CHAPTER I

INTRODUCTION

1.1 Background

Tablets are the most popular pharmaceutical dosage forms, with numerous advantages such as providing patients compliance, precise dosage, easy to manufacture, can be produced at relatively low cost, highly more stable than oral liquid dosage forms, portable, and its ability to be moulded into a variety of shapes (Tiwari *et al*. 2011; Marwaha, Sandu & Marwaha, 2010; Behera *et al*. 2009; Gohel & Jogani, 2005; Jivraj, Martini & Thomson, 2000; Alderborn, 2002; Bandelin, 1989). Tablets can be manufactured by the following techniques: wet granulation, dry granulation and direct compression (Bolhuis & Chowhan, 1996; Michaud *et al.*, 1998; Patel & Patel, 2009). Wet granulation method needs more unit processes in the production of tablets while dry granulation requires more processing control and has low reproducibility. As for direct compression, it only involves two primary processes, namely mixing and compression to produce tablets. Therefore direct compression is the most appropriate technology and preferred method for pharmaceutical industries in manufacturing of tablets (Govedarica *et al*., 2011; Patel & Patel, 2009; Shankar *et al.*, 2012; Weisser *et al.* 2001). The method offers simplicity and is cost effectiveness, uses lesser processing steps, and requires lesser validations and maintenance of equipment, shorter processing time, fewer excipients, and poses fewer stability issues for heat or moisture sensitive drugs (Bolhuis & Chowhan, 1996; Gohel & Jogani, 2005; Patel & Patel, 2009).

"Direct compression" is a term used to describe the process of tablet manufacturing, in which tablets are formed by compressing directly from powder mixtures consisting of

active ingredient(s) and suitable material aids which are also known as excipients (Bolhuis & Chowhan, 1996; Gohel & Jogani, 2005; Weisser *et al.,* 2001). Hence, directly compressible materials refer to tablet excipients specifically used in the direct compression formulations. Since most of the active pharmaceutical ingredients are poorly compressible and lack flow properties, addition of directly compressible excipients in the formulations is required to allow such active ingredients be compressed into satisfactory tablets (Marwaha, Sandhu, & Marwaha, 2010; Gohel & Jogani, 2005; Shangraw, 1989). Therefore, directly compressible excipients should be free flowing, compressible and exhibit high dilution potential. The free flowing property is needed to ensure uniformity of die filling powder mixtures, compressibility is required to facilitate the formation of compacts and dilution potential of the excipients should be high to have the tablets at optimum weight (Li *et al.*, 2004; Marwaha, Sandhu & Marwaha, 2010; Jivraj, Martini & Thomson, 2000; Prescott & Hossfeld, 1994; Rudnic & Schwartz, 2005).

With the growing popularity of direct compression method, a demand for directly compressible excipient is increasing (Shittu *et al*., 2012; Marwaha, Sandhu & Marwaha, 2010). Starch and its derivatives have a broad range of applications both in food and non-food sectors. This is due to its relative inertness, diverse functionalities, year-round availability, and low cost (Cisneros *et al.,* 2009). In pharmaceutical field, starch is ranked among the top ten excipients in oral solid dosage forms (Riley *et al.*, 2008). It is widely used as a pharmaceutical excipient primarily in tablet and capsule formulations functioning as a diluent, binder and disintegrant (Okunlola & Odeku, 2011; Odeku & Picker-Freyer, 2010; Kibbe, 2000; Shangraw, 1989; Bolhuis & Chowhan, 1996). Several different pharmaceutical starches are available on the market, including corn, cassava, wheat, and potato (Burrell, 2002). Worldwide, corn starch is the most widely used starch in tablet

formulations due to its availability (Riley *et al.*, 2008). However, starches are not suitable to be used as excipients in direct compression formulations due to compression problems, poor flow properties and high lubricant sensitivity (Odeku & Picker-Freyer, 2010; Jivraj, Martini, & Thomson, 2000; Bolhuis & Chowhan, 1996). Physical and chemical modifications of starches have been applied to improve their properties as direct compression excipients. Modified rice starch was introduced as a direct compression filler-binder with commercial name Era-Tab® or Primotab®. Rice starch was physically modified by a spray drier to produce a spherical agglomerated particle. It has excellent flow and binding properties (Bos *et al.,* 1992). Korhonen *et al.* (2002) investigated the effects of various starch acetate powders on the direct compression characteristics. They reported that all powders were free flowing and easily formed bonding. Alebiou & Itiola (2002) had comparatively evaluated the compression characteristics of natural and fully pregelatinised forms of sorgum, plantain and corn starches. The study concludes that pregelatinisation increases compression characteristics at low pressure and facilitates plastic deformation. Gohel & Jogani (2005) in their review reported that dextrinised form of rice, corn, wheat and tapioca starches exhibited very good flow properties, compressibility and disintegration qualities for direct compression tableting, with dextrinised tapioca starch appeared the best. Odeku, Schmid, & Picker-Freyer (2008) had investigated pregelatinised starches of four tropical *Dioscorea* species as excipient in direct compression. *Dioscorea* starches were fully pregelatinised followed by either oven drying or freeze drying. The results obtained indicated that pregelatinisation improved flowability and compressibility of *Dioscorea* starches with freeze dried pregelatinised *Dioscorea* starches showed higher compactibility. In related development, Odeku & Picker-Freyer (2010) found that the freeze dried pregelatinised *Dioscorea* starches were non-disintegrating and could find application as directly compressible excipients for controled drug delivery. Adedokun & Itiola (2011)

comparatively studied the effectiveness of native and pregelatinized trifoliate yams, rice and corn starches as disintegrants in paracetamol tablets. They found that the pregelatinised starches produced better disintegrant properties than natural starches. Apeji, Oyi, & Musa (2011) and Shittu *et al*. (2012) converted cassava starch into directly compressible microcrystalline starch by enzymatic hydrolysis using α-amylase enzyme. Results of the evaluations revealed that microcrystalline cassava starch showed improvement in compression properties and dilution potential of the native starch.

Pregelatinisation is one of the typical physical modification adopted to prepare directly compressible materials, the method has proven able to render starches flowable and directly compressible (British Pharmacopeia/BP 2007; Kibbe, 2000; Odeku, Schmid, & Picker-Freyer, 2008; United States of Pharmacopeia/USP 27; USP 30). For example, corn starch has been successfully modified into pregelatinised form and is commonly used as direct compressible excipients with commercial name Uni-pure® DW (National Starch & Chemical Co., USA), Uni-pure® LD (National Starch & Chemical Co., USA), Starch® 1500 (Colorcon Inc., USA) and Spress® B820 (Grain Processing Corp., USA) (Zhang, Law & Chakrabarti, 2003). Pregelatinised starch is included in the pharmacopoeias as an official excipient (BP 2007; Kibbe, 2000; USP 27; USP 30). Modification of starches by pregelatinisation offers various advantages, such as the simplest method, low cost, environmentally friendly and produce non-toxic product, therefore there is no need to undergo the necessary safety testing (Jayakody *et al.,* 2009; Kibbe, 2000; Tharanathan, 2005).

Sago starch is one of the commercial starches derived from the stem of sago palm (*Metroxylon sagu*) and becoming an increasingly important socioeconomic crop in South

East Asia. It has its own unique characteristics, but some of its physicochemical properties are quite similar to common starches such as potato and cassava (Abdorreza, Cheng, & Karim, 2011). The palm grows in high humid tropical countries like Malaysia, Indonesia, Thailand, Philippines, Vietnam and Papua New Guinea. Its trunk contains a large amount of starch and is used as food. Sago starch has also been applied in food industries; biotechnology industries and other industries such as in the production of biodegradable plastic, adhesives, paper and textile (Abd-Aziz, 2002; Karim *et al.* 2008; Nor Nadiha *et al*., 2010; Singhal *et al.* 2008; Teng, Chin, & Yusof, 2011).

Malaysia is one of the three leading countries of sago starch producers in the world, together with Indonesia and Papua New Guinea. In Malaysia, the state of Sarawak is the largest sago-growing areas and is now the biggest exporter of sago starch in the world (Singhal *et al.,* 2008) with main usage for food products (Pimpa *et al.*, 2007a). In the pharmaceutical field, investigation on the literatures revealed that there have been many researches on the utilisation of sago starch as potential pharmaceutical excipients, such as: sago starch has been evaluated as a binder in comparison with various commercial binders such as corn starch, tapioca starch, pregelatinised starches and polyvinylpyrrolidone, sago starch showed prolonged disintegration time (Sinchaipanid *et al.,* 1995). Sago starch showed faster disintegration properties as compared to papaya starch (Gangwar *et al.,* 2010). Preparation and evaluation of carboxymethylated sago starch as tablet superdisintegrant has been conducted by Singh *et al.* (2011). The results revealed that its efficacy as tablet disintegrant was comparable to sodium starch glycolate, an official superdisintegrant (Singh *et al.*, 2011). Acetylated sago starch has been prepared and found to be useful as a carrier for controlled drug delivery (Singh & Nath, 2012). However, research on the application of a local sago starch as directly compressible material in

tableting has not been reported yet. Therefore, this research aimed to study the potential of a local sago starch in its pregelatinised forms as a new excipient in directly compressed tablets.

1.2 Justification

The demand for directly compressible excipients is increasing as a consequence of the growing popularity of direct compression method in the manufacturing of tablets (Shittu *et al*. 2012; Marwaha, Sandhu & Marwaha, 2010). In an attempt to optimise the use of local sources, a local sago starch was selected in this study with a view of establishing its potential as a source of directly compressible excipients. Sago starch is renewable, cheap and abundantly available locally (Pimpa *et al.,* 2007b). Its availability is guaranteed since the sago starch industry in Malaysia is well established especially in the state of Sarawak, which is now the world's biggest exporter of sago (Singhal *et al.* 2008). Although a lot of research on sago starch has been conducted, however a study on pregelatinised sago starch from local resources, particularly as a directly compressible material in tableting has not been conducted yet. Up to now local pharmaceutical industries are still depending on the imported directly compressible excipients for their need. Thus, research on locally available starches such as sago starch to reduce dependency on such imported excipients is definitely of value not only in increasing the local content of pharmaceutical products and improving the trade balance, but also in the development of local pharmaceutical excipient industries.

Pregelatinisation method was adopted in this study with various reasons. It is the simplest method in the manufacturing of directly compressible excipients (Tharanathan, 2005). The method is also cheap. In the processing, it only involves heat and aqueous medium without addition of the chemicals, therefore it is environmentally friendly, producing non-toxic

product and without undergoing necessary safety testing (Jayakody *et al.*, 2009; Kibbe, 2000). Furthermore, the pregelatinisation method has proven to be effective in converting starches into flowable and directly compressible starches (BP 2007; Kibbe, 2000; Odeku, Schmid, & Picker-Freyer, 2008; USP 27; USP 30). For instance, corn starch has been successfully modified into pregelatinised form and marketed as flowable and compressible starch with commercial names of Uni-pure® DW (National Starch & Chemical Co., USA), Uni-pure® LD (National Starch & Chemical Co., USA), Starch® 1500 (Colorcon Inc., USA) and Spress® B820 (Grain Processing Corp., USA). These excipients are widely used as a direct compression material in tablet formulations (Zhang, Law, & Chakrabarti, 2003).

1.3 Research objectives

This study was conducted with the aims to explore the potential of a local sago starch which is abundantly available, as a new source of directly compressible material for tableting. Subsequently the study aimed:

- To characterise the properties of sago starch
- To convert sago starch into pregelatinised forms with different interventions, namely difference in heating time
- To comparatively evaluate the characteristics of sago starch and pregelatinised forms of sago starch at the molecular level
- To comparatively evaluate the characteristics of local sago starch, pregelatinised sago starches, Spress® B820 and Avicel PH 101 as a directly compressible material at the particle and powder level

- To develop direct compression formulations of Paracetamol tablet containing different types of directly compressible materials, namely a selected pregelatinised sago starch obtained from this study, Spress® B820 and Avicel PH 101.
- To comparatively evaluate the tablets resulted from the above formulations according to the official requirements and non-official requirements

1.4 Thesis outline

This thesis describes the potential of pregelatinised sago starches as directly compressible material for tableting using two commonly used commercial directly compressible materials i.e Avicel PH 101 and Spress® B820 as the benchmarks. The sago starch grade was characterised according to the USP specifications and its chemical compositions were determined. Sago starch was converted into its pregelatinised forms at different heating time, i.e. 15, 30, 45 and 60 minutes. Effect of pregelatinisation was analysed to characterise their amylose content, molecular structure, types of crystal, degree of crystallinity, thermal characteristics and degree of gelatinisation. Comparative evaluations of the characteristics of sago starch, pregelatinised sago starches and Avicel PH 101 and Spress® B820 as directly compressible material were carried out, covering shape and surface texture of particles, viscosity, swelling power, water solubility index, particle size distribution, loss on drying, porosity, densities, flowability, compressibility, mechanical properties and lubricant sensitivity. Finally, the best directly compressible pregelatinised sago starch was selected; its dilution potential and performances in developed tablet formulations using Paracetamol as a model drug were evaluated in comparison against Avicel PH 101 and Spres® B820.

CHAPTER 2

LITERATURE REVIEW

2.1 Sago starch

2.1.1 Sago palm

Sago starch is derived from the pith of sago palm with botanical name *Metroxylon sagu*, the most important species producing starch of genus *Metroxylon* in the Palmae family. *Metroxylon sagu* is native to South Pacific Island; with thevcentre of diversity in Papua New Guinea, extending to South East Asia countries such as Indonesia, Malaysia, Thailand, Philippines and Vietnam through Melanisia (Karim *et al.* 2008; Singhal *et al.*, 2008). Sago palm primarily grows in freshwater swamps or in dry land with sufficient water supply and dies after flowering only once (Flach, 1997; McClatchey *et al*., 2006). The palm produces an erect trunk, often over 9 m high with 0.5 – 1.0 m in diameter at the base, loaded with starch. Sago palm achieves its maturity and is ready for harvesting at about 9 – 12 years of age, the palms are felled just before flowering, the time when accumulation of starch reaches maximum. The productivity of sago palm per land area is the highest among the starchy crops; the palm could produce starch 3 to 4 times higher than that of rice, corn, or wheat and about 17 times higher than that of cassava (Karim *et al.*, 2008; Malviya *et al.*, 2010; Singhal *et al.*, 2008; Radley, 1976). Malaysia, Indonesia and Papua New Guinea are the three leading countries of sago starch producers in the world. In Malaysia, the state of Sarawak is the largest sago-growing areas and is now the biggest exporter of sago starch in the world (Singhal *et al.*, 2008).

2.1.2 Extraction of sago starch

A sago palm is felled and the trunk is cut lengthwise. The starchy pith is then removed, kneaded with water and filtered through sieves to release the starch. The pith is subjected to several washings and straining to extract the starch from fibrous residue. The starch milk is allowed to run into troughs and settle. The water layer is decanted to obtain the settled starch and followed by sun-drying. In large scale, the palm trunk is split lengthwise into segments and debarked. The pith is then fed into a mechanical rasper to form finer pieces and facilitate the release of starch granules. The process is continued by passing the finer pieces through a hammer mill via a belt conveyor for further disintegration. The resulting starch slurry is then passed through a series of centrifugal sieves to separate coarse fibres. A series of cyclone separator is used to further purify the starch, which is then dried using a rotary vacuum drum dryer and hot air drying (Karim *et al.*, 2008).

In order to produce high quality sago starch, matured palms and efficiency of extraction method are required. Starch produced from immature palms contains more impurities and tends to brown due to the presence of polyphenol compounds and polyphenol oxidase activity in the starch. The polyphenol oxidase is facilitated by acidic pH and further promoted by ions such as copper and iron present in the water used for extraction and purification processes. Therefore, usage of water containing such ions in the extraction processes should be avoided. The browning of sago starch could be whitened by oxidative bleaching agents such as sodium hypochlorite and bisulphite (Flach, 1997; Karim *et al.*, 2008; Pei-Ling, Mohamed, & Karim, 2006; Singhal *et al.*, 2008).

In order to improve the quality of sago flour, the Sago Advisory Board of Malaysia was established in 1950. The board had set a minimum standard in terms of colour and amount

of fibre. The standard was then altered by Standards and Industrial Research Institute of Malaysia (SIRIM), who set the basic requirements for industrial-grade sago starch and edible food-grade sago starch (Yiu *et al.,* 2008). Table 2.1 and Table 2.2 show the requirements for industrial sago starch and edible sago starch.

Table 2.1: Requirements for industrial sago starch (MS468 1976).

No.	Characteristics	Requirements
1	Starch content	60% minimum
2	Moisture content	15% maximum
3	Total ash (dry basis)	0.5% maximum
4	Crude fibre (dry basis)	1% maximum
5	Particle size (through sieve of mesh 125)	65% minimum
6	Colour (tintometer readings)	0.4 red + 0.5 yellow
7	pH of aqueous extract	4 minimum

Adapted from Karim *et al.* (2008).

Table 2.2: Requirements for edible sago starch (MS470 1992).

No.	Characteristics	Requirements
1	Moisture content	13% maximum
2	Total ash (dry basis)	0.2% maximum
3	pH of aqueous extract	4.5 to 6.5
4	Crude fibre (dry basis)	0.1% maximum
5	Peak viscosity (6% dry basis suspension)	600 BU
6	Colour ("L" value)	90 minimum
7	Sulphur dioxide	30 ppm maximum
8	Particle size (through 125 mm or 120 mesh size)	99.0% minimum

Adapted from Karim *et al.* (2008).

2.1.3 Composition and structure

2.1.3.1 Amylose and amylopectin

All types of starches have chemical formula of $(C_6H_{10}O_5)_n$, where n is between 300 to 1000 (Aggarwal & Dollimore, 1998). Starches, regardless of plant source, are mainly made up of two glycans that are amylose and amylopectin. Both amylose and amylopectin

contain α-D-glucose as basic monomer units (Hoover, 2001; Jayakody & Hoover, 2008; Tester, Karkalas, & Qi, 2004).

Figure 2.1 shows the molecular structure of amylose. Amylose is a type of relatively long linear polymer of 99% (1,4)-α-D-glucan linkages and (1%) (1,6)-α-D linkages. This means that amylose is mainly composed of D-glucose units that are interconnected through α-linkages between carbon-1 of one unit and carbon-4 of the next unit. The molecular weight of amylose is in the range of 1-10 × 10^5 and its degree of polymerisation vary from 324 to 4920 (Jayakody & Hoover, 2008; Tester, Karkalas, & Qi, 2004).

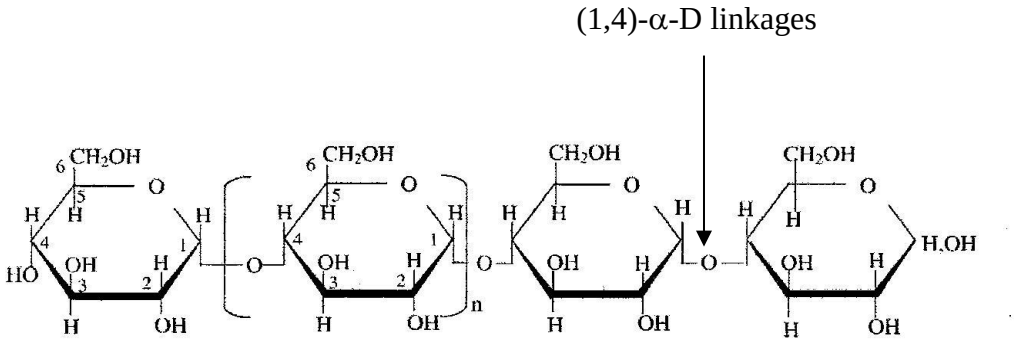

Figure 2.1: The molecular structure of amylose (Tester, Karkalas & Qi, 2004).

Amylopectin is a highly branched polymer consisting of 95% (1,4)-α-D linkages between the glucose unit to form the polymer chains with 5% (1,6)-α-D linkages to form the branching points (Aggarwal & Dollimore, 1998; Jayakody & Hoover, 2008). Hoover (2001) as well as Solomans & Fryhle (2000) further described that the branching of amylose structure between carbon-1 of one glucose unit to carbon-6 of another take place at intervals of about 20 to 25 glucose units. The molecular weight of amylopectin is around 1 × 10^7 to 1 × 10^9 with degree of polymerization from 9600 – 15900 (Jayakody & Hoover, 2008). Figure 2.2 shows the molecular structure of amylopectin (Tester, Karkalas & Qi,

2004). D-glucose units are interconnected through (1,4)-α-D linkages with (1,6)-α-D linkages as branching points.

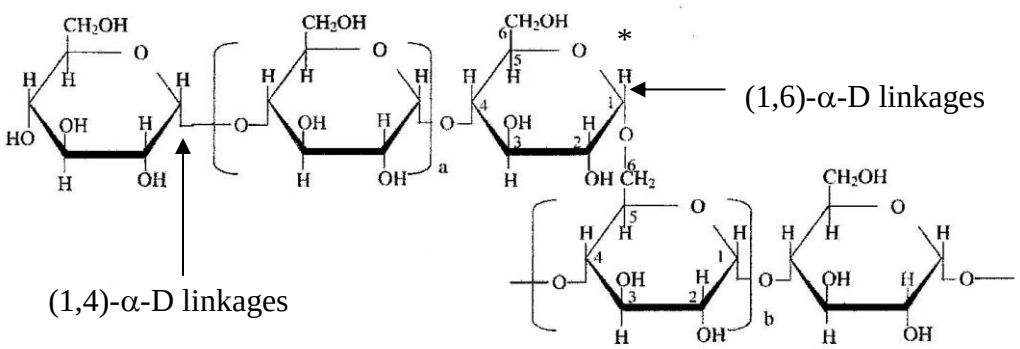

Figure 2.2: The molecular structure of amylopectin (Tester, Karkalas & Qi, 2004).

The relative proportion of amylose to amylopectin may vary according to the botanical origin of the starch and the proportion has a significant influence on starch performance as a tablet excipient (Lin & Czuchajowska, 1998).

Typically, the range of amylose content in the starch is about 10 – 38%. As examples, cassava has around 18.6 – 23.6% amylose, potato 25% amylose and corn 28% amylose. However, there are some exceptions; for instance genetically manipulated high amylose corn starch contains about 70% amylose and genetically modified waxy corn starch contains 90 – 100% amylopectin (Ahmad *et al.*, 1999; Hoover, 2001). According to Ahmad *et al.* (1999), the amylose content and the molecular weight of the sago starches from different origin were found to be different significantly. The amylose content varies between 24% and 31%. The differences could be due to the different stages of harvesting. The molecular weight of amylose was found to be in the range of 1.41×10^5 to 2.23×10^6 and amylopectin 6.70×10^6 to 9.23×10^9; the differences were as a result of different

processing in the factory, notably the water used (Ahmad *et al.,* 1999; Mohamed *et al.,* 2008). Sago starch had the average-number degree of polymerization between 2490 and 5090. The gelatinisation temperature of sago starches varied from 69.5 to 70.2°C, which is higher than potato, corn and pea, but is relatively low when compared to sweet potato and yam starches (Karim *et al.*, 2008).

2.1.3.2 Non-carbohydrate components

In addition to amylose and amylopectin, starch granules also contain other minor constituents or proximate composition, namely protein, lipid, ash, crude fibre and minerals such as calcium, magnesium, phosphorus, potassium and sodium (Tester, Karkalas & Qi, 2004).

Lipid may be contained in starch for up to 2% w/w. For protein, it contains less than 0.6% w/w in starch weight and the proteins occur commonly on the surface or embedded within the matrix of granules. Starches also contain relatively small quantities of minerals that are approximately 0.4% w/w. Tattiyakul *et al.* (2010) conducted a study on the proximate analysis of *Dioscorea hispida* starch and the results showed that it consists of 12.8% moisture, 86.6% carbohydrate, 0.13% protein, 0.13% lipid and 0.33% crude fibre. As reported by Rai (2005), corn starch is composed of 7.74% moisture, 1.22% lipid, 1.21% protein and 0.36% ash whereas potato starch composed of 9.37% moisture, 0.32% lipid, 0.61% protein and 0.19% ash.

Ahmad *et al.* (1999) found that the proximate compositions of sago starches from different origin did not vary significantly. The studies revealed that moisture content varied in the

sago starch between 10.6% and 20.0%, ash between 0.06% and 0.43%, crude fat between 0.10% and 0.13%, fibre between 0.26% and 0.32%, and crude protein between 0.19% and 0.25%.

2.1.3.3 Physicochemical properties of sago starch.

Starch is in the form of granules that exist naturally and stored in parts of the plant including grains, roots, tubers, seeds, stem piths, leaves, fruit and pollen. Size and shape of starch granules are typical of the botanical sources. Sago starch granules vary from 10 to 50 μm with an average of 32 μm, are oval polygonal shaped, with some of truncated oval granules (Kerr, 1968; Wang, Powell, & Oates, 1995). Rice starch granules are the smallest among the commercial starches; their size is from 3 to 10 μm with the shape polygonal and is sometimes found in clusters. Corn starch granules are all round shaped and polygonal with sizes from 5 to 20 μm. Wheat starch granules are elliptical shape with no distinct striations, they show larger granules (22 to 36 μm) and smaller granules (2 to 10μm), where a faint centric hilum can be seen only in the larger granules. Cassava starch granules are round or oval with indentation on one side and some fissures centric hilum, the granules vary from 5 to 25 μm. Potato starch granules vary greatly in size (15 to 85 μm); they are egg-shaped, concentric striations with distinction a dot or short line eccentric hilum situated in the smaller end of the granule (Karim *et al.* 2008; Kerr, 1968).

Starch is semi-crystalline in nature with varying degree of crystallinity of 20 – 40%. The crystallinity is associated with the amylopectin component, whereas the amorphous region mainly represents amylose (Hood & Mercier, 1978; Jacobs & Delcour, 1998; Jayakody & Hoover, 2008). Figure 2.3 shows a model of the starch granule structure, with growth rings.

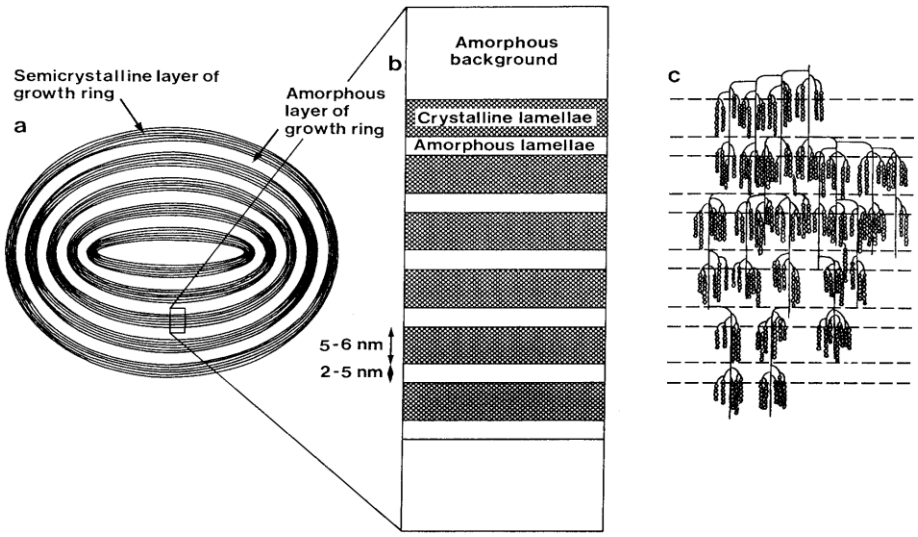

Figure 2.3: Schematic representation of starch granule (Jacobs & Delcour, 1998).

The multiple concentric layers of growth rings consist of alternating crystalline and amorphous layers of higher and lower density respectively. The higher dense layer consists of alternating crystalline and amorphous lamellae (semicrystalline layer), with thickness between 120 and 400 nm. Crystalline lamellae (5 – 6 nm) are formed mainly by amylopectin double helices branches pack into a crystalline lattice in parallel fashion, whereas amorphous lamellae (2 – 5 nm) contains the amylopectin branching points (Figure 2.3c). The lower dense layer of the growth ring, which is as thick as the higher dense layer, is amorphous (amorphous layer), where amylose is located and contains more water (Copeland *et al.*, 2009; Jacobs & Delcour, 1998). Analysis by X-ray diffraction (XRD) indicates that the amylopectin double helices may exhibit either A-, B- or C-crystalline forms. The double helices of A-crystalline forms show more compact structure than B-crystalline forms (open structure), as C-crystalline forms are actually a combination of A- and B-crystalline forms (Copeland *et al.*, 2009). In a study of 12 sago starches from different origins, all the granules of sago starches exhibit a C-type X-ray diffraction pattern

due to the relatively high amylose content, which is in the range of 24 – 31% (Ahmad, *et al.,* 1999; Ahmad & Williams, 1999; Teng, Chin, & Yusof, 2011).

The amorphous regions of granules are mainly composed of amylose and amylopectin branch point (Ratnayake & Jacson, 2006). The ratio of amylose and amylopectin content can affect the functional properties of the starch, such as swelling power, water binding capacity (water solubility), temperature gelatinization and peak viscosity (Copeland *et al.,* 2009; Riley, Wheatly, & Asemota, 2006; Tester & Morrison, 1990). Swelling properties are basically affected by the appearance of amylopectin. Amylose contributes to the stickiness and acts as an inhibitor of swelling, especially when there is a formation of amylose-lipid complex (Copeland *et al.,* 2009; Mohamed *et al.,* 2008; Tester & Morrison, 1990). Starches with high swelling powers and water binding capacity facilitate disintegration and dissolution rate of tablets when they are used as binders in the tablet formulations. Sago starch have swelling power and water solubility (water binding capacity) that increase with temperature, and the magnitude is quite similar to cassava and potato starches but higher than corn and pea starches (Mohamed *et al.*, 2008).

Sago starches were reported to possess two types of pasting properties. The first type showed a maximum consistency, immediately followed by a sharp drop in consistency. On the other hand, the second type showed a plateau when the maximum consistency was achieved. This pasting profile was found to be similar to cassava and sweet potato starches (Ahmad *et al.*, 1999). At the same solid concentration, sago starch paste was observed to be similar to sweet potato and cassava starch pastes, but softer if compared to cereal starch pastes. The viscosity order of starch pastes ranging from high to low is potato, sago,

cassava, sweet potato, rice, corn and wheat. Sago starch possessed low adhesiveness but the cohesiveness was high. The gel of sago starch was found to be firm (Karim *et al.*, 2008).

Gelatinisation temperature of most starches is between 60 and 80°C. (Copeland *et al.*, 2009). Starches with low amylose content tend to have high gelatinisation temperatures as the granules are more crystalline and less amorphous (Riley, Wheatly, & Asemota, 2006). The gelatinisation temperature of sago starches varied from 69.5 to 70.2°C which is higher than potato, corn and pea, but is relatively low if compared to sweet potato and yam starches (Karim *et al.*, 2008).

2.1.3.4 Uses of sago starch

Sago starch has been used traditionally as staple food for many coastal communities in Papua New Guinea and traditional Borneo people living near swamp, where sago palm grows (Abd-Aziz, 2002; Sopade & Kiaka, 2001). Sago flour is used in a variety of recipes such as sago pudding, sago cones, savory sago pancakes and *tabaloi* biscuits. In Sarawak, sago starch is widely utilized to produce sago pearls. Sago pearls are made by pressing the slightly wet sago starch through a sieve. The small particles of wet starch are then rolled around and heated in a round bottom pan until the outside gelatinised and subsequently dried, sorted and sold. The pearls are used in the preparation of "three-palm pudding" which is sago pearls cook in coconut milk and and topped with sugar from *Arenga pinnata* (Flach, 1997; Karim *et al.*, 2008; Singhal *et al.*, 2008).

Sago starch has found its uses in food industry as well as various non-food industries. In the food industry, sago starch is commonly used as ingredients, functioning as thickener,

stabiliser and gelling agent in various food products, such as soups, baby food and pudding due to its viscous property upon gelatinisation (Karim *et al.,* 2008; Mohamed *et al.,* 2008; Malviya *et al.,* 2010; Singhal *et al.,* 2008). Sago starch is also used in the production of kuey teow, vermicelli, biscuits, bread, noddle, fish cracker and some other foods (Abd-Aziz, 2002; Mohamed *et al.*, 2008; Pimpa *et al.*, 2007a; Singhal *et al.*, 2008).

In non-food industries, sago starch is utilised to produce adhesives for plywood, paper and textile (Abd-Aziz, 2002; Flach, 1997) as biodegradable filler in plastics to produce biodegradable packaging (Abdorreza, Cheng, & Karim, 2011; Flach, 1997; Ishiaku *et al.,* 2002). Sago starch has some uses in the biotechnology field to produce ethanol (Abd-Aziz, 2002; Flach, 1997), fermentable sugar, lactic acid, monosodium glutamate (Aziz, 2002; Singhal *et al.,* 2008) and cyclodextrin (Charoenlap *et al.,* 2004). Sago starch also found application in livestock and poultry feed formulations (Flach, 1997).

In pharmaceutical field, applications of sago starch as tablet excipients have been studied by several researchers. Sinchaipanid *et al*. (1995) conducted a preliminary study on the performance of sago starch as a binder and was comparatively evaluated against commercial binding agents: they are corn starch, tapioca starch, pregelatinised starches (Era gel, EG® and Starch® 1500, S1500), and polyvinylpyrrolidone K 30 (PVP). Tablets were prepared by wet granulation method with 2% level as the binder, using hydrochlorothiazide as an active ingredient. It was concluded that sago starch prolongs the disintegration time; therefore it is only suitable as a binding agent in the tablet formulations of which dissolution is not the primary concern or in formulations containing sufficient disintegrants. Disintegration properties of sago starch in comparison against papaya starch were studied by Gangwar *et al.* (2010). Tablets were prepared by wet granulation method. The study

found that both sago starch and papaya starch possess significant disintegration properties with sago starch appeared superior to papaya starch. Singh *et al.* (2011) has modified sago starch into carboxymethylated form in an attempt to improve disintegration properties of sago starch. The disintegrating properties of carboxymethylated sago starch were further evaluated. The results revealed that its efficacy as tablet disintegrant was comparable to sodium starch glycolate, an official disintegrant. Research on acetylated sago starch as tablet excipients has also been conducted. It was reported that the acetylation of sago starch prolongs disintegration time and rendered the drug to be released in a controlled manner, thus it was found to be useful as a carrier for drug control delivery (Singh & Nath, 2012). Further research on the modification of sago starch, especially by pregelatinisation for direct compression tablet excipients, has not been conducted yet.

2.2 Pharmaceutical tablets

Tablets are pharmaceutical solid dosage forms, containing one or more active ingredients and excipients, prepared by compressing the uniform volume of the powder mixtures (Alderborn, 2002). They are the most popular pharmaceutical dosage forms for several reasons. Tablets are convenient and simple to administer, easy to dispense, is portable and hence, provide patient compliance. Tablets are in dry form, less bulky with relatively low moisture content, and the hydrolysis reactions can be avoided. Therefore, tablets are physically and chemically more stable than liquid dosage forms. Furthermore, with the available technology, tablets can be manufactured to provide accurate dosing of the drug, the unpleasant taste of drugs can be coated to improve patient's acceptance and can be mass produced with consistent quality, or in relative term, cheaper price (Alderborn, 2002; Bandelin, 1989). However, there are some disadvantages of tablets as a pharmaceutical dosage form. Tablets are not suitable for patients with difficulty in

swallowing, especially for children. It has longer time in giving effect as compared to the solution dosage form; therefore tablets are not suitable for patients who are critically ill. The effectiveness of tablets that are poor water soluble or poorly absorbable active ingredients is low due to bioavailability problems. Some active ingredients, when given in the form of tablets, may cause local irritation to the gastrointestinal mucosa (Alderborn, 2002).

Tablets may be classified based on route of administration such as oral tablets, sub-lingual tablets, buccal tablets, rectal tablets and vaginal tablets. Another classification of tablets can be based on the formulation characteristics such as immediate release tablets, effervescent tablets, melt in mouth or fast dissolving tablets and delayed release or extended release tablets. In terms of manufacturing processes, machineries and excipients used in the tableting are similar (Parmar & Rane, 2009).

As a pharmaceutical dosage form, tablets should have good quality and carry the following attributes: tablets must contain the correct dosage and able to release drug in a controlled and reproducible way. The appearance of tablets must be elegant and its weight, size and drug content must be uniform. Tablets should have sufficient mechanical strength to withstand fracture and erosion during manufacture, packaging, transporting and use. Tablet should be biocompatible and physically, chemically and microbiologically stable during the lifetime of the product (Alderborn, 2002; Bandelin, 1989).

Tablet compaction

Compaction is the transformation of powders into a compact of defined shape by powder compression and is the principle process involved in the formation of tablets. The

compaction process can be described by a number of sequential phases. It starts initially with the transitional repacking of the particles in the die cavity. These particles will then rearrange into a closer packing order where the porosity and volume will be reduced (Alderborn, 2002). This process will continue until the increasing friction limits further movement between particles.

At this stage, the subsequent compression force applied will cause the deformation or fragmentation of the particles (Alderborn, 2002). There are two types of deformation; elastic deformation and plastic deformation. Elastic deformation is a reversible type of deformation where the shape of the particles will only change temporarily. The powder will return to its former structure after the compression force is removed (Alderborn, 2002; Rudnic & Schwartz, 2005). Meanwhile, plastic deformation is defined as an irreversible or permanent deformation which increases the formation of permanent interparticle contact region. This will cause the formation of interparticle bond during compression (Alderborn, 2002; Jivraj, Martini, & Thomson, 2000). This is considered as the most critical phase in the consolidation process because excessive compression force may lead to brittle fracture and the fast application of the compression force may lead to de-bonding of the compacts during the stress relaxation stage (Rudnic & Schwartz, 2005). For both elastic and plastic deformation, the degree of deformation is dependent on the applied compression force (Alderborn, 2002).

The increasing compression force can also lead to fragmentation, where the particles fracture into smaller sizes and create more new surfaces for bonding (Alderborn, 2002; Jivraj, Martini, & Thomson, 2000). The cycle of deformation and fragmentation will repeat throughout the compression process. Finally, elastic recovery of the tablet formed occurs

during the decompression phase. The tablet formed will then be ejected from the compaction machine by the special pushing device (Alderborn, 2002).

2.2.1 Manufacturing tablets by direct compression

There are three main modes of tablet manufacturing: wet granulation, dry granulation and direct compression (Gohel & Jogani, 2005; Parmar & Rane, 2009). Wet granulation is the oldest method and consists of more unit processes (Table 2.3) in the manufacturing of tablets (Patel & Patel, 2009). Granulation is carried out by addition of binder solution to the powder mixture, followed by passing the wetted mass to a screen of the desired mesh size and dried. The dried granule is then subjected to second screening to obtain smaller size of granules (Bandelin, 1989). Wet granulation is applied with the objective to improve the flow, density and compressibility of particles by size enlargement and densification (Bandelin, 1989; Parmar & Rane, 2009). Wet granulation method is preferred to dry granulation because of dust elimination, single pot processing and uniformity of tablets containing low dosage of active ingredient can be achieved (Bandelin, 1989; Parmar & Rane, 2009). Dry granulation (roll compaction or slugging) is a process involving compaction of dry powder at high pressure to form large compacts or slugs, followed by milling and dry screening of the slugs to obtain the desired granules size. This method does not use heat and moisture in the processing (Parmer & Rane, 2009). However, dry granulation requires more control of processing variables, and reproducibility of the products is difficult to be achieved (Patel & Patel, 2009). Because of that, it is no longer the method of choice to produce tablets (Bolhuis & Chowhan, 1996).

Direct compression is a technique which involves compaction of the bulk material that consists of ingredients composite to form a tablet without the use of granulation (Prescott &

Hossfeld, 1994). Mixing and compressing are the only steps involved in direct compression to produce the finished tablets. Due to its simplicity, direct compression technique has gained popularity and is preferable in tablet production with a number of advantages (Table 2.4).

Table 2.3: Comparison of wet granulation, dry granulation and direct compression steps in the tablet manufacture (Bandelin, 1989; Bolhuis & Chowhan, 1996; Gohel & Jogani, 2005).

Step	Wet Granulation	Dry Granulation	Direct compression
• 1	• Weighing	• Weighing	• Weighing
• 2	• Mixing	• Mixing	• Mixing
• 3	• Moistening	• Compressing into slugs	
• 4	• Wet screening	• Dry screening	
• 5	• Drying	• Admixing of disintergrant and lubricant	
• 6	• Dry Screening	• Compressing	
• 7	• Admixing of disintergrant and lubricant		• Admixing of lubricant
• 8	• Compressing		• Compressing

Direct compression has economic and time scale advantages. It requires less unit processes therefore needs less space, less equipment, lower labour cost, less processing time and less energy consumption compared to dry and wet granulations. The method eliminates stability issue for active ingredients that are sensitive to the moisture and heat. Another advantage of tablets prepared by direct compression is higher dissolution rate as the tablets disintegrate into the primary particle instead of into granules (Bolhuis & Chowhan, 1996; Jivraj, Martini, & Thomson, 2000; Shangraw, 1989).

However, direct compression also has its limitations. It is only applicable to tablets containing low dose of active ingredient, preferably less than 30% of the formulation due to tablet size and weight limitation (Jivraj, Martini, & Thomson, 2000). It is not suitable for poor flow active ingredients. Other than that, direct compression is susceptible to particle segregation during blending prior to compaction if there are variations in particle size distribution, particle shape and particle density of drug substances and excipients (Bolhuis & Chowhan, 1996). Hence, physical and physicomechanical properties of active pharmaceutical ingredients and excipients that are used in direct compression need to be defined and controlled as variation in these properties can seriously interfere the tableting properties. Table 2.4 shows the advantages and limitations of the methods of tablet manufacturing.

Table 2.4: The advantages and limitations of wet granulation, dry granulation and direct compression methods in the tablet manufacture (Bandelin, 1989; Parmar & Rane, 2009; Patel & Patel, 2009; Shangraw, 1989).

Method of manufacturing	Advantages	Limitations
Wet granulation (aqueous)	Suitable for most compounds	High cost: more time, space and energy consuming process
	Improve flowability	Required special equipment
	Reduce elasticity	Stability issues for heat-moisture sensitive active ingredients
	Improve hydrophilicity	Less powder recovery
	Reduce potential of segregation	
	Reduce dust production	
Wet granulation (non-aqueous)	Suitable for heat sensitive drugs	Expensive equipment
	Vacuum drying reduce need for heat	Solvent recovery, health and environment issues
		Required organic facility
Dry granulation	Eliminate heat and moisture	Dusty and slow process
		Not suitable for most compounds
		Low reproducibility
Direct compression	Eliminate heat and moisture	Limited to lower dose of active ingredients
	Simple and economical process	Potential of segregation
		Costly excipients
		Dusty

2.2.2 Materials in direct compression

Spray dried lactose is the first excipient designed for direct compression; it was introduced in the early sixties. Since then, many excipients have been introduced on the pharmaceutical market as directly compressible excipients. To function as directly compressible excipients, they need to comply with a number of requirements, such as high

flowability, high compressibility and high loading capacity (Bolhuis & Chowhan, 1996; Gohel & Jogani, 2005; Marwaha, Sandhu, & Marwaha, 2010).

Flowability

The directly compressible excipients should be free flowing to ensure the powder blend flow rapidly and homogenously for uniformed die filling, which in turn contributes to the uniformity of tablet weight and content. This is very important especially when using a high speed rotary tablet machine, the amount of powder blend transferred into die cavities should have reproducibility of ± 5% (Bolhuis & Chowhan, 1996; Gohel & Jogani, 2005).

High compressibility

High compressibility is required to ensure the compacted mass remain bonded after the release of compaction pressure. Compactibility of the excipient can be evaluated through the relationship between tablet crushing strength and the pressure load (Bolhuis & Chowhan, 1996; Gohel & Jogani, 2005).

Loading capacity

Loading capacity or dilution potential can be defined as the ability of the directly compressible excipient to retain its compression properties when being diluted with a poorly compressible active ingredient or material (Marwaha, Sandhu, & Marwaha, 2010). Most of the active ingredients are poorly compressible, therefore dilution potential of the excipient should be high to allow the final weight of tablets be minimised (Gohel & Jogani, 2005; Marwaha, Sandhu, & Marwaha, 2010).

Other properties required are good blending properties, low lubricant sensitivity, physically and chemically stable when in contact with moisture, air and heat, worldwide continuous availability, inert chemically, compatible with all the substances and have batch to batch reproducibility (Jivraj, Martini, & Thomson, 2000).

However, there is no single excipient that can fulfill all the requirements. Available direct compression excipients that are commonly used are microcrystalline cellulose (MCC), dicalcium phosphate dehydrate, α-lactose monohydrate and starch (Bolhuis & Chowhan, 1996; Hwang & Peck, 2001; Jivraj, Martini, & Thomson, 2000). Various types of these filler-binders exist with distinct differences in their particle properties, thus may affect the compression and tablet characteristics (Hwang & Peck, 2001). A combination of two or more filler-binders is preferable in order to obtain a mixture with desired properties (Bolhuis & Chowhan, 1996).

2.2.3 Modification of starch

Starch has a wide application in the production of pharmaceuticals due to its adhesive, thickening, gelling and swelling properties, as well as its immediate availability and low cost. It became a valuable ingredient in the pharmaceutical industry as fillers, binders and disintegrants in tablet formulation (Kunle *et al*., 2003; Odeku & Picker-Freyer, 2007; Riley, Wheatly, & Asemota, 2006). Native starches are generally attributed by poor flowability, high hygroscopicity and high lubricant sensitivity; therefore it can function only as excipient in wet granulation, (Bolhuis & Chowhan, 1996; Riley *et al.*, 2008). Besides that, generally native starches are not compressible, and when used in high concentrations it causes reduced tablet strength (Parmar & Rane, 2009). Native starches are

often subjected to modification either by chemical or physical means to enhance, specify and extend their applications (Reimerdes, 1993).

Chemical modification involves changing of the molecular structure of starch, namely amylose and amylopectin with the use of chemicals or enzymatic reaction in specific temperature, pH and concentration of starch and reagents used (Fang *et al.*, 2004; Rowe, Shekey, & Owen, 2006). Chemical modifications are widely implemented (Zavareze & Dias, 2011). However, they are relatively expensive, require toxicological data and are time consuming (Gohel & Jogani, 2005; Akram, Naqvi, & Gahugar, 2011).

Physical modification on the other hand relies on the application of shear force, compression force, physical blending or thermal treatment to produce starches with favourable physical properties (Breuninger, Piyachomkwan, & Sriroth, 2009). Physical modification has been gaining wider acceptance because no by-products of chemical reagents are present in the modified starch (Zavareze, & Dias, 2011), it is relatively simple and economical (Akram, Naqvi, & Gahugar, 2011; Gohel & Jogani, 2005), and the physical modified starches are considered natural materials with high safety (Jacobs & Delcour, 1998).

2.2.3.1 Chemical modifications

(i) Acid and enzymatic modification

Modification of starches by acid is the earliest method of starch modification (Tharanathan, 2005). Acid modified starches are prepared by reacting concentrated starch slurry with low concentration of a mineral acid, such as hydrochloric acid (HCl), sulfuric acid (H_2SO_4), or

oxalic acid ($C_2H_2O_4$) below the gelatinisation temperature of starch (Abdorreza *et al.,* 2012). When the desired conversion is reached, the acid is neutralised and the starch is recovered. This acid hydrolysis process is controlled by acid concentration, reaction time and temperature (Abdorreza *et al*., 2012). Effect of acid treatment on starch causes depolymerisation, with the modified acid starches exhibit higher solubility, lower viscosity (Abdorreza *et al*., 2012) and greater degree of crystallinity (Atichokudomchai & Varavinit, 2003; Shujun *et al.*, 2006)

Acidic modification of starch has been carried out by Atichokudomchai & Varavinit (2003). In their studies, tapioca starch was hydrolyzed by suspending in 6% of hydrochloric acid at room temperature for different suspending times without stirring. The resulting spray-dried modified starch powder showed an increase in crushing strength of tablets due to increase in crystallinity.

Hydrolysis of starch can also be done through an enzymatic reaction using α-amylase (Wang, Powell, & Oates, 1995). The reaction is specific; α-amylase only breaks the α-1,4 linkages present in starch (Aggarwal & Dollimore, 1998).The enzyme actions on starch granule caused partial hydrolysis and dissolution of amorphous regions of the starch leading to an increase in the degree of crystallinity; the modified starch produced is also known as microcrystalline starch (Apeji, Oyi, & Musa, 2011). Microcrystalline cassava starch was reported to have been evaluated for their physiochemical characteristics. A further study on their tableting properties revealed that both microcrystalline starches were applicable for direct compression excipients (Apeji, Oyi, & Musa, 2011; Shittu *et al.*, 2012).

(ii) Cross-linked modification

Cross-linking reaction involves replacement of hydrogen bonding between starch chains by chemical reagents, such as epichlohydrin, phosphorus oxychloride, metaphosphate, citric acids and adipic acid that leads to the formation of covalent bridge or intermolecular cross-linking of molecules (Tran, Piyachomkwan, & Sriroth, 2007; Tharanathan, 2005; Zou, Liu, & Eliasson, 2004).

Cross-linking treatment is a method to strengthen the starch granule, resulting resistance to high temperature, low pH, high shear and leads to increased stability of the swollen starch granule (Tharanathan, 2005). The cross-linked starches exhibit increased gelatinisation temperature and resistance to swelling. Increased degree of cross-linking leads to increased gelatinisation temperature and reduced swelling. Cross-linking starch is used as a polymeric base for controlled drug release and very highly cross-linking starches are useful as dusting powders for surgical gloves (Tharanathan, 2005; Visvarungroj & Remon, 1990).

(iii) Acetylation of starch

Acetylation is esterification of starch, where the hydroxyl groups in the α-D-glucopyranose units of starch are substituted by acetyl groups (Singh & Nath, 2012; Wilkins *et al.,* 2003). Acetylated starches provide lower gelatinisation temperature and higher peak viscosity. Degree of acetylation strongly determines the physicochemical properties of starch acetates. As the degree of acetylation increases, the starch acetate changes to more hydrophobic, therefore slowing the drug release rate (Korhonen *et al.* 2002). Investigation on the application of starch acetate revealed that it has a potential to be used as direct compression excipient (Korhonen *et al.* 2000). Acetylated potato starch

(Tuovinen, Peltonen, & Jarvinen, 2003) and acetylated sago starch (Singh & Nath, 2012) were reported to be useful as a carrier for drug control delivery.

(iv) Carboxymethylation of starch

Carboxymethyl starch is prepared by a reaction of starch and sodium monochloroacetate in the alkaline environment of sodium hydroxide. The hydroxyl groups of starch molecules are substituted by sodium monochloroacetate to produce carboxymethyl starch. The carboxymethyl starch possesses properties of lower gelatinisation temperature and able to swell in cold water (Nattalpulwat, Purkkao, & Suwitayaphan, 2009; Noor Fadzlina, Karim, & Teng, 2005). The higher the degree of substitution, the more the carboxylated starch is soluble in water (Noor Fadzlina, Karim, & Teng, 2005). Carboxymethylated starch is classified as superdisintegrant and is an official excipient with the name sodium starch glycolate (BP 2007; Kibbe, 2000; USP 27; USP 30). In the tablet formulations, sodium starch glycolate is widely used as a disintegrant in tablets prepared either by direct compression or wet granulation processes (Kibbe, 2000). Sodium starch glycolate is also found to be extensively used as excipient in orally fast disintegrating tablets (Fu *et al.*, 2004; Singh *et al.*, 2011; Thakur & Kashi, 2011). A number of researchers have synthesised carboxymethyl starch from different botanical resources. Nattalpulwat, Purkkao, & Suwitayaphan (2009) reported that carboxymethylated yam starch can be used as an excellent tablet disintegrant in low concentration, and another group of researchers, Singh *et al.* (2011) found that carboxymethylated sago starch performances are comparable to official superdisintegrant i.e. sodium starch glycolate.

2.2.3.2 Physical modifications

(i) Spray drying

Spray drying is a process involving spraying of solution or suspension in the form of droplets through atomiser into a hot drying chamber, resulting evaporation of the moisture and recovery of the dried product from the air. The products are porous, spherical agglomorates uniform in shape and size (Bolhuis & Chowhan, 1996). Spray dried rice starch product was introduced as a direct compression excipient in 1992 by Erawan Pharmaceutical Research and Laboratory Co. Ltd., Bangkok, Thailand with the commercial name Era-Tab® or Primotab®. It has excellent flow and binding properties. In tablet formulations prepared by direct compression, spray dried rice starch can be used as a single excipient or in combination with other excipients. Combination with microcrystalline cellulose should be avoided, because of the poor flowability of the blends and slow disintegration of tablets produced (Bos *et al.,* 1992). A study by Mitrevej, Sinchaipanid, & Faroongsarng (1996) on the comparative evaluation of direct compression filler, spray dried rice starch was reported to be more flowable, compressible, less lubricant sensitivity and higher dilution potential/loading capacity than pregelatinised starch. Evaluation of the compact material made with Era-Tab® showed a higher crushing strength and a lower friability than pregelatinised starch (Hsu *et al*., 1997). However, all spray dried directly compressible excipients showed poor reworkability, since the original spherical shape of the excipient is lost upon tableting (Gohel & Jogani, 2005).

(ii) Co-process modification

Co-process is combining two or more established excipients with the aim to obtain a product with functionality improvements and masking undesirable properties of individual excipient (Gohel & Jogani, 2005; Marwaha, Sandhu, & Marwaha, 2010). Co-processed

directly compressible excipients are simple physical mixture of two or more excipients, prepared by wet granulation (Akram, Naqvi, & Gauhar, 2011), or by dispersing or dissolving the excipients followed by co-drying such as drum drying and spray drying (Gonnissen, Remon, & Vervait, 2007; Marwaha, Sandhu, & Marwaha, 2010; Patel & Bhavsar; 2009).

Starlac® (Roquette) is an example of commercially available co-processed directly compressible excipient involving starch. It is composed of 85% α-lactose and 15% native corn starch; the excipients show characteristics of good flow and low lubricant sensitivity (Marwaha, Sandhu & Marwaha, 2010). A directly compressible co-processed microgranules comprising of lactose (7 parts), microcrystal cellulose (2 parts) and corn starch (1 part) was developed by Akram, Naqvi, & Gauhar (2011). The co-processed micro granules were spherical, excellent flow, high compressibility and better binding properties. They recommended it as a new co-processed directly compressible excipient. Another group of researchers, Shankar *et al.* (2012) produced a co-processed excipient consisting of pregelatinised potato starch (7.5 parts) and microcrystalline cellulose (2.5 parts). It exhibited high swelling (400%) and excellent flow properties. As blends with poor flow selected drugs, it showed good to excellent properties. Tablets of sulphamethoxazole, paracetamol and aceclofenac prepared by direct compression method employing the said co-processed excipient were of good physical qualities and complied with official requirements for dissolution rate. The study concluded that a co-processed excipient consisting of pregelatinised potato starch (7.5 parts) and microcrystalline cellulose (2.5 parts) was found to be promising for directly compressible tablet excipients.

2.3 Pregelatinised starch

Pregelatinisation is the simplest of all starch modifications (Tharanathan, 2005). The processes are economical and environmentally friendly (Jayakody *et al.*, 2009), producing a nontoxic and nonirritant excipient (Kibbe, 2000). Pregelatinised starches are prepared by subjecting aqueous starch slurry to heat to rupture all or part of the starch granules and subsequently dried, rendering the starch flowable and compressible (Adedokun & Itiola, 2010; Bolhuis & Chowhan, 1996; Kibbe, 2000; Odeku, Schmid, & Picker-Freyer, 2008). These processes are required to control the starch-to-moisture ratio, temperature and heating time (Zavareze & Dias, 2011). Starch granules are insoluble in cold water. When starch is heated, the granules absorb water and swelling. At higher temperature or continuous heating, starch granules swell to a greater extent and crystallites melt causing the leaching of amylose from the granules. These phenomena are known as gelatinisation, where the aqueous starch slurry is changed into gel or paste-like mass (Fourmann, Carrot, & Mignard, 2003; Jacobs & Delcour, 1998; Loisel *et al.*, 2006; Ratnayake & Jacson, 2006). It was reported that swelling is the primary property of amylopectin (Ratnayake & Jacson, 2006).

Pregelatinised starches are available as a fully or partially pregelatinised form (Kibbe, 2000; Parmar & Rane, 2009). Fully pregelatinised starches are used as binders in wet granulation formulations (Colorcon, 2009), swelling rapidly and soluble in cold water to form strong binding properties (Heinze, 2003; Parmar & Rane, 2009). However, fully pregelatinised starches lose their disintegrant properties much due to gelatinisation (Colorcon, 2009). Therefore addition of separate disintegrants in the formulations are required (Parmar & Rane, 2009).

Partially pregelatinised starches are pregelatinised starches designed specifically for direct compression and are also known as compressible starches (Bolhuis & Chowhan, 1996; Kibbe, 2000). Partially pregelatinised starches consist of native and fully pregelatinised starches, making them useful as a binding agent and a disintegrant in the wet granulation and direct compression formulations (Colorcon, 2009; Parmar & Rane, 2009). Partially pregelatinised starches exhibit good flow and compressible, therefore able to form bonding in direct compression (Gohel & Jogani, 2005). They also showed increasing solubility in cold water, self-lubrication and multifunctionality (act as binders and disintegrants at the same time). In the tablet formulations, partially pregelatinised starches can be incorporated up to 75% in wet granulation process and up to 50% in direct compression process. It was noted that different suppliers provide different degree of gelatinisation, which is a key factor to product performances (Parmar & Rane, 2009). Chemically, compressible starch does not differ from starch (USP 30/NF25).

Pregelatinised starch is an official excipient in the pharmacopoeias. According to the BP 2007, pregelatinised starch is prepared from maize starch, potato starch or rice starch by mechanical processing in the presence of water, with or without heat, to rupture all or part of the starch granules and subsequent drying. It contains no added substances but it may be modified to render it compressible and to improve its flow characteristics.

According to USP 30/ NF25, pregelatinised starch is starch that has been chemically and/or mechanically processed to rupture all or part of the starch granules in the presence of water and subsequently dried. Some type of pregelatinised starch may be modified to render them compressible and flowable in character.

Pregelatinised corn starch has been developed successfully as a commercial excipient with the brand names Uni-pure® DW (National Starch & Chemical Co., USA), Uni-pure® LD (National Starch & Chemical Co., USA), Starch® 1500 (Colorcon Inc., USA) and Spress® B820 (Grain Processing Corp., USA). These excipients are compressible and widely used as a direct compression material in tablet formulations (Zhang, Law & Chakrabarti, 2003). Therefore, pregelatinised sago starch may show similar functions. However, due to variation in ratio of amylose and amylopectin among starches, difference in properties can be expected.

Starch 1500® is also known as compressible starch that was specifically designed for direct compression excipients (Bolhuis & Chowhan, 1996). It is partially pregelatinised corn starch, which is more compressible and flowable than its native form (Gohel & Jogani, 2005). During manufacturing, some of the hydrogen bonding between amylose and amylopectin in the corn starch are ruptured, resulting in the pregelatinised starch to consist of native and fully pregelatinised corn starch (Jivraj, Martini & Thomson, 2000). Starch 1500® has properties of fair binding and dilution capacity, good disintegration and self-lubricating. It needs a high pressure to produce tablets and shows high lubricant sensitivity (Gohel & Jogani, 2005). It also shows extreme softening effect when being mixed with alkaline stearate lubricant, such as magnesium stearate. Therefore, the usage of such lubricant should be avoided or kept lower below 0.5%. Because of that, stearic acid is a preferred lubricant to pregelatinised starch (Jivraj, Martini, & Thomson, 2000).

Starch 1500® is a multifunction excipient; as binder, disintegrant, filler, flow-aid and self-lubricant properties. Versatile, it is effective in various processing methods for manufacturing tablets such as direct compression, dry granulation or wet granulation. It is

also effective with moisture and low drug dosage; therefore it enhances the functionality of other common excipients in the formulations. Possessing self-lubricating properties, it reduces the need of high levels of lubricants, improving mechanical strength of tablets and dissolution rate. However, it readily thickens or gels in cold water (unlike native starch), making the properties unsuitable for reconstituted products. It also has its disadvantages; with moisture content of about 13 – 14% (the USP requirements), tablet formulations containing Starch 1500® tend to stick on the dies when the bulk of powder is compressed. Starch 1500® is prepared by physical modification, resulting in combined benefits of soluble and insoluble functionality such as partial solubility, increased particle size, improve flow properties and compressibility. Starch 1500® has a mixture of properties of both native and fully gelatinised starches, making it useful as both a binder and disintegration in wet granulated formulations.

Alebiou & Itiola (2002) evaluated the compressional characteristics of native and fully pregelatinised forms of sorghum, plantain and corn starches and the mechanical properties of their tablets. The study showed that pregelatinisation increases swelling and water retention capacity. Pregelatinisation also increases densification of the starches during die filling at low pressure and facilitates a faster onset of plastic deformation of the starches, but appears to reduce the amount of plastic deformation during compression process. For mechanical properties, pregelatinisation resulted in lower tensile strength and brittle fracture index of the starch tablets.

Odeku, Schmid, & Picker-Freyer (2008) have investigated material and tablet formation properties of pregelatinised forms of four tropical *Dioscorea* species: *Dioscorea rotunda, Dioscorea dumetorum, Dioscorea oppositifolia* and *Dioscorea alata*. *Dioscorea* starches

were fully pregelatinised followed by either oven drying or freeze drying and used as excipient in direct compression. Evaluation on tablet formation properties revealed that pregelatinisation improved flowability and compressibility of *Dioscorea* starches, with freeze dried pregelatinised *Dioscorea* starches showing higher compactibility. It was reported that the freeze dried pregelatinised forms of *Dioscorea dumetorum* and *Dioscorea oppositifolia* starches produced non-disintegrating tablets, indicating to have potential as excipients for controled drug delivery. Odeku & Picker-Freyer (2010) then investigated the freeze dried pregelatinised forms of *Dioscorea dumetorum* and *Dioscorea oppositifolia* starches as directly compressible excipients for sustained release using diclofenac sodium and caffeine as the model drugs. The results obtained showed that the amount of drug release from the matrices, the release rate and mechanism of release were dependent on the *Dioscorea* starch used and the concentration of drug present in the matrix tablets. Thus freeze dried pregelatinised forms of *Dioscorea dumetorum* and *Dioscorea oppositifolia* starches could find application as excipients for controlled drug delivery.

Adedokun & Itiola (2010) comparatively studied material properties and compaction characteristics of natural and fully pregelatinised forms of white trifoliate yam, yellow trifoliate yam, rice and corn starches. Pregelatinisation increased swelling power and solubility as well as flowability as indicated by lower Hausner's ratio. Fully pregelatinised starches exhibited more densification than natural starches during compression and produce tablets with lower tensile strength and brittle fracture index. In their following study, it was found that pregelatinised starches produced better combined disintegrant (endo-exo-disintegrants) properties than natural starches in paracetamol tablets prepared by wet granulation. However, all the tablets produced passed the official disintegration time test (Adedokun & Itiola, 2011).

CHAPTER 3

EXPERIMENTAL

3.1 Materials

A local sago starch (Food grade, Nee Seng Ngeng & Sons Sago Industries Sdn Bhd), pure amylose (02522HC, Sigma-Aldrich, USA) and amylopectin from potato (GA15140, Fluka Chemie GMBH, UK), four batches of pregelatinised sago starch prepared (PS1, PS2, PS3 and PS4), Spress® B820 (pregelatinized corn starch, lot S0615476, GPC, Muscatine, Iowa), Avicel® PH101 (lot 11363, Fluka, Ireland), Paracetamol (BP grade supplied by Euro Chemo-Pharma Sdn. Bhd.), magnesium stearate (Peter Greven, Nederland C.V.), sodium starch glycolate (BP grade supplied by Euro Chemo-Pharma Sdn. Bhd.).

3.2 Equipment

Drying oven (FD115, Binder, Germany), digital overhead stirrer (WiseStir$_{TM}$ HD-30D, Daihan Scientific Co., Seoul, Korea), analytical sieve shaker (Retsch GmbH, Haan, Germany), halogen moisture analyzer (HR73, Mettler Toledo, Switzerland), laboratory mill (MX-895M, National), advance X-Ray Diffractometer (D8, Bruker AXS, Germany), FT-IR spectrophotometer (IFS66v/S, Germany), solid state NMR (Broker AV 400 WB, Germany), Differential Scanning Calorimeter (DSC 822^{e}, Mettler Toledo, Switzerland), scanning electron microscope (XL-30 ESEM, Philips, Eindhoven, Holland), light microscope (Nikon Eclipse 80i, Nikon Instruments Inc., Japan), tapped density tester (JV2000, Dr.Schleuninger Pharmaton AG, Solothurn, Germany), helium pycnometer (AccuPyc II 1340, Micromeritics, Norcross, USA), semi-automated granule and powder flow tester (BEP-Auto, Dr.Schleuniger Pharmaton, Nottingham, UK), cube mixer (Type KB 15/UG, Hensenstamm, Germany), motor drive (Type AR401, ERWEKA,

Hensenstamm, Germany), single punch compaction machine (MTCM-1, Globepharma Inc, New Brunswick, NJ), tablet hardness tester (Version 4.5, 6D, Dr. Schleuniger Pharmaton, USA), friability tester (TAR10, ERWEKA, Germany) , disintegration tester (ZT41, ERWEKA, Germany), dissolution tester (DA-60, ERWEKA), Climacell (MMM, Medcenter Einrichtungen GmbH, Munich, Germany).

3.3 Methods

3.3.1 Pharmacopoeial characterisation of sago starch

Sago starch was characterised according to the starch monograph in the United States Pharmacopoeia 27 (USP 27) as below:

3.3.1.1 Identification

A smooth mixture of sago starch (1 g) was prepared and stirred into 15 ml of boiling water for 2 minutes. The product was cooled and 3 drops of iodine test standard was added.

3.3.1.2 pH test

Aqueous dispersion of sago starch at 20% w/v was prepared and agitated continuously at a moderate rate for 5 minutes; pH of the dispersion was immediately measured using a pH meter.

3.3.1.3 Residue on ignition

Sago starch (2 g) was heated to char, cooled and moistened with 2.0 M sulfuric acid. It was gently reheated until no white fumes were released and then be ignited at 800 ± 25^{o}C

for 30 minutes. The cooled residue was weighed and the percentage of residue was calculated.

3.3.1.4 Iron

The residue was dissolved in 8 ml of hydrochloric acid and diluted with water to 100 ml. The solution (25 ml) was justified with water to 47 ml. Ammonium peroxydisulfate (25 mg) and 30% w/v of ammonium thiocynate solution (5 ml) was then added. The colour of the solution must not be darker than that of the standard solution.

3.3.1.5 Oxidizing substances

Aqueous dispersion of sago starch at 2% w/v was prepared and swirled for 5 minutes. The clear supernatant (30 ml) was transferred to a conical flask. Glacial acetic acid (1 ml) and potassium iodide (1 g) were added. The mixture was swirled and allowed to stand for 25 to 30 minutes in the dark area. Starch test standard (1 ml) was then added. The mixture was titrated with 0.002 M sodium thiosulphate to the disappearance of the starch-iodine colour. A blank determination was performed and any necessary correction was made.

3.3.1.6 Sulphur dioxide

Aqueous dispersion of sago starch (10% w/v) was prepared and filtered. The clear filtrate (100 ml) was added with starch test standard (3 ml) and titrated with 0.01M iodine until the first permanent blue colour was formed.

3.3.1.7 Loss on drying

Sago starch (1 g) was dried in the oven at temperature 100 – 105 ^{o}C for 4 hours. The percentage loss in weight was calculated as loss on drying.

3.3.1.8 Microbial limit test

Sago starch was tested for the absence of *Salmonella sp* and *Escherichia coli*. The starch was cultured in agar medium and incubated at room temperature for 12 to 24 hours.

3.3.2 Determination of chemical compositions

3.3.2.1 Amylose and amylopectin

Amylose content was determined using iodine-amylose complex principle (Farhat, Oguntona, & Neale, 1999). A quantity of sago starch (100 mg) was placed into a 100 ml volumetric flask and heated with 1 ml of 99% ethanol and 9 ml 1 M sodium hydroxide in the water bath at 95°C for 30 minutes. The starch solution was allowed to cool and its volume was made up to 100 ml using distilled water. A portion of the starch solution (5 ml) was transferred into a 50 ml volumetric flask and added with 25 ml of distilled water, 0.5 ml of 1 M acetic acid and 1 ml iodine solution. The solution was shaken and left to stand for 20 minutes. The absorbance of the solution was then measured by a spectrophotometer at 620 nm. The measurements were done in triplicate. Potato amylose and amylopectin were used as the standard. Table 3.1 shows the standard curve to determine the amylose content.

Table 3.1: Standard curve for determination of amylose content.

Concentrations of amylose (% w/v)	Amount of amylose (mg)	Amount of amylopectin (mg)
0	0	100
10	10	90
20	20	80
30	30	70
40	40	60
50	50	50

3.3.2.2 Lipid

Dried sago starch (2 g) was extracted with hexane using soxhlet apparatus for 4 hours. The solvent was vaporised by means of Buchi Rotary Evaporator System under vacuum at 335 mbar, boiling at 40˚C for 30 minutes. The lipid content was then calculated by the difference between the weight of flask and extracted fat with the weight of empty flask. The analysis was conducted in triplicate (AOAC, 2005).

3.3.2.3 Protein

Protein content in sago starch was determined according to the USP 30. Aqueous dispersion of sago starch (0.1%) was prepared. The dispersion was subjected to centrifugation at 9000 rpm for 15 minutes. The absorbance was measured at 280 nm against a blank reagent. The concentration of protein in the sample was determined by the albumin calibration curve. The measurements were done in triplicate.

3.3.3 Preparation of pregelatinised sago starches

Aqueous slurry of 20% w/v sago starch was heated in the water bath (Grant SUB 36, England) at 65°C while stirring at 700 RPM (WiseStir$_{TM}$ HD-30D, Daihan Scientific Co., Seoul, Korea) for 15 minutes. The resulting paste of sago starch was dried in the oven WTB Binder (Geprcifte Sicherheit, Germany) at 40°C for 48 hours. The dried mass was powdered in a laboratory mill. All the starches were passed through a sieve (180 μm aperture) and stored in a tightly-sealed white container before used. Another three batches were prepared with different heating times of 30, 45 and 60 minutes respectively. The four batches of pregelatinised sago starch (PS) prepared are shown in Table 3.2. The method was modified from Adedokun & Itiola (2010) and Odeku, Schmid, & Picker-Freyer (2008).

Table 3.2: Preparation of pregelatinised sago starch (PS) using 20% w/v aqueous slurry of sago starch.

Batch	Heating time
PS1	15 minutes
PS2	30 minutes
PS3	45 minutes
PS4	60 minutes

3.3.4 Powder Characterisations

3.3.4.1 Amylose content determination

The procedure to determine amylose content of pregelatinised sago starches (PS1, PS2, PS3, and PS4) was in the same manner as 3.3.2.1.

3.3.4.2 FT-IR Spectroscopy

FT-IR spectra were obtained on FT-IR spectrophotometer (Model: IFS66v/S) using KBr disc containing 1% sample. The disc was scanned over a wave number range 4000-400 cm^{-1} interval with a 4 cm^{-1} resolution.

3.3.4.3 NMR Spectroscopy

The NMR spectra of the starches were recorded at room temperature on a Broker AV400 solid state NMR at frequency of 100.6 MHz for ^{13}C analyses. ^{13}C NMR spectra were observed under cross polarisation magic angle sample spinning (CPMAS) with spinning rate at 7 kHz. The chemical shift was determined using tetramethylsilane TMS (0 ppm) as an internal standard.

3.3.4.4 X-ray diffraction (XRD)

The X-ray diffraction patterns of the starches were recorded using a D8 Advance X-Ray Diffractometer- Bruker AXS (Germany) with CuK_{α} monochromatised radiation, running at 40 kV and 40 mA at ambient temperature. The scanning region of the diffraction angle 2θ was from 2° to 40° with step interval of 0.02 and scanning rate of 2°/min. The total run time was 60 minutes. Degree of crystallinity of the starches was calculated using X-ray diffraction height method (Terinte, Ibbett, & Schuster, 2011) as written below:

$$C = 100 \times \frac{(I_{cr} - I_{non-cr})}{I_{cr}} \qquad (3.1)$$

where, C expresses the apparent crystallinity (%), I_{cr} indicates the maximum intensity of the peak of the crystalline starch and $I_{non\text{-}cr}$ is the maximum intensity of the peak of amorphous starch i.e located in the valley between the peaks. Figure 3.1 shows an example on how the degree of crystallinity was calculated based on the height of the peak in XRD.

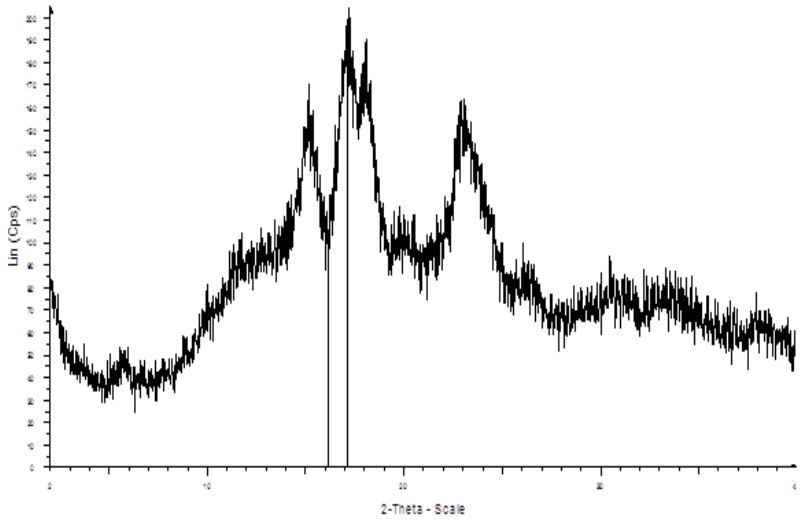

Figure 3.1: An example for the determination of the degree of crystallinity in a starch sample using XRD height method.

A second method to obtain the degree of crystallinity of the starches is by calculating the area of crystallinity in the X-Ray diffractogram obtained, using the following formula (Nuwamanya *et al.*, 2010):

$$\text{Area} = \frac{A_c}{A_c + A_m} \qquad (3.2)$$

where, the area expresses the apparent crystallinity (%), A_c indicates the area of crystallinity of the peak and A_m is the area of the amorphous region in the starch. Figure 3.2 shows an example on the determination of the degree of crystallinity based on the area under the peaks in the XRD.

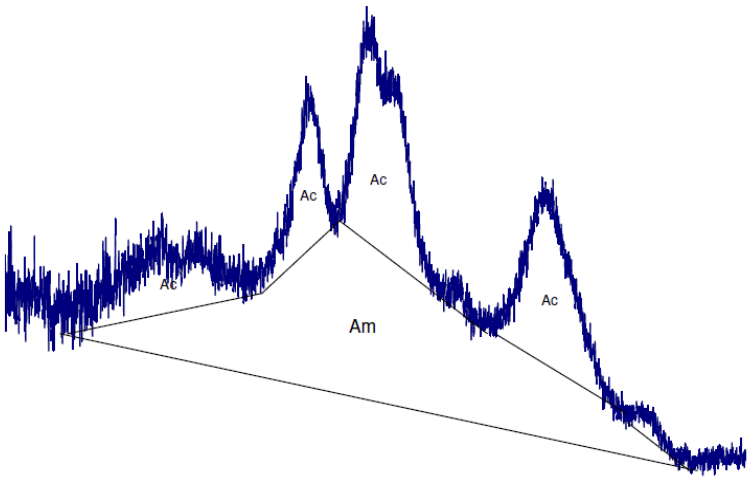

Figure 3.2: An example for the determination of the degree of crystallinity in a starch sample using the XRD area method (Nuwamanya *et al.*, 2010).

The height and area were calculated using OriginLab's OriginPro version 8.5.1 software.

3.3.4.5 Differential Scanning Calorimetry (DSC)

Thermal characteristics of the starches were analysed using a Differential Scanning Calorimeter (Mettler Toledo, DSC 822^{e}). The DSC was calibrated with indium and an empty aluminium pan was used as a reference. Starch dispersions with a dry starch to water ratio of 1:2 were prepared. Each of the starch dispersion was transferred into an aluminium pan and hermetically sealed. The dispersions were equilibrated at room temperature for 24 hours. The aluminium pan was then put in the DSC cell and heated from 40 to 120°C at 5°C/min. The onset (T_o), peak (T_p) and conclusion (T_c) temperatures and the melting enthalpy (ΔH) in J/g of dry starch were recorded. All reported values were the mean of triplicate measurements (Atichokudomchai & Varavinit, 2002). Degree of gelatinisation (DG) of the starch was determined by the following formula (Baks *et al.*, 2007; Marshall *et al.*, 1993):

$$DG = 1 - \frac{\Delta Hp}{\Delta Hn} \qquad (3.3)$$

where ΔH_p is the enthalpy of pregelatinised sago starch and ΔH_n is the enthalpy of native sago starch.

3.3.4.6 Scanning Electron Microscopy

Powder samples were mounted on stub and coated with gold, their three dimensional images were taken from Scanning Electron Microscopy (FEI Quanta 200 FESEM) at an accelerating voltage from 10 to 12.5 kV (Odeku, Schmid, & Picker-Freyer, 2008).

3.3.4.7 Viscosity

Viscosity for all powders (2% w/v) were determined by Brookfield viscometer (Brookfield Eng. Labs Inc) using a spindle no.1 with rotation speed of 100 rpm at 25°C. The reading of viscosity was recorded after 60 seconds of the spindle rotation. (Brookfield Dial Viscometer Operating Instruction, n.d).

3.3.4.8 Swelling power (SP) and water solubility index (WSI)

Swelling power and water solubility index were determined in triplicate. Dispersion of the powder sample (2% w/v) was prepared in centrifuge tube. The tube was heated at 25^0C, 37^0C, 45^0C, 55^0C, 65^0C, 75^0C and 85^0C for 30 minutes in a water bath (Grant Sub-36, Grantz Instrument, Royston, England) with controlled shaking at interval of 5 and 10 minutes. The tubes were cooled to room temperature and centrifuged (Universal 32, Hettich Zentrifugen, Germany) at 8000 rpm for 15 minutes. The supernatant was carefully poured out and the wet sediment was weighed, W_w. The wet sediment was then dried in the oven at

60^0C for 120 hours and weighed, W_d. SP and WSI were calculated as below (modified from Li & Yeh, 2001):

$$\text{SP (g/g)} = \frac{W_w}{W_d} \quad (3.4)$$

$$\text{WSI (\%)} = 100 \times \left(1 - \frac{W_d}{W_0}\right) \quad (3.5)$$

3.3.4.9 Particle size distribution

Particle size distribution was determined by light microscope (Nikon Eclipse 80i, Nikon Instruments Inc., Japan). Diameter of 300 particles projected was measured horizontally. Mean projected diameter and particle size distribution were reported.

3.3.4.10 Loss on drying

The procedures employed to determine loss on drying of each of the powder sample was in the same manner as 3.3.1.7.

3.3.4.11 Porosity

The total porosity (ε) of a powder was calculated from the different value of true density ρ_T and bulk density ρ_0 divided by true density ρ_T. Average was obtained from the five calculated values.

$$\varepsilon \text{ (total)} = \left(1 - \frac{\rho_0}{\rho_T}\right) \times 100\% \quad (3.6)$$

3.3.4.12 Densities

The bulk (ρ_0) and tapped densities (ρ_t) of the powders were determined using tapped density tester (JV2000, Dr. Schleuninger Pharmaton AG, Solothurn, Germany). A 250 ml

glass cylinder was filled with 100 g of powder sample and placed on top of the tapped density tester and bulk volume was recorded. The cylinder was then tapped 1000 times to a constant volume and the tap volume was recorded. Bulk and tapped densities were calculated based on the ratio of weight to volume. The procedure was done in triplicate. Mean and standard deviation were reported (modified from Apeji, Oyi, & Musa, 2011; Picker & Brink, 2006; Shah, Tawakkul, & Khan, 2008). True density (ρ_T) of the materials was determined by a Helium Pycnometer (AccuPyc 1330, Micromeritics, USA) (Kibbe, 2000). The powder sample was weighed and loaded into the sample cell. True volume was obtained by calculating the difference in helium pressure before and after loading sample. Each sample was tested in triplicate (Cao *et al.*, 2008; Zhang, Law, & Chakrabarti, 2003).

3.3.4.13 Powder flowability

(i) Carr's Compressibility Index and Hausner ratio

Carr's Compressibility Index and Hausner ratio were calculated from the data of bulk density (ρ_0) and tapped density (ρ_t). The following formulas were used (Shah, Tawakkul, & Khan, 2008; Staniforth, 2002):

$$\text{Carr's Compressibility Index, CI} = \left(1 - \frac{\rho_0}{\rho_t}\right) \times 100\% \qquad (3.7)$$

$$\text{Hausner ratio, HR} = \frac{\rho_t}{\rho_0} \qquad (3.8)$$

(ii) Angle of repose

Angle of repose was determined by fixed height cone method. The height (Y) and the diameter (X) of the pile of the powder formed from the experiment of flow rate determinations were measured. The angle of repose, α (°) was calculated according to the formula below.

$$\text{Angle of repose, } \tan \alpha = \frac{2Y}{X} \qquad (3.9)$$

The measurements were in triplicate (Shah, Tawakkul, & Khan, 2008; Staniforth, 2002)

(iii) Flow rate

The flow rate was determined using a steel funnel semi-automated flowability tester (BEP-Auto, Dr. Schleuniger Pharmaton, Nottingham, UK) with an orifice of 15 mm. A quantity of sample powder (100 mg) was filled into the steel funnel. Time required for the sample powder to completely discharge from the funnel was recorded. The determinations were done in triplicate (modified from BP 2007; Shah, Tawakkul, & Khan, 2008).

3.3.5 Compression and mechanical properties of powders in compact form

3.3.5.1 Preparation of compacts

Enerpac GA3 Single Punch Machine (Globe Pharma, New Brunswick) equipped with a set of round flat-faced stainless steel tooling with diameter 8.00 mm was used in the preparation of compacts. Prior to the compression, suspension of magnesium stearate in alcohol 95% was used to lubricate the punch faces and the die wall. Ten different compression pressures (from 20 to 200 MPa) were used to prepare the compacts from each material. Sample of powder (300 ± 3mg) was loaded manually into the die and the determined compression pressure was applied for 3 seconds. The process was repeated three times for each level of compression pressure. The compact weight, dimensions (diameter and thickness) and hardness were measured after storage for 24 hours (adopted from Busignies *et al.*, 2006; Kibbe, 2000; Narayan & Hancock, 2003; Sonnergaard, 1999; Sonnergaard, 2000; Sun, 2006; Zhang, Law, & Chakrabarti, 2003). This data was used to

calculate relative density, porosity and degree of volume reduction using the formula below:

$$D = \frac{\rho_A}{\rho_T} \quad (3.10)$$

$$\varepsilon = 1 - D \quad (3.11)$$

$$C = 1 - \frac{\rho_0}{\rho_A} \quad (3.12)$$

Where D is the relative density of a powder compact at pressure P, ρ_A is the apparent density of a powder compact at pressure P, ρ_T is the true density of a powder, ε is the porosity a powder compact at pressure P, C is the degree of volume reduction of a powder compact at pressure P and ρ_0 is the bulk density of a powder.

3.3.5.2 Analysis of compression properties

Compression properties of the powder compacts were analysed according to the Heckel and the Kawakita equations (Equations 3.13 & 3.14) (Zhang, Law, & Chakrabarti, 2003).

$$\ln\left(\frac{1}{[1-D]}\right) = kP + A \quad (3.13)$$

$$\frac{P}{C} = \frac{P}{a} + \frac{1}{ab} \quad (3.14)$$

The Heckel equation is widely used to relate relative density, D, of the powder bed under compression at applied compression pressure, P. Heckel plots of ln (1 / [1 - D]) versus P was established. The slope of the linear plot indicated the value of constant k, whereas the intercept of the plot give the value of constant A. The constant k reflects the deformation of particle under compression and the reciprocal of constant k is known as mean yield pressure, P_y, of the powder. The constant A is related to the particle rearrangement and die

filling before deformation and bonding of the discrete particles. The constant A obtained was used to calculate the relative density, D_a, using the formula below:

$$D_a = 1 - e^{-A} \qquad (3.15)$$

The relative density at zero compression pressure, D_0, is related to the initial rearrangement phase as a result of die filling, while the relative density, D_b, describes the rearrangement phase at low pressure and can be calculated from the formula below;

$$D_b = D_a - D_0 \qquad (3.16)$$

The Kawakita equation is used to study the relationship between volume reduction of a powder and the pressure applied. The constant a and b can be determined by constructing a plot of P / C versus P. Constant a is indicative of total volume reduction of the powder bed, while the constant b is indicative of plasticity of the powder and its reciprocal value, P_k, is related to yield strength of the particles.

3.3.5.3 Analysis of mechanical properties

Mechanical properties of powder compacts were evaluated by calculating the tensile strength using the formula below:

$$T = \frac{2F}{\pi dt} \qquad (3.17)$$

where, T is tensile strength of the compact, F is force required to fracture the compact, d is diameter of the compact and t is thickness of the compact. The use of tensile strength in the evaluations was to allow dimension of compacts to be taken into consideration. All measurements were done in triplicate.

3.3.6 Lubricant sensitivity

Magnesium stearate that was previously pre-sieved through 25 μm was added to each of the sample powder at concentrations of 0%, 0.25%, 0.5%, 0.75% and 1% and mixed in a cube mixer (Type KB 15/UG, Hensenstamm, Germany) attached to a motor drive (Type AR401, ERWEKA, Hensenstamm, Germany) for 5 minutes at 200 rpm. The mixture was compressed into compacts (300 mg) using single punch compaction machine (MTCM-1, Globepharma Inc, New Brunswick, NJ) and die/punch set of 8.33 mm size at different compression pressure, ranging from 20 to 120 MPa. The process was repeated three times for each level of compression pressure. Compacts were stored for 24 hours post compression. The compact's hardness, dimension (diameter and thickness) was determined. Plot of compact hardness, H versus compression applied, P was made for all sample powder. The lubricant sensitivity ratio, LSR for each sample powder was then calculated using the formula below (modified from Almaya & Aburub, 2008; Busignies *et al.*, 2006):

$$\text{LSR (\%)} = \frac{(H_0 - H)}{H_0} \times 100\% \qquad (3.18)$$

where H_0 is compact hardness without lubricant, and H is compact hardness with lubricant at highest compression pressure applied.

3.3.7 Loading capacity

Paracetamol is poorly compressible, thus it is suitable to be used as a model drug for loading capacity test (Bolhuis & Chowhan, 1996; Gonnissen, Remon, & Vervaet, 2007; Govedarica *et al.*, 2011). Paracetamol powder was added to the sample powder at concentrations of 0 %, 10 %, 20 %, 30 %, 40 %, 50 %, 60% and 70% and mixed in a cube mixer (Type KB 15/UG, Hensenstamm, Germany) attached to a motor drive (Type AR401, ERWEKA, Hensenstamm, Germany) for 5 minutes at 200 rpm. The mixture was

compressed into compacts (300 mg) using single punch compaction machine (MTCM-1, Globepharma Inc, New Brunswick, NJ) and die/punch set of 8.33 mm size at different compression pressure, ranging from 20 to 120 MPa. The process was repeated three times for each level of compression pressure. Compacts were stored for 24 hours post compression. Compact's hardness and dimension (diameter and thickness) was determined and the compact's tensile strength was calculated. Accordingly, a plot of compact tensile strength versus compression applied was made for all powder mixture and the area under plotted curves (AUC) was calculated using trapezoidal method. Area ratio was determined by dividing the AUC of the powder mixture and the AUC pure powder sample. Plot of area ratio versus the percentage (%) of paracetamol in the mixture was constructed for each of the powder sample. Linear regression and back extrapolation to zero area ratios gave the values of dilution potential (adopted from Busignies *et al.*, 2006; Habib *et al.*, 1996).

3.3.8 Formulation and evaluation of Paracetamol tablets containing selected pregelatinised sago starch

3.3.8.1 Preparation of tablets

The effectiveness of selected pregelatinised sago starch as a directly compressible material in the tablet formulations was evaluated and compared with Avicel PH 101 and Spress® B820. Paracetamol was used as a model drug while sodium starch glycolate and magnesium stearate were used as disintegrant enhancer and lubricant, respectively. Paracetamol tablets were formulated as tabulated in Table 3.3 and prepared by direct compression method. All ingredients (except magnesium stearate) were mixed with paracetamol for 10 minutes in the cube mixer at 200 rpm. Magnesium stearate was then added and mixed for another 3 minutes. The powder mixtures were compressed into tablets using single punch compaction machine (MTCM-1, Globepharma Inc., New Brunswick,

NJ) and die/punch set of 10.00 mm size at predetermined compression pressure, to obtain tablets with the same degree of hardness (90 – 110 N). The tablets produced were stored in a desiccator for 24 hours prior further evaluations (Hsu *et. al.*, 1997).

Table 3.3: Paracetamol tablet formulations

Ingredient (mg)	**Formulation**				
	1	**2**	**3**	**4**	**5**
Paracetamol	120.0	120.0	120.0	120.0	120.0
Avicel PH 101	229.1			70.0	70.0
Spress® B820		229.1		145.1	
Selected pregelatinised sago starch			229.1		145.1
Sodium starch glycolate				14.0	14.0
Magnesium stearate	0.9	0.9	0.9	0.9	0.9

3.3.8.2 Evaluation of Tablets

(i) Uniformity of weight

Twenty tablets of each formulation were randomly selected and weighed on individual tablet basis. The mean weight and standard deviation of the twenty tablets were reported. Since the mass of a tablet is 350 mg, the deviation of individual tablet mass should not exceed the limits of ±5 % from the average tablet mass (BP 2007; USP 27).

(ii) Hardness and dimension

Hardness and dimension (thickness and diameter) of tablets were determined using multipurpose tablet hardness tester (Model 6D, Dr. Schleuniger Pharmatron). Ten tablets of each formulation were used in this test, means and standard deviations were calculated (BP 2007; USP 27).

(iii) Friability

For friability test of each formulation, twenty tablets were selected randomly, dusted and weighed. The tablets were placed in a friability tester (ERWEKA-TAR10) and rotated at 25 rotations per minute for four minutes. The tablets were then dusted and reweighed to calculate the percentage loss of weight (BP 2007; USP 27).

(iv) Disintegration

Six tablets of each batch were randomly selected for disintegration test using a disintegration apparatus (ERWEKA-ZT41) in the distilled water medium at a constant temperature of 37.0 ± 0.5°C. The disintegration time was taken when no granule of the tablets was left in the disintegration apparatus. The mean and standard deviations of six readings were reported (BP 2007; USP 27).

(v) Dissolution

Dissolution tests were conducted using a dissolution tester (DA-60) in 900 mL dissolution medium of buffer phosphate pH 5.8 maintained at temperature of 37.0 ± 0.5°C with paddle rotation speed at 50 rotations per minute. Continuous sampling technique was performed every 5 minutes for 30 minutes. 5 mL sample was collected each time and an equal volume of fresh dissolution medium was replaced in. The amounts of the dissolved drug were determined using UV-Visible spectrophotometer (UV-1601, Shimadzu) at wavelength of 243 nm. A dissolution curve was then prepared by plotting between percentages of drug dissolved versus time. Six tablets of each formulation were tested (USP 27). Dissolution efficiency was determined by calculating the area under the dissolution curve (AUC) using trapezoidal method (Ngwuluka *et al.*, 2010).

(vi) Short-term accelerated stability study

The method adopted was according to ICH (2003). The tablets resulted were kept in closed glass containers at 40 ± 2°C / 75 ± 5% RH for 3 and 6 months and the tablets were evaluated in the same manner as above for uniformity of weight, hardness, dimension, friability, disintegration and dissolution.

3.3.9 Data analysis

The difference in means of data were analysed by using t-test, and analysis of variance (ANOVA) tests. Results with $p<0.05$ is considered to be significantly different.

CHAPTER 4

RESULTS AND DISCUSSION

4.1 Pharmacopoeial specification and chemical composition

Table 4.1 shows that the sago starch used in this study met the requirements of USP 27 for starch. The chemical composition of sago starch listed in Table 4.2 revealed it contains 26.33% of amylose and traces of lipid (0.12%) and protein (0.20%), therefore the amylopectin content in the sago starch can be considered to be about 73.67%. The results are in agreement with previous studies conducted by Ahmad *et al.* (1999).

Table 4.1: Pharmacopoeial characterisation of sago starch according to USP 27.

Test	Specification	Results
Identification	Product is translucent or whitish jelly and give reddish violet to deep blue colour with iodine	Conform
pH	5.0 – 7.0	5.93±0.06
Residue on Ignition	Not more than 0.5%	Conform
Iron	Not more than 0.002%	Conform
Sulphur Dioxide	Not more than 0.008%	Conform
Oxidizing substance	Not more than 0.002%	Conform
Loss on Drying	Not more than 15%	12.81±0.12
Microbial limit tests	Absence of *Salmonella sp* and *E.coli*	Conform

Table 4.2: Amylose, lipid and protein contents.

Test	Content
Amylose (%)	26.33±0.58
Lipid (%)	0.12±0.01
Protein (%)	0.20±0.01

4.2 Powder Characterisations

4.2.1 Amylose content

Table 4.3: Amylose content of sago starch and its pregelatinised forms.

Powder sample	Sago starch	PS1	PS2	PS3	PS4
Amylose content(%)	26.33±0.58	25.00±1.00	24.33±0.58	20.67±1.15	17.00±1.00

Note: n=3 for each powder.

Table 4.3 shows pregelatinisation decreased significantly ($p<0.05$) amylose content of sago starch. This was due to the leaching of amylose during pregelatinisation (Fourmann, Carrot, & Mignard, 2003; Jacobs & Delcour, 1998; Loisel *et al.*, 2006; Ratnayake & Jacson, 2006) and increasing heating time for pregelatinisation resulted in decreasing amylose content ($p<0.05$).

4.2.2 Fourier Transform Infrared spectroscopy (FT-IR)

Figures 4.1 – 4.5 show FTIR spectra of sago starch and pregelatinised sago starches (PS1, PS2, PS3 and PS4.

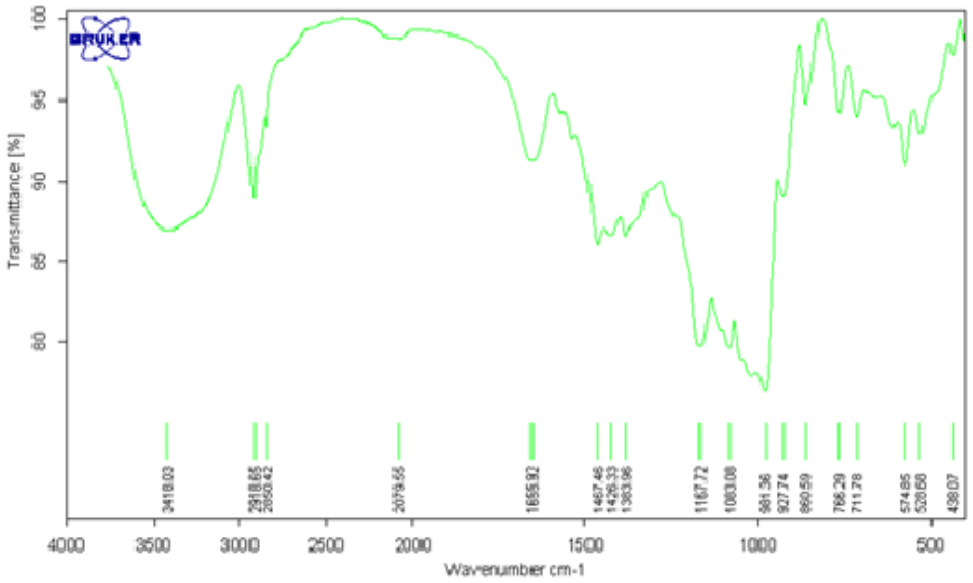

Figure 4.1: FT-IR spectra of sago starch.

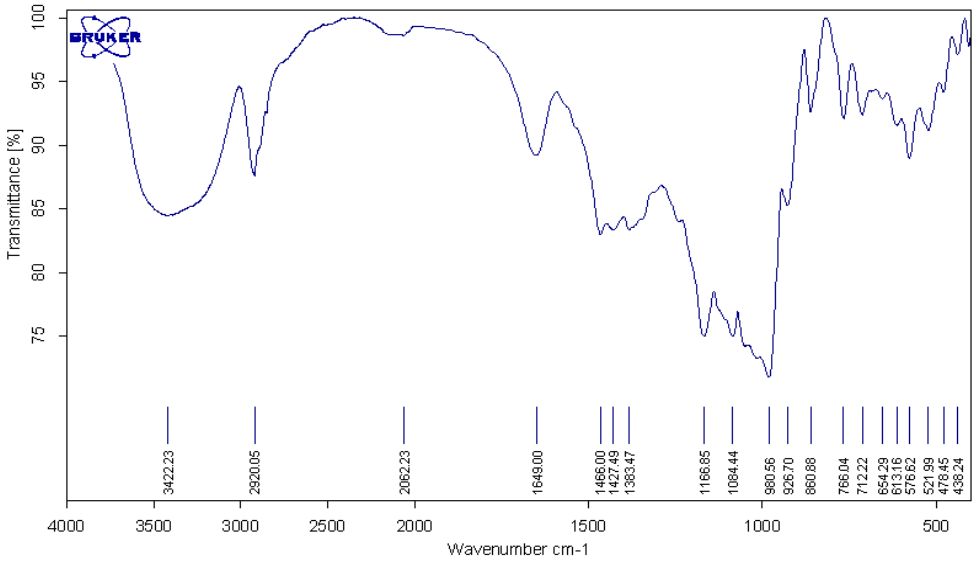

Figure 4.2: FT-IR spectra of pregelatinised sago starch PS1.

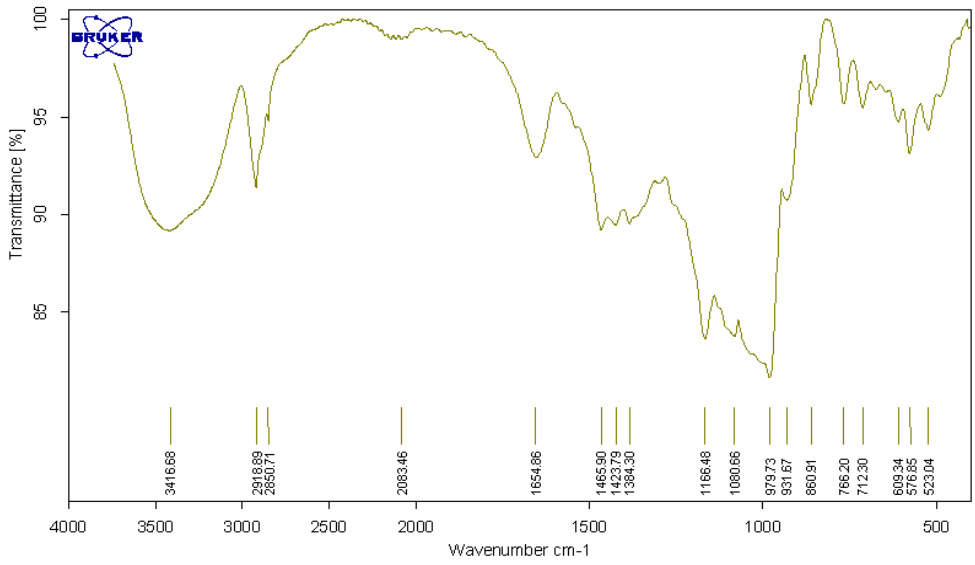

Figure 4.3: FT-IR spectra of pregelatinised sago starch PS2.

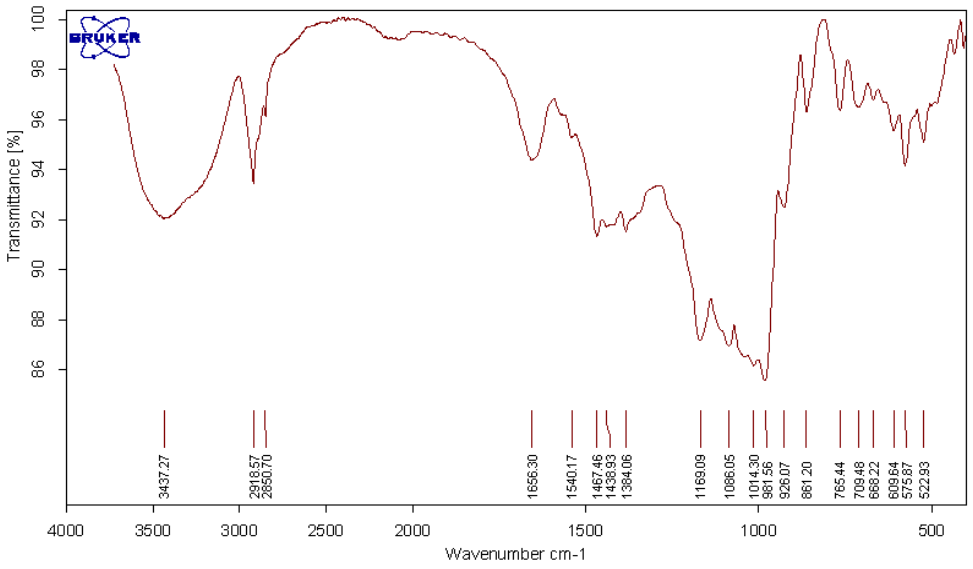

Figure 4.4: FT-IR spectra of pregelatinised sago starch PS3.

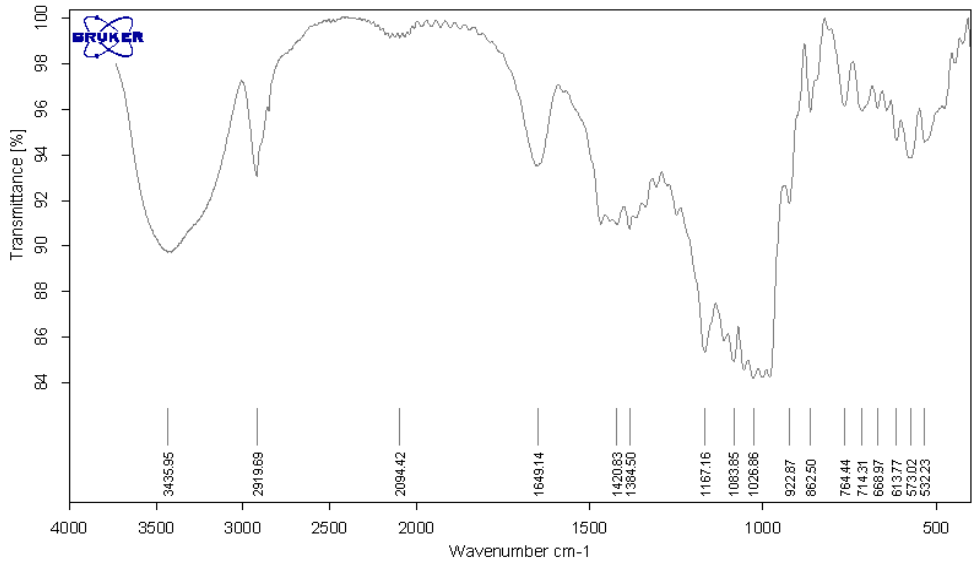

Figure 4.5: FT-IR spectra of pregelatinised sago starch PS4.

FTIR spectra were used to verify the changes of chemical structure (Singh & Nath, 2012) as the result of pregelatinisation. The FT-IR spectra analyses revealed that there were no new sharp bands found in the pregelatinised sago starches (Figures 4.2 – 4.5), indicating

that pregelatinisation did not change the chemical structure of sago starch. The characteristic of a strong, broad band between 927 cm^{-1} and 1200 cm^{-1} with three peaks at 980 cm^{-1}, 1084 cm^{-1} and 1166 cm^{-1}, associated with (C-O-H), (C-C) and (C-O), is a glycosidic linkage. Another characteristic of sharp bands is the three peaks at 1649 cm^{-1}, 2920 cm^{-1} (refers to the C-H stretching of starch molecules) and 3422 cm^{-1} (refers to O-H group of starch). The two sharp bands at 1645 cm^{-1} and 1411 cm^{-1} are characteristics of bound water and C-H bonding present in the starch molecules (Sun *et al.*, 2000; Ummi-Shafiqah *et al.*, 2012).

4.2.3 NMR Spectroscopy

Figures 4.6 – 4.10 show ^{13}C-NMR spectra of sago starch and pregelatinised sago starches (PS1,PS2, PS3 and PS4).

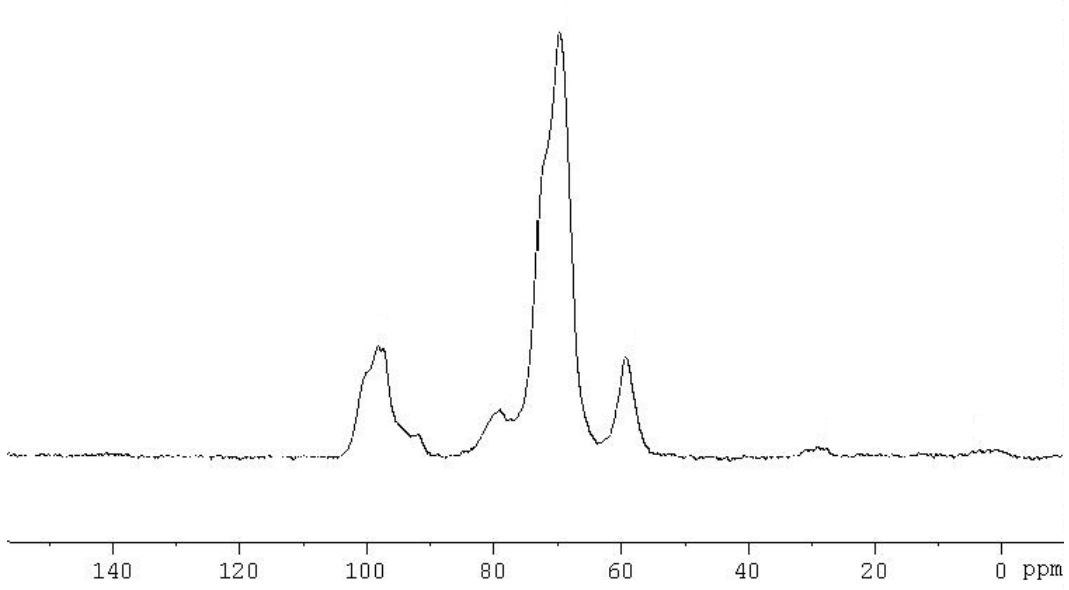

Figure 4.6: ^{13}C-NMR Spectra of sago starch (δ: 98.0, 78.9, 69.7 and 59.2 ppm).

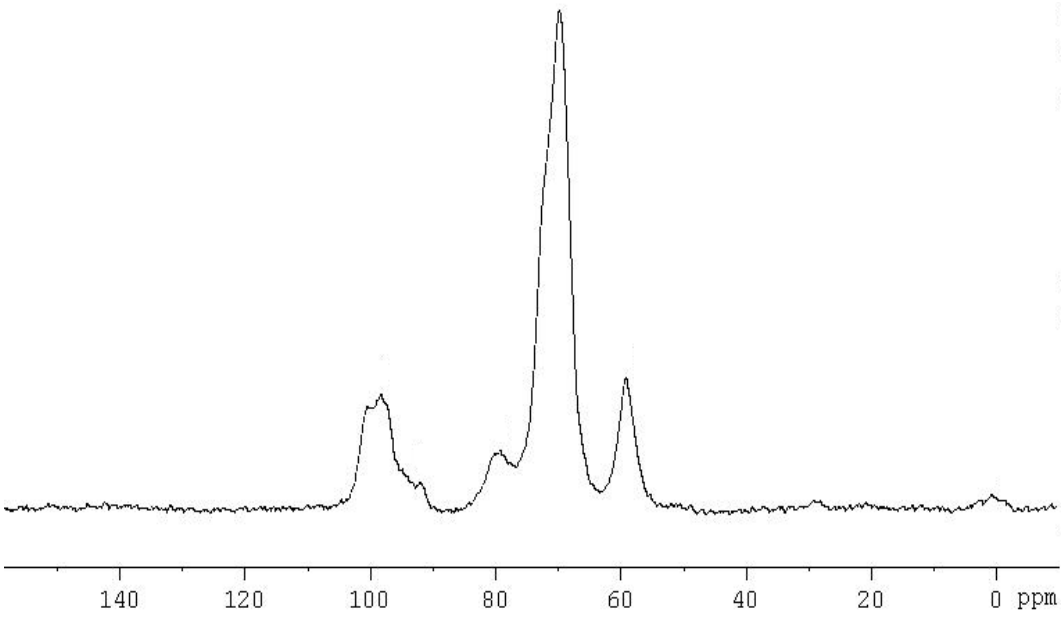

Figure 4.7: ^{13}C-NMR Spectra of PS1 (δ: 98.2, 79.2, 69.7 and 59.0 ppm).

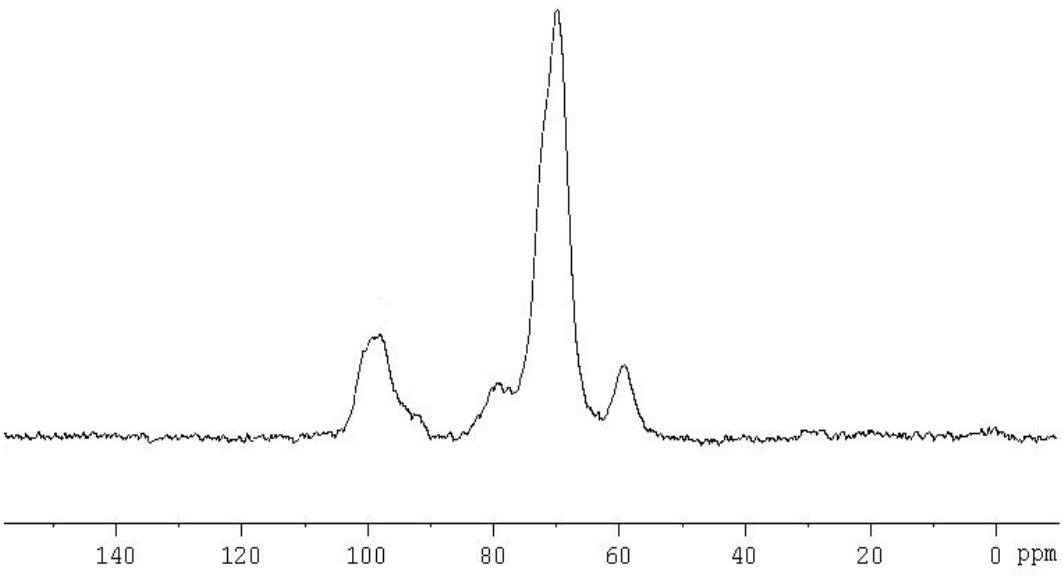

Figure 4.8: ^{13}C-NMR Spectra of PS2 (δ: 98.0, 79.2, 69.7 and 59.0 ppm).

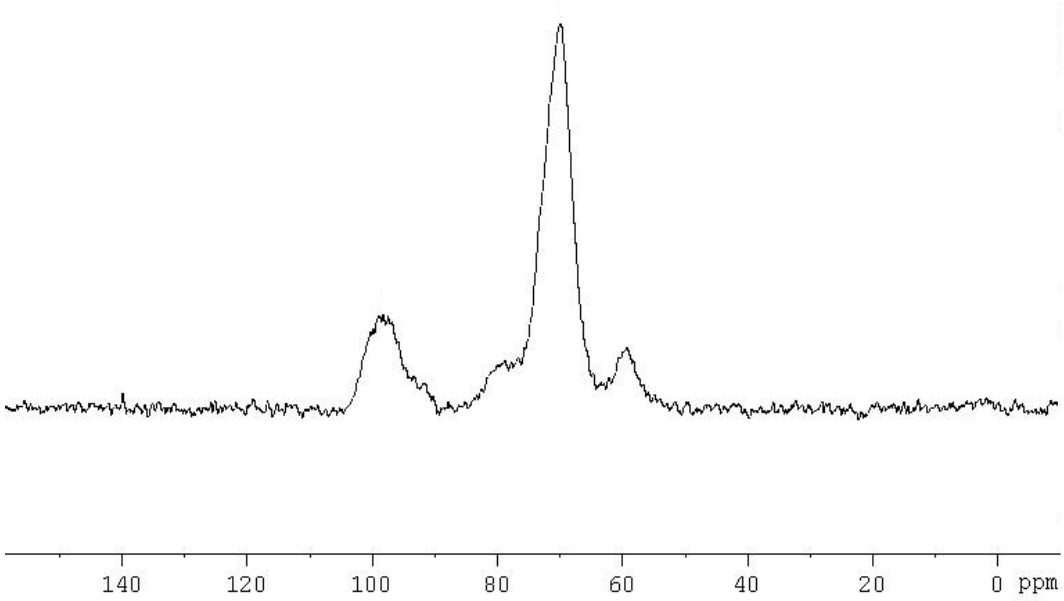

Figure 4.9: ^{13}C-NMR Spectra of PS3 (δ: 98.1, 79.1, 69.7 and 59.1 ppm).

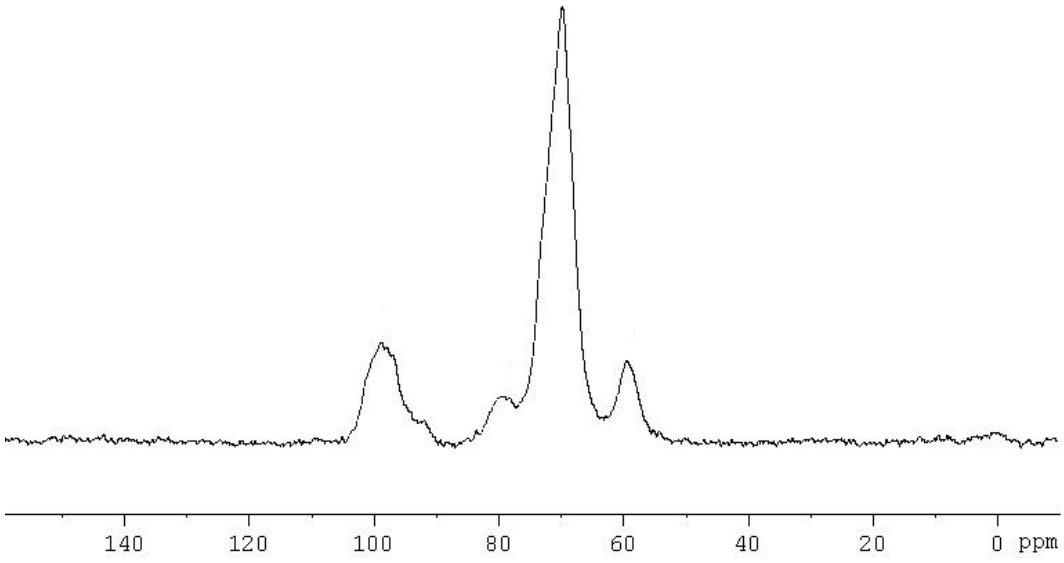

Figure 4.10: ^{13}C-NMR Spectra of PS4 (δ: 98.6, 79.1, 69.7 and 59.4 ppm).

From the ^{13}C-NMR spectra, it was shown that there are no significant chemical structure changes for sago starch after pregelatinisation. Chemical shift (δ) variations shown from the studies were of minor significance. This could be due to when the starch is

heated in excess water, the crystalline structure of starch granule is disrupted (Hoover, 2001; Morgan *et al*., 1995). In the presence of water with heat, the water molecule tends to diffuse and be uptaken by the starch granules. This resulted in the uncoiling and dissociation of double helical structure of linear starch chains, leading to loss of the organised structure of starch. However, the basic monomer structure of D-glucose unit found in both amylose and amylopectin components of starch remains uninterrupted. Thus, the ^{13}C-NMR spectra of the PS showed no chemically important differences in comparison with the native starch spectra. This suggests that pregelatinisation of starch will only disrupt the hydrogen bonding between linear starch chains leading to disorganisation of the double helical structure of starch but the basic monomer backbone will be unaffected (Hoover, 2001).

4.2.4 X-ray diffraction

Diffraction patterns of sago starch and pregelatinised sago starches (PS1, PS2, PS3, PS4) are presented in Figures 4.11 and 4.12 (a) – (d). The diffraction patterns as well as the degree of crystallinity for the sago starch samples are tabulated in Tables 4.4 and 4.5.

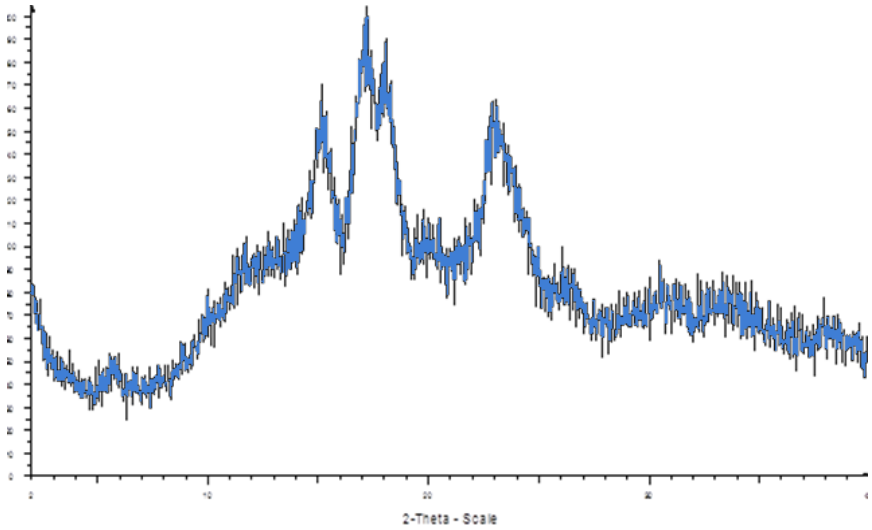

Figure 4.11: X-ray diffractogram of sago starch.

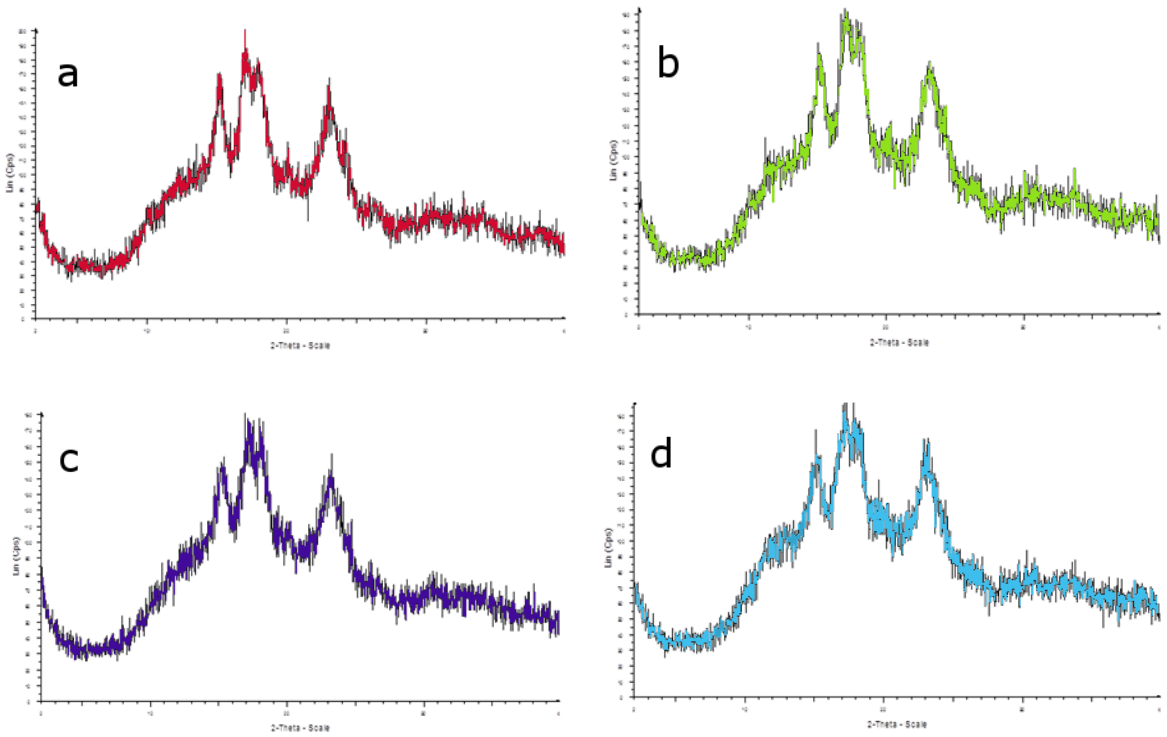

Figure 4.12: X-ray diffractogram of: (a) PS1, (b) PS2, (c) PS3, and (d) PS4.

Table 4.4: Diffraction pattern of sago starches.

Sample powder	Diffraction peaks at 2θ value (°angle)							Diffraction pattern
	5°	15°	17°	18°	20°	22°	23°	
Sago starch	5.60	15.11	16.95	17.97	19.93		23.15	C
PS1		15.13	16.98	18.06	19.64		23.18	A
PS2		15.14	17.03	18.11	19.89		23.24	A
PS3		15.16	17.11	18.15	20.12		23.28	A
PS4		15.09	17.11	18.16	19.46		23.18	A

Table 4.5: Degree of crystallinity of sago starches.

Sample powder	Degree of crystallinity (%)	
	Area	Height
Sago starch	52.00 ± 1.03	52.49 ± 1.63
PS1	39.75 ± 2.88	48.57 ± 1.28
PS2	37.39 ± 0.82	46.93 ± 2.00
PS3	36.32 ± 0.39	47.83 ± 2.92
PS4	35.11 ± 1.10	45.64 ± 3.63

Note: n=3 for each sample.

It was observed that sago starch exhibits characteristics of C-type diffraction pattern, characterised by a weak peak at 2θ: 5.60° and strong peaks at 2θ: 15°, 17°, 18° and 23° (Ahmad *et al.*, 1999; Karim *et al.*, 2008). All of the pregelatinised sago starches showed an A type pattern, characterized by strong peaks at 2θ: 15°, 17°, 18° and 23° (Kaur, Fazilah, & Karim, 2011). In addition, pregelatinised sago starches showed similar X-ray diffraction patterns as that of native sago starch, except at the peak of 2θ: 5.60°. However, the peaks of native sago starch appeared sharper compared to its pregelatinised forms, indicating that the native sago starch showed more crystalline region. This study showed pregelatinisation reduced degree of crystalinity ($p<0.05$) and as the heating time for pregelatinisation increased, the degree of crystallinity decreased ($p<0.05$) as suggested by Ummi-Shafiqah *et al.* (2012). The degree of crystallinity was calculated using the height method (Equation 3.1) and the area method (Equation 3.2), with results of the peak height method gave significantly higher ($p<0.05$) degree of crystalinity than the area method. Terinte, Ibbett & Schuster (2011) stated that eventhough the height method is very useful and simple, it only measures relative degree of crystallinity and therefore should not be used to indicate the absolute area of crystalline and non-crystalline of the material.

4.2.5 Differential Scanning Calorimetry

Figures 4.13(a) – (d) show the thermogram of sago starch and pregelatinised sago starches (PS), i.e PS1, PS2, PS3 and PS4. Transition temperatures with the gelatinisation, namely onset or gelatinisation (T_o), peak (T_p), conclusion (T_c) temperatures as well as the melting enthalpy (ΔH) in J/g and degree of gelatinisation of the starches were recorded in Table 4.6. DSC curves showed pregelatinisation increased significantly ($p<0.05$) the gelatinisation temperature (T_o), peak temperature (T_p), and degree of gelatinisation (DG); it

also decreased significantly ($p<0.05$) the gelatinisation temperature range ($T_c - T_o$) and the melting enthalpy (ΔH) of sago starch. The effects became more pronounced ($p<0.05$) with the increasing heating time for pregelatinisation; the transition temperatures change as more amylose leaches ($p<0.05$), the degree of gelatinisation (DG) increases as more heat is absorbed by the starch granules and the melting enthalpy (ΔH) decreases as more crystalline part reduces ($p<0.05$) (Fourmann, Carrot, & Mignard, 2003; Jacobs & Delcour, 1998; Loisel *et al.*; Ratnayake & Jacson, 2006; Ummi-Shafiqah *et al.*, 2012). In particular, it was observed that PS exhibited higher gelatinisation temperature than sago starch. The delay in gelatinisation is due to excess water penetrating into the amorphous region during the heating process, resulting in hydration and limited swelling. The swelling of amorphous region put a stress on the crystalline region, thereby disrupting the polymer chain of the starch. Eventually, the suppressed swelling led to high temperature (Perera, Hoover, & Martin, 1997).

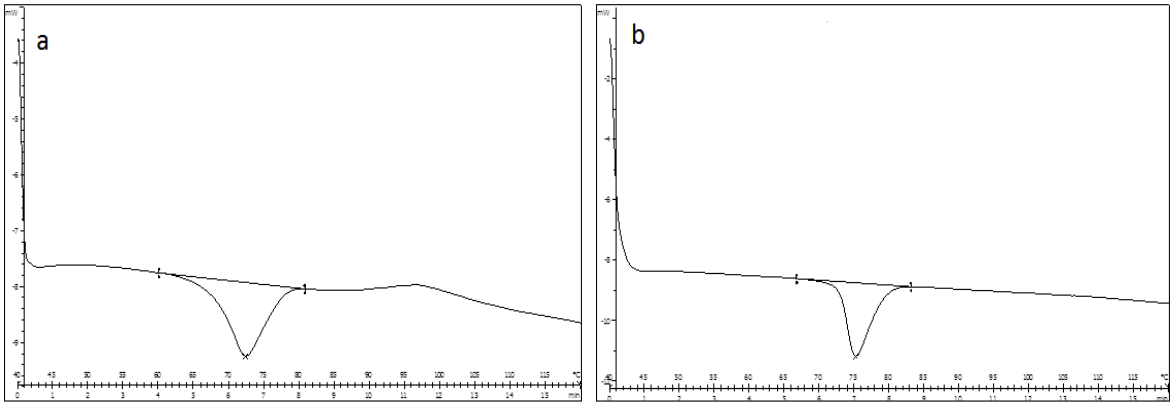

Figure 4.13: Thermogram of (a) Sago, (b) PS1, (c) PS2, (d) PS3, and (e) PS4.

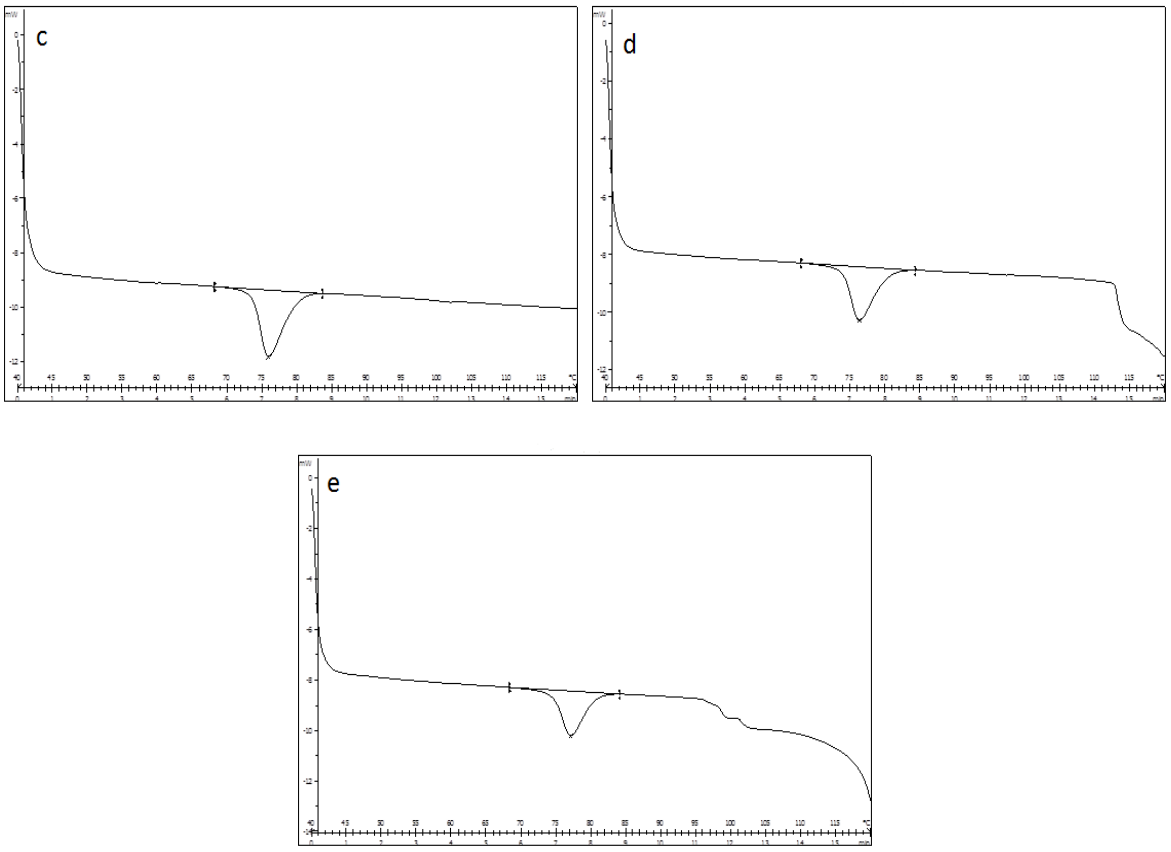

Figure 4.13, continued: Thermogram of (a) Sago, (b) PS1, (c) PS2, (d) PS3, and (e) PS4.

Table 4.6: Differential scanning calorimetry data for each powder sample.

Powder sample	T_o±SD (°C)	T_p±SD (°C)	T_c±SD (°C)	$T_c - T_o$ ±SD (°C)	ΔH±SD (J/g)	DG±SD (%)
Sago starch	67.11±0.35	71.94±0.14	78.07±0.58	10.96±0.84	3.62±0.31	0.00±0.00
PS1	72.78±0.46	74.96±0.51	78.98±1.03	6.20±0.62	3.27±0.29	9.67±0.34
PS2	73.25±1.07	75.45±1.44	79.46±1.72	6.20±0.66	3.10±0.26	14.43±1.36
PS3	73.90±0.74	76.18±1.07	80.06±1.46	6.16±0.76	2.64±0.23	27.17±0.59
PS4	74.13±0.10	76.45±0.18	79.75±0.54	5.62±0.50	2.37±0.22	34.40±2.89

Note: n=3 for each sample.

4.2.6 Scanning Electron Microscopy

Scanning electron microscopy was used to study the shape and surface texture of Avicel PH 101, Spress® B820, sago starch and pregelatinised sago starch granules (PS): PS1, PS2, PS3, -PS4. The results are presented in Figures 4.14 and 4.15.

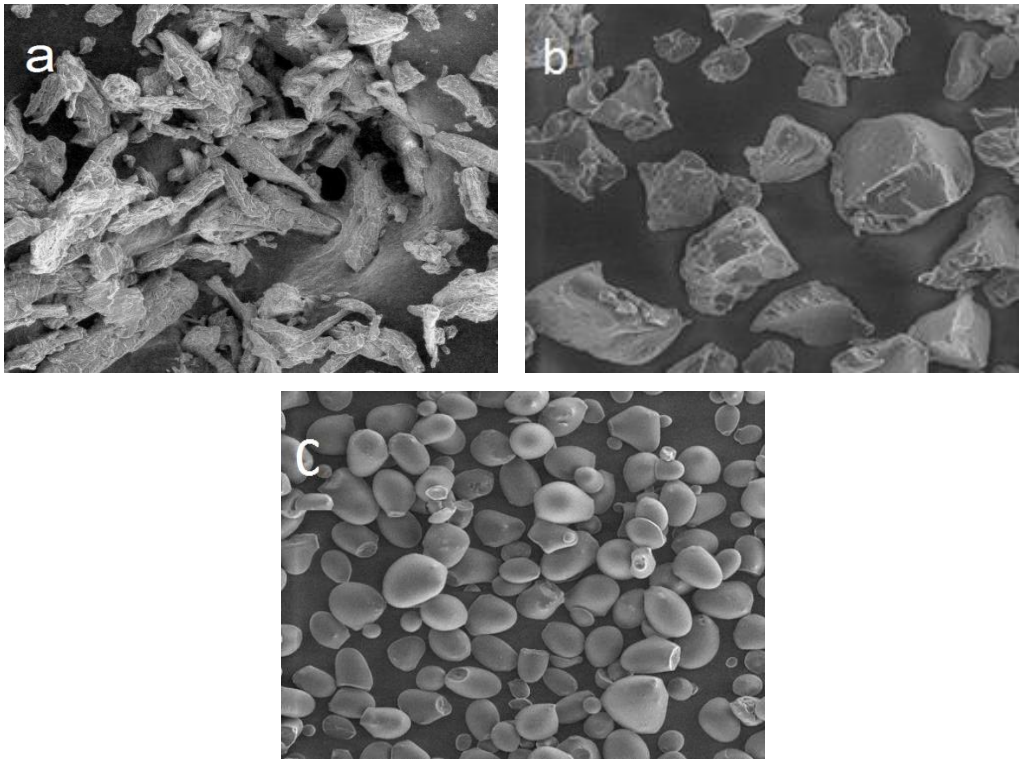

Figure 4.14: SEM photographs of (a) Avicel PH 101, (b) Spress® B820 and (c) sago starch.

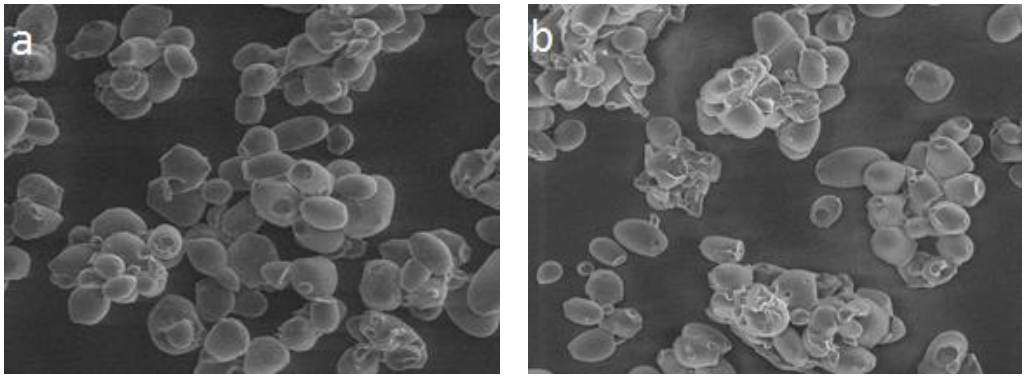

Figure 4.15: Images of pregelatinised sago starches (PS) at different heating times observed with scanning electron microscope: (a) PS1 (15 minutes), (b) PS2 (30 minutes), (c) PS3 (45 minutes) and (d) PS4 (60 minutes).

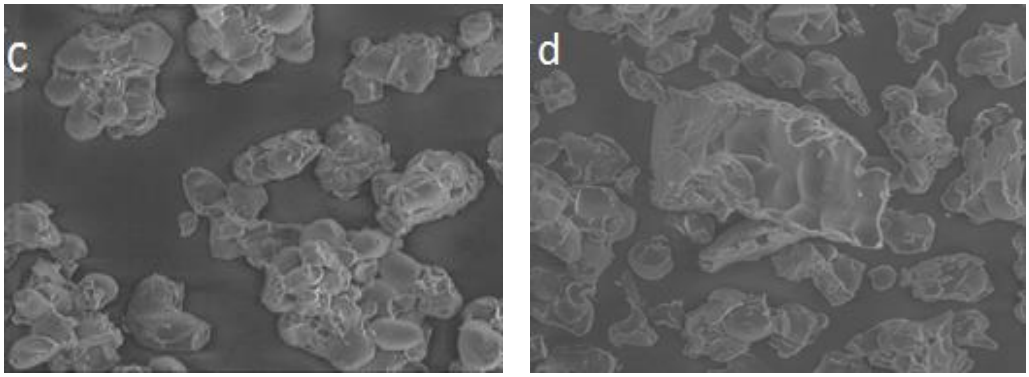

Figure 4.15, continued: Images of pregelatinised sago starches (PS) at different heating times observed with scanning electron microscope: (a) PS1 (15 minutes), (b) PS2 (30 minutes), (c) PS3 (45 minutes) and (d) PS4 (60 minutes).

From Figure 4.14, it can be seen that Avicel PH 101 exhibits fibrous rodlike structure, and far from spherical shape. Spress® B820 appears as granules with irregular shape and surface structure. These observations were similar to the previous studies (Ahmad *et al.*, 1999; Bolhuis & Chowhan, 1996; Kerr, 1968; Kibbe, 2000; Noor Fadzlina, Karim & Teng, 2005; Ohwoavworhua, Adelakun & Okhamafe, 2007; Singh & Nath, 2012; Yaacob *et al.*, 2011). After pregelatinisation with heating time for 15 minutes (PS1) and 30 minutes (PS2), the starch granules started swelling and a small part of them was gelatinised; there were no obvious impact on the surface texture and shape of the granules (Figure 4.15a and 4.15b). By prolonging the heating time to 45 minutes (PS3) and 60 minutes (PS4), more sago starch granules were gelatinised, resulting the loss of their surface smoothness and showed more irregular shapes (Figure 4.15c and 4.15d). This is because the amount of water that diffuses into starch granules and amount of heat received by the starch granules are larger during prolonged heating time. This resulted in the starch granules swelling to a greater extent and crystallites melt, causing more granules to be gelatinised which lead to the change of shape and size of the starch granules (Jacobs & Delcour, 1998; Loisel *et al.*, 2006; Ratnayake & Jacson, 2006). This study found that

Avicel PH 101 exhibits the most irregular shape and the roughest surface, followed by Spress® B820, PS4, PS3, PS2, PS1 and sago starch.

4.2.7 Viscosity

Table 4.7 shows viscosities of all powder samples, with each value that were significantly different ($p<0.05$). Within sago starch group, pregelatinisation significantly increased ($p<0.05$) the viscosity of sago starch, with increased heating time causing increasing viscosity ($p<0.05$). As pregelatinised starches showed lower amylose content and higher DG, therefore they are able to absorb water more readily and swell, causing increased viscosity ($p<0.05$) at low temperatures (Puspitowati & Driscoll, 2007; Riley, Wheatly, & Asemota, 2006). In comparison, PS4 showed lower viscosity than Spress® B820 but higher than Avicel PH 101.

Table 4.7: Viscosity of each powder sample at 2% w/v, 25°C.

Powder sample	Avicel PH 101	Spress® B820	Sago starch	PS1	PS2	PS3	PS4
Viscosity (cPS)	8.57± 0.39	15.18± 0.30	10.09± 0.19	10.77± 0.22	11.19± 0.08	12.06± 0.15	13.14± 0.26

Note: n=3 for each sample.

4.2.8 Swelling power and water solubility index

In the pharmaceutical applications, swelling power (SP) and water solubility index (WSI) of starch need to be evaluated to assess the functional properties of starch as a disintegrant in order to release the active ingredient(s) from the dosage forms, such as tablets and capsules (Bandelin, 1989; Bolhuis & Chowan, 1996; Kibbe, 2000). Temperatures for the test were selected to evaluate the ability of sago starch and

pregelatinised sago starches (PS) to dissolve in cold water, as well as to see the change in swelling power and water solubility as the temperature increases. Tables 4.8 – 4.9 and Figures 4.16 – 4.17 shows the swelling power as well as the water solubility index of sago starch, pregelatinised sago starches (PS) i.e. PS1, PS2, PS3, PS4 and Spress® B820 at various temperatures.

Table 4.8: Swelling power (SP) of sago starch, PS1, PS2, PS3, PS4 and Spress® B820.

Powder sample	Swelling power (%) ± SD						
	25°C	35°C	45°C	55°C	65°C	75°C	85°C
Sago starch	3.00± 0.05	2.98± 0.02	3.00± 0.02	3.01± 0.02	2.99± 0.02	20.71± 1.92	26.42± 0.61
PS1	3.08± 0.02	3.11± 0.00	3.13± 0.02	3.22± 0.22	4.82± 0.02	18.88± 0.17	24.01± 0.25
PS2	3.50± 0.01	3.53± 0.03	3.54± 0.45	3.57± 0.07	4.19± 0.05	14.84± 0.25	19.95± 0.21
PS3	3.50± 0.05	3.66± 0.04	3.70± 0.04	3.69± 0.02	4.05± 0.03	12.82± 0.16	16.34± 0.21
PS4	3.77± 0.04	3.76± 0.03	3.77± 0.01	3.98± 0.02	4.00± 0.03	13.01± 0.12	15.39± 0.09
Spress® B820	5.91± 0.15	5.94± 0.07	5.95± 0.11	6.46± 0.10	10.05± 0.10	12.09± 0.19	13.84± 0.15

Note: n=3 for each sample.

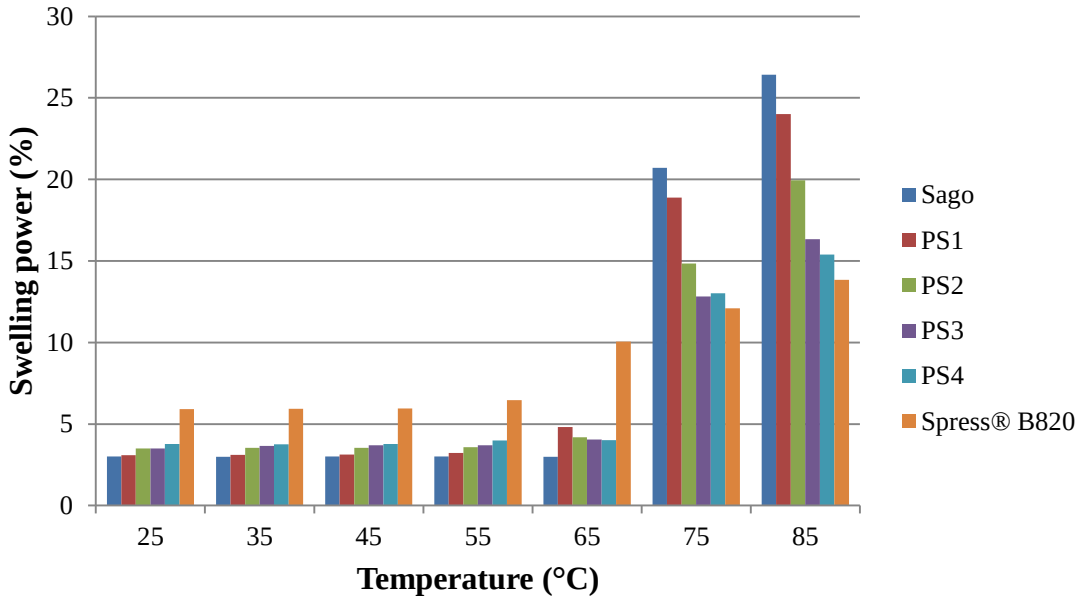

Figure 4.16: The effect of temperature on the swelling power (SP) of sago starch, PS1, PS2, PS3, PS4 and Spress® B820.

Table 4.9: Water solubility index (WSI) of sago starch, PS1, PS2, PS3, PS4 and Spress® B820.

Powder sample	Water solubility index (g/g)±SD						
	25°C	35°C	45°C	55°C	65°C	75°C	85°C
Sago starch	5.00± 1.00	5.33± 0.29	5.83± 0.76	6.17± 0.29	6.67± 0.76	30.50± 6.94	59.00± 1.00
PS1	6.00± 0.50	6.33± 0.58	6.83± 0.29	7.00± 0.50	7.17± 0.58	23.67± 0.58	40.00± 0.50
PS2	7.33± 0.29	7.50± 0.50	7.67± 0.58	7.67± 0.29	8.50± 0.50	24.67± 1.15	33.83± 0.76
PS3	9.83± 0.76	9.83± 0.29	10.17± 0.76	10.33± 0.29	10.67± 0.29	25.17± 0.76	29.33± 0.76
PS4	10.50± 0.87	10.50± 0.50	10.83± 0.29	10.83± 0.29	12.17± 0.29	23.67± 0.76	28.00± 0.50
Spress® B820	19.61± 3.69	19.00± 1.00	19.17± 1.44	21.78± 2.17	22.33± 0.58	34.67± 1.15	36.67± 0.76

Note: n=3 for each sample.

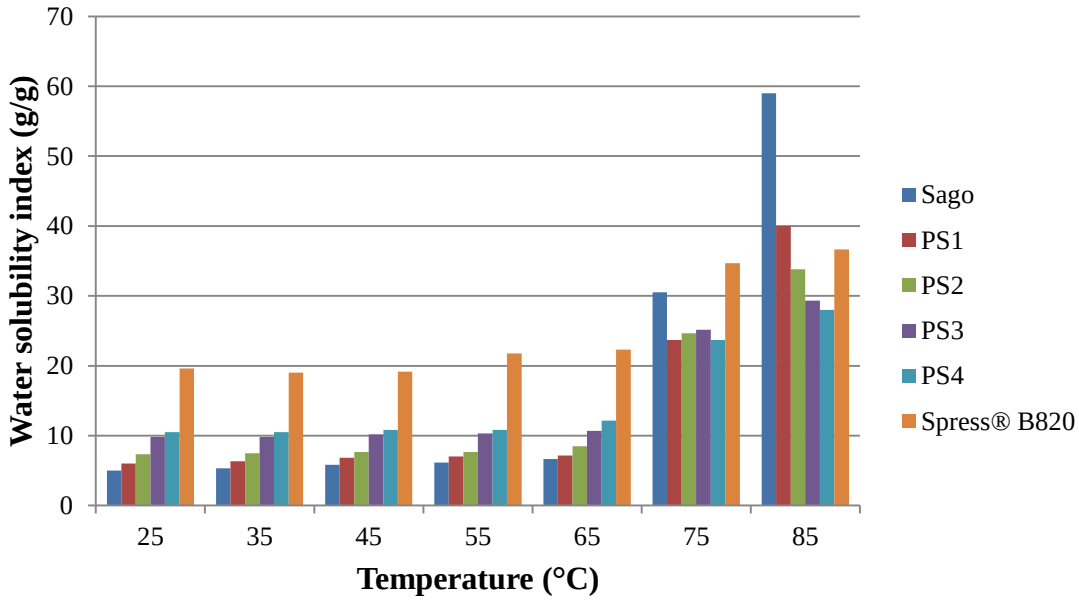

Figure 4.17: The effect of temperature on the water solubility index (WSI) of sago starch, PS1, PS2, PS3, PS4 and Spress® B820.

The results showed pregelatinised sago starches (PS) exhibited significantly higher ($p<0.05$) SP and WSI than sago starch up to 55˚C and 65˚C respectively; increasing the heating times for pregelatinisation resulted in the significant increment ($p<0.05$) of both SP and WSI. This was due to the fact that gelatinisation caused disruption of granules structure as indicated by the increasing degree of gelatinisation (DG) (Table 4.6), causing the starch molecules to dissolve and swell (Ratnayake & Jacson, 2006). Besides that, since the amylose content of PS is lower than sago starch (Table 4.3), it weakens inhibition of the swelling through the formation of complex amylose-lipid molecules (Riley, Wheatly, & Asemota, 2006; Tester & Morrison, 1990). Statistical analysis revealed that SP and WSI of sago starch, PS1, PS2, PS3 and PS4 were significantly influenced ($p<0.05$) by the temperature, their DG and amylose contents. By these explanations, therefore PS4 exhibited the highest SP and WSI within the sago starch group, but inferior in comparison to Spress® B820 at any temperatures of the study. The results at temperatures above 55˚C and 65˚C however, are the opposite, where sago starch showed higher SP and WSI

respectively than PS. This could be due to more disruption of granules structure, increasing the leaching of amylose and amylopectin from the starch granules and also disassociation of amylose-lipid complexes as the temperature increases (Ratnayake & Jacson, 2006; Tester & Morrison, 1990). Overall, this study found that SP and WSI increase with increasing temperatures ($p<0.05$) and there was a strong correlation ($p<0.05$, $R^2 = 0.926$) between SP and WSI at any temperature used in this study.

4.2.9 Particle size and size distribution

Since a collection of particles is in a range of sizes (Martin, Bustamante, & Chun, 1993), expression of the size of a material is more useful in its particle size distribution (Parrot, 1989). Particle size distribution of sago starch, pregelatinised sago starches (PS) and two commercial directly compressible excipients commonly used, i.e. Avicel PH 101 and Spress® 820 (Zhang, Law, & Chakrabarti, 2003) were analysed. The results are presented in Table 4.10 and Figures 4.18 - 4.24.

Table 4.10: Particle size of each powder sample.

Powder sample	Avicel PH 101	Spress® B820	Sago starch	PS1	PS2	PS3	PS4
Mean particle size , diameter (μm)	56.70 ±11.51	89.30 ±20.29	32.10 ±10.72	75.9 ± 20.97	86.70 ±19.78	87.80 ± 16.52	88.00 ±18.98

Note: n=300 for each sample.

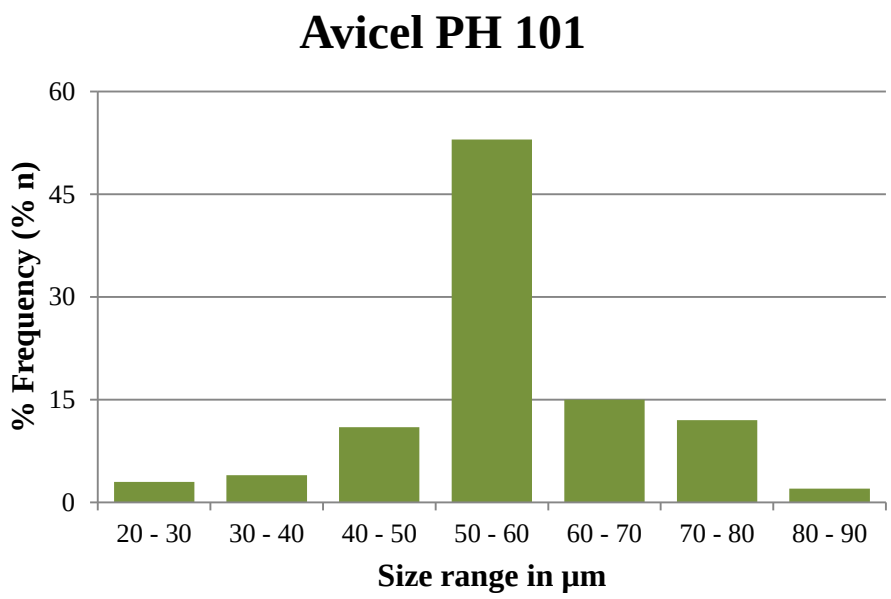

Figure 4.18: Particle size distribution Avicel PH 101.

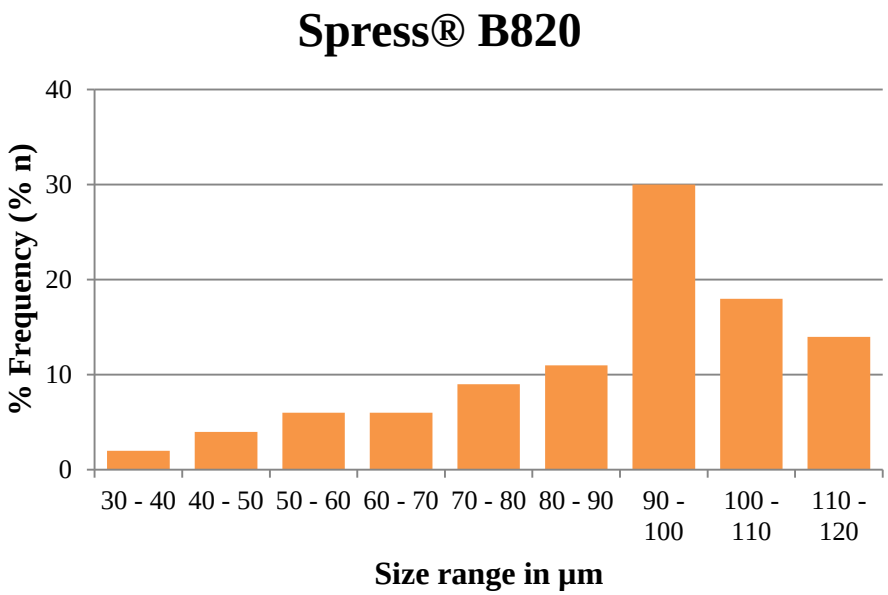

Figure 4.19: Particle size distribution Spress® B820.

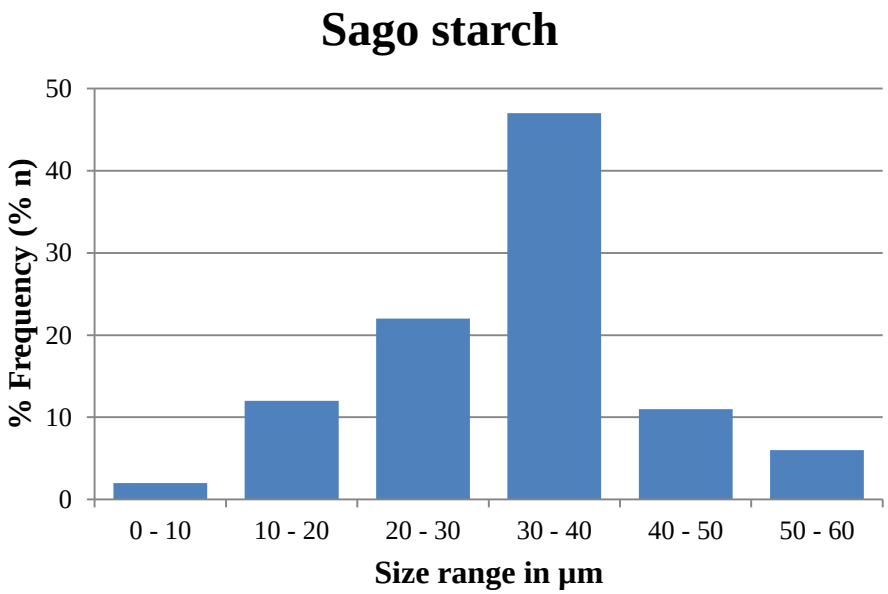

Figure 4.20: Particle size distribution sago starch.

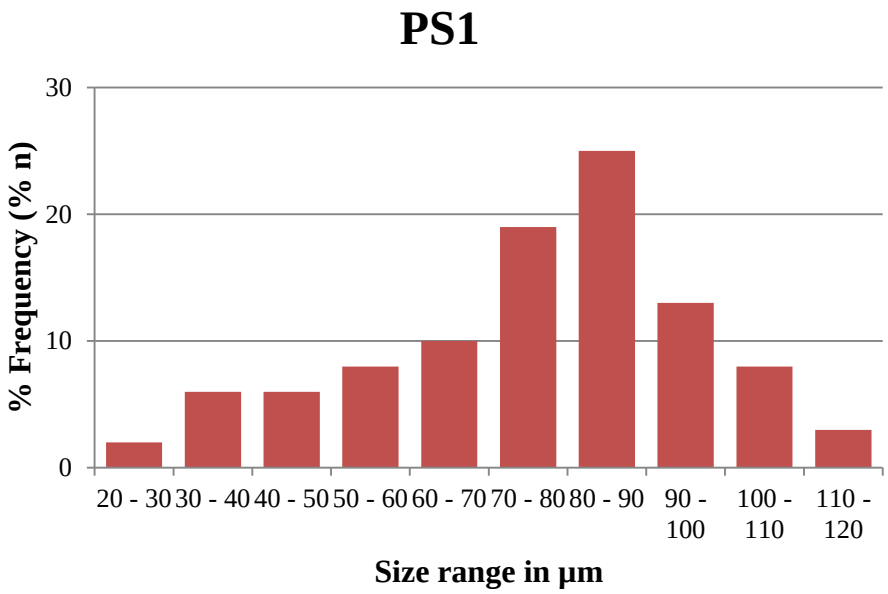

Figure 4.21: Particle size distribution PS1.

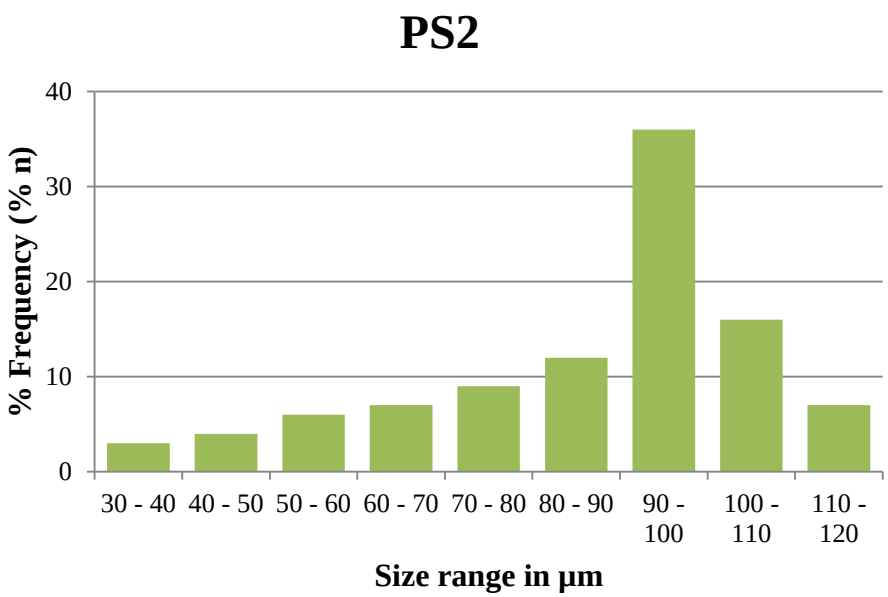

Figure 4.22: Particle size distribution PS2.

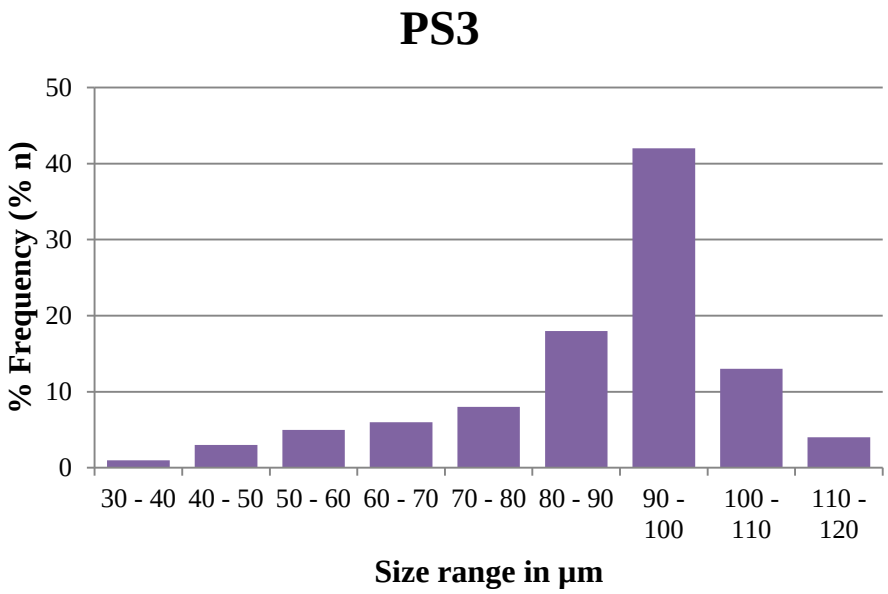

Figure 4.23: Particle size distribution PS3.

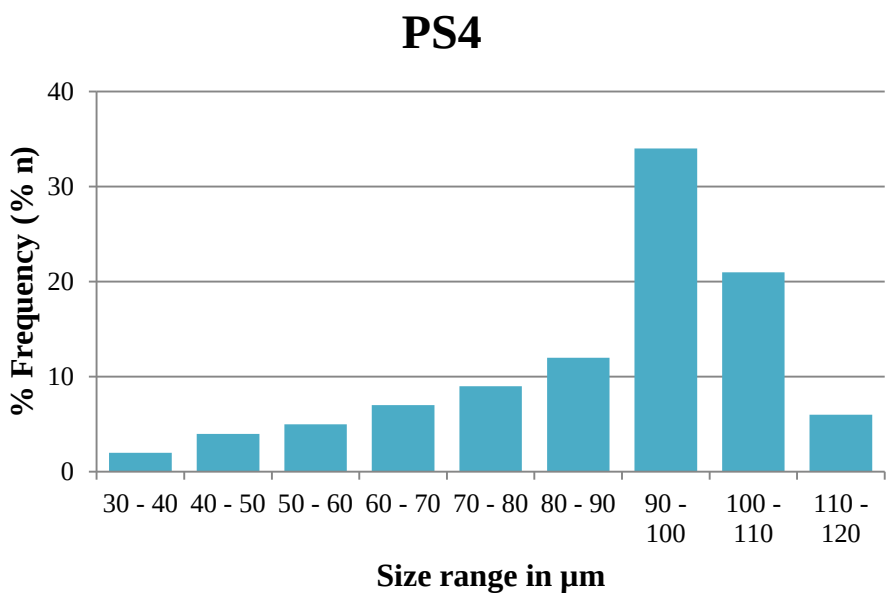

Figure 4.24: Particle size distribution PS4.

From the figures presented, it can be observed that the particle size distributions for all of the sample powders are unimodal and positively skewed with mean diameter different significantly ($p<0.05$). The mean diameter for sago starch was 32.10 µm. This was in agreement with the results reported by Ahmad *et al.* (1999) where the size of sago starch granules were in the range of 20 to 40 µm, and by Wang, Powell, & Oates (1995), in the range of 10 to 50 µm. After pregelatinisation, the mean size of pregelatinised sago starch granules increased significantly ($p<0.05$), with mean diameters for PS1, PS2, PS3 and PS4 as 75.9 µm, 86.70 µm, 87.80 µm and 88.00 µm respectively. It was noted that the longer heating time applied in the pregelatinisation produced significantly different ($p<0.05$) mean diameter for the pregelatinised sago starches. As seen in Figure 4.21 – 4.24, the longer the heating time applied, the more starch granules were gelatinised and agglomerated, therefore the greater the size. The mean diameter for Avicel PH 101 was found to be 56.70 µm and Spress® B820 89.30 µm. These results did not differ much with the works conducted by Zhang, Law, & Chakrabarti (2003), where the mean diameters of Avicel PH 101 and

Spress® B820 were 56.30 µm and 93.90 µm respectively. Comparing the mean diameter of Avicel PH 101 and Spress® B820 against sago starch and its pregelatinised forms, sago starch exhibited smaller mean diameter than Avicel PH 101 and all pregelatinised sago starches showed higher mean diameter than Avicel PH 101 but lower than Spress® B820. These differences in particle size distributions would affect their functionality as direct compression excipients. An optimum particle size distribution will determine some other properties such as flowability and content uniformity (Brittain, 1995). It is generally accepted that the larger particle size exhibits better flow properties, and up to a critical size range above which the powder flow does not show any improvement (Abdullah & Geldart, 1999; Randal, 1995). In the tablet manufacturing, a larger particle size would help to reduce dust generation (Joshi & Duriez, 2004). In contrast, small particles exhibit poor powder flow and therefore such powders are not suitable for use as direct compressed tablet excipients (Abdullah & Geldart, 1999; Nagel & Peck, 2003). However, powders with smaller particles contain higher number of particles per unit weight and have a higher potential to achieve homogeneity in the powder-powder mixing (Odeku & Picker-Freyer, 2007). Besides that, smaller powders possess a larger surface area and provide more contact points, thus producing better powder compressibility in the tableting (Martin, Bustamante, & Chun, 1993).

It is important to appreciate the properties of both active ingredients and tableting excipients i.e. particle shape and size distribution, friction and adhesion profile, true and bulk densities and compaction parameters. There are four aspects which are crucial for direct compression formulations: blend uniformity, blend flowability, compressibility and lubricity (McCormick, 2005). Lacking in any of these aspects can result in poor tablet quality.

4.2.10 Loss on drying, densities and porosity

Results obtained for the loss on drying, densities as well as porosity of each powder sample are tabulated in Table 4.11. Each of the properties is discussed in its own subsection.

Table 4.11: Loss on drying, densities and porosity of each sample.

Powder	% Loss on drying±SD[b]	Density (g/cm^3)±SD[c]			% Porosity (ε) ±SD[d]
		True (ρ_T)	Bulk (ρ_0)	Tap (ρ_t)	
Avicel PH 101	5.19±0.06	1.58 ±0.00	0.35±0.00	0.44±0.00	77.84±0.00
Spress® B820	9.91±0.02	1.50±0.00	0.64±0.00	0.71±0.00	57.33±0.00
Sago starch	12.81±0.12	1.55±0.00	0.63±0.00	0.73±0.00	59.35±0.00
PS 1	11.86±0.06	1.52±0.00	0.53±0.01	0.63±0.01	64.91±0.38
PS 2	11.72±0.08	1.52±0.00	0.53±0.00	0.63±0.01	65.13±0.00
PS 3	11.38±0.13	1.52±0.00	0.53±0.00	0.62±0.01	65.13±0.00
PS 4	10.39±0.41	1.51±0.00	0.52±0.01	0.61±0.01	65.34±0.38

Note: [a]n=300 for each powder, [b]n=3 for each powder, [c]n=3 for each powders at every density, and [d]n=3 for each powders.

4.2.10.1 Loss on drying

Table 4.11 shows % loss on drying (moisture content) of the powder samples and their values are significantly different ($p<0.05$). Within sago starch group, pregelatinisation decreases significantly ($p<0.05$) moisture content of sago starch and increasing heating time for pregelatinisation further decreased ($p<0.05$) its moisture content. Moisture content is reflecting the affinity of the powder for moisture (Parrott, 1989). All the powders examined were within United States Pharmacopoeia 27 (USP 27) for moisture content specifications, where moisture content of Avicel PH 101 does not exceed 7% and none of the moisture content for the starches was more than 14%. In comparison, Avicel PH 101 exhibited the lowest moisture content (5.19%), followed by Spress® B820 (9.91%), PS4 (10.39%), PS3 (11.38%), PS2 (11.32%), PS1 (11.86%) and sago starch (12.81%). The moisture content of Avicel PH 101 and Spress® B820 in this study is similar to those

determined by Zhang, Law, & Chakrabarti (2003), where their moisture contents were 5.1% and 9.8% respectively. In general, the moisture content of the powders decreases with increasing particle size ($p<0.05$). This is because the larger particle provides smaller surface area than the smaller particle; therefore the larger particle has less capacity to absorb moisture (Martin, Bustamante & Chun, 1993). The results of moisture content for sago starch, PS1, PS2, PS3 and PS4 were found to correspond with their degree of crystallinity ($p<0.05$, $R^2 = 0.790$ by area method), where the powder with a higher degree of crystallinity showed a higher moisture content. Low moisture content would avoid formation of liquid bridges between particles and eliminates powder flow problems. When adsorbed moisture is present at high concentration, the powders become cohesive resulting in poor flow (Nagel & Peck, 2003) and may affect the chemical stability of the tablets (Lieberman, Lachman & Schwartz, 1990). However, moisture content is also required to facilitate compaction during tableting, of which would affect the physicochemical properties of tablets, such as hardness, disintegration and dissolution (Faqih *et al.*, 2007). Therefore, moisture content of the powders needs to be optimised.

4.2.10.2 Densities

Density is defined as the ratio of the mass of powder to its volume. There are three types of density i.e true density, bulk density and tap density. True density refers to the mass of a powder divided by its powder volume, bulk density is the mass of a powder divided by its bulk volume and tap density is the mass of a powder divided by its bulk volume after tapping (Martin, Bustamante, & Chun, 1993; Newman, 1995). Results for the true, bulk and tap densities of the powders are presented in Table 4.11.

The true density of Avicel PH 101 of 158 g/cm^3 was the highest, followed by sago starch 1.55 g/cm^3, pregelatinised sago starches (PS1, PS2, PS3) 1.52 g/cm^3, PS4 1.51 g/cm^3, and Spress® B820 1.50 g/cm^3. It was found that the true density of the powders was dependent on the internal porosity and the size of the particles ($p<0.05$). Avicel PH 101 is a crystalline powder composed of porous particles (Bolhuis & Chowhan, 1996); as such Avicel PH 101 is left with a lowest actual powder volume resulting in the highest true density of the powders (Table 4.11). As shown in Table 4.10 and Figure 4.20 - 4.26, Spress® B820 and all pregelatinised sago starches (PS4, PS3, PS2 and PS1) have mean particle size (diameter) with significantly larger value ($p<0.05$) than sago starch. This was due to the formation of the agglomerate granular; therefore the actual volume of granular Spress® B820 and pregelatinised sago starches are higher than actual volume of granular sago starch, thus resulting in their lower true density (Table 4.11). True density plays a critical role in determination of powder porosity, particle mechanical properties and powder flowability (Cao *et al.*, 2008).

As for bulk density, Spress® B820 exhibited the highest value i.e. at 0.64 followed by sago starch 0.63 g/cm^3, pregelatinised sago starches (PS1, PS2, PS3) 0.53 g/cm^3, PS4 0.52 g/cm^3, and Avicel PH 101 0.35 g/cm^3. According to Martin, Bustamante, & Chun (1993), bulk density of a powder is affected by particle size distribution, particle shape and cohesiveness of the particles. Avicel PH 101 appeared as the smallest size after sago starch and the lowest moisture content among the powders (Tables 4.10 & 4.11). However, due to its fibrous particles (Ohwoavworhua, Adelakun & Okhamafe, 2007) and matchstick-like or rodlike structure (Bolhuis & Chowhan, 1996) as shown in Figure 4.14, particles of Avicel PH 101 were packed in irregular manner to give large voids among the particles. As a

result, Avicel PH 101 showed the highest bulk volume and lowest bulk density (Table 4.11).

Sago starch exhibited smaller mean particle size (diameter) and higher moisture content than pregelatinised sago starches (Tables 4.10 & 4.11). Smaller particle size may pack in such a way that leaves narrower gaps between the particles. In addition with the oval shape and higher cohesiveness as indicated by higher moisture content, sago starch particles pack closer to each other. Because of that, sago starch has smaller bulk volume and therefore produces higher bulk density. Conversely, the particle size of the pregelatinised sago starches were larger, lesser moisture content and more irregular in shape with rougher surface texture, thus the packing showed larger voids. This resulted in higher bulk volume and therefore lower bulk density. In this context, particle with larger size and lower moisture content will produce lower bulk density ($p<0.05$) (Table 4.11). However, this trend is not applicable for Spress® B820. Although its particle size is larger and its moisture content is lower than both sago starch and pregelatinised sago starches (PS1, PS2, PS3, and PS4), Spress® B820 exhibited higher bulk density than both of them. This could be due to the particles packing properties, where more of the small particles lie in between the larger ones to form lower bulk volume.

The mean value of tap density obtained for sago starch was 0.73 g/cm^3. It was the highest among the rest of the powders, followed by Spress® B820 0.71 g/cm^3, pregelatinised sago starches (PS1, PS2) 0.63 g/cm^3, PS3 0.62 g/cm^3, PS4 0.61 g/cm^3 and Avicel PH 101 0.44 g/cm^3 (Table 4.11). Tapping actions would allow smaller particles slip between the larger ones to form lower bulk volume, consequently tap density is always higher than bulk density (Table 4.11) and thus the sequence should be similar to the bulk density. However,

sago starch exhibited an exception, where its tap density is the highest (0.73 g/cm^3) instead of Spress® B820 (0.71 g/cm^3). This is probably due to the small particle size and high cohesiveness or moisture content ($p<0.05$) of the sago starch and the tapping treatment causes the particles of sago starch packing become closer to give low bulk volume and high tap density.

Overall, it was noted that the densities (true, bulk and tap densities) of the pregelatinised sago starches were significantly different ($p<0.05$) from their unmodified form (sago starch) and the densities decreased ($p<0.05$) as the heating time for pregelatinisation increased.

In powder technology, densities affect several other physical characteristics such as mixing uniformities, flow properties, compressibility, tablets porosity and their dissolution. If there are significant differences in the particle densities between the drug substance and excipients, this may lead to segregation during mixing of the powders. When segregation is occurring during compaction process, it will influence the content uniformity of the end product. Particles with high density and low-internal porosity tend to have free-flowing characteristics (Nagel & Peck, 2003; Nokhodchi, 2005). Particles which are hard and dense require higher compression to produce cohesive compacts. Furthermore, when higher compression is applied during tableting, the resulting tablet would exhibited longer disintegration times and slower dissolution rate (Lieberman, Lachman, & Schwartz, 1990; Swarbrick & Boylan, 2002). In addition, the knowledge of the densities of the active ingredients and excipients can provide perspective to the size of the final tablet as well as the choice of size and type of processing equipment. Hence, the bulky powder or low bulk density powder requires a larger packaging size and limits the percentage of active

ingredient/s contained (Lieberman, Lachman, & Schwartz, 1990; Sinko, 2006; Swarbrick & Boylan, 2002). Therefore a powder with high bulk density is preferable for a direct compression tablet excipient than a powder with low bulk density.

4.2.10.3 Porosity

The consequences of differences in density ($p<0.05$) were reflected in the total porosity. According to Newman (1995), total porosity is a combination of the void volume and pores within the particles (interparticulate and intraparticulate pores). Hence, it can be calculated from the volume measurements (true volume and bulk volume) or the density values (true density and bulk density) and can be expressed in percentage (Equation 3.5). As presented accordingly in Table 4.11, Avicel PH 101 (77.84%) showed the highest total porosity, followed by PS4 (65.34%), PS3 & PS2 (65.13%), PS1 (64.91%), sago starch (59.35%) and Spress® B820 (57.33%). Porosity could provide information on flow properties of powders (Guerin *et al.,* 1999), and powders with high density and low internal porosity tend to be free flowing (Martin, Bustamante, & Chun, 1993).

4.2.11 Flow properties

Flowability of powders is crucial in the manufacturing of tablets, since it would determine the uniformity of weight and content as well as the hardness of tablets. Therefore, determination of flow properties is very essential prior to tableting. Powder flow properties are commonly evaluated by measurements of Carr's compressibility index (CI, %) and Hausner ratio (HR) through determination of bulk density and tap density, and measurement of angle of repose and powder flow rate through an orifice flow tester (Guerin *et al.,* 1999; Schüssele & Bauer-Brandl, 2003; Shah, Tawakkul, & Khan, 2008).

4.2.11.1 The Carr's compressibility index (CI, %) and Hausner ratio (HR)

The Carr's compressibility index (CI) and Hausner ratio (HR) were calculated according to Equations (3.6) and (3.7) respectively. The results were tabulated in Table 4.12 and the values showed significant difference ($p<0.05$) among the powders. The CI and HR are qualitative assessment and indirect methods to determine flowability of a powder through measurements of its bulk and tap density (Shah, Tawakkul, & Khan, 2008). These are based on the fact that the densification of a powder occurred during the determination of tapped density which is influenced by the powder bridge strength and interparticulate frictions, factors that affect the flowability of a powder. In this case, CI is a measure of the powder bridge strength and HR is a measure of the interparticulate frictions. The lower CI or HR of the powders indicates their flowability is better than the higher ones (Abdullah & Geldart, 1999; Carr, 1965; Santomaso, Lazzaro, & Canu, 2003; Shah, Tawakkul, & Khan, 2008).

Table 4.12: Flow properties of each powder sample.

Powder sample	Carr's compressibility index, (CI,%)±SD	Hausner ratio, (HR)±SD	Angle of repose, α (°)±SD	Flow rate (g/s)±SD
Avicel PH 101	20.45±0.00	1.26±0.00	41.87±0.51	1.27±0.06
Spress® B820	9.86±0.00	1.11±0.00	30.23±0.46	6.39±0.24
Sago starch	13.70±0.00	1.16±0.00	-	-
PS1	15.79±0.14	1.19±0.00	32.20±0.40	4.84±0.14
PS2	15.42±0.78	1.18±0.01	31.93±0.61	5.01±0.25
PS3	14.97±0.78	1.18±0.01	30.97±0.45	5.46±0.17
PS4	14.67±0.13	1.17±0.00	30.37±0.23	5.90±0.35

Note: n=3 for each powder for all properties.

Table 4.13: Scale of flowability (Carr, 1965).

Carr's compressibility index (CI, %)	Flow character	Hausner ratio (HR)
1 – 10	Excellent	1.00 – 1.11
11 – 15	Good	1.12 – 1.18
16 – 20	Fair	1.19 – 1.25
21 – 25	Passable	1.26 – 1.34
26 – 31	Poor	1.35 – 1.45
32 – 37	Very poor	1.46 – 1.59
> 38	Very, very poor	> 1.60

Based on Table 4.13, Avicel PH 101 (CI: 20.45%, HR: 1.26) was rated as passable. Spress® B820 (CI: 9.86%, HR: 1.11) was rated as excellent flow. Sago starch (CI: 13.70%, HR: 1.16) and pregelatinised sago starches PS4 (CI: 14.67%, HR: 1.17), PS3 (CI: 14.97%, HR: 1.18), PS2 (CI: 15.42%, HR: 1.18) were rated as having good flow. Pregelatinised sago starch PS1 (CI: 15.79%, HR: 1.19) was rated as fair flow. The ranking of rates for CI and HR has a similar pattern and highly correlated ($p<0.05$, $R^2 = 0.998$) since it is derived from the same data, i.e. their value of bulk densities and tap densities. According to Martin, Bustamante, & Chun (1993), bulk density and tap density are influenced by particle size, porosity and cohesiveness (moisture content) of the powders, and this study found these three factors, either individually or in combinations (partly or fully), were statistically proven ($p<0.05$) to be affecting the CI and HR values of the powders evaluated. Based on the values of CI and HR obtained, Spress® B820 appeared to have the best flow characteristics, followed by sago starch, pregelatinised sago starches (PS4, PS3, PS2 and PS1 respectively) and Avicel PH 101.

It was observed that sago starch has CI and HR values lower than its pregelatinised forms ($p<0.05$), which can be translated that sago starch has better flowability (Table 4.12). This

finding could be related to the characteristics of particle size, porosity and cohesiveness of the sago starch ($p<0.05$) which contributed to the higher bulk density of sago starch (Martin, Bustamante, & Chun, 1993) than its pregelatinised forms (Table 4.11). Another factor is that the higher bulk density of sago starch could be the impact of frictional and abrasive forces during tapping, where the sago starch powders breakdown, hence the result might not be a true measure of the powder flow (Shah, Tawakkul, & Khan, 2008).

Among the pregelatinised sago starches, PS4 exhibited the best flow properties, as indicated by its lowest CI and HR values, and then followed by PS3, PS2 and PS1. Referring to Tables 4.10 & 4.11, the extension of heating time in the preparation of pregelatinised sago starches significantly ($p<0.05$) increased their particle size and reduced their moisture content. Particle size and moisture content are two factors that are indirectly related to the flow rate of the powder, where the bigger particle size are more free flowing and the higher moisture content presents the more cohesive powder (Newman, 1995).

Evaluations of powder flow through determination of CI and HR are simple (Guerin *et al.*, 1999) and fast (Santomaso, Lazzaro, & Canu, 2003). However, the results obtained should be supported with other measurements of powder flow, since these methods do not assess all the factors influencing flow properties of powder (Amidon, 1995).

4.2.11.2 Angle of repose

Angle of repose is a qualitative assessment of measuring internal cohesive and frictional effects in a loose powder, therefore it is an indirect method to determine flow characteristic of a powder (Martin, Bustamante, & Chun, 1993; Nagel & Peck, 2003;

Santomaso, Lazzaro & Canu, 2003; Staniforth, 2002). Table 4.14 shows angle of repose (°) which corresponds to the flow property.

Table 4.14: Angle of repose (°) and flow property (Carl, 1965).

Flow Property	Angle of repose (°)
Excellent	25 – 30
Good	31 – 35
Fair (aid not needed)	36 – 40
Passable (may hang up)	41 – 45
Poor (must agitate, vibrate)	46 – 55
Very poor	56 – 65
Very, very poor	> 66

Angle of repose of the powders was calculated according to Equation (3.8) and the results are tabulated in Table 4.12. The flowability of the powders was rated based on their angle of repose value. Powders with lower angle of repose indicate higher flowability than the higher ones (Table 4.14). Spress® B820 and pregelatinised sago starch PS4, with angles of repose 30.23° and 30.37º respectively, were rated as excellent flow; pregelatinised sago starches (PS3, PS2 and PS1), with angles of repos 30.97º, 31.93º and 32.20º respectively, were rated as good flow and Avicel PH 101 with angle of repose 41.87º was rated passable (may hang up). Sago starch failed to flow through the funnel of flow tester, therefore according to Table 4.14 its angle of repose can be considered to be more than 66º and rated as having very, very poor flow. Based on the results above, the sequence of decreasing flowability was Spress® B820 > pregelatinised sago starches (PS4 > PS3 > PS2 > PS1) > Avicel PH 101> sago starch, which was similar to the sequence of their particle size (Table 4.10). This indicated that angle of repose of the powders evaluated were significantly affected by their particle size ($p<0.05$).

This study showed that pregelatinisation process significantly decreases the angle of repose of the sago starch ($p<0.05$). It was observed that the longer the time adopted for pregelatinisation, the angle of repose was reduced significantly ($p<0.05$). PS4 appeared comparable against Spress® B820; both are categorised under excellent flow (Table 4.14) but their angle of reposes are different significantly ($p<0.05$). Avicel PH 101 was rated as poor flow as its compressibility index (CI) value is more than 20%. A powder with such CI value is not free flowing and has a tendency to create bridges in the hopper (Bhimte & Tayade, 2007). A limitation in measuring the angle of repose is when the powder presented a high moisture content (Bhimte & Tayade, 2007). In this study, moisture content of the powders evaluated were significantly ($p<0.05$) impacting their angle of repose. Sago starch for instance, with its moisture content of 12.81% was cohesive and as a result, sago starch failed to pass through the funnel. Introducing vibration to the funnel may be made, however such intervention might produce invariability in the measurement (Santomaso, Lazzaro, & Canu, 2003; Shah, Tawakkul, & Khan, 2008). Statistical analysis showed angle of reposes of the powders evaluated were significantly influenced by both their particle size and moisture content with very strong correlation ($p<0.05$, $R^2 = 0.996$).

4.2.11.3 Flow rate

Measurement of flow rate is a direct method of measuring flowability of the powder. Unlike indirect methods such as angle of repose, Compressibility index (CI) and Hausner ratio, this method is more dynamic and produces quantitative data (Staniforth, 2002). Results of the flow rate measurements are presented in Table 4.12. Spress® B820 has the highest flow rate (6.53 g/s) followed by PS4 (5.90 g/s), PS3 (5.46 g/s), PS2 (5.01 g/s), PS1 (4.84), Avicel PH 101 (1.27 g/s) and sago starch (failed to flow).

The ranking of flow rate of the powders above was in agreement with their respective particle size (Table 4.10), in which Spress® B820 was found to be the largest and sago starch was the smallest. This is because as the particle size increase, cohesiveness of powders is expected to decrease (Abdullah & Geldart, 1999; Staniforth, 2002). Larger particle size have smaller surface area and weaker friction among the particles, thus it facilitates better flow properties (Martin, Bustamante, & Chun, 1993). Reducing interparticulate frictions was also contributed by the presence of the fine particles to cover up the rough surfaces of the larger ones (Meyer & Zimmermann, 2004). However, this surface texture factor was only applicable for Spress® B820 and pregelatinised sago starches (PS4, PS3, PS2 and PS1).

The study also found that moisture content influenced the flow rate of the powders, with the exception of Avicel PH 101. The results showed that those with higher moisture content exhibited slower flow rate (Tables 4.11 & 4.12). This was due to the stronger cohesion and friction among the powders that impede powder flow (Faqih *et al.*, 2007; Nokhodchi, 2005).

The poor flow of Avicel PH 101 was mainly contributed by its particle shape, which is far from spherical (Abdullah & Geldart, 1999; Newman, 1995; Santomaso, Lazzaro, & Canu, 2003). Avicel PH 101 is fibrous particles with rodlike structures (Ohwoavworhua, Adelakun & Okhamafe, 2007; Bolhuis & Chowhan, 1996). As a result, entanglements between particles arise and hamper the flowability.

The failure of sago starch to flow in this study could be related to the mean particle size of 32.10 µm (Table 4.10) and moisture content of 12.8 (Table 4.11). Generally, powders with

particle size smaller than 30 μm tend to agglomerate and aggregate (Meyer & Zimmermann, 2004; Nagel & Peck, 2003; Verwijs, 2007). The presence of high moisture content in the powder would facilitate the formation of liquid bridges between the particles and develop powder caking (Nagel & Peck, 2003; Nokhodchi, 2005).

This study found that by converting the sago starch into pregelatinised forms it was able to change its flow characteristics from a cohesive powder to flowable powders. The flow rate of pregelatinised sago starches were in accordance with the heating time used in the preparation of pregelatinised sago starches (Table 4.12) and has a significant impact on the flow rate of the powders ($p<0.05$). Although the shapes of pregelatinised sago starches appeared to be more irregular than sago starch (Figure 4.17), they showed better flowabilty. This was because their particle size was bigger than those of sago starch (Gonnisen, Remon, & Vervaet, 2007). PS4, which was prepared with the longest heating time, exhibited the fastest flow rate among the pregelatinised sago starches. This was understandable due to the fact that PS4 appeared to have the largest mean particle size (Table 4.10) and the lowest moisture content (Table 4.11) than other pregelatinised sago starches. These results support the proposal that modification of starches by pregelatinisation would convert them into flowable powders (BP 2007; Kibbe, 2000; Odeku, Schmid, & Picker-Freyer, 2008, USP 27; USP 30). PS4 flow rate was comparable to Spress® B820 with ($p<0.05$) but superior to Avicel PH 101.

In general, statistical analysis shows that flow rates of the powders evaluated were significantly influenced by their particle size and moisture content with very strong correlation ($p<0.05$, $R^2 = 0.988$).

From the flow study above, the sequence of powder flowability by densification (CI and HR measurements) is the same as those obtained from the angle of repose and flow rate measurements, with the exception of sago starch. On the other hand, powder flowability by angle of repose was fully in agreement with the results obtained from the flow rate measurement.

4.3 Powder characterisations in compact form

Tables 4.15 – 4.21 showed all parameters required to analyse the compression and mechanical properties of Avicel PH 101, Spress® B820, sago starch, PS1, PS2, PS3 and PS4. The compression and mechanical properties for all samples are discussed in its own section.

Table 4.15: Parameters for analysis of compression and mechanical properties of Avicel PH 101.

P (MPa)	Hardness (N)	ρ_A (g/ml)	D	1 - D	ln 1/1 - D	C	P/C	T (MPa)
20	90.33± 1.53	0.88± 0.01	0.56±0.01	0.44±0.01	0.81±0.01	0.59±0.02	34.12±1.37	1.08±0.03
40	196.00±5.29	1.11± 0.01	0.70±0.01	0.30±0.01	1.21±0.02	0.68±0.01	58.54±0.49	2.97±0.09
60	291.00±3.61	1.26± 0.00	0.79±0.00	0.21±0.00	1.56±0.00	0.72±0.00	83.33±0.00	5.00±0.08
80	349.67±0.58	1.32± 0.01	0.83±0.01	0.17±0.00	1.77±0.00	0.73±0.00	109.59±0.00	6.28±0.06
100	402.67±2.08	1.36± 0.00	0.86±0.00	0.14±0.00	1.97±0.00	0.74±0.00	135.14±0.00	7.48±0.01
120	452.00±2.00	1.39± 0.01	0.88±0.01	0.12±0.01	2.12±0.09	0.75±0.00	160.00±0.00	8.60±0.03
140	459.00±1.73	1.44± 0.01	0.91±0.00	0.09±0.00	2.41±0.00	0.76±0.00	184.21±0.00	8.95±0.05
160	465.67±1.15	1.45± 0.00	0.92±0.00	0.08±0.00	2.53±0.00	0.76±0.00	210.53±0.00	9.23±0.05
180	478.33±1.53	1.47± 0.01	0.93±0.01	0.07±0.01	2.67±0.14	0.76±0.00	236.82±0.00	9.62±0.08
200	480.00±1.00	1.48± 0.01	0.94±0.00	0.06±0.00	2.81±0.00	0.76±0.00	263.16±0.00	9.72±0.03

Note: P = compression pressure, ρ_A = apparent density, D = relative density, C= degree of volume reduction, T = tensile strength, ε (porosity) = 1 – D, and n=3 for all parameters.

Table 4.16: Parameters for analysis of compression and mechanical properties of Spress® B820.

P (MPa)	Hardness (N)	ρ_A (g/ml)	D	1 - D	ln 1/1 - D	C	P/C	T (MPa)
20	20.33± 1.53	1.00± 0.01	0.67±0.01	0.33±0.01	1.10±0.02	0.36±0.01	55.58±1.55	0.27±0.02
40	40.33± 1.53	1.07± 0.01	0.71±0.01	0.29±0.01	1.25±0.02	0.40±0.01	99.19±1.41	0.59±0.03
60	70.67± 1.15	1.24± 0.01	0.83±0.01	0.17±0.01	1.75±0.03	0.48±0.00	125.00±0.00	1.19±0.02
80	107.33±1.53	1.28± 0.01	0.85±0.01	0.15±0.01	1.92±0.04	0.50±0,00	160.00±0.00	1.87±0.04
100	127.67±2.08	1.32± 0.01	0.88±0.01	0.12±0.01	2.15±0.05	0.52±0.00	192.31±0.00	2.31±0.06
120	148.33±1.53	1.35± 0.01	0.90±0.01	0.10±0.01	2.31±0.10	0.53±0.01	227.87±2.51	2.76±0.04
140	181.67±2.89	1.37± 0.01	0.91±0.01	0.09±0.01	2.45±0.07	0.53±0.01	262.52±2.82	3.44±0.06
160	188.33±2.08	1.39± 0.01	0.93±0.01	0.07±0.01	2.62±0.08	0.54±0.00	296.30±0.00	3.60±0.05
180	222.67±2.52	1.41± 0.01	0.94±0.01	0.06±0.01	2.82±0.17	0.55±0.01	329.29±3.50	4.28±0.08
200	224.00±2.00	1.42± 0.00	0.95±0.00	0.05±0.00	3.00±0.00	0.55±0.00	363.64±0.00	4.33±0.05

Note: P = compression pressure, ρ_A = apparent density, D = relative density, C= degree of volume reduction, T = tensile strength, ε (porosity) = 1 – D, and n=3 for all parameters.

Table 4.17: Parameters for analysis of compression and mechanical properties of sago starch.

P (MPa)	Hardness (N)	ρ_A (g/ml)	D	1 - D	ln 1/1 - D	C	P/C	T (MPa)
20								
40	20.33± 2.08	0.99± 0.01	0.64±0.01	0.36±0.01	1.03±0.02	0.36±0.01	110.11±1.73	0.28±0.03
60	33.00± 3.61	1.01± 0.01	0.66±0.01	0.34±0.01	1.07±0.02	0.38±0.01	159.31±2.47	0.44±0.04
80	33.67± 3.06	1.04± 0.01	0.67±0.01	0.33±0.01	1.10±0.02	0.39±0.01	203.42±2.96	0.48±0.05
100	40.33± 1.15	1.06± 0.01	0.68±0.00	0.32±0.00	1.14±0.00	0.41±0.00	243.90±0.00	0.59±0.02
120	48.33± 1.53	1.07± 0.00	0.69±0.00	0.31±0.00	1.17±0.00	0.41±0.00	292.68±0.00	0.72±0.02
140	49.00± 3.00	1.09± 0.01	0.70±0.01	0.30±0.01	1.21±0.02	0.42±0.01	330.75±4.47	0.74±0.05

Note: P = compression pressure, ρ_A = apparent density, D = relative density, C= degree of volume reduction, T = tensile strength, ε (porosity) = 1 – D, and n=3 for all parameters.

Table 4.18: Parameters for analysis of compression and mechanical properties of PS1.

P (MPa)	Hardness (N)	ρ_A (g/ml)	D	1 –D	ln 1/1 - D	C	P/C	T (MPa)
20								
40	27.33± 1.53	0.93± 0.01	0.62±0.00	0.38± 0.00	0.96±0.00	0.43±0.01	93.06±2.17	0.35±0.02
60	35.33± 3.06	0.95± 0.01	0.63±0.01	0.37± 0.01	1.00±0.02	0.44±0.01	136.41±3.10	0.46±0.04
80	47.33± 3.06	0.97± 0.01	0.65±0.00	0.35± 0.00	1.05±0.00	0.45±0.01	177.84±3.96	0.63±0.04
100	53.67± 1.53	0.99± 0.01	0.66±0.00	0.34± 0.00	1.08±0.00	0.46±0.00	217.39±0.00	0.73±0.02
120	64.33± 1.53	1.01± 0.00	0.67±0.00	0.33± 0.00	1.11±0.00	0.48±0.01	251.77±3.07	0.89±0.02
140	71.00± 2.00	1.02± 0.00	0.68±0.00	0.32± 0.00	1.14±0.00	0.48±0.00	291.67±0.00	1.00±0.04
160	76.00± 2.00	1.03± 0.01	0.69±0.00	0.31± 0.00	1.17±0.00	0.49±0.01	328.80±3.93	1.08±0.03
180	81.00± 2.00	1.05± 0.00	0.70±0.00	0.30± 0.00	1.20±0.00	0.49±0.01	365.00±8.66	1.17±0.03
200	83.67± 1.15	1.06± 0.00	0.71±0.00	0.29± 0.00	1.24±0.00	0.50±0.01	402.72±4.71	1.21±0.02

Note: P = compression pressure, ρ_A = apparent density, D = relative density, C= degree of volume reduction, T = tensile strength, ε (porosity) = 1 – D, and n=3 for all parameters.

Table 4.19: Parameters for analysis of compression and mechanical properties of PS2.

P (MPa)	Hardness (N)	ρ_A (g/ml)	D	1 -D	ln 1/1 – D	C	P/C	T (MPa)
20								
40	28.00± 3.00	0.95± 0.01	0.63±0.01	0.37± 0.01	0.98±0.01	0.44±0.01	90.24±1.17	0.36±0.05
60	47.67± 5.51	0.99± 0.01	0.65±0.01	0.35± 0.01	1.06±0.02	0.46±0.01	129.51±1.60	0.65±0.08
80	70.00± 2.00	1.03± 0.01	0.68±0.01	0.32± 0.01	1.13±0.02	0.49±0.01	164.40±1.96	0.99±0.04
100	79.33± 4.04	1.06± 0.01	0.70±0.00	0.30± 0.00	1.20±0.00	0.50±0.00	200.00±0.00	1.16±0.07
120	89.67± 1.53	1.09± 0.00	0.72±0.00	0.28± 0.00	1.27±0.00	0.51±0.00	235.29±0.00	1.35±0.03
140	97.67± 2.52	1.11± 0.01	0.73±0.01	0.27± 0.01	1.31±0.04	0.52±0.01	267.54±2.93	1.49±0.05
160	102.33±2.52	1.13± 0.00	0.74±0.00	0.26± 0.00	1.34±0.00	0.53±0.00	301.89±0.00	1.60±0.05
180	106.33±2.52	1.14± 0.00	0.75±0.00	0.25± 0.00	1.39±0.00	0.54±0.00	333.33±0.00	1.67±0.04
200	112.67±3.06	1.18± 0.02	0.77±0.02	0.23± 0.02	1.48±0.07	0.55±0.01	363.72±6..61	1.83±0.08

Note: P = compression pressure, ρ_A = apparent density, D = relative density, C= degree of volume reduction, T = tensile strength, ε (porosity) = 1 – D, and n=3 for all parameters.

Table 4.20: Parameters for analysis of compression and mechanical properties of PS3.

P (MPa)	Hardness (N)	ρ_A (g/ml)	D	1 -D	ln 1/1 - D	C	P/C	T (MPa)
20								
40	35.33± 0.58	0.95± 0.00	0.63±0.00	0.37± 0.00	0.99±0.00	0.44±0.00	90.91±0.00	0.46±0.01
60	70.33± 1.53	0.97± 0.01	0.64±0.00	0.36± 0.00	1.02±0.00	0.45±0.01	132.36±1.67	0.94±0.02
80	77.33± 2.52	1.02± 0.00	0.67±0.00	0.33± 0.00	1.12±0.00	0.48±0.00	166.67±0.00	1.08±0.05
100	83.67± 4.16	1.04± 0.01	0.68±0.00	0.32± 0.00	1.14±0.00	0.49±0.00	204.08±0.00	1.19±0.06
120	93.67± 3.51	1.06± 0.01	0.70±0.01	0.30± 0.01	1.19±0.02	0.50±0.00	240.00±0.00	1.36±0.06
140	100.33±2.52	1.09± 0.01	0.72±0.00	0.28± 0.00	1.27±0.00	0.51±0.01	272.75±3.05	1.51±0.04
160	112.67±4.51	1.12± 0.02	0.74±0.02	0.26± 0.02	1.35±0.07	0.53±0.01	306.46±8.80	1.74±0.08
180	123.33±3.01	1.16± 0.01	0.76±0.01	0.24± 0.01	1.44±0.02	0.54±0.01	331.31±3.50	1.97±0.06
200	134.00±3.00	1.21± 0.01	0.80±0.01	0.20± 0.01	1.59±0.03	0.56±0.00	357.14±0.00	2.23±0.06

Note: P = compression pressure, ρ_A = apparent density, D = relative density, C= degree of volume reduction, T = tensile strength, ε (porosity) = 1 – D, and n=3 for all parameters.

Table 4.21: Parameters for analysis of compression and mechanical properties of PS4.

P (MPa)	Hardness (N)	ρ_A (g/ml)	D	1 –D	ln 1/1 - D	C	P/C	T (MPa)
20	38.33± 1.53	1.00± 0.01	0.66±0.00	0.34± 0.00	1.08±0.00	0.48±0.01	41.96±0.51	0.53±0.02
40	59.67± 2.08	1.04± 0.01	0.68±0.01	0.32± 0.01	1.15±0.02	0.50±0.01	80.54±0.94	0.85±0.03
60	72.67± 1.53	1.06± 0.01	0.70±0.00	0.30± 0.00	1.20±0.00	0.51±0.01	118.43±1.36	1.06±0.03
80	102.33±1.53	1.11± 0.01	0.73±0.01	0.27± 0.01	1.32±0.02	0.53±0.01	150.98±2.85	1.57±0.03
100	120.67±3.06	1.16± 0.02	0.76±0.01	0.23± 0.01	1.46±0.05	0.55±0.01	181.86±3.31	1.94±0.07
120	143.00±2.65	1.23± 0.01	0.81±0.01	0.19± 0.01	1.66±0.05	0.58±0.01	208.11±2.10	2.41±0.06
140	160.33±2.52	1.28± 0.03	0.84±0.02	0.16± 0.02	1.86±0.16	0.59±0.02	236.06±6.03	2.81±0.11
160	179.00±1.00	1.32± 0.01	0.87±0.01	0.13± 0.01	2.07±0.05	0.61±0.01	263.76±2.52	3.25±0.03
180	188.67±1.15	1.36± 0.01	0.89±0.01	0.11± 0.01	2.24±0.05	0.61±0.01	293.49±2.75	3.52±0.05
200	204.33±1.53	1.40± 0.01	0.92±0.01	0.08± 0.01	2.49±0.14	0.63±0.01	319.17±2.97	3.92±0.05

Note: P = compression pressure, ρ_A = apparent density, D = relative density, C= degree of volume reduction, T = tensile strength, ε (porosity) = 1 – D, and n=3 for all parameters.

4.3.1 Compression properties

Figure 4.25 shows Heckel plot of the powders evaluated and their constants are listed in Table 4.22.

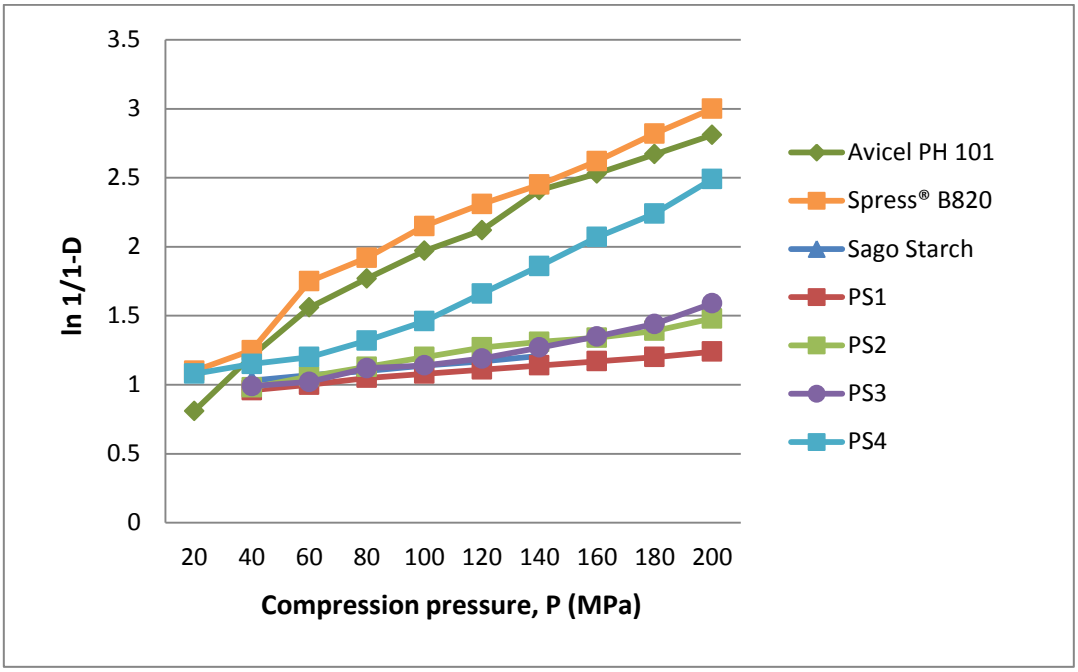

Figure 4.25: The graphs of ln 1/1-D versus compression pressure, P for the powders.

Table 4.22: Heckel plot constants and parameters of the powders.

Powder	Plot constants			Parameters			
	k	A	R^2	D_0	D_a	D_b	P_y
Avicel PH 101	0.0106	0.8147	0.9709	0.22	0.56	0.34	94.34
Spress® B820	0.0104	0.9973	0.9754	0.43	0.63	0.20	96.15
Sago starch	0.0018	0.9606	0.9984	0.41	0.62	0.21	555.56
PS1	0.0017	0.9036	0.9939	0.35	0.59	0.24	588.24
PS2	0.0029	0.8880	0.9852	0.35	0.59	0.24	344.83
PS3	0.0035	0.8094	0.9617	0.35	0.55	0.20	285.71
PS4	0.0080	0.7700	0.9680	0.34	0.54	0.20	125.00

Constant k values were obtained from the slope of the Heckel plots with the linearity in the range of 0.9617 – 0.9984 for all of the powders evaluated. The strong linearity indicates that the plastic deformation was dominant (Odeku & Itiola, 2007). Mean

yield pressure (P_y), which is the reciprocal of k, is the pressure or stress when the plastic deformation starts (Paronen & IIkka, 1996). Thus, lower value of P_y indicates greater plasticity of the materials (Busignies *et al.*, 2006; Odeku & Itiola, 2007). The intercept of the plots give values of constant A, which is related to the particle rearrangement before deformation and bonding (Shittu *et al.*, 2012) and it reflects the densification of powders in the early stage of compaction (Mitrevej, Sinchaipanid, & Faroongsarng, 1996). D_0 is densification at zero pressure as a result of die filling and is equal to the ratio of bulk density at zero pressure to the true density (relative bulk density), D_b is densification due to movement and rearrangement of particle (densification of fragmentation) and D_a is total densification of plastic deformation before interparticle bonding becomes appreciable (Hsu *et al.*, 1997; Mitrevej, Sinchaipanid, & Faroongsarng, 1996; Shittu *et al.*, 2012).

Referring to Table 4.22, overall the P_y value for Avicel PH 101 is lower ($p<0.05$) than all of the starches, indicating that Avicel PH 101 is more plastic and the onset of its plastic deformation occurred at the lower pressures. These results were similar to the previous study by Zhang, Law, & Chakarabarti (2003), where Avicel PH 101 was found to perform plastic deformation under pressure. With exception of PS1, it was observed that the P_y value of sago starch was found to be higher ($p<0.05$) than its pregelatinised forms, suggesting that pregelatinised sago starches have greater plasticity than the sago starch ($p<0.05$) and the P_y values decreased with an increase in the degree of gelatinisation (Table 4.15, $p<0.05$). A similar research was conducted by Alebiowu & Itiola (2002) on sorghum, plantain and corn starches concluded that pregelatinisation of the starches improved their plasticity. The plasticity of PS4 was the highest among the pregelatinised sago starches but slightly lower than Spress® B820 ($p<0.05$) as indicated by their P_y values (Table 4.22).

According to Patel, Kaushal, & Bansal (2007), in general the particle shape will affect the value of P_y. Material with irregular particles will show a lower P_y values with higher compressibility as compared to the materials that consists of regular particles (Alderborn, 2002; Korhonen *et al.*, 2002; Paronen & IIkka, 1996). As discussed previously, among the powders evaluated Avicel PH 101 was the most irregular in shape, followed by Spress® B820, PS4, PS3, PS2, PS1 and sago starch. The study found that the sequence of decreasing P_y values of the powders was in line with the increasing irregularity degree of particle shape ($p<0.05$, $R^2= - 0.950$). Bouvard (2000) and Paronen & IIkka (1996) stated that materials with irregular shape tend to deform plastically and enhanced by the presence of rough surface. The mean yield pressure (P_y) of larger particle was also consistently lower than the smaller particle ($p<0.05$) (Table 4.22 and Table 4.10). Thus, it can be concluded that materials with greater particle size have greater ability to deform plastically under the same compression force as compared to smaller particle (Bouvard, 2000; Korhonen *et al.*, 2002; Nokhodchi *et al.*, 2007; Patel, Kaushal, & Bansal, 2007). From statistical analysis, this study showed that plasticity of the powders evaluated were significantly influenced ($p<0.05$) by their degree of shape irregularity and size. Avicel PH 101 was found to have the lowest P_y value even though its average particle size was the second lowest among the powders evaluated. This indicated that the plastic deformation of Avicel PH 101 was dominated by its irregular shape and rough surface texture (Bouvard, 2000; Paronen & IIkka, 1996). Besides that, structurally Avicel PH 101 is fibrous in nature; such materials are known to exhibit excellent plastic deformation (Almaya & Aburub, 2008). PS1 showed an exception, where it has a lower plasticity than the sago starch, although all of the factors discussed above were in favour of PS1 (higher degree of gelatinisation, higher degree of shape irregularity and higher average of particles size) to

have higher plasticity. However, results from the Heckel plot analysis showed otherwise, as indicated by its P_y value, which was higher than the sago starch (P_y value and k was significantly different). A possible explanation is that the plastic deformation in sago starch and PS1 was dominated by the degree of particle shape irregularity (Bouvard, 2000; Paronen & IIkka, 1996). These were based on the facts that the average particle size and the gelatinisation degree between the sago starch and PS1 were significantly different ($p<0.05$), while from the SEM analysis (Figure 4.17), as has been discussed previously (Section 4.2.6), there were no obvious dissimilarity for the surface texture and shape between sago starch and PS1 granules. According to Zhang, Law, & Chakarabarti (2003), group of starch performs plastic and fragmentation deformation, while Heckel equation presumed that the changes in the volume of the powder bed after particle rearrangement are solely due to the plastic deformation (Patel, Kaushal, & Bansal, 2007). This renders the Heckel equation to have less discriminative power (Patel, Kaushal, & Bansal, 2007; Sonnergaard, 1999).

The D_0 value for the Avicel PH 101 was the lowest among the powders tested. This was probably the initial densification as a result of die filling affected by fibrous rod-like structure of Avicel PH 101 (Ohwoavworhua, Adelakun, & Okhamafe, 2007; Bolhuis & Chowhan, 1996), thus interfering the initial packing in the die resulting to produce low densification. Within the sago starch group, sago starch showed higher D_0 value than all of its pregelatinised forms (Table 4.22), indicating that pregelatinisation of sago starch did not enhance its densification at zero pressure. Sago starch showed smaller particle size (Table 4.10) than its pregelatinised forms resulting in higher densification. Within the pregelatinised sago starches, PS4 exhibits the lowest D_0 value due to having the largest particle size among the rest, although their D_0 values were of minimal difference ($p<0.05$).

As for Spress® B820, although it has a larger average particle size than the sago starch group, it exhibited higher D_0 value. This was probably due to the particles packing arrangement of Spress® B820, where its small particles filled interparticle void, forming better densification (Bouvard, 2000; Korhonen *et al.*, 2002; Nokhodchi *et al.*, 2007; Patel, Kaushal, & Bansal, 2007).

Avicel PH 101 also possessed the highest D_b value, suggesting that Avicel PH 101 experienced the most fragmentation among the powders tested at low pressure. Within the sago starch group, it can be seen that the D_b values for PS1 and PS2 were higher than the sago starch. This is probably due to the fragile agglomerates of PS1 and PS2 as a result of the short pregelatinisation process applied, which was only 15 minutes and 30 minutes respectively. However, the values of D_b decreases with increasing pregelatinisation time as in the case for PS3 and PS4, which was pregelatinised for 45 minutes and 60 minutes respectively. This longer pregelatinisation time would probably produce stronger agglomerates, thus resulting in lower fragmentation under low pressure (lower D_b value). Lower value of D_b is also an indication of the particles' higher resistance to move (Ohwoavworhua, Adelakun, & Okhamafe, 2007). In comparison, D_b value for Spress® B820 was the same as PS3 and PS4.

This study found that the ranking of D_a values was Spress® B820 > sago starch > PS1 > PS2 > Avicel PH 101 > PS3 > PS4. The lower value of D_a indicates such powder has lower densification (Ohwoavworhua, Adelakun, & Okhamafe, 2007). Referring to Table 4.22, it was observed that within the sago starch group, pregelatinisation decreased their D_a values ($p<0.05$) and the values decrease with increasing particle size ($p<0.05$). According to

Ohwoavworhua, Adelakun, & Okhamafe (2007), D_a value correlated with the particle contact area, thus as expected PS4 showed the lowest D_a value since PS4 exhibited the largest particle size in the group, hence the smallest contact area. Spress® B820 has the largest average particle size among the powders evaluated, but showed the highest D_a value. This could be due to the particles of Spress® B820 packing arrangement, by which it is able to form a large surface contact as indicated by its highest initial densification, D_o (Patel, Kaushal, & Bansal, 2007; Sonnergaard, 2000). Avicel PH 101 was found to have the lowest D_0 value among the powders, but its D_a value is in-between the D_a values of PS2 and PS3 (Table 4.22). This is because the particles of Avicel PH 101 underwent the highest fragmentation (D_b value) resulting in higher surface area.

Figure 4.26 shows Kawakita plots for the powders evaluated, and the Kawakita constants are tabulated in Table 4.23.

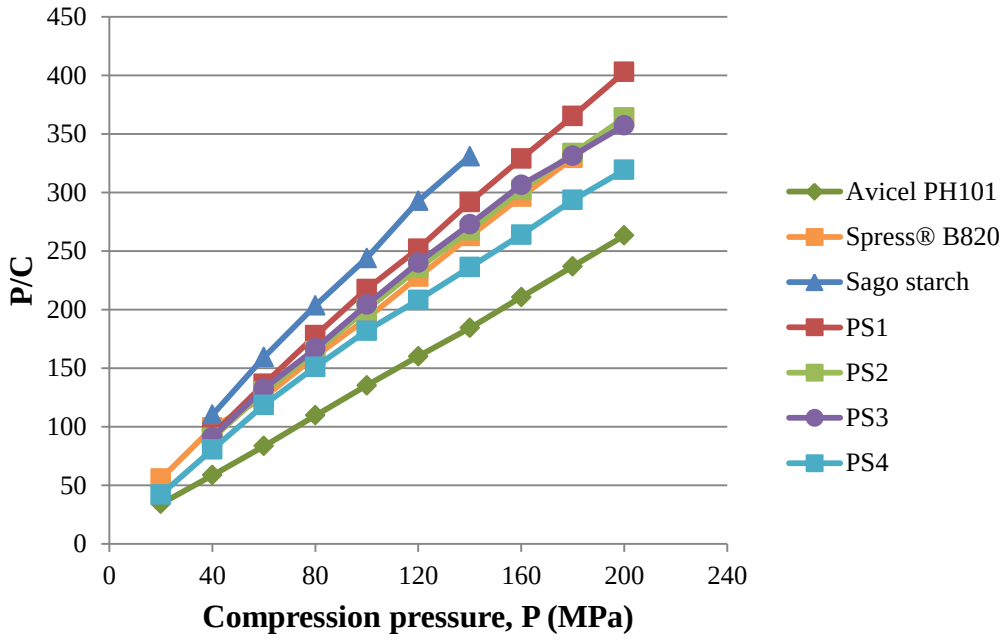

Figure 4.26: The graphs of P/C versus compression pressure, P for the powders.

Table 4.23: Kawakita plot constants of the powders.

Powder	a	b	R^2	D_i (1 – a)	P_k
Avicel PH 101	0.7868	0.1621	0.9999	0.21	6.17
Spress® B820	0.6174	0.0646	0.9994	0.38	15.48
Sago starch	0.4534	0.0887	0.9989	0.55	11.27
PS1	0.5216	0.0889	0.9993	0.48	11.25
PS2	0.5860	0.0633	0.9990	0.41	15.80
PS3	0.5970	0.0515	0.9953	0.40	19.42
PS4	0.6609	0.0658	0.9957	0.34	15.20

The plots showed a linear relationship at any compression pressures applied with a correlation coefficient (R^2) of 0.9953 and above. From the table, constant a (slope) is indicative of total volume reduction of the powder bed (compressibility), D_i (1 – a) is related to the initial relative density at low pressure and b is a constant where its reciprocal value, P_k, is related to the yield strength of the particles (Alebiowu & Itiola, 2002; Shittu, *et al.,* 2012). In terms of constant a, Avicel PH 101 was the most compressible among the powders evaluated. Within the sago starch category, PS4 was found to be the most compressible, followed by PS3, PS2, PS1 and sago starch. This indicated that pregelatinisation increased compressibility of the sago starch ($p<0.05$) and the degree of compressibility increased with increasing degree of gelatinisation ($p<0.05$). As for Spress® B820, its compressibility was higher than PS3 but lower than PS4. These results of constant a values were in line with the mean yield pressure (P_y) values obtained from the Heckel analysis above, where a powder with lower mean yield pressure would generally demonstrate higher compressibility (Alderborn, 2002; Korhonen *et al.,* 2002; Paronen & IIkka, 1996). Table 4.23 shows the D_i (1 – a) value for the sago starch was the highest, followed by PS1, PS2, PS3, Spress® B820, PS4 and Avicel PH 101. This indicated that the sago starch has the highest packing at low compression pressure. The results were in accordance with the fact that packing of a powder under compression pressure is

determined by its deformation tendency (Shittu *et al.,* 2012) and this study showed that the D_i (1 – a) values corresponded with their plasticity (P_y value). In terms of constant b, Avicel PH 101 showed the lowest yield strength among the powders evaluated. It was observed that overall the yield strengths of pregelatinised sago starches were higher than sago starch itself ($p<0.05$) with the exception of PS1, where its P_k value was slightly lower than sago starch ($p<0.05$, Table 4.23). Generally, the yield strength of the sago starch increased as the gelatinisation degree increases ($p<0.05$), although PS3 demonstrated a higher yield strength than PS4 ($p<0.05$). As for Spress® B820, its yield strength was slightly higher than PS4 ($p<0.05$) but below PS3 ($p<0.05$). According to Alebiowu & Itiola (2002), yield strength value (P_k) relates to the amount of plastic deformation occurring during compression process and this is responsible for the tensile strength value, where the lower in the value of P_k, the higher in the tensile strength. Excluding Avicel PH 101, the P_k values obtained from the Kawakita equation above were inconsistent with the tensile strength determination findings (Tables 4.15 – 4.21 and Figure 4.30), where Avicel PH 101 was found to have the highest radial tensile strength at any of the compression pressure applied. It was then followed by Spress® B820, PS4, PS3, PS2, PS1 and sago starch. These differences could be contributed by the different ability of the powders to form compacts under predetermined range of the compression pressure used in the study, which was from 20 to 200 MPa. As such, plots of the Kawakita equations were found to be using different ranges of compression pressures, as happened to sago starch versus PS1 and PS3 versus PS4. Sago starch powder only formed compacts under a shorter range of compression pressures (40 to 140 MPa) while PS1 formed compacts under a larger range of compression pressure of 40 to 200 MPa. As for PS3, it formed compacts from 40 to 200 MPa while PS4 was shown to form compacts at a larger range of compression pressure than PS3, i.e 20 to

200 MPa. Kawakita parameter is pressure-dependent; with such different ranges of compression pressure, these will impact on the curve fitting when P/C is plotted against P (Denny, 2002; Patel, Kaushal, & Bansal, 2007). The poor correlation between the yield strengths (P_k) obtained from Kawakita equation and the tensile strengths above was in agreement with the review as reported by Denny (2002), where he found that there have not been a good correlation between yield strength (P_k) and mechanical properties of a powder.

4.3.2 Mechanical properties

Figures 4.27 – 4.30 show the graphs of various mechanical properties for each powder evaluated.

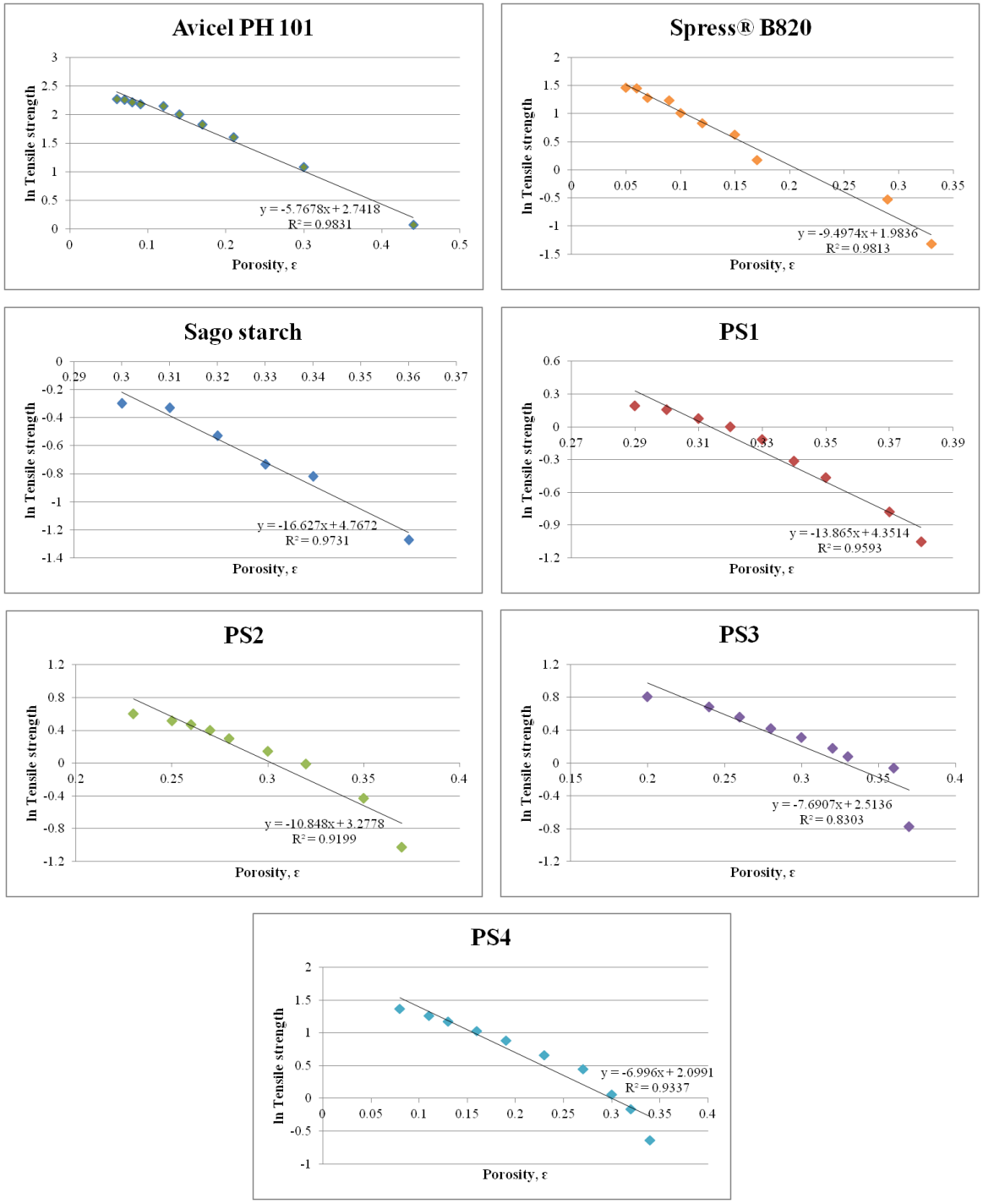

Figure 4.27: Plots of ln tensile strength vs porosity for each powder evaluated.

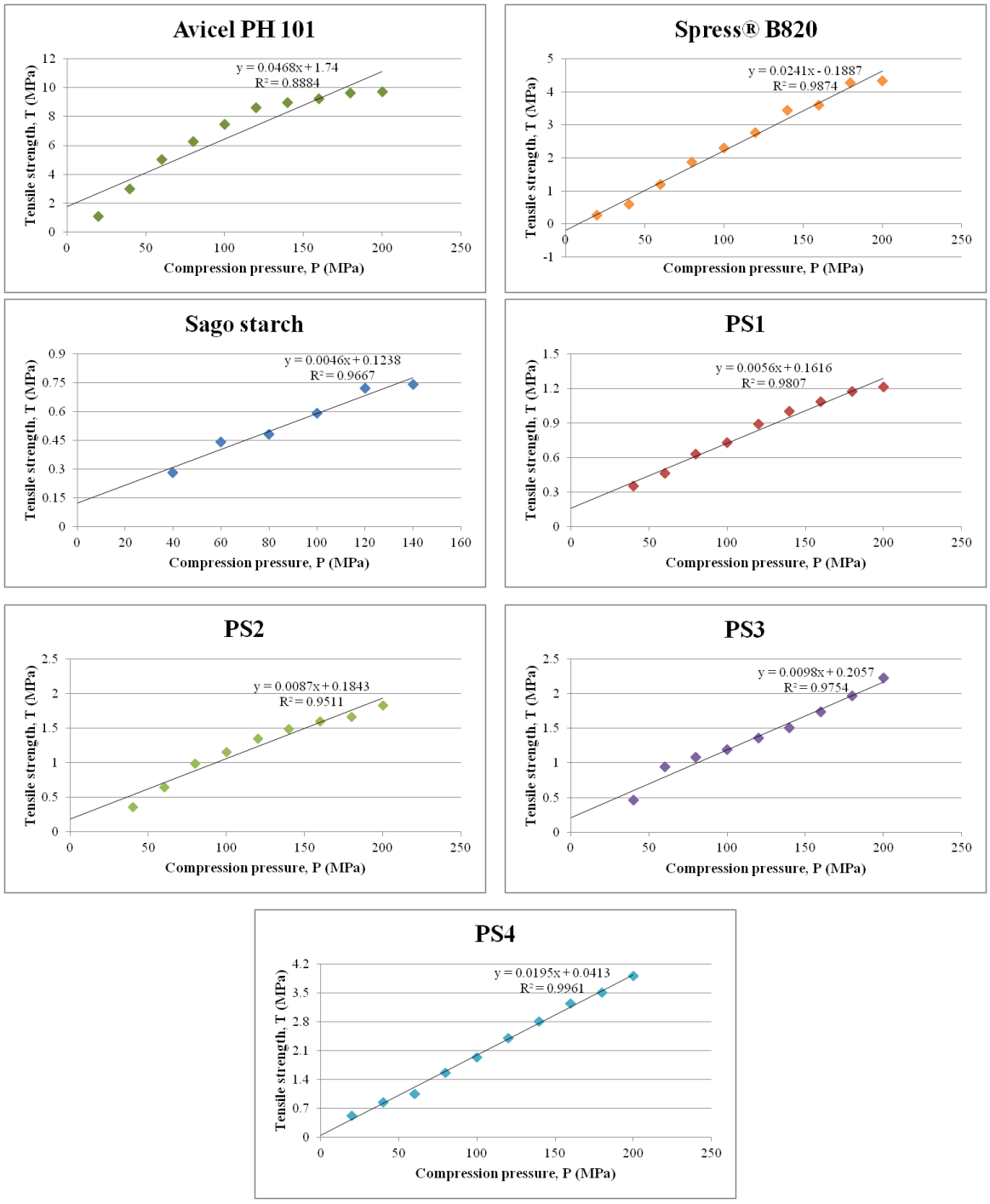

Figure 4.28: Plots of tensile strength vs compression pressure for each powder evaluated.

Table 4.24: AUC for each of the powder's tensile strength vs compression pressure.

Powder	Avicel PH 101	Spress® B820	Sago starch	PS1	PS2	PS3	PS4
AUC	1270.6	446.8	54.8	134.8	200.1	222.7	392.7

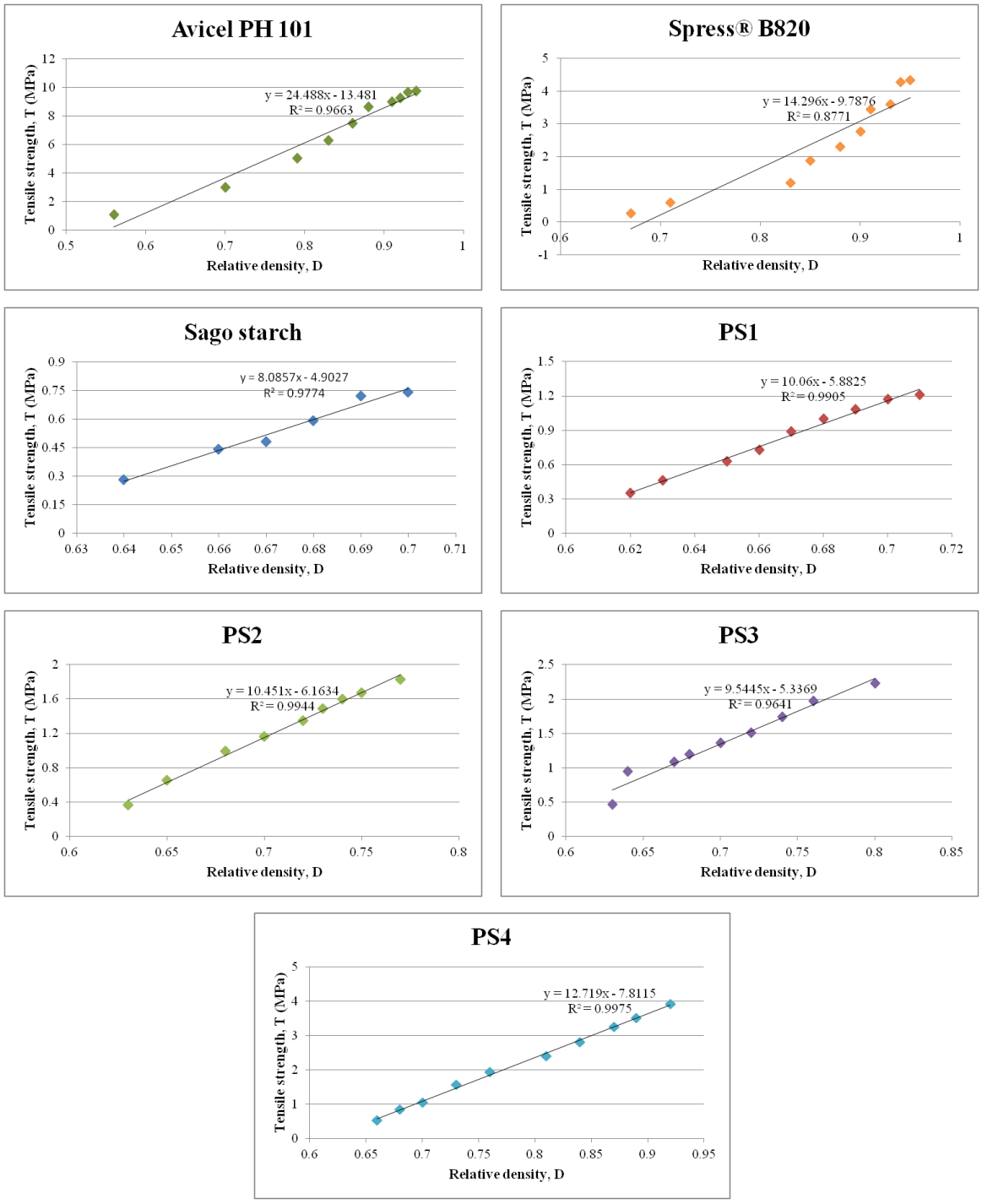

Figure 4.29: Plots of tensile strength vs the relative density for each powder evaluated.

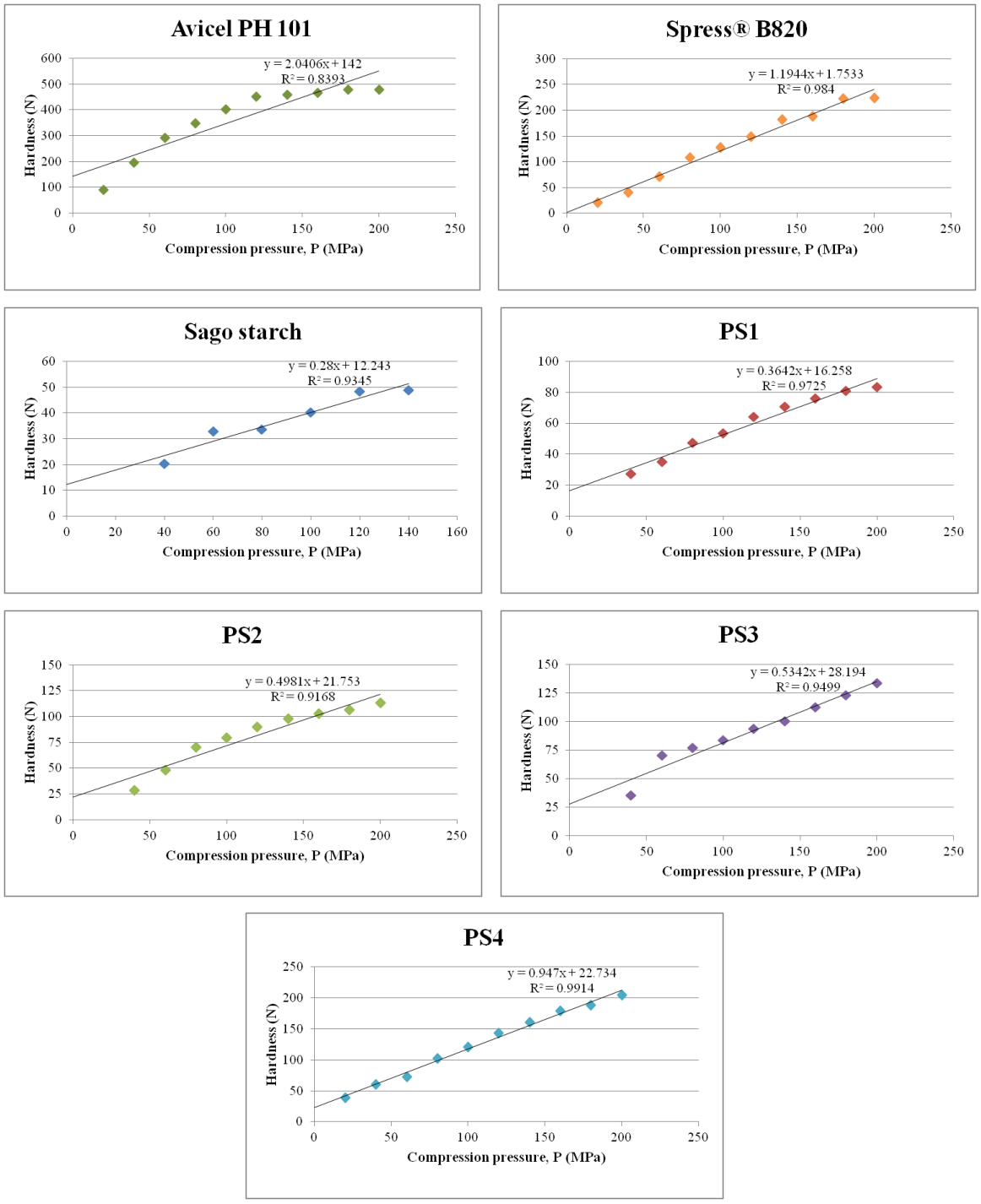

Figure 4.30: Plots of hardness versus compression pressure of each powder evaluated.

The compact hardness and radial tensile strength indicate the mechanical properties of the directly compressible materials. As shown by Figure 4.28 and 4.30, strong linear relationships were found for the plots of tensile strength versus compression pressure (R^2: 0.8884 – 0.9961) and the plots of hardness versus compression pressure (R^2: 0.9168 – 0.9914). Tensile strength and hardness increased with increasing compression pressure. At any of the same compression pressure applied, Avicel PH 101 was revealed to have the highest radial tensile strength and the hardest compacts, as indicated with its highest compactibility, followed by Spress® B820, PS4, PS3, PS2, PS1 and sago starch (Figures 4.27 and 4.28). These results showed that Avicel PH101 underwent the greatest degree of plastic deformation compared to the other starch groups, as confirmed by its lowest mean yield pressure (P_y) obtained from the Heckel plot analyses (Odeku, Schmid, & Picker-Freyer, 2008). The ranking of the compactibility above was also supported by their respective area under the curve of tensile strength versus pressure (Habib *et al.,* 1996), where the larger area indicates a higher compactibility (Table 4.24 and Figure 4.28).

The excellent hardness of Avicel PH 101 compacts was contributed by hydrogen bonding (Bolhuis & Chowhan, 1996). Under compression pressure, Avicel PH 101 experienced plastic deformation, producing smaller particles with larger surface area of contact and facilitated the formation of hydrogen bonding between the plastically deformed close particles. The bonding formation was also eased by the presence of optimum moisture content (5.19%) within the porous structure of Avicel PH 101 (Table 4.11) of which it acts as an internal lubricant to smoothen the flow within the individual microcrystalline particles during plastic deformation, thus enforcing the formation of hydrogen bonding (Bolhuis & Chowhan, 1996; Zhang, Law, & Chakrabarti, 2003). These findings were

similar to previous studies where applying compression pressure on Avicel PH 101 would produce excellent compact hardness (Zhang, Law, & Chakrabarti, 2003).

In comparison, the hardness and tensile strength of all starches, namely Spress® B820, PS4, PS3, PS2, PS1 and sago starch were much lower than Avicel PH 101 at any of the compression pressure applied. This is because the plastic deformation of starches that occurred during compression is too slow to form interparticle bonding (Bolhuis & Chowhan, 1996; Zhang, Law, & Chakrabarti, 2003), as indicated by their mean yield pressure (P_y) values obtained from the Heckel plot analyses (Table 4.22).

For the sago starch group, their compactibilities (hardness and tensile strength) increased with increasing degree of gelatinisation ($p< 0.05$), in the rank order of PS4 > PS3 > PS2 > PS1 > sago starch. Sago starch, PS1, PS2 and PS3, with degree of gelatinisation (DG) 0%, 9.67%, 14.43% and 27.17% respectively (Table 4.5), were not able to form compacts at 20 MPa, indicating they required more compression pressure to initiate the plastic deformation. The results showed that the compacts were only able to be formed starting at compression pressure of 40 MPa with the compacts hardness and tensile strength differing significantly ($p<0.05$) at any of the same compression pressure. Under conditions of the test, the hardness of the sago starch compacts were less than 60 N, indicating the compacts were generally weak (Odeku, Schmid, & Picker-Freyer, 2008) and the compacts exhibited brittle fracture at compression pressure above 140 MPa, due to the destruction of particle bonding as a result of the excessive force applied. Meanwhile, PS4 with DG of 34.40% was able to be compressed into compacts at lower compression pressure, i.e at 20 MPa, similar to Avicel PH 101 and Spress® B820. PS4 compacts tensile strength and hardness was the

strongest among the pregelatinised sago starches and is slightly lower than Spress® B820 ($p<0.05$). The study also found that the order of compact hardness and tensile strength among sago starch, PS1, PS2, PS3, PS4 and Spress® B820 were significantly ($p<0.05$) influenced by their particle size,particle shape and moisture content, both either stand alone or in any combinations of these three factors. As shown by sago starch, more number of smaller particles with larger number of contact points was produced during compression, causing the distribution of pressure applied on each contact point to be relatively lower, thus resulting in the softer compacts (Zhang, Law, & Chakrabarti, 2003). According to Kibbe (2000), starches are poorly compact; as such starches with too low moisture content are not suitable as direct compression materials. Hence, moisture content is needed to enhance compressibility and facilitate plastic deformation of glassy starches (Bolhuis & Chowhan, 1996). Though moisture content is required to facilitate the formation of compact, its presence should be at optimum state (Faqih *et al.*, 2007). Adsorbed water at optimum quantity will increase the number of solid bridges and enhance particle-particle interactions. It may also penetrate each other between adjacent particles resulting in the stronger attraction forces (Bolhuis & Chowhan, 1996). High moisture content, as shown by sago starch (Table 4.11), produced the weakest compact strength among the starch group evaluated. This was because the high moisture content formed multilayer water or free water at the surface of the particles, reducing interparticle attraction forces and thus weakening the compact strength (Bolhuis & Chowhan, 1996).

Plots of tensile strength versus relative density of the powder compacts are presented in Figure 4.29. It can be seen that there is a strong correlation between tensile strength and relative density for all of the powders with R^2 values in the range of 0.8771 – 0.9975. The

increased tensile strength was followed by the increasing relative density. This was probably due to the decreasing porosity of the compact powders to which provide larger surface contacts and eventually facilitate the formation of the stronger interparticulate bonding (Adedokun & Itiola, 2011) as shown in Figure 4.27 (ln tensile strength vs porosity). It was noted that, even though Spress® B820 showed lower compacts porosity than Avicel PH 101 at any of the same compression pressures, its compacts' tensile strengths were weaker. This is due to the fact that the plasticity and compactibility of Spress® B820 was lower than Avicel PH 101, as has been explained above.

4.3.3 Lubricant sensitivity

Tables 4.25 – 4.26 and Figure 4.31 show the effects of various concentrations of magnesium stearate on the hardness of Avicel PH 101 at different compression pressures.

Table 4.25: Mixture of Avicel PH 101and magnesium stearate.

P (MPa)	Hardness (N)				
	Concentration of magnesium stearate (%)				
	0	0.25	0.5	0.75	1.00
20	90.33±1.53	63.67±1.52	60.33±1.52	50.33±2.08	50.00±2.00
40	196.00±5.29	161.00±1.73	153.67±1.52	148.67±1.53	148.67±1.53
60	291.00±3.61	254.67±1.15	250.67±2.52	241.67±1.53	241.67±1.53
80	349.67±0.58	334.33±3.06	322.33±1.52	312.67±3.06	312.33±2.52
100	402.67±2.08	377.67±2.08	368.33±2.08	362.67±2.08	362.33±2.52
120	452.00±2.00	429.67±0.58	420.00±2.00	410.00±2.00	410.00±2.00

Note: P = compression pressure, n= 3 for all concentrations.

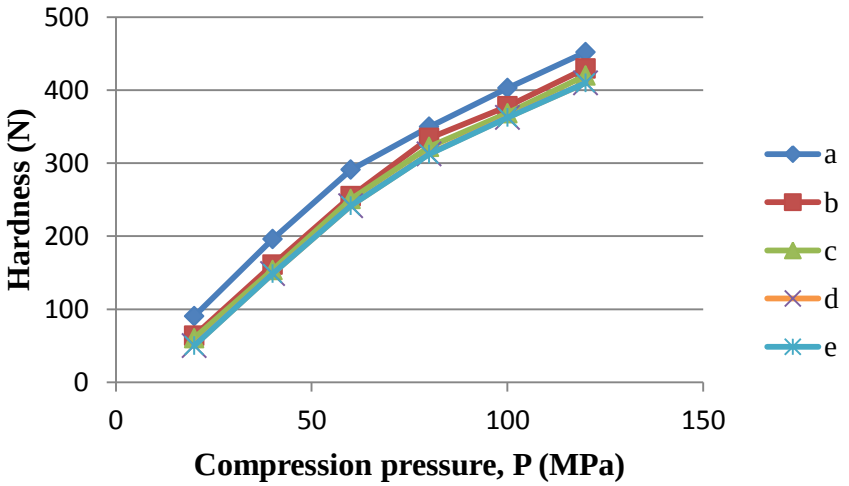

Figure 4.31: Effect of various concentrations of magnesium stearate on hardness of Avicel PH 101tablets; a, 0% w/w; b, 0.25% w/w; c, 0.50% w/w; d, 0.75% w/w; e, 1.00% w/w.

Table 4.26: R^2 values of the various slopes of the concentrations of magnesium stearate and Avicel PH101.

Concentration of magnesium stearate (%)	Y = mX + C		
	m	C	R^2
0	3.5529	48.2420	0.9719
0.25	3.6567	14.201	0.9759
0.50	3.5914	11.1560	0.9767
0.75	3.5876	3.2000	0.9760
1.00	3.5881	3.0027	0.9760

Tables 4.27 – 4.28 and Figure 4.32 shows the effects of various concentrations of magnesium stearate on the hardness of Spress® B820 at different compression pressures.

Table 4.27: Mixture of Spress® B820 and magnesium stearate.

P (MPa)	Hardness (N)				
	Concentration of magnesium stearate (%)				
	0	0.25	0.5	0.75	1.00
20	20.33±1.53	-	-	-	-
40	40.33±1.53	5.00±0.00	6.67±0.58	8.33±0.58	3.33±0.58
60	70.67±1.15	21.00±1.00	13.00±2.00	9.67±0.58	6.33±0.58
80	107.33±1.53	23.67±0.58	15.00±1.00	11.00±0.00	6.67±0.58
100	127.67±2.08	27.33±2.52	18.00±1.00	12.33±0.58	7.67±1.15
120	148.33±1.53	34.00±0.00	20.00±1.00	13.33±0.58	7.67±0.58

Note: P = compression pressure, n=3 for all concentrations.

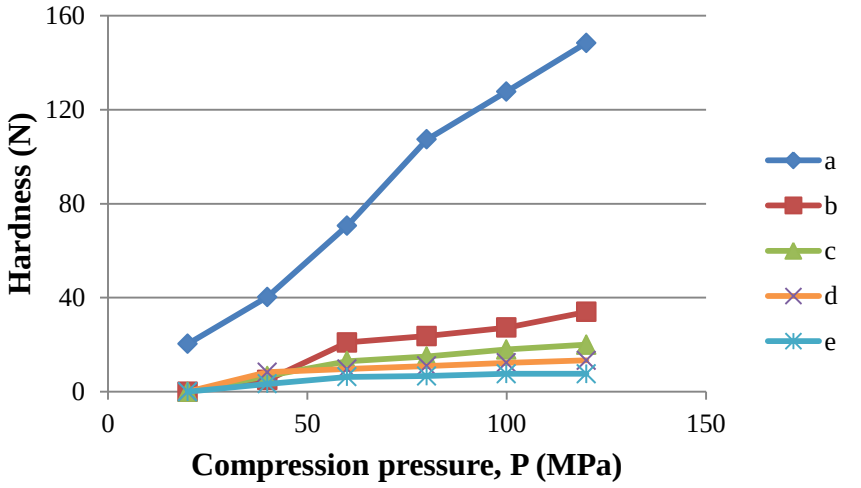

Figure 4.32: Effect of various concentrations of magnesium stearate on hardness of Spress® B820 tablets; a, 0% ww; b, 0.25% w/w; c, 0.50% w/w; d, 0.75% w/w; e, 1.00% w/w.

Table 4.28: R^2 values of the various slopes of the concentrations of magnesium stearate and Spress® B820.

Concentration of magnesium stearate (%)	Y = mX + C		
	m	C	R^2
0	1.3410	-8.0913	0.9904
0.25	0.3424	-5.4660	0.9370
0.50	0.1943	-1.4873	0.9357
0.75	0.1143	1.1120	0.7901
1.00	0.0739	0.1073	0.8279

Tables 4.29 – 4.30 and Figure 4.33 shows the effects of various concentrations of magnesium stearate on the hardness of sago starch at different compression pressures.

Table 4.29: Mixture of sago starch and magnesium stearate.

P (MPa)	Hardness (N)				
	Concentration of magnesium stearate (%)				
	0	0.25	0.5	0.75	1.00
20	-	-	-	-	-
40	20.33±2.08	16.33±1.15	14.67±1.53	5.00±0.00	5.33±0.58
60	33.00±3.61	25.00±3.00	24.00±1.73	22.00±2.00	16.33±1.53
80	33.67±3.06	27.00±1.00	26.00±1.00	26.00±2.65	20.00±1.00
100	40.33±1.15	31.33±1.53	29.00±1.00	27.00±2.65	21.00±1.00
120	48.33±1.53	37.00±1.00	32.67±1.53	29.33±0.58	25.33±2.52

Note: P = compression pressure, n= 3 for all concentrations.

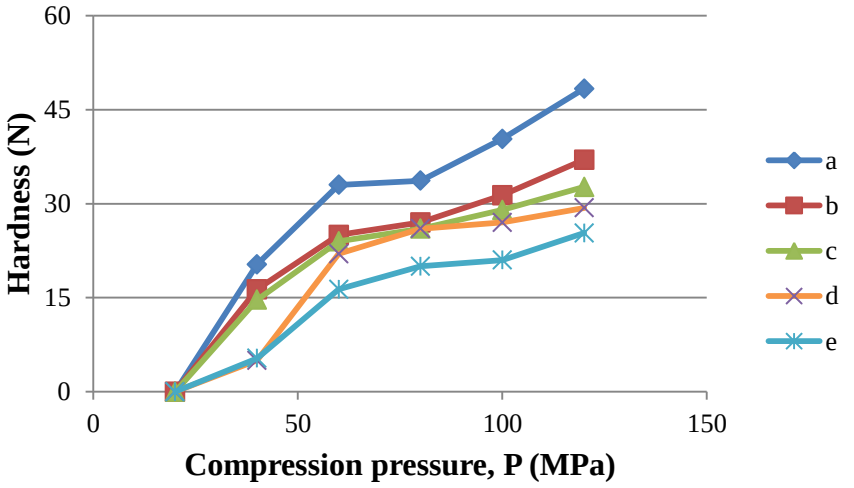

Figure 4.33: Effect of various concentrations of magnesium stearate on hardness of sago starch tablets; a, 0% w/w; b, 0.25% w/w; c, 0.50% w/w; d, 0.75% w/w; e, 1.00% w/w.

Table 4.30: R^2 values of the various slopes of the concentrations of magnesium stearate and sago starch.

Concentration of magnesium stearate (%)	Y = mX + C		
	m	C	R^2
0	0.4319	-0.9553	0.8970
0.25	0.3314	0.4233	0.8956
0.50	0.2976	0.2227	0.8670
0.75	0.3095	-3.4433	0.8574
1.00	0.2533	-3.068	0.9218

Tables 4.31 – 4.32 and Figure 4.34 shows the effects of various concentrations of magnesium stearate on the hardness of PS1 at different compression pressures.

Table 4.31: Mixture of PS1 and magnesium stearate.

P (MPa)	Hardness (N)				
	Concentration of magnesium stearate (%)				
	0	0.25	0.5	0.75	1.00
20	-	-	-	-	-
40	27.33±1.53	8.33±0.58	7.67±1.53	4.00±0.00	3.00±0.00
60	35.33±3.06	12.33±0.58	11.33±1.15	9.67±1.15	5.67±0.58
80	47.33±3.06	14.00±1.00	13.00±1.00	12.67±3.06	8.33±0.58
100	53.67±1.53	18.00±2.65	16.00±1.00	14.33±0.58	9.33±1.53
120	64.33±1.53	20.33±2.52	19.67±1.15	16.67±0.58	12.00±1.00

Note: P = compression pressure, n= 3 for all concentrations.

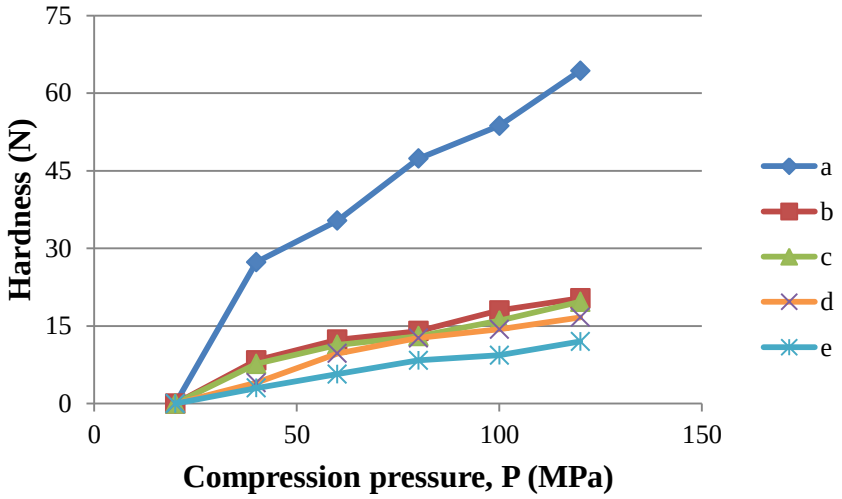

Figure 4.34: Effect of various concentrations of magnesium stearate on hardness of PS1 tablets; a, 0% w/w; b, 0.25% w/w; c, 0.50% w/w; d, 0.75% w/w; e, 1.00% w/w.

Table 4.32: R^2 values of the various slopes of the concentrations of magnesium stearate and PS1.

Concentration of magnesium stearate (%)	Y = mX + C		
	m	C	R^2
0	0.5895	-3.2687	0.9390
0.25	0.1890	-1.0680	0.9376
0.50	0.1786	-1.2227	0.9464
0.75	0.1676	-2.1773	0.9581
1.00	0.1166	-1.7767	0.9847

Tables 4.33 – 4.34 and Figure 4.35 shows the effects of various concentrations of magnesium stearate on the hardness of PS2 at different compression pressures.

Table 4.33: Mixture of PS2 and magnesium stearate.

P (MPa)	Hardness (N)				
	Concentration of magnesium stearate (%)				
	0	0.25	0.5	0.75	1.00
20	-	-	-	-	-
40	28.00±3.00	14.00±1.00	7.33±0.58	4.67±0.58	3.00±0.00
60	47.67±5.51	21.67±0.58	14.33±1.53	11.00±0.00	6.67±0.58
80	70.00±2.00	26.00±2.00	15.00±1.00	14.00±0.00	7.67±0.58
100	79.33±4.04	31.33±1.53	25.00±1.00	15.00±1.00	9.33±0.58
120	89.67±1.53	31.67±1.15	26.00±2.00	19.33±0.58	11.33±0.58

Note: P = compression pressure, n= 3 for all concentrations.

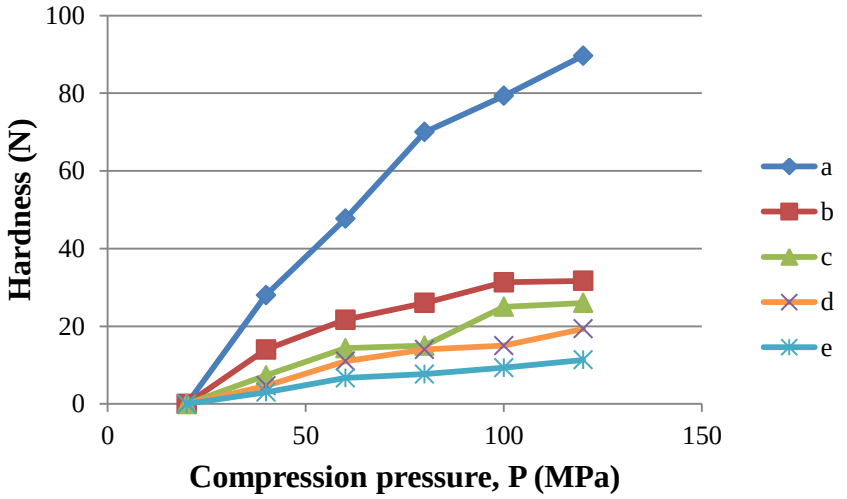

Figure 4.35: Effect of various concentrations of magnesium stearate on hardness of PS2 tablets; a, 0% w/w; b, 0.25% w/w; c, 0.50% w/w; d, 0.75% w/w; e, 1.00% w/w.

Table 4.34: R^2 values of the various slopes of the concentrations of magnesium stearate and PS2.

Concentration of magnesium stearate (%)	Y = mX + C		
	m	C	R^2
0	0.8924	-10.0220	0.9632
0.25	0.3067	-0.6887	0.8948
0.50	0.2624	-3.7580	0.9556
0.75	0.1866	-2.3973	0.9569
1.00	0.1095	-1.3307	0.9637

Tables 4.35 – 4.36 and Figure 4.36 shows the effects of various concentrations of magnesium stearate on the hardness of PS3 at different compression pressures.

Table 4.35: Mixture of PS3 and magnesium stearate.

P (MPa)	Hardness (N)				
	Concentration of magnesium stearate (%)				
	0	0.25	0.5	0.75	1.00
20	-	-	-	-	-
40	35.33±0.58	11.00±1.00	9.67±0.58	5.67±1.15	3.65±0.92
60	70.33±1.53	21.67±1.53	17.33±2.52	12.00±2.00	6.00±1.00
80	77.33±2.52	26.00±1.00	20.67±1.53	14.33±0.58	7.00±1.00
100	83.67±4.16	27.68±0.58	22.67±1.15	17.33±1.53	9.33±1.15
120	93.67±3.51	31.67±1.53	24.67±1.15	18.00±2.00	10.33±0.58

Note: P = compression pressure, n= 3 for all concentrations.

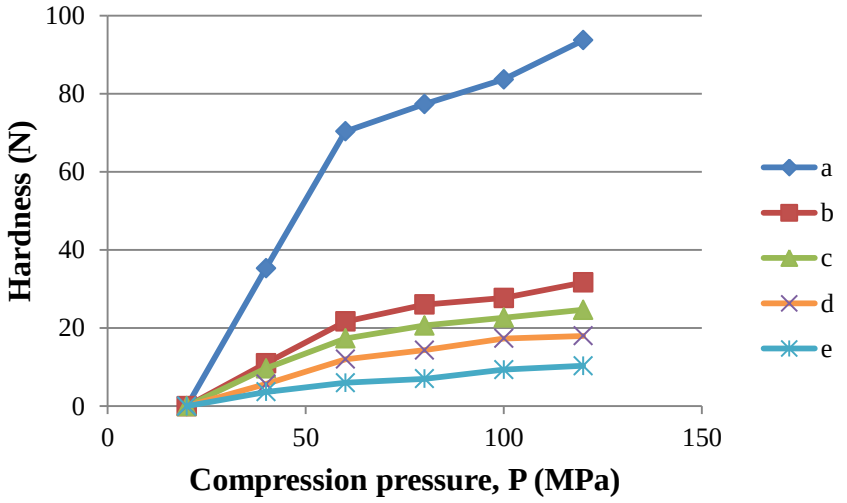

Figure 4.36: Effect of various concentrations of magnesium stearate on hardness of PS3 tablets; a, 0% w/w; b, 0.25% w/w; c, 0.50% w/w; d, 0.75% w/w; e, 1.00% w/w.

Table 4.36: R^2 values of the various slopes of the concentrations of magnesium stearate and PS3.

Concentration of magnesium stearate (%)	Y = mX + C		
	m	C	R^2
0	0.8862	-1.9820	0.8714
0.25	0.3039	-1.6020	0.9050
0.50	0.2367	-0.7340	0.8931
0.75	0.1819	-1.5093	0.9252
1.00	0.0996	-0.9173	0.9590

Tables 4.37 – 4.38 and Figure 4.37 shows the effects of various concentrations of magnesium stearate on the hardness of PS4 at different compression pressures.

Table 4.37: Mixture of PS4 and magnesium stearate.

P (MPa)	Hardness (N)				
	Concentration of magnesium stearate (%)				
	0	0.25	0.5	0.75	1.00
20	38.33±1.53	7.00±1.00	6.00±0.00	4.67±0.58	3.00±1.00
40	59.67±2.08	12.00±1.73	11.33±0.58	8.33±0.58	6.00±1.00
60	72.67±1.53	19.67±1.53	15.33±1.53	11.00±1.00	7.67±0.58
80	102.33±1.53	29.67±1.53	22.67±1.15	13.67±1.53	9.33±1.15
100	120.67±3.06	34.33±1.53	28.67±1.53	16.33±1.53	11.33±1.15
120	143.00±2.65	43.67±1.53	32.00±2.00	23.33±2.08	11.67±0.58

Note: P = compression pressure, n= 3 for all concentrations.

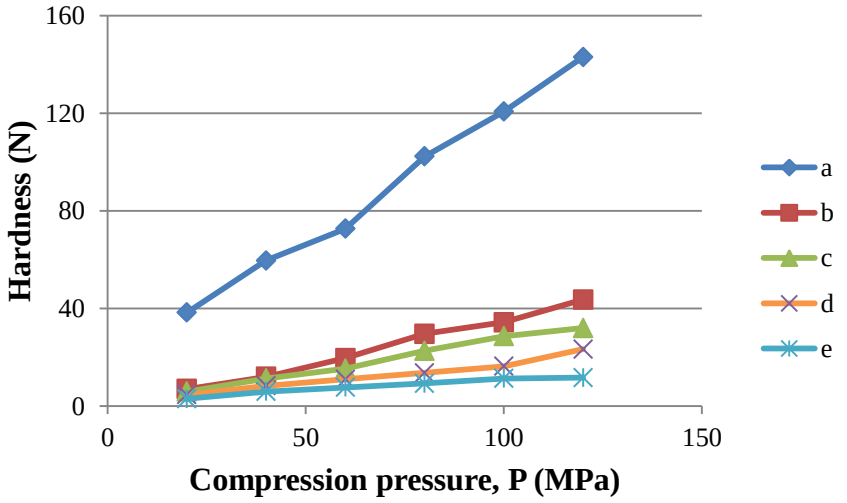

Figure 4.37: Effect of various concentrations of magnesium stearate on hardness of PS4 tablets; a, 0% w/w; b, 0.25% w/w; c, 0.50% w/w; d, 0.75% w/w; e, 1.00% w/w.

Table 4.38: R^2 values of the various slopes of the concentrations of magnesium stearate and PS4.

Concentration of magnesium stearate (%)	Y = mX + C		
	m	C	R^2
0	1.0514	15.8440	0.9934
0.25	0.3719	-1.644	0.9914
0.50	0.2705	0.3973	0.9916
0.75	0.1714	0.8913	0.9636
1.00	0.0871	2.0667	0.9618

The results for the effect of various concentrations of magnesium stearate on the lubricant sensitivity ratio (LSR) of each sample are tabulated in Table 4.39. Figures 4.38 – 4.41 show the comparison of the LSR for each sample at different concentrations of magnesium stearate.

Table 4.39: Lubricant sensitivity ratio (LSR) of each sample at various concentrations.

Powder	LSR (%)			
	Concentration of magnesium stearate (%)			
	0.25	0.5	0.75	1.00
Avicel PH 101	4.94 ±0.32	7.08±0.86	9.29±0.88	9.29±0.73
Spress® B820	77.08 ±0.23	86.51±0.77	91.02±0.30	94.83±0.38
Sago starch	23.41 ±2.56	32.43±1.44	39.29±0.89	47.58±5.14
PS1	62.20±1.46	68.88±2.08	74.07±1.48	81.35±1.48
PS2	64.96 ±0.91	71.02±1.95	78.44±0.67	87.36±0.63
PS3	66.20±0.44	73.64±1.49	80.82±1.42	88.96±0.70
PS4	69.45±1.50	77.62±1.37	83.67±1.60	91.84±2.58

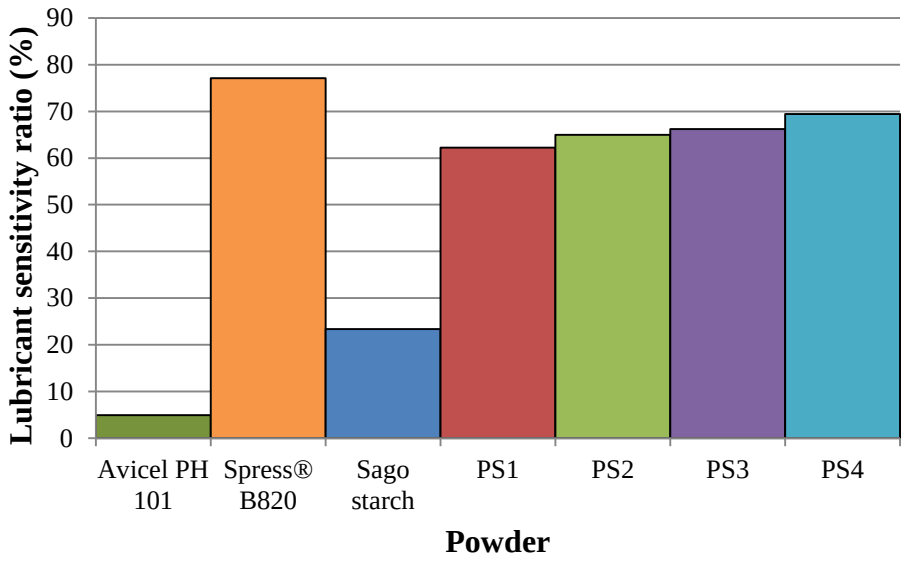

Figure 4.38: Effect of 0.25% w/w magnesium stearate on the lubricant sensitivity ratio (LSR) of the powders.

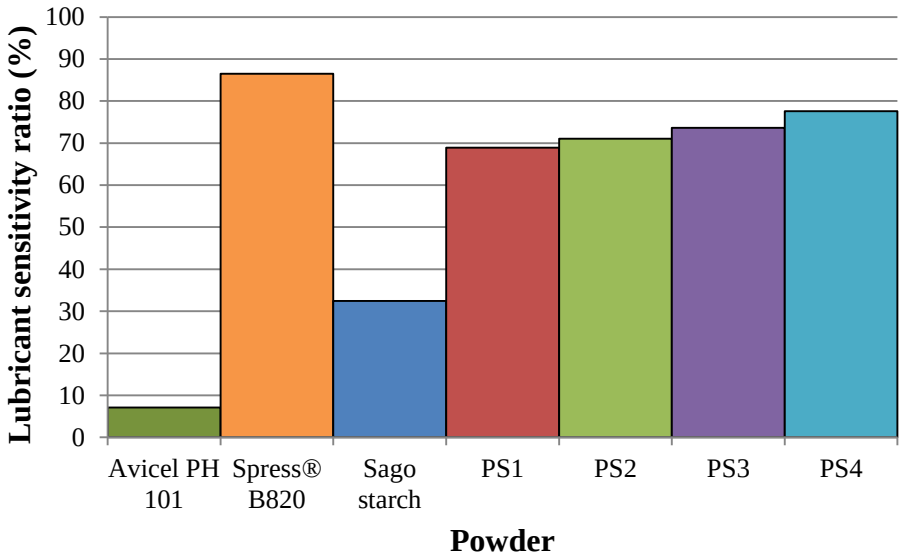

Figure 4.39: Effect of 0.50% w/w magnesium stearate on the lubricant sensitivity ratio (LSR) of the powders.

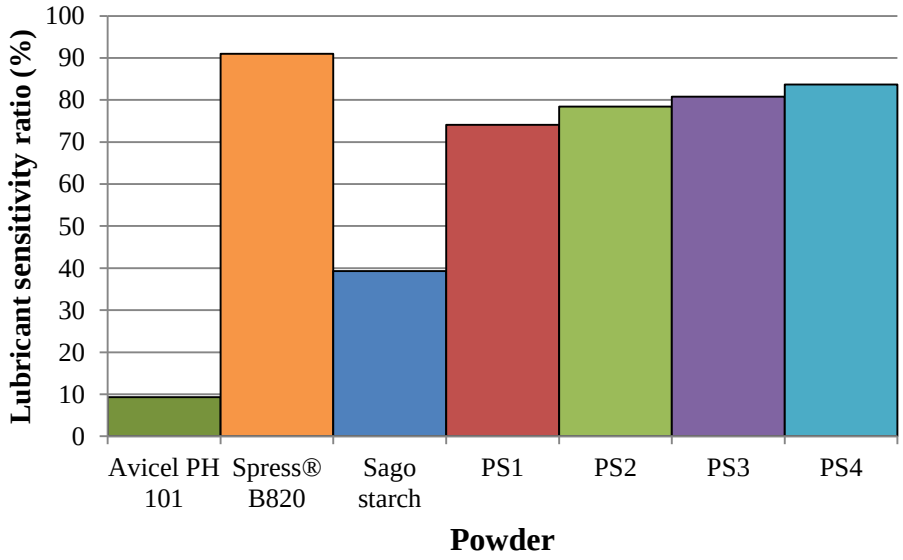

Figure 4.40: Effect of 0.75% w/w magnesium stearate on the lubricant sensitivity ratio (LSR) of the powders.

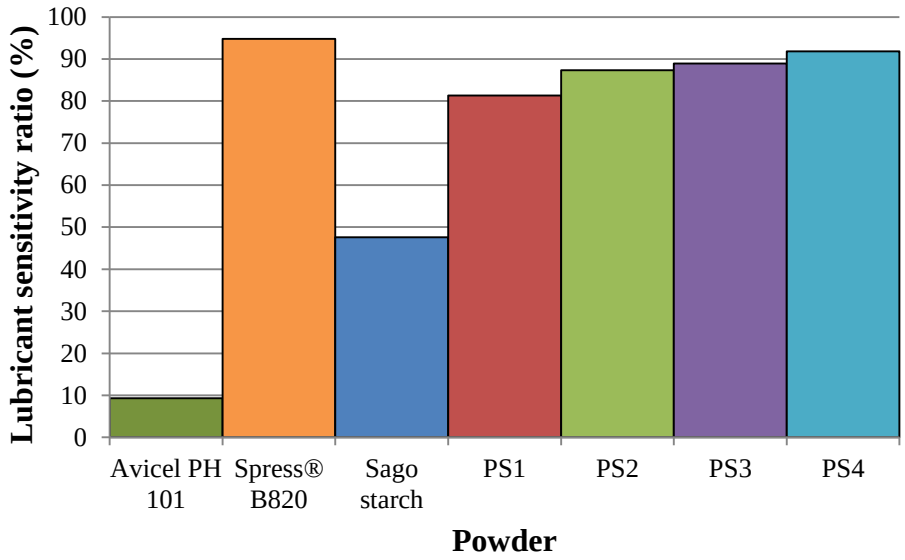

Figure 4.41: Effect of 1.00% w/w magnesium stearate on the lubricant sensitivity ratio (LSR) of the powders.

Lubricant sensitivity was carried out to evaluate the amount of lubricant that can be added before the tablet hardness fall below the minimum requirement, which is about 40 N. Magnesium stearate is most commonly used as a lubricant with multifunctionality including antiadherent, reduction of friction and glidant to enhance flow. It has a high lubricant efficiency and low friction coefficient, making it suitable for the test. However, its effectiveness as lubricant is counterproductive with the effects it has in reducing the tablet hardness (Almaya & Aburub, 2008; Bastos, Friedrich, & Beck, 2008; Yüksel *et al.*, 2007).

Tables 4.25 – 4.38 and Figures 4.31 – 4.37 showed the effect of various concentration of magnesium stearate to the compacts hardness at various compression forces. The results showed that the compact hardness decreased with increasing concentration of magnesium stearate and the hardness increased with increasing compression forces. The hardness of the compacts decreased due to the formation of magnesium stearate film at the surface of the powder, which acts as a barrier and limiting the site for bonding, consequently lowering the

compacts strength (Bastos, Friedrich, & Beck, 2008; Bolhuis & Hölzer, 1996; Odeniyi, Alfa, & Jaiyeoba, 2008). Under the conditions of the test, the hardness of Avicel PH 101 compacts was slightly decreased by the presence of magnesium stearate. It has been reported that Avicel PH 101 was the least affected by the presence of magnesium stearate (Jivraj, Martini, & Thomson, 2000; Mitrevej, Sinchaipanid, & Faroongsarng, 1996), though prolonging the mixing time may cause strong decrease in its compacts hardness (Bolhuis & Chowhan, 1996). On the other hand, the compacts hardness of sago starch, PS1, PS2, PS3, PS4 and Spress® B820 were noticeably decreased with the increase in concentration of magnesium stearate. This result is similar to previous reports that found starch-based materials to be highly sensitive towards lubricant magnesium stearate (Bolhuis & Chowhan, 1996; Jivraj, Martini, & Thomson, 2000; Mitrevej, Sinchaipanid, & Faroongsarng, 1996). The study showed that the lubricated powder of Avicel PH 101 produced compacts with hardness in the range between 50 N and 429 N (Table 4.25 and Figure 4.33) while the lubricated powders of sago starch, PS1, PS2, PS3, PS4 and Spress® B820 produced very weak compacts with hardness below 40 N, a minimum requirement for acceptable tablet hardness (Rudnic & Schwartc, 2005). However, PS4 was an exception; its lubricated powder was able to produce acceptable compact hardness when the concentration of magnesium stearate was 0.25% with minimum compression pressure of 120 N. Due to these reasons, many previous reports suggested that starches and their derivatives should not be lubricated with magnesium stearate or alternatively, keep the concentration below 0.5%, stearic acid is suggested to be used as lubricant instead (Jivraj, Martini, & Thomson, 2000; Mitrevej, Sinchaipanid, & Faroongsarng, 1996).

Lubricant sensitivity ratio (LSR) is the ratio between the decrease of compacts hardness due to mixing with a lubricant and the hardness of unlubricated compacts (Bolhuis & Hölzer, 1996). LSR is used as a quantitative measure to express sensitivity of powder to lubricant and the higher value of LSR means the powder is more sensitive to the addition of lubricant (Almaya & Aburub, 2008; Bolhuis & Hölzer, 1996).The results show the LSR increased as the magnesium stearate concentrations becomes higher for all of the powders evaluated ($p<0.05$) with a very strong correlation (Table 4.39). The overall order of increasing lubricant sensitivity (least to most sensitive) was Avicel PH 101, sago starch, PS1, PS2, PS3, PS4 and Spress® B820.

Figures 4.38 – 4.41 shows that Avicel PH 101 has the least LSR among the powders evaluated. This could be contributed by its high compactibility (Bolhuis & Chowhan, 1996) and poor flow properties which slows the distribution and formation of magnesium stearate film during the mixing process (Almaya & Aburub, 2008; Bolhuis & Hölzer, 1996). Avicel PH 101 also showed the lowest bulk density which indicates poor flow properties. This low bulk density causes high friction during consolidation which disturbs the already formed magnesium stearate film to enhance the bonding formation (Bolhuis & Hölzer, 1996). The irregular shape and rough surface texture showed by Avicel PH 101 caused the layer of magnesium stearate around the Avicel PH 101 particles to discontinue; some of it was trapped in the cavities and asperities. As a result a perfect film layer of magnesium stearate failed to be formed (Bolhuis & Hölzer, 1996).

By referring to (Table 4.39 and Figures 4.38 – 4.41), all of the starches was clearly sensitive to the addition of magnesium stearate. This was because they underwent high

plastic deformation as proven by their Heckel plots (Figure 4.25) and bonded by cohesion force (Bolhuis & Hölzer, 1996). Sago starch was found to have lower LSR than its pregelatinised forms ($p<0.05$). As tabulated in Tables 4.10 and 4.12, sago starch has the smallest average particle size and the most poor flow rate. Therefore in the mixing process, such particles created weak shear force and caused the rate of formation magnesium stearate film at the surface of the particles to be very slow (Almaya & Aburub, 2008; Bolhuis & Hölzer, 1996).

Within the pregelatinised sago starches, the results showed the LSR increased with increasing gelatinisation degree ($p<0.05$). This indicated that the sensitivity of the pregelatinised sago starches was dominantly influenced by their average particle size and flow properties; the factors that determined the formation of magnesium stearate film. This study showed that pregelatinisation of sago starch resulted in increasing average particle size and flow properties (Tables 4.10 &4.12), thus as expected PS4 was found to have the highest LSR value (most sensitive to the magnesium stearate) followed by PS3, PS2, and PS1. This explanation was also applied to Spress® B820; it has a higher LSR value ($p<0.05$) than PS4 because the former showed a larger average particle size and better flow properties (Almaya & Aburub, 2008; Bolhuis & Hölzer, 1996). In general, this study found that the LSR of the powders evaluated were significantly ($p<0.05$) influenced by the concentration of magnesium stearate, their particle size and flow rate, either alone or in combination.

4.3.4 Loading capacity

Tables 4.40 – 4.41 and Figure 4.42 shows the effect of various concentrations of Paracetamol on the tensile strength of Avicel PH 101 at different compression pressure.

Table 4.40: Mixture of Avicel PH 101 and Paracetamol.

P (MPa)	Tensile strength, T (MPa)					
	Concentration of paracetamol (%)					
	0	10	20	30	40	50
20	1.08±0.03	1.06±0.01	1.01±0.01	0.70±0.02	0.47±0.02	0.37±0.04
40	2.97±0.09	2.94±0.07	2.41±0.09	1.81±0.06	1.18±0.01	0.91±0.02
60	5.00±0.08	4.90±0.06	3.27±0.09	2.71±0.03	2.04±0.05	1.67±0.05
80	6.28±0.06	6.20±0.07	4.15±0.06	3.78±0.12	2.62±0.07	2.05±0.06
100	7.48±0.01	7.13±0.19	4.83±0.04	4.53±0.08	3.10±0.16	2.51±0.09
120	8.60±0.03	7.35±0.18	5.63±0.06	4.70±0.09	3.76±0.04	2.63±0.03

Note: P = compression pressure, n= 3 for all concentrations of paracetamol.

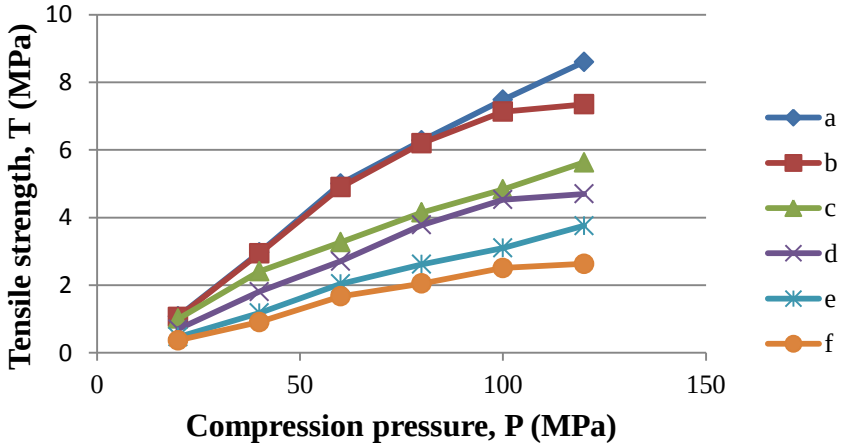

Figure 4.42: Compaction profile of Avicel PH 101 and paracetamol mixture, a, 0% w/w paracetamol; b, 10% w/w paracetamol; c, 20% w/w paracetamol; d, 30% w/w paracetamol; e, 40% w/w paracetamol; f, 50% w/w paracetamol.

Table 4.41: R^2 values of the various slopes of the concentrations of paracetamol and Avicel PH101.

Concentration of paracetamol (%)	Y = mX + C		
	m	C	R^2
0	0.0749	-0.0060	0.9833
10	0.0647	0.3980	0.9390
20	0.0446	0.4260	0.9850
30	0.0418	0.1153	0.9671
40	0.0326	-0.0840	0.9921
50	0.0235	0.0420	0.9611

Tables 4.42 – 4.43 and Figure 4.43 shows the effect of various concentrations of Paracetamol on the tensile strength of Spress® B820 at different compression pressure.

Table 4.42: Mixture of Spress® B820 and Paracetamol.

P (MPa)	Tensile strength, T (MPa) Concentration of paracetamol (%)					
	0	10	20	30	40	50
20	0.27±0.02	0.16±0.01	0.12±0.01	0.10±0.01	0.06±0.01	0.03±0.00
40	0.59±0.03	0.41±0.02	0.28±0.03	0.21±0.01	0.13±0.02	0.08±0.01
60	1.19±0.02	0.74±0.01	0.57±0.04	0.34±0.02	0.24±0.04	0.15±0.04
80	1.87±0.04	1.31±0.04	1.07±0.07	0.61±0.05	0.41±0.03	0.29±0.04
100	2.31±0.06	1.59±0.02	1.35±0.02	0.94±0.06	0.66±0.03	0.58±0.03
120	2.76±0.04	2.12±0.05	1.77±0.05	1.61±0.05	1.10±0.05	0.87±0.05

Note: P = compression pressure, n= 3 for all concentrations of paracetamol.

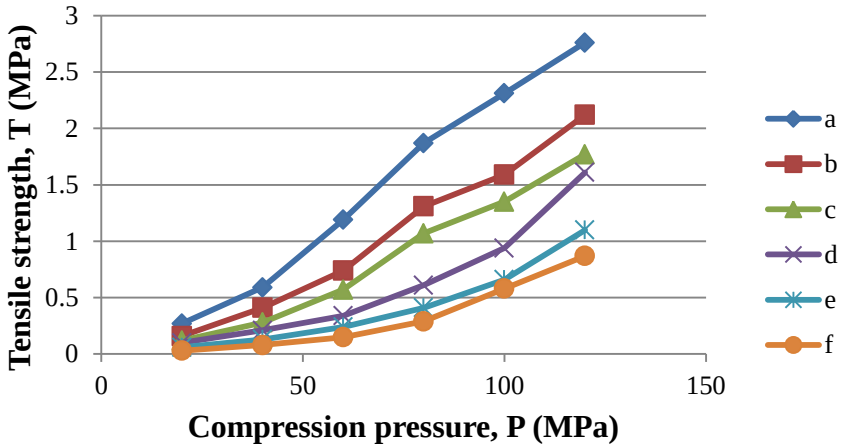

Figure 4.43: Compaction profile of Spress® B820 and paracetamol mixture, a, 0% w/w paracetamol; b, 10% w/w paracetamol; c, 20% w/w paracetamol; d, 30% w/w paracetamol; e, 40% w/w paracetamol; f, 50% w/w paracetamol.

Table 4.43: R^2 values of the various slopes of the concentration of paracetamol and Spress® B820.

Concentration of paracetamol (%)	Y = mX + C		
	m	C	R^2
0	0.0261	-0.3307	0.9920
10	0.0199	-0.3660	0.9866
20	0.0171	-0.3360	0.9822
30	0.0143	-0.3660	0.8957
40	0.0099	-0.2627	0.9044
50	0.0083	-0.2507	0.9014

Tables 4.44 – 4.45 and Figure 4.44 shows the effect of various concentrations of Paracetamol on the tensile strength of PS4 at different compression pressure.

Table 4.44: Mixture of PS4 and Paracetamol.

P (MPa)	Tensile strength, T (MPa) Concentration of paracetamol (%)					
	0	10	20	30	40	50
20	0.53±0.02	0.28±0.01	0.18±0.02	0.11±0.01	0.08±0.01	0.04±0.00
40	0.85±0.03	0.57±0.01	0.33±0.01	0.22±0.02	0.16±0.01	0.11±0.02
60	1.06±0.03	0.72±0.03	0.55±0.04	0.37±0.03	0.25±0.03	0.17±0.01
80	1.57±0.03	1.22±0.05	1.03±0.03	0.59±0.04	0.40±0.01	0.26±0.02
100	1.94±0.07	1.56±0.03	1.40±0.03	0.89±0.02	0.66±0.04	0.58±0.03
120	2.41±0.06	1.95±0.02	1.71±0.04	1.55±0.03	1.08±0.05	0.84±0.03

Note: P = compression pressure, n= 3 for all concentrations of paracetamol.

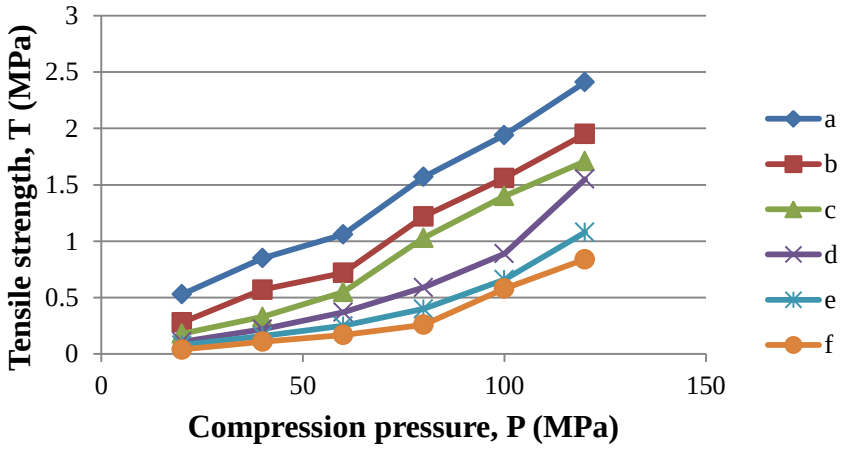

Figure 4.44: Compaction profile of PS4 and paracetamol mixture, a, 0% w/w paracetamol; b, 10% w/w paracetamol; c, 20% w/w paracetamol; d, 30% w/w paracetamol; e, 40% w/w paracetamol; f, 50% w/w paracetamol.

Table 4.45: R^2 values of the various slopes of the concentration of paracetamol and PS4.

Concentration of paracetamol (%)	Y = mX + C		
	m	C	R^2
0	0.0188	0.0753	0.9866
10	0.0169	-0.1320	0.9826
20	0.0162	-0.2673	0.9761
30	0.0135	-0.3213	0.8938
40	0.0095	-0.2267	0.8978
50	0.0079	-0.2167	0.8900

NOTE: Area ratio is AUC of each mixture of paracetamol and Avicel or Spress or PS4 divided by the AUC of plain Avicel or Spress or PS4

Table 4.46: Area ratio of each of the powder mixture and various concentration of paracetamol.

Powder	% Paracetamol (W/W)	AUC (MPa^2)	Area ratio
Avicel PH 101	0	531.4	1.00
	10	507.5	0.96
	20	359.6	0.68
	30	310.6	0.58
	40	221.1	0.42
	50	172.8	0.33
Spress® B820	0	149.5	1.00
	10	103.8	0.69
	20	84.3	0.56
	30	59.1	0.40
	40	40.4	0.27
	50	31.0	0.21
PS4	0	137.8	1.00
	10	103.7	0.75
	20	85.1	0.62
	30	58.0	0.42
	40	41.0	0.30
	50	31.2	0.23

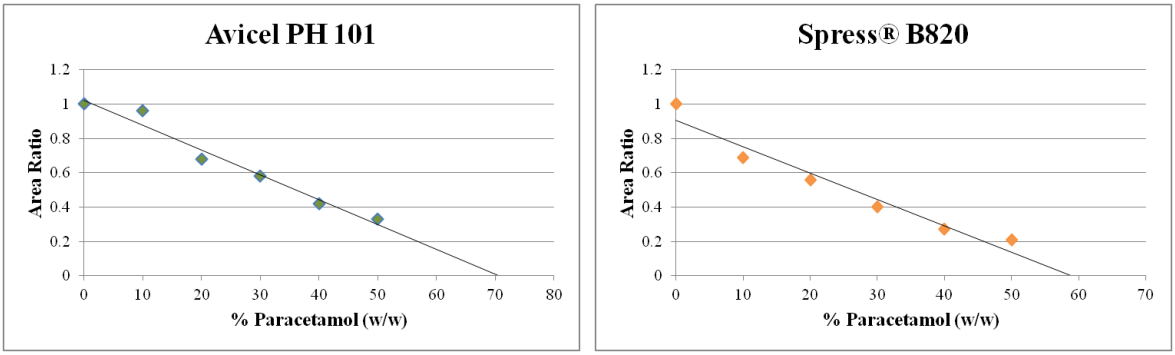

Figure 4.45: Plot between area ratio of the powders and concentration of paracetamol.

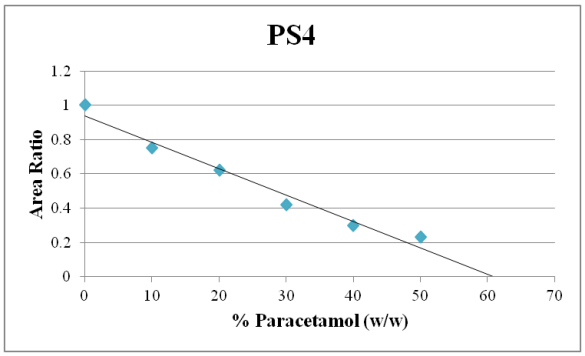

Figure 4.45, continued: Plot between area ratio of the powders and concentration of paracetamol

Table 4.47: Dilution potential/ loading capacity (% w/w paracetamol) values.

Powder	Loading capacity (% w/w)	Y = aX + b		
		a	b	R^2
Avicel PH 101	70.61	-0.0145	1.0238	0.9692
Spress® B820	59.16	-0.0153	0.9052	0.9495
PS4	60.97	-0.0154	0.939	0.9707

This study found that PS4 is the best candidate for directly compressible excipient in terms of flow properties and compressibility among the pregelatinised sago starches. Therefore PS4 was selected for further loading capacity evaluation. Figures 4.42 – 4.44 illustrate the compaction profiles of Avicel PH 101, Spress® B820 and PS4 at various Paracetamol concentrations. It shows that the tensile strength of the compacts reduced significantly ($p<0.05$) with increasing Paracetamol concentration, showing a very strong linear correlationship (Tables 4.41, 4.43 and 4.45). Based on the compression study, Avicel PH 101, Spress® B820 and PS4 underwent plastic deformation, therefore reduction of the tensile strength profiles upon Paracetamol loading was expected since Paracetamol itself is poorly compressible (Bolhuis & Chowhan, 1996; Gonnissen, Remon, & Vervaet, 2007; Govedarica *et al.*, 2011). Consequently, the area under plotted curves (AUC) of the tensile strength versus compression pressure decreased with increasing Paracetamol content (Table 4.46). The area ratio, which was obtained by dividing the AUC of the powder mixture and

the AUC of pure powder sample, is presented in the same table. Figure 4.45 shows plots of the area ratio versus percentage (%) of Paracetamol, where the plots are linear with very strong correlation (Table 4.47). Linear regression and back extrapolation to zero area ratios gave the loading capacity values (Habib *et al.,* 1996), which reflects the minimum amount of the excipient to form a tablet with the poorly compressible active ingredient (Patel & Patel, 2009; Saigal *et al.*, 2009). The higher loading capacity value indicated that such directly compressible excipient has the ability to retain its compression properties upon incorporation of a poorly compressible active ingredient at the lower excipient quantity (Marwaha, Sandhu & Marwaha, 2010). High loading capacity of the directly compressible excipient is preferable, as it eases the final weight of tablets to be at minimum (Gohel & Jogani, 2005).The loading capacity value for Avicel PH 101, Spress® B820 and PS4 are presented in Table 4.47 and shows the decreasing ranking of the loading capacity as Avicel PH 101 > PS4 > Spress® B820. The loading capacity of Avicel PH 101 is much more higher compared to PS4 and Spress® B820 and thus confirming the reports that microcrystalline cellulose group including Avicel PH 101 is the most compressible with the highest loading capacity among the available directly compressible excipients (Apeji *et al.*, 2010; Saigal *et al.*, 2009; Shangraw, 1989). The high loading capacity of Avicel PH 101 was contributed by factors such as the ability to bind other materials during compression and also because of its low density that impacts to high covering power of other excipients and wide range of particle sizes that allow such excipient to provide optimum packing arrangement (Bolhuis & Chowhan, 1996; Shangraw, 1989). The loading capacity of PS4 was found to be higher than Spress® B820 with a difference of about 1.81%, indicating PS4 has an ability to hold slightly higher amount of Paracetamol. This could be attributed by the lower bulk density of PS4 than Spress® B820 (Bolhuis & Chowhan, 1996;

Shangraw, 1989) as presented in (Table 4.11). This study found that the loading capacity Avicel PH 101 reached up to 70.16% w/w of Paracetamol, a relatively higher loading capacity compared to a previous study, which was 65% w/w of Paracetamol (Laovachirasuwan *et al.,* 2010). The difference of loading capacities obtained was related to the fact that the experiment conditions applied were different, such as ranges of the compression pressure and the composition of the powder mixtures (with or without the lubricant). Based on the literature reviews conducted so far, information on the loading capacity for pregelatinised starches relative to Paracetamol is not available. However Shangraw (1989) stated that, the loading capacity of the pregelatinised starch is minimal and this study found that the loading capacities of PS4 and Spress® B820 relative to Paracetamol were 60.97% and 59.16% respectively.

4.4 Evaluation of Paracetamol tablets

4.4.1 Tablet composition

Table 4.48: Paracetamol tablet formulations.

Ingredient (mg)	Formulation				
	1	2	3	4	5
Paracetamol	120.0	120.0	120.0	120.0	120.0
Avicel PH 101	229.1			70.0	70.0
Spress® B820		229.1		145.1	
Pregelatinised sago starch (PS4)			229.1		145.1
Sodium starch glycolate				14.0	14.0
Magnesium stearate	0.9	0.9	0.9	0.9	0.9

Based on the evaluations conducted in this study, PS4 was the best possible choice for directly compressible material compared to the other pregelatinised sago starches, i.e. PS1, PS2 and PS3. Therefore, tablets containing Paracetamol as a model active ingredient were prepared with the purpose of evaluating the performances of PS4 as a directly

compressible material in the formulation of Paracetamol tablets and to compare it with two commercially available directly compressible materials, namely Avicel PH 101 and Spress® B820. The formulations of Paracetamol tablets are presented in (Table 4.48). Flow properties of the powder mixtures from each of the formulations were evaluated through measuring their bulk densities and the results were presented in Table 4.49. Based on the Carr's compressibility index and Hausner ratio obtained, Formulation 1 was rated as passable, Formulations 2, 3 and 4 were rated as good flow, and Formulation 5 was rated as fair flow.

Table 4.49: Tap testing of powder mixtures.

	Formulation				
	1	2	3	4	5
Bulk density (g/cm^3) ± SD	0.36±0.01	0.60±0.01	0.55±0.01	0.54±0.00	0.50±0.01
Tapped density (g/cm^3) ± SD	0.46±0.01	0.68±0.00	0.64±0.01	0.63±0.01	0.60±0.01
Carr's compressibility index (CI, %) ± SD	22.46±1.25	11.27±0.85	14.12±1.35	13.82±0.80	16.58±0.16
Hausner ratio (HR) ± SD	1.29±0.02	0.12±0.01	1.17±0.02	1.16±0.01	1.20±0.00

4.4.2 Uniformity of weight and dimension

The requirements for the physical tests' for all tablets were compiled, namely their uniformity of weight, friability, hardness and disintegration test. The diameter of the tablets resulted from all of the five formulations are similar according to the die and size of punches used in this study. They were found to have similar uniformity of weight to the basic formulation, which was set at 350 mg, and not more than two tablets deviate from the average weight by more than 5% as specified by USP 27. The thickness of the tablets (Table 4.50) were significantly different ($p<0.05$) for each of the formulation, as a result of

the variation in compression pressure required to produce tablets with the hardness at 90 to 110 N as predesigned in this study.

Table 4.50: Evaluation of paracetamol tablets.

Evaluations	Formulation				
	1	2	3	4	5
Thickness (mm)[a]	3.96±0.05	3.55±0.03	3.66±0.03	3.59±0.02	3.62±0.01
Diameter(mm)[a]	9.90±0.01	9.88±0.01	9.90±0.01	9.88±0.00	9.90±0.00
Hardness (N)[a]	92.91±4.37	103.50±6.72	103.50±7.46	98.70±5.17	109.10±5.00
Uniformity of weight (mg)[b]	347.82±1.00	348.79±0.76	350.05±1.29	350.06±0.93	349.40±1.05
Friability (%)	0.38	0.48	0.51	0.54	0.43
Disintegration time (min)[c]	0.23±0.05	1.41±0.16	1.33±0.12	0.57±0.37	0.44±0.18

Note: [a]n=10 for all formulations, [b]n=20 for all formulations and [c]n=6 for all formulations.

4.4.3 Hardness

The hardness value of the tablets shows the ability of the tablets to withstand physical pressure during handling, packaging and transportation. Although tablets with hardness of 40 N complied with the minimum requirement for satisfactory tablets (Ngwuluka *et al.,* 2010), the Paracetamol tablets in this study were designed to have hardness between 90 and 110 N. Besides that, it was also intended to avoid the effects resulted from the various hardness of the Paracetamol tablets on their disintegration and dissolution properties (Ngwuluka *et al.,* 2010).

It was found that the tablets formulated with Avicel PH 101 (Formulation1), Spress® B820 (Formulation 2) and PS4 (Formulation 3) needed compression pressure of 40, 160 and 120 MPa respectively to produce Paracetamol tablets with the hardness of 90 to 110 N. Formulation 1 required the lowest compression pressure due to the effect of Avicel PH 101, which has an excellent compactibility properties at low pressure (Bastos, Friedrich, & Beck,

2008; Odeniyi, Alfa, & Jaiyeoba, 2008; Zhang, Law, & Chakrabarti, 2003) as seen in the results of the compression properties study (Section 4.3.1). Bolhuis & Chowhan (1996) and Nogami *et al.* (1969) reported that the extremely good compactibility properties of microcrystalline celluloses such as Avicel PH 101 are due to its stronger cohesive force to form hydrogen bonding. The higher hardness of the tablets containing Avicel PH 101 (Formulation 1) than those containing Spress® B820 (Formulation 2) or PS4 (Formulation 3) were contributed by the formation of hydrogen bonding on the larger surface area and higher plasticity of the Avicel PH 101 (Bolhuis & Chowhan, 1996; Bastos, Friedrich, & Beck, 2008, Odeku, Schmid, & Picker-Freyer, 2008; Nogami *et al.*, 1969). The results also found that the tablets containing Spress® B820 (Formulation 2) needed a higher compression pressure to obtain the tablets with the desired hardness of 90 – 110 N than those containing PS4 (Formulation 3). Although Spress® B820 exhibited higher plasticity than PS4 (Section 4.3), however the study also found that it showed higher sensitivity to magnesium stearate lubricant (Section 4.3.3) and have a larger particle size than PS4 (Section 4.2.9). Excipients that are sensitive to magnesium stearate would soften the tablets (Shangraw, 1989), while excipients with large particle size indicates that their total surface area is small and therefore can only provide a small contact point to form bonding between the particles (Bolhuis & Chowhan, 1996; Govedarica, *et al.*, 2011; Odeniyi, Alfa, & Jaiyeoba, 2008). Due to these reasons, Paracetamol tablets formulated with Spress® B820 (Formulation 2) needs a higher compression pressure than those formulated with PS4 (Formulation 3). To avoid using excessive compressing pressure to produce the tablets, modification of the formulations was carried out by substituting some portion of Spress® B820 and PS4 in Formulation 2 and Formulation 3 respectively with the same amount of Avicel PH 101 as shown by Formulation 4 and 5 (Table 4.48). The results showed that to

obtain the tablets with hardness between 90 and 110 N, Formulation 4 needed a lower compression pressure, i.e. at 140 MPa compared to Formulation 2, i.e. at 160 MPa. Although Formulation 5 required the same compression pressure as Formulation 3, i.e. at 120 MPa, however it produced a higher hardness of the Paracetamol tablets (Table 4.50). This indicates that Avicel PH 101 significantly improved the compactibility of the powder mixtures, thus supporting the previous report that Avicel PH 101 shows extremely good binding properties as a dry binder in direct compression formulations (Bolhuis & Chowhan, 1996).

4.4.4 Friability

Friability of the tablets from all of the formulations met the requirements of USP 27 for friability of uncoated tablets, which was below 1% (Table 4.50). This indicates that all the tablets possessed good mechanical resistance (Obaidat & Obaidat, 2011) and were well protected against various abrasive motions during production and subsequent use (Okunlola & Odeku, 2011).

4.4.5 Disintegration

All of the tablets showed disintegration time less than 2 minutes (Table 4.50), thus meeting with the USP 27 and BP 2007 specifications for disintegration time, where uncoated tablets are required to disintegrate within 15 minutes. This shows that all of the directly compressible excipients used in the formulations possessed good disintegration properties. However, statistical analysis found that the five formulations showed significant ($p<0.05$) differences in disintegration time. Paracetamol tablets that were formulated with Avicel PH 101 (Formulation 1) showed faster disintegration time than those formulated

with Spress® B820 (Formulation 2) and PS4 (Formulation 3). The faster disintegration time of the tablets formulated with Avicel PH 101 (Formulation 1) was attributed to the ability of the water to penetrate into the porous hydrophilic tablet matrix of Avicel PH 101 by means of capillary action to subsequently disrupt the hydrogen bonding of the particles, hence weakening the tablet's strength (Bhimte & Tayade, 2007; Bolhuis & Chowhan, 1996). Penetration of water into the Avicel PH 101 matrix was extremely faster than into Spress® B820 matrix or PS4 matrix due to the fact that intraparticular pores of Avicel is about 90% of the total surface area (Bolhuis & Chowhan, 1996; Nogami *et al.*, 1969). Besides that, Formulation 1, which contained Avicel PH 101, was found to produce Paracetamol tablets with the hardness of (92.91±4.37) N, while Formulation 2 (Spress® B820) and Formulation 3 (PS4) produced Paracetamol Tablets with the hardness of (103.50±6.72) N and (103.50±7.46) N respectively (Table 4.50). Tablets with lower hardness will provide larger pore size and thus result in faster penetration of water into the tablets than those tablets with higher hardness (Bolhuis & Chowhan, 1996). Consequently, Formulation 1 showed faster disintegration time than Formulation 2 and 3. Pregelatinised starches have been known to act as a disintegrant by wicking and swelling in the presence of moisture (Bolhuis & Chowhan, 1996). This research found that Spress® B820 exhibited higher swelling properties than PS4 (Section 4.2.8; Table 4.8). Theoretically, excipients with greater swelling power should produce tablets with the faster disintegration time (Gangwar *et al.*, 2010). However, since Spress® B820 was found to be more sensitive to the magnesium stearate lubricant than PS4, the distribution of magnesium stearate on the particle surface of Spress® B820 was more uniform than those on the particle surface of PS4 (Bolhuis & Hölzer, 1996). Therefore, Paracetamol tablets formulated with Spress® B820 (Formulation 2) was more hydrophobic and less accessible by the aqueous medium

than those of the tablets formulated with PS4 (Formulation 3), causing the tablets of Formulation 2 to exhibit longer disintegration time than the tablets of Formulations 3 (Mitrevej, Sinchaipanid, & Faroongsarng, 1996). Formulation 4 and 5 were modifications of Formulations 2 and 3 respectively, where the portion of Spress® B820 and PS4 were substituted by the same amount of Avicel PH 101 and sodium starch glycolate (Table 4.48), with the purpose to obtain Paracetamol tablets with faster disintegration time. The results showed that Paracetamol tablets of Formulation 4 and 5 exhibited significantly faster disintegration time than the tablets of Formulation 2 and 3 respectively (Table 4.50, $p<0.05$) Hence, Avicel PH 101 and sodium starch glycolate proved to be useful as complimentary disintegration agents. According to the reports (Jivraj, Martini, & Thomson, 2000), microcrystalline cellulose such as Avicel PH 101 is regarded by many formulation scientists of having superior disintegration properties for direct compression excipient. This could be due to the porous structure of Avicel PH 101, as such accelerated the water penetration into the tablet matrix and hastened the swelling of Spress® B820 and PS4 to disintegrate the Tablets (Bhimte & Tayade, 2007; Nogami *et al.*, 1969). As for sodium starch glycolate, it absorbs water rapidly, causing the granules to increase enormously in size and thus leading to faster disintegration time (Obaidat & Obaidat, 2011).

4.4.6 Dissolution

Dissolution test was performed to predict in vivo drug bioavailability. It is one of the most important quality control and official tests for pharmaceutical solid dosage forms such as tablets (Özkan *et al.*, 2000). Therefore, drug products should comply with the dissolution requirement as required by the Official Books (Pharmacopoeias). The USP 27 specified that for uncoated Paracetamol tablet, the tablet should release 80% Paracetamol

within 30 minutes to ensure the tablets would have no bioavailability problems (Ngwuluka *et al.*, 2010). Based on this specification, this study found that only Paracetamol tablets formulated with Avicel PH 101 (Formulation 1) may have bioavailability problems (Table 4.51). Dissolution profiles of Paracetamol tablets obtained from the five formulations above are shown in Figure 4.46.

Table 4.51: Dissolution test.

Time (minutes)	Paracetamol released (%)				
	Formulation				
	1	2	3	4	5
5	25.39±5.23	42.36±7.82	56.07±6.71	82.51±3.23	82.05±0.69
10	36.21±6.42	64.89±10.66	65.67±5.55	85.41±3.86	84.86±3.03
15	41.69±8.50	76.30±7.28	70.59±5.38	100.00±0.24	99.95±0.29
20	48.53±9.85	82.88±0.92	84.56±3.11	100.40±0.09	100.27±0.04
25	57.80±11.55	100.23±0.33	100.28±0.36	100.61±0.03	100.60±0.28
30	62.49±6.76	100.65±0.15	100.68±0.36	100.69±0.07	100.89±0.14

Note: n=6 for all formulations.

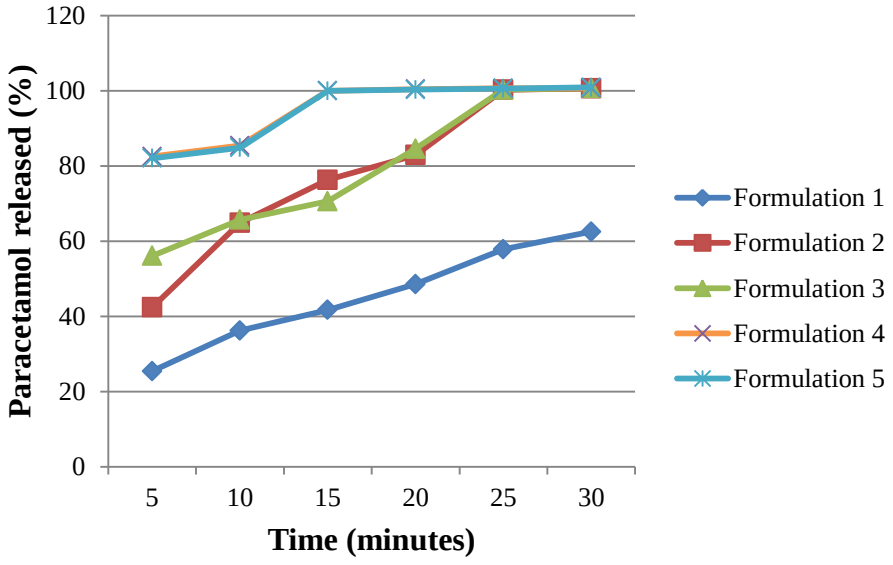

Figure 4.46: Plot of percentage of paracetamol released over time for the dissolution test of each formulation.

Table 4.52: Area under the curve (AUC) and dissolution efficiency for each formulation.

Formulation	1	2	3	4	5
AUC	63.48	105.90	140.18	206.28	205.13
	154.00	268.13	304.35	419.80	417.28
	194.75	352.98	340.65	463.53	462.03
	225.55	397.95	387.88	501.00	500.55
	265.83	457.78	462.10	502.53	502.18
	300.73	502.20	502.40	503.25	503.73
	-	-	-	-	-
Sum	1204.33	2084.93	2137.56	2596.38	2590.88
DE (%)	40.14	69.50	71.25	86.55	86.36

Paracetamol tablets formulated with Avicel PH 101 (Formulation 1) showed incomplete dissolution of Paracetamol within 30 minutes; it did not even reached 80% of Paracetamol that should be released as required by the USP 27. This was connected to the insolubility of Avicel PH 101 in the dissolution medium, causing small particles of Paracetamol to be trapped in the deformed Avicel PH101, making it difficult to be released in the dissolution medium and thus slowed the wetting and dissolution rate (Mitrevej, Sinchaipanid, & Faroongsarng, 1996; Saigal *et al.*, 2009). Dissolution profiles of Paracetamol from the tablets formulated with Spress® B820 (Formulation 2) and PS4 (Formulation 3) were comparable (Figure 4.48) and did not differ significantly ($p<0.05$). The two Formulations complied with the USP 27 requirements for dissolution of uncoated Paracetamol tablet. In fact, the tablets released more than 80% of Paracetamol within 20 minutes and completely released 100% of Paracetamol within 25 minutes. Although Spress® B820 and PS4 swelled and formed a viscous gel when in contact with the dissolution medium, of which enables blockage of the tablet pores and hindered further water uptake, nevertheless the formation of a viscous gel in these two formulations were interrupted with the presence of Paracetamol in the formulations, allowing the dissolving medium to penetrate into the

tablet matrix and facilitate the dissolution (Mitrevej, Sinchaipanid, & Faroongsarng, 1996). To improve the dissolution rate of Paracetamol, the super disintegrant sodium starch glycolate was introduced into the formulations (Formulation 4 and Formulation 5). The results showed that both Formulations showed excellent dissolution profiles, releasing more than 80% of Paracetamol within 5 minutes, and within 15 minutes Formulation 4 completely released Paracetamol while Formulation 5 almost fully released Paracetamol i.e. 99.95%.

The dissolution performance for each of the formulation was evaluated by its dissolution efficiency (Ngwuluka *et al.,* 2010). Dissolution efficiency is known as area under the dissolution curve (AUC) between defined time points t_1 and t_2 and the area under curve can be calculated using trapezoidal method (Anderson *et al.*, 1998). In this study, $t_1 = 0$ and $t_2 =$ 30 minutes. Dissolution profiles of the tablet formulated with various different excipients are said to be equivalent when the differences between them are within appropriate limits, usually about ± 10%. Dissolution efficiencies of each of the Paracetamol tablet from different formulations are tabulated in Table 4.52. It was revealed that the range of dissolution efficiencies is large, i.e. from 40.14 – 86.55, hence the dissolution profiles are not equivalent. Paracetamol tablets formulated with Avicel PH 101 (Formulation 1) showed lower dissolution efficiency than those formulated with pregelatinised starches, namely Spress® B820 (Formulation 2) and PS4 (Formulation 3), with the range between 40.14 and 71.25 (more than 10% difference) (Table 4.52). This indicated that Paracetamol tablets formulated with Avicel PH 101 (Formulation 1) could be dissimilar in bio-equivalency than those formulated with Spress® B820 (Formulation 2) and PS4 (Formulation 3). In comparison between Formulation 2 and 3, their dissolution efficiency has a very slight

difference, i.e. between 69.50 and 71.25 respectively (far below 10% difference), thus their dissolution profiles are equivalent and therefore could be reasoned to be similar in their bio-equivalency. Substitution of Spress® B820 in Formulation 2 and PS4 in Formulation 3 with the same quantity of Avicel PH 101 and sodium starch glycolate as shown in Formulation 4 and 5 (Table 4.48) resulted in significant increase ($p<0.05$) of their dissolution efficiency, from 69.50 (Formulation 2) to 86.55 (Formulation 4) and from 71.25 (Formulation 3) to 86.36 (Formulation 5) (Table 4.52). It can be seen that the differences of the dissolution efficiency caused by the substitution above were more than 10%, therefore the presence of Avicel PH 101 and sodium starch glycolate in the formulations of Paracetamol tablets (Formulation 4 and 5) improved their dissolution performances and possibly enhanced bio-equivalency. In comparison between Formulation 4 and 5, they showed a narrow dissolution efficiency difference (0.19%). This indicated that Paracetamol tablets formulated with the same concentration of Spress® B820 (Formulation 4) and PS4 (Formulation 5) to have equivalent dissolution profiles and may also be similar in bio-equivalency.

4.4.7 Short-term accelerated stability study

Formulation 4, together with Formulation 5, showed a superior release profile among all of the formulations, therefore they were selected for the accelerated stability study. The tablets were evaluated for uniformity of weight, dimension, hardness, friability, disintegration and dissolution after 3 months and 6 months of storage at accelerated stability study conditions 40 ± 2°C / 75 ± 5% RH (ICH, 2003). The results of tablet evaluations at the initial stage were used as references for the study. The results showed that all parameters evaluated as above for Formulations 4 and 5 after 6 months of storage at

the accelerated stability study conditions were found to be almost similar ($p<0.05$) to that of the references respectively (Tables 4.53 – 4.55 and Figures 4.47 & 4.48).

Table 4.53: Stability study results of Formulation 4 and 5 after 3 months and 6 months of storage at conditions 40 ± 2°C / 75 ± 5% RH.

Evaluations	Formulation 4			Formulation 5		
	Reference	3 months	6 months	Reference	3 months	6 months
Thickness (mm) ±SD	3.59 ±0.02	3.60 ±0.01	3.61 ±0.02	3.62 ±0.01	3.62 ±0.02	3.62 ±0.03
Diameter (mm) ±SD	9.88 ±0.00	9.90 ±0.02	9.90 ±0.02	9.90 ±0.00	9.91 ±0.02	9.92 ±0.03
Hardness (N) ±SD	98.70 ±5.17	100.00 ±2.21	100.40 ±3.60	109.10 ±5.00	107.40 ±2.55	106.50 ±2.37
Uniformity of weight (mg) ±SD	350.06 ±0.93	348.79 ±0.66	348.68 ±0.89	349.40 ±1.05	348.97 ±0.76	348.75 ±0.55
Friability (%)	0.54	0.54	0.58	0.43	0.46	0.46
Disintegration time (min) ±SD	0.57 ±0.37	0.56 ±0.04	0.58 ±0.06	0.44 ±0.18	0.47 ±0.03	0.45 ±0.04

Note: [a]n=10 for both formulations, [b]n=20 for both formulations and [c]n=6 for both formulations.

Table 4.54: Stability study results of dissolution test for Formulation 4 and 5 after 3 months and 6 months of storage at conditions 40 ± 2°C / 75 ± 5% RH.

Time (minutes)	Paracetamol released (%)					
	Formulation 4			Formulation 5		
	Reference	3 months	6 months	Reference	3 months	6 months
5	82.51 ±3.23	82.17 ±3.17	78.88 ±1.09	82.05 ±0.69	81.81 ±0.74	79.16 ±1.76
10	85.41 ±3.86	85.05 ±3.84	85.83 ±2.09	84.86 ±3.03	84.72 ±3.06	84.07 ±1.03
15	100.00 ±0.24	99.84 ±0.28	99.54 ±0.38	99.95 ±0.29	99.73 ±0.43	99.70 ±0.18
20	100.40 ±0.09	100.24 ±0.18	100.06 ±0.11	100.27 ±0.04	100.27 ±0.15	100.11 ±0.10
25	100.61 ±0.03	100.47 ±0.10	100.13 ±0.06	100.60 0.28	100.49 ±0.17	100.10 ±0.09
30	100.69 ±0.07	100.57 ±0.08	100.13 ±0.10	100.89 ±0.14	100.76 ±0.08	100.11 ±0.09

Note: n=6 for both formulations.

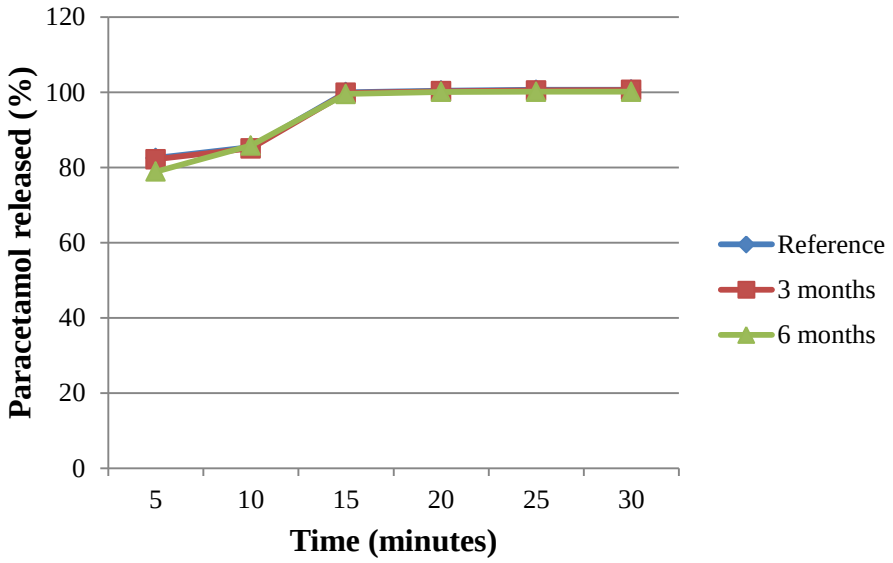

Figure 4.47: Comparison of Paracetamol released (%) between the reference, 3 months and 6 months of storage at conditions 40 ± 2°C / 75 ± 5% RH for Formulation 4.

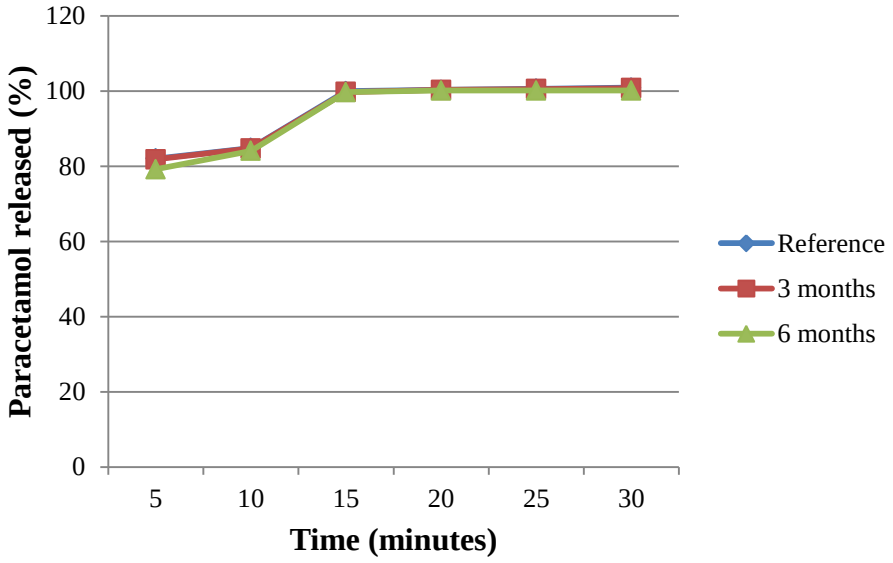

Figure 4.48: Comparison of Paracetamol released (%) between the reference, 3 months and 6 months of storage at conditions 40 ± 2°C / 75 ± 5% RH for Formulation 5.

Table 4.55: Area under the curve (AUC) and Dissolution efficiency for the stability studies of both Formulation 4 and Formulation 5 after 3 months and 6 months of storage at conditions 40 ± 2°C / 75 ± 5% RH.

	Formulation 4			Formulation 5		
	Reference	After 3 months	After 6 months	Reference	After 3 months	After 6 months
AUC	205.43	205.43	197.00	204.53	204.53	197.90
	418.05	418.05	411.78	416.33	416.33	408.08
	462.23	462.23	463.43	461.13	461.13	459.43
	500.20	500.20	499.00	500.00	500.00	499.53
	501.78	501.78	500.48	501.90	501.90	500.53
	502.60	502.60	500.65	503.13	503.13	500.53
	-	-	-	-	-	-
Sum	2590.28	2632.86	2572.34	2587.01	2587.02	2566.00
Dissolution efficiency (%)	86.34	87.76	85.75	86.53	86.23	85.53

CHAPTER 5

CONCLUSION

The results showed that sago starch met the requirements for starches in the USP 27. Sago starch contained 26.33% amylose with traces of fat and protein, therefore it can be considered to contain about 73.67% amylopectin. FT-IR spectra of sago starch is characterized by a strong, broad band between 927 cm^{-1} and 1200 cm^{-1} with three peaks at 980 cm^{-1}, 1084 cm^{-1} and 1166 cm^{-1} and another characteristic of sharp bands are the three peaks at 1649 cm^{-1}, 2920 cm^{-1} and 3422 cm^{-1} (refer to O-H group of starch). ^{13}CNMR spectra of sago starch showed chemical shifting at 98.0, 78.9, 69.7 and 59.2 ppm with the highest intensity at 69.7 ppm. Sago starch exhibited C-type diffraction pattern with the degree of crystallinity calculated to be 52.49% (by height method) or 52.00% (by area method). Sago starch showed gelatinisation temperature (T_o) at 67.11°C, peak temperature (T_p) at 71.94 °C, conclusion temperature (T_c) at 78.07°C, gelatinisation temperature range ($T_c - T_o$) of 10.96°C and the melting enthalpy (ΔH) of -3.62 in J/g. Sago starch granules appeared oval, two round shapes with smooth surface texture with its viscosity value at 8.57 cPS (room temperature). Sago starch showed swelling below 5% and water solubility about 10% at temperature 65°C and below. Sago starch is found to have mean diameter particle size of 32.10 µm, moisture content of 12.81%, bulk density of 0.63 (g/cm^3), true density of 1.55 (g/cm^3), tap density of 0.73 (g/cm^3) and porosity of 59.35 %. The powder of sago starch exhibited poor compressibility, flow properties and high lubricant sensitivity.

Sago starch was converted into pregelatinised forms at 65°C with different heating times, that is for 15(PS1), 30(PS2), 45(PS3) and 60(PS4) minutes, and followed by oven drying.

The pregelatinised sago starches (PS) obtained were characterised and evaluated as directly compressible excipient. The FT-IR spectra analyses revealed that there were no new sharp bands found in the pregelatinised sago starches and chemical shift variations shown by ^{13}CNMR were of minor significance, indicating that pregelatinisation did not change the chemical structure of sago starch. XR-D patterns of sago starch showed characteristics of C-type and PS showed of A-type, with the peaks of sago starch appeared sharper, indicating it has more crystalline region and increasing the heating times significantly decreased the degree of crystallinity. DSC curves showed pregelatinisation increased the gelatinisation temperature (T_o), peak temperature (T_p), and degree of gelatinisation (DG); it also narrowed the gelatinisation temperature range ($T_c - T_o$) and decreased the melting enthalpy (ΔH) of sago starch, as the impact become more pronounced with the increasing heating time. Sago starch granules are oval, two round shapes with smooth surface texture. After pregelatinisation with heating time of 15 minutes (PS1) and 30 minutes (PS2), the starch granules started swelling and a small part of them was gelatinised; however there were no obvious effect on the surface texture and shape of the granules. By prolonging the heating time i.e. 45 minutes (PS3) and 60 minutes (PS4), more sago starch granules were gelatinised, resulting in the loss of their surface smoothness and showed more irregular shapes.

PS showed higher swelling power (SP) at $\leq 55^{\circ}$C and higher water solubility index (WSI) at $\leq 65^{\circ}$C than sago starch. The longer heating time produced PS with lower amylosa content, higher viscosity, SP and WSI. The mean diameter of sago starch was 32.10 µm; after pregelatinisation its mean diameter increased significantly, with the mean diameter for PS1, PS2, PS3 and PS4 were 75.9 µm, 86.70 µm, 87.80 µm and 88.00 µm respectively. In

comparison, mean diameter for Avicel PH 101 was 56.70 µm and Spress® B820 was 89.30 µm. All of the powders met the USP 27 for moisture content specifications. Avicel PH 101 exhibited the lowest moisture content (5.19%), followed by Spress® B820 (9.91%), PS4 (10.39%), PS3 (11.38%), PS2 (11.32%), PS1 (11.86%) and sago starch (12.81%). The true density of Avicel PH 101 of 158 g/cm^3 was the highest, followed by sago starch 1.55 g/cm^3 , pregelatinised sago starches (PS1, PS2, PS3) 1.52 g/cm^3 , PS4 1.51 g/cm^3 and Spress® B820 1.50 g/cm^3. As for bulk density, Spress® B820 exhibited the highest value i.e. at 0.64 followed by sago starch 0.63 g/cm^3 , pregelatinised sago starches (PS1, PS2, PS3) 0.53 g/cm^3, PS4 0.52 g/cm^3 and Avicel PH 101 0.35 g/cm^3. Tap density for sago starch at 0.73 g/cm^3 was the highest, followed by Spress® B820 0.71 g/cm^3, pregelatinised sago starches (PS1, PS2) 0.63 g/cm^3, PS3 0.62 g/cm^3, PS4 0.61 g/cm^3 and Avicel PH 101 0.44 g/cm^3. This indicated that pregelatinisation modified the particle densities of sago starch and the different heating times applied for pregelatinisation did not affect the densities of PS but increased the total porosity of powder. Hence, PS4 showed the highest total porosity followed by PS3 & PS2 (65.13%), PS1 (64.91%), sago starch (59.35%). As for Avicel PH 101, it showed total porosity (77.84%) and Spress® B820 (57.33%).

Powder flow properties are commonly evaluated by measurements of Carr's compressibility index (CI, %), Hausner ratio (HR), angle of repose and powder flow rate through an orifice flow tester. Avicel PH 10 (CI: 20.45%, HR: 1.26) was rated as passable. Spress® B820 (CI: 9.86%, HR: 1.11) was rated as excellent flow. Sago starch (CI: 13.70%, HR: 1.16), PS4 (CI: 14.67%, HR: 1.17), PS3 (CI: 14.97%, HR: 1.18) and PS2 (CI: 15.42%, HR: 1.18) were rated as having good flow while PS1 (CI: 15.79%, HR: 1.19) was rated as fair flow. In terms of angle of repose, Spress® B820 and PS4 showed angle of repose

30.23° and 30.37º respectively were rated as excellent flow. PS3, PS2 and PS1 with angle of reposes 30.97º, 31.93º and 32.20º respectively were rated as good flow and Avicel PH 101 with angle of repose 41.87° was rated passable. Sago starch failed to flow, therefore was rated as very, very poor flow. Results of flow rate measurements showed Spress® B820 has the highest flow rate (6.53 g/s) followed by PS4 (5.90 g/s), PS3 (5.46 g/s), PS2 (5.01 g/s), PS1 (4.84), Avicel PH 101 (1.27 g/s) and Sago starch (failed to flow). The ranking of the powders flow rate was in agreement with their respective particle size and moisture content, with the exception of Avicel PH 101. The poor flow of Avicel PH 101 was mainly contributed by its particle shape, which is far from spherical. Overall, this study found that pregelatinisation improved the flowability of sago starch. Flowability of PS4 was comparable to Spress® B820 but superior to Avicel PH 101.

Compressibility of the powders was analyzed by Heckel and Kawakita equations. Heckel plots for all of the powders were linear in the range of 0.9617 – 0.9984. The strong linearity indicates that the plastic deformation was dominant. The mean yield pressure (P_y) value for Avicel PH 101 was lower than all of the starches, indicating that Avicel PH 101 is more plastic and the onset of its plastic deformation occurred at lower pressures. In general, it was observed that the P_y value of sago starch was found to be higher than its pregelatinised forms, suggesting that pregelatinised sago starches have greater plasticity than the sago starch ($p<0.05$) and the P_y values decreased with an increase in the degree of gelatinisation. The plasticity of PS4 was the highest among the pregelatinised sago starches but slightly lower than Spress® B820 ($p<0.05$). The study found that the sequence of decreasing P_y values of the powders was in line with the increasing degree of particle shape irregularity ($p<0.05$) and surface roughness. The mean yield pressure (P_y) of larger particle was also

consistently lower than the smaller particle with the exception of Avicel PH 101, where its plastic deformation was dominated by irregular particle shape and rough surface texture. Kawakita plots for all of the powders showed a linear relationship at any compression pressures applied with correlation coefficient (R^2) $\geq$ 0.9953. Based on the values of constant a, Avicel PH 101 was the most compressible among the powders evaluated. Within the sago starch category, PS4 was found to be the most compressible, followed by PS3, PS2, PS1 and sago starch. This indicated that pregelatinisation increased compressibility of sago starch ($p<0.05$). As for Spress® B820, its compressibility was lower than PS4.

The compact hardness and radial tensile strength indicate the mechanical properties of the directly compressible materials. At any of the same compression pressure applied, Avicel PH 101 was revealed to have the highest radial tensile strength and the hardest compacts, indicating it has the highest compactibility. It is followed by Spress® B820, PS4, PS3, PS2, PS1 and sago starch. These results showed that Avicel PH101 underwent the greatest degree of plastic deformation compared to the other starches group, as confirmed by its lowest mean yield pressure (P_y) obtained from the Heckel plot analyses. The ranking of the compactibility above was also supported by their respective area under the curve of tensile strength versus pressure, where the larger area indicates a higher compactibility.

Under conditions of the test, the hardness of Avicel PH 101 compacts was slightly decreased by the presence of magnesium stearate, but the decrease was statistically significant ($p<0.05$). It has been reported that Avicel PH 101 was the least affected by the presence of magnesium stearate. On the other hand, the compacts hardness of sago starch,

PS1, PS2, PS3, PS4 and Spress® B820 were noticeably decreased with the increase in concentration of magnesium stearate. The results showed that the lubricant sensitivity ratio (LSR) increased as the magnesium stearate concentrations increased. The overall order of increasing lubricant sensitivity was Avicel PH 101< Sago starch< PS1< PS2< PS3< PS4< Spress® B820. This study found that PS4 was the best candidate for directly compressible excipient in terms of flow properties, compressibility and compactibility among the pregelatinised sago starches. Its loading capacity value relative to Paracetamol was 60.97% W/W, in comparison to Avicel PH 101 and Spress® B820 which were 70.16% and 59.16% W/W respectively.

PS4 was evaluated for its functionality as a directly compressible excipient in comparison with Avicel PH 101 and Spress® B820 in the five formulations of Paracetamol tablet. The powder mixtures from Formulations 2, 3 and 4 showed good flowability, while Formulation 5 showed fair flow and Formulation 1 was rated as passable. The diameter of the tablets resulted from all of the five formulations are similar according to the die and size of punches used in this study. The thickness of the tablets were considerably different ($p<0.05$) for each of the formulation, as a result of the variation in compression pressure required to produce tablets with the predetermined hardness at 90 to 110 N. All of the Paracetamol tablets produced complied with the official requirements for uniformity of weight, friability and disintegration times (BP 2007; USP 27).

Tablets formulated with Avicel PH 101 (Formulation1), Spress® B820 (Formulation 2) and PS4 (Formulation 3) required compression pressure of 40, 160 and 120 MPa respectively to produce Paracetamol tablets with the hardness of 90 to 110 N. Although Spress® B820

exhibited higher plasticity than PS4, however it showed higher sensitivity to magnesium stearate lubricant, therefore it needed a higher compression pressure. Formulation 1 showed the shortest disintegration time, followed by Formulation 3 and Formulation 2. Their disintegration times were less than 2 minutes, signifying the three formulations showed good disentigration properties. However, Formulation 1 did not release 80% of Paracetamol as required by the USP 27. This was connected to the insolubility of Avicel PH 101 in the dissolution medium, causing small particles of Paracetamol to be trapped in the deformed Avicel PH101, making it difficult to be released in the dissolution medium. Formulation 2 and Formulation 3 released > 80% of Paracetamol within 20 minutes and completely released Paracetamol within 25 minutes. Although Spress® B820 and PS4 swelled and formed a viscous gel when in contact with the dissolution medium, however the viscous gel formation was interrupted by Paracetamol, allowing the dissolving medium to penetrate into the tablet matrix and facilitate the dissolution. Formulation 1, Formulation 2 and Formulation 3 showed dissolution efficiency of 40.14, 69.50 and 71.25 respectively. The differenct dissolution efficiency between Formulation 1 and Formulation 2 or Formulation 3 was >10%. This indicated that Formulation 1 could be dissimilar in bio-equivalency with Formulation 2 or Formulation 3. In comparison between Formulation 2 and 3, their dissolution efficiency was far below 10% difference; therefore their dissolution profiles are equivalent and could be similar in bio-equivalency.

Paracetamol tablet formulations were developed by replacing a portion of Spress® B820 in Formulation 2 and PS4 in Formulation 3 with Avicel PH 101 and Sodium starch glycolate in Formulation 2 and Formulation 3, subsequently they were identified as Formulation 4 and 5 respectively. To produce Paracetamol tablets with hardness between 90 and 110 N,

Formulation 4 required lower compression pressure, i.e. at 140 MPa than Formulation 2, i.e. at 160 MPa. Even though Formulation 5 required the same compression pressure as Formulation 3, i.e. at 120 MPa, however it produced greater hardness of Paracetamol tablets. This shows that Avicel PH 101 significantly improved the compactibility of the formulations ($p<0.05$). Formulation 4 and 5 exhibited notably faster disintegration time ($p<0.05$) than Formulation 2 and 3 respectively. Hence, Avicel PH 101 and sodium starch glycolate proved to be useful as complimentary disintegration agents. They showed excellent dissolution profiles, releasing > 80% of Paracetamol within 5 minutes, and within 15 minutes Formulation 4 completely released Paracetamol while Formulation 5 almost fully released Paracetamol i.e. 99.95%. Formulation 4 and 5 showed dissolution efficiencies of 86.55% and 86.36% respectively, which is significantly higher ($p<0.05$) than the dissolution efficiencies of Formulation 2 and 3. Hence, the presence of Avicel PH 101 and sodium starch glycolate improved the dissolution performances. Formulation 4 and 5 showed a narrow dissolution efficiency difference (0.19%). This indicated that both Formulation 4 and 5 have equivalent dissolution profiles and may also be similar in bio-equivalency. Formulation 4 and 5 exhibited superior release profile among all of the formulations; therefore they were selected for the accelerated stability study. The tablets were evaluated in terms of uniformity of weight, dimension, hardness, friability, disintegration, and dissolution after 3 and 6 months of storage at accelerated stability study conditions of 40 ± 2°C / 75 ± 5% RH. The results of tablet evaluations at the initial stage were used as references for the study. It was found that all parameters evaluated as above for Formulations 4 and 5 after 3 and 6 months of storage at the accelerated stability study conditions were found to be almost similar ($p<0.05$) to that of the references respectively.

Overall, the aim of the study has been achieved. PS4 demonstrated its potentiality as a new directly compressible excipient with functional properties comparable to Spress® B820. For future work, PS4 may be produced an industrial scale by using a drum dryer and its application in tablet formulations should be extended with various suitable model drugs.

REFERENCES

Abd-Aziz, S. (2002). Review: Sago starch and its utilisation. Journal of Bioscience and Bioengineering, 94(6), 526 – 529.

Abdorreza, M. N., Cheng, L. H., & Karim, A. A. (2011). Effect of plastisizers on thermal properties and heat sealability of sago starch films. Food Hydrocolloids, 25, 56 – 60.

Abdorreza, M. N., Robal, M., Cheng, L. H., Tajul, A. Y., & Karim, A. A. (2012). Physicochemical, thermal, and rheological properties of acid-hydrolized sago (Metroxylon sagu) starch. LWT- Food Science and Technology, 46, 135 - 141.

Abdullah, E. C., & Geldart, D. (1999). The use of bulk density measurements as flowability indicators. Powder Technology, 102(2), 151 – 165.

Adedokun, M. O., & Itiola, O. A. (2010). Material properties and compaction characteristics of natural and pregelatinized forms of four starches. Carbohydrate Polymers 79, 818 – 824.

Adedokun, M. O., & Itiola, O. A. (2011). Disintegration activities of natural and pregelatinized trifoliate yams, rice and corn starches in paracetamol tablets. Journal of Applied Pharmaceuttical Science 1(10), 200–206.

Aggarwal, P., & Dollimore, D. (1998). A thermal analysis investigation of partially hydrolyzed starch. Thermochimica Acta, 319, 17 – 25.

Ahmad, F. B., & Williams, P. A. (1999). Effect of salt on the gelatinization and the rheological properties of sago starch. Journal of Agriculturul and Food Chemistry, 47, 3359 – 3366.

Ahmad, F. B., Williams, P. A., Doublier, J. L., Durand, S., & Buleon, A. (1999). Physico-chemical characterisation of sago starch. Carbohydrate Polymers. 38: 361-370.

Akram, M., Naqvi, S. B. S., & Gahugar, S. (2011). Development of co-processed micro granules for direct compression. International Journal of Pharmacy and Pharmaceutical Sciences, 3(2), 64 – 69.

Alderborn, G. (2002). Tablets and compaction. In M.E. Aulton, *Pharmaceutics: The science of dosage form design* (pp. 397 – 440). London: Churchill Livingston.

Alebiou G., & Itiola O. A. (2002). Conpressional characteristics of native and pregelatinised forms of sorghum, plantain, and corn starches and the mechanical properties of their tablets. Drug Development and Industrial Pharmacy, 28(6), 663 – 672.

Almaya, A., & Aburub, A. (2008). Effect of particle size on compaction of materials with different deformation mechanisms with and without lubricants. AAPS Pharmsci Tech., 9(2), 414 – 418.

Amidon, G. E. (1995). Physical and Mechanical Property Characterization of Powders. In H.G. Brittain, *Physical characterisation of pharmaceutical solids* (pp. 281 – 319). New York: Marcel Dekker Inc.

Anderson, N. H., Bauer, M., Boussac, N., Khan-Malek, R., Munden, P., & Sardaro, M. (1998). An evaluation of fit factors and dissolution efficiency for the comparison of in vitro dissolution profile. Journal of Pharmaceutical and Biomedical Analysis, 17, 811 – 822.

AOAC. (2005). The Officials Methods of Analysis of the Association of Official Analytical Chemists (18th ed.). Arlington, Virginia: The Association of Official Analytical Chemists.

Apeji, Y. E., Oyi, A., Musa, M., & Olowosulu, A.K. (2010). Investigation of the direct compression properties of microcrisstaline starch (MCS) as a filler / binder / disintegrant in metronidazole tablet formulation. International Journal of Pharmaceutical Research and Innovation, 1, 8 – 14.

Apeji, Y. E., Oyi, A. R., & Musa, M. (2011). Studies on the physicochemical properties of microcrisstaline starch obtained by enzimatic hydrolysis using α-amylase enzime. Pharmacophore, 2(1), 9 – 15.

Atichokudomchai, N., Shobsngob, C., & Padvaravinit, S. (2001) A study of some physicochemical properties of high-crystalline tapioca starch. Starch/Stärke. 53, 577 – 583.

Atichokudomchai, N., & Varavinit, S. (2003). Characterization and utilization of acid-modified cross-linked tapioca starch in pharmaceutical tablets. Carbohydrate Polymers, 53, 263 – 270.

Atichokudomchai, N., Varavinit, S., & Chinachoti, P. (2004) A study of ordered structure in acid-modified tapioca starch by ^{13}C CP/MAS solid-state NMR. Carbohydrate Polymers. 58, 383 – 389.

Baks, T., Ngene, I.S., Soest, J. J. G., Janssen, A. E. M., & Boom, R. M. (2007). Comparison of methods to determine the degree of gelatinisation for both high and low starch concentrations. Carbohydrate Polymers, 67, 481 – 490.

Bandelin, F. J. (1989). Compressed tablets by wet granulation. In H.A. Lieberman, L. Lachman, & J.B. Schwartz, *Pharmaceutical dosage Forms: Tablets* (pp. 131 – 193). New York: Marcel, Decker, INC.

Bastos, M. O., Friedrich, R. B., & Beck, R. C. R. (2008). Effect of filler-binders and lubricants on physicochemical properties of tablets obtained by direct compression: A 2^2 factorial design. Latin American Journal of Pharmacy, 27(4), 578 – 583.

Behera, A. K., Nayak, A. K., Mohanty, B. R., & Barik, B. B (2009). Development and optimisasion of losartan potasium tablets. International Journal of Applied Pharmaceutics, 2(2), 15 – 19.

Bhimte, N. A., & Tayade, P. T. (2007). Evaluation of microcrystalline cellulose prepared from sisal fibers as a tablet excipient: A technical note. AAPS PharmSciTech, 8(1), E1 – E7.

Bolhuis, G. K., & Chowhan, Z. T. (1996). Materials for direct compaction. In G. Alderborn, & C. Nström, *Pharmaceutical powder compaction technology* (pp. 419 – 500). New York: Marcel Dekker Inc.

Bolhuis, G. K., & Hölzer A. W. (1996). Lubricant sensityvity. In G. Aldebron and C. Nystrom, *Pharmaceutical Powder Compaction Technology*, (pp. 517 – 560). New York: Marcel dekker.

Bos, C. E., Bolhuis, G. K., Lerk, C. F., & Duineveld, C. A. A. (1992). Evaluation of modified rice starch, a new excipient for direct compression. Drug Development and Industrial Pharmacy, 18(1), 93 – 106.

Brittain, H. G. (1995). Overview of physical characterization methodology. In H.G. Brittain, *Physical characterisation of pharmaceutical solids* (pp. 1 – 35). New York: Marcel Dekker Inc.

Breuninger, W. F., Piyachomkwan, K., & Sriroth, K. (2009). Tapioca/cassava starch: Production and use. In J. BeMiller & R. Whistler, *Starch: Chemistry and Technology* (pp. 541 – 568). New York: Elsevier.

Bouvard, D. (2000). Densification behaviour of mixtures of hard and soft of powders under pressure. Powder Technology, 3(3), 231 – 239.

Burrell, M. (2002). Starch: The need for improved quality or quantity – An overview. Oxford Journal, 54(382), 451 – 456.

Busignies, V., Leclerc, B., Porion, P., Evesque, P., Couarraze, G., & Tchoreloff, P. (2006). Compaction behaviour and new prespective approach to the compressibility of binary mixtures of pharmaceutical excipients. European Journal of Pharmaceutics and Biopharmaceutics, 64(1), 66 – 74.

Cao, X., Leyva, N., Anderson, S. R., & Hancock, B. C. (2008). Use of prediction methods to estimate true density of active pharmaceutical ingredients. International Journal of Pharmaceutics, 355, 231 – 237.

Carr, R. L. (1965). Evaluating flow properties of solids. Chem. Eng, 72, 163 – 168.

Charoenlap, N., Dharmsthiti, S., Sirisansaneeyakul, S., & Lertsiri, S. (2004). Optimization of cyclodextrin production from sago starch. Bioresource Technology, 92, 49 – 54.

Cisneros, F. H., Zevillanos, R., & Cisneros, L. Z. (2009). Characterization of starch from Two Ecotypes of Andean Achira Roots (*Canna edulis*). Journal of Agricultural and Food Chemistry, 57(10), 7363 – 7368.

Colorcon. (2009). Starch 1500®, partially pregelatinized maize starch, used as a binder disintegrant in high shear wet granulation comparison to povidone and croscarmellose sodium. Application Data, 1 – 9.

Copeland, L., Blazek, J., Salman, H., & Tang, M. J. (2009). Form and functionality of starch. Food Hydrocolloids, 23, 1527 – 1534.

Denny, P. J. (2002). Compaction equation: A comparison of Heckel and Kawakita equation. Powder Technology, 127(2), 162 – 172.

Fang, J. M., Fowler, P. A., Sayers, C., & Williams, P. A. (2004). The chemical modification of a range of starchs under aqueous reaction conditions. Carbohydrate Polymers, 55, 283 – 289.

Faqih, A. M. N., Mehrota, V., Hammond, S. V., & Muzzio, F. J. (2007). Effect of moisture and magnesium stearate concentration on flow properties of cohesive granular materials. International Journal of Pharmaceutics. 336(2), 338 – 345.

Farhat, I. A., Oguntona, T., & Neale, R. J. (1999). Characterisation of starches from West African yams. Journal of the Science of Food and Agriculture, 79, 2105 – 2112.

Flach, M. (1997). Sago palm. *Metroxylon sagu* Rottb. Promoting the conservation and use of underutilized and neglected crops.13. Institute of Plant Genetics and Crop Plant Research/International Plant Genetics resources Institute, Rome, Italy.

Fourmann, S. B, Carrot, C., & Mignard, N. (2003). Gelatinization and gelation of corn starch followed by dynamic mechanical spectroscopy analysis. Rheol Acta, 42, 110 – 117.

Fu, Y., Yang, S., Jeong, S. H., Kimura, S., & Park, K. (2004).Orally fast disintegrating tablets: Developments, technologies, taste-masking and clinical studies. Critical Review in Drug Therapeutic Carrier Systems, 21(6), 433 – 475.

Gangwar, S., Singh, S., Garg, G., Gerg, V., & Sharma, P.K. (2010). To compare the disintegrating properties of papaya starch and sago starch in paracetamol tablets. International Journal Pharmacy and Pharmaceutical Sciences, 2(2), 148 – 151.

Gohel, M. C., & Jogani P. D. (2005). A Review of co-processed directly compressible excipients. Journal of Pharmacy Pharmaceutical Science, 8(1),76 – 93.

Gonnissen, Y., Remon, J. P., & Vervait, C. (2007). Development of directly compressible powders via co-spray drying. European Journal of Pharmaceutics and Biopharmaceutics, 67, 220 – 226.

Govedarica, B., Injac, R., Dreu, R., & Srcic, S. (2011). Formulation and evaluation of immediate release tablets with different types of paracetamol powders prepared by direct compression. African Journal of Pharmacy and Pharmacology, 5(1), 31 – 41.

Guerin, E., Tchoreloff, P., Leclerc, B., Tanguy, D., Deleuil, M., & Couarraze, G. (1999). Rheological characterization of pharmaceutical powders using tap testing, shear cell and mercury porosimeter. International Journal of Pharmaceutics. 189, 91 – 103.

Habib, Y., Augsberger, L., Reier, G., Wheatley, T., & Shangraw, R. (1996). Dilution Potential: A new prespective. Pharmaceutical Development and Technology, 1(2), 205 – 212.

Heinze, F. (2003). New opportunities – speciality pregelatinised starch excipients. Business Briefing: Pharmatech, 1 – 5.

Hood, L. F., & Mercier, C. (1978) Molecular structure of unmodified and chemically modified manioc starches. Carbohydrate Research, 61: 53-66.

Hoover, R. (2001). Composition, molecular structure, and physicochemical properties of tuber and root starches: A review. Carbohydrate Polymers, 45, 253 – 267.

Hsu, S. H., Tsai, T. R., Chuo, W. H & Cham, T. M. (1997). Evaluation of Era-Tab as a direct compression excipient. Drug Development and Industrial Pharmacy, 23(7), 711 – 716.

Hwang, R. & Peck, G. R. (2001). A systematic evaluation of the compression and tablet characteristics of various types of lactose and dibasic calcium phosphate. Pharmaceutical Technology North America 2001, 25(6), 54 – 61.

ICH (2003). Guideline on stability testing of new drug subtances and products. European Medicines Agency. London, UK.

Ishiaku, U. S., Pang, K. W., Lee, W. S., & Mohd. Ishak, Z. A. (2002). Mechanical Properties and enzymic degradation of thermoplastics and granular sago starch filled poly (ε-caprolactone). European Polymer Journal, 58, 393 – 401.

Jacobs, H., & Delcour, J. A. (1998). Hydrothermal modifications of granular starche, with retention of the granular structure: A review. Journal of Agriculturul and Food Chemistry, 46(8), 2895 – 2904.

Jayakody, L. & Hoover, R. (2008). Effect of annealing on the molecular structure and physicochemical properties of starches from different botanical origins: A review. Carbohydrate Polymers, 74, 691 – 703.

Jayakody, L., Hoover, R. Liu, Q., & Donner, E. (2009). Study on the tuber starches III. Impact of annealing on the molecular structure and physicochemical properties of yam (*Dioscorea* sp) starches grown in Srilanka.: A review. Carbohydrate Polymers, 76, 145 – 153.

Jivraj, M., Martini, L. G., & Thomson, C. M. (2000). An overview of the different excipients useful for the direct compression of tablets. Pharmaceutical Science & Technology Today, 3(2), 58 – 63.

Joshi, A, A., & Duriez, X. (2004). Added functionality excipients: An answer to challenging Formulations. Pharmaceutical Technology, Excipients & Solid Dosage Forms, 12 – 19.

Karim, A. A., Pei-Ling, A. T., Manan, D. M. A., & Zaidul, I. S. M. (2008). Starch from the sago (Metroxylan sagu) Palm Tree-Properties, Prospects, and Challenges as a New industrial Source for Food and Other Uses. Comprehensive Reviews in Food Science and Food Safety,7, 215 – 228.

Kaur, B., Fazilah, A., & Karim, A. A. (2011). Alcoholic-alkaline treatment of sago starch and its effects on physicochemical properties. Food and Bioproducts Processing, 89, 463 – 471.

Kerr, R. W. (1968). Chemistry and Industry of Starch. In *Occurence and Variaties of Starch* (pp. 3 – 17). New York: Academic Press Inc.

Kibbe, A. H. (2000). Handbook of pharmaceutical excipients. London: American Pharmaceutical Assosiation and Pharmaceutical Press.

Korhonen, O., Raatikainen, P., Harjunen, P., Nakari, J., Suihko, E., Peltonen, S., Vidgren, M., & Paronen, P. (2000). Starch-acetates multifuntional direct compression excipients. Pharmaceutical research, 17(9), 1138 – 1143.

Korhonen, O., Pohja, S., Peltonen, S., Suihko, E., Vidgren, M., Paronen, P., & Ketolainen, J. (2002). Effects of physical properties for starch acetate powders on tableting. AAPS PharmSciTech, 3(4), 1 – 9.

Kunle, O. O., Ibrahim, Y. E., Emeja, M. O., Shaba, S., & Kunle, Y. (2003). Extraction, physicochemical and compaction properties of tacca starch – a potential pharmaceutical excipient. Starch, 55, 319 – 325.

Laovachirasuwan, P., Peerapattana, J., Srijesdaruk, V., Chitropas, P., & Otsuka, M. (2010). The performance of modified glutinous rice starch as a direct compression filler. Procceding of The 2nd Annual International Conference of Northeast Pharmacy Research 2010, (pp. 32 – 35). Faculty of Pharmacy, Mahasarakham University, Thailand.

Li, J. Y., & Yeh, A. I. (2001). Relationship between thermal, rheological characteristics, and swelling power for various starches. Journal of Food Engineering, 50, 141-148.

Li, Q., Rudolph, V., Weigl, B., & Earl, A (2004). Interparticle van der Waals force in powder flowability and compactibility. International Journal of Pharmaceutics, 1(2), 77 – 93.

Lieberman, H. A., Lachman, L., & Schwartz, J. B. (1990) *Pharmaceutical dosage forms: Tablets.* 2nd ed. New York: Marcel Dekker Inc.

Lin, P. Y., & Czuchajowska, Z. (1998). Role of Phosphorus in Viscosity, Gelatinization, and Retrogradation of Starch. American Association of Cereal Chemists , 75(5), 705-709.

Loisel, C., Maache-Rezzoug, Z., Esneault, C., & Doublier, J. L. (2006). Effect of hydrothermal treatment on the physical and rheological properties of maize starches. Journal of Food Engineering, 73, 53 – 64.

Malviya, R., Srivastava, P., Pandurangan, A., Bansal, M., & Sharma, P.K. (2010). Brief review on thermo-rheological properties of starch obtained from *"Metroxylon sagu"*. World Applied Sciences Journal, 9(5), 553 – 560.

Marshall, W. E., Wadsworth, J. I., Verma, L. R., & Velupillai, L. (1993). Deterrmining the degree of gelatinization in parboiled rice: Comparison of a subjective and an objective method. Cereal Chem., 70(2), 226 – 230.

Martin, A., Bustamante, P., & Chun, A. H. C. (1993). Micromeritics. In *Physical pharmacy: Physical chemical principles in the pharmaceutical science* (pp. 423 – 452). Philadelphia, London: Lea & Febiger.

Marwaha, M., Sandhu, D., & Marwaha, R. K. (2010). Coprocessing of excipients: A review on excipient development for improved tabletting perfoemance. International Journal of Applied Pharmaceutics, 2(3), 41 – 47.

McClatchey, W., Manner, H. I. & Elevitch, C. R. (2006). *Metroxylon amicarum, M.paulcoxii, M.sagu, M.salomonense, M.vitiense, and M.warburgii (sago palm)* : Species Profiles for Pacific Island Agroforestry [online]. Holualoa, Hawaii. Permanent Agriculture Resources (PAR). Available: http://www.traditonaltree.org [Accessed 30 July 2008].

McCormick, D. (2005). Evolutions in direct compression. Pharmaceutical Technology, 29(4), 52 – 57.

Meyer, K., & Zimmermann, I. (2004). Effect of glidants in binary powder mixtures. Powder Technology, 139(1), 40 – 54.

Michaud, J. M. L., Provoost, D. R., & Bogaert, E. V. (1998). Free-flowable directly compressible starch as binder, disintegrant and filler for compression tablets and hard gelatine capsules. United States Patent. US6143324A.

Mitrevej, A., Sinchaipanid, N., & Faroongsarng, D. (1996). Spray-dried rice starch: Comparative evaluation of direct compression fillers. Drug Development and industrial Pharmacy, 22(7), 587 – 594.

Mohamed, A., Jamilah, B., Abbas, K. A., Abdur Rahman, R., & Roselina, K. (2008). A review on physicochemical and thermorheological properties of sago starch. American Journal of Agricultural and Biological Sciences, 3(4), 639 – 646.

Morgan, K.R., Furneaux, R.H., & Larsen, N.G. (1995) Solid-state NMR studies on the structure of starch granules. Carbohydrate Research, 276, 387 – 399.

Nagel, K. M., & Peck, G. E. (2003). Investigating the effects of excipients on the powder flow characteristics of theophylline anhydrous powder formulations. Drug Development and Industrial Pharmacy, 29(3), 277 – 287.

Narayan, P., & Hancock, B. C. (2003). The relationship between the particle properties, mechanical behavior and surface roughness of some pharmaceutical excipient compacts. Materials Science and Engineering A, 355(1-2), 24 – 36.

Nattalpulwat, N., Purkkao, N., & Suwitayaphan, O. (2009). Preparation and application of carboxymethyl yam (*Dioscorea esculenta*) starch. AAPS PharmSciTech, 10(1), 193 – 198.

Newman, A. W. (1995). Micromeritics. In H.G. Brittain, *Physical characterisation of pharmaceutical solids* (pp. 253 – 280). New York: Marcel Dekker Inc.

Ngwuluka, N. C., Idiakhoa, B. A., Nep, I. E., Ogaji, I., & Okafor, I. S. (2010). Formulation and evaluation of paracetamol tablets manufactured using the dried fruit of *Phoenic dactilyfera* Linn as an excipient. Research in Pharmaceutical Biotechnology, 2 (3), 25 – 32.

Nogami, H., Nagai, T., Fukuoka, E., & Sonobe, T. (1969). Disintegration of the Aspirin tablets containing Potato starch and Microcrystalline Cellulose in various concentration. Chem. Pharm. Bull., 17(7), 1450 – 1455.

Nokhodchi, A. (2005). An overview of the effect of moisture on compaction and compression. Pharmaceutical Technology 2005, 46 – 66.

Nokhodchi, A., Maghsoodi, M., Zaedah, D. H., & Jalali, M. B. (2007). Preparation of agglomerated crystals for improving flowability and compactibility of poorly flowable and compressible drugs and excipient. Powder technology, 175(2), 73 – 81.

Nor Nadiha, M. Z., Fazilah, A., Bhat, R., & Karim, A. A. (2010). Comparative suceptibilities of sago, potato and corn starches to alkali treatment. Food Chemistry, 121, 1053 – 1059.

Noor Fadzlina, Z. A., Karim, A. A., & Teng, T. T. (2005). Physicochemical properties of carboxymethylated sago (*Metroxylon sagu*) starch. Journal of Food Science, 70(9), C560 – C567.

Nuwamanya, E., Baguma, Y., Emmambux, N., & Rubaihayo, P. (2010).Crystalline and pasting properties of cassava starch are influenced by its molecular properties. African Journal of Food Science, 4(1), 008 – 015.

Obaidat, A. A., & Obaidat, R. M. (2011). Development and evaluation of fast-dissolving tablets of meloxicam-ß-cyclodextrin complex prepared by direct compression. Acta Pharm, 62, 83 – 91.

Odeku, O. A., & Itiola, O. A. (2007). Compaction properties of three types starch. Iranian Journal of Pharmaceutical Research, 6(1), 17 – 23.

Odeku, O. A., & Picker-Freyer, K. M. (2007). Analysis of the material and tablet formation properties of four *Dioscorea* starches. Starch, 59, 430 – 444.

Odeku O. A., & Picker-Freyer K. M. (2010). Freeze-dried pregelatinised Dioscorea starches as tablet matrix for sustained release. Journal Excipient & Food Chem., 1(2), 21 – 32.

Odeku, O. A., Schmid, W., & Picker-Freyer, K. M. (2008). Material and tablet properties of pregelatinized (thermally modified) *Dioscorea* starches. European Journal of Pharmaceutics and Biopharmaceutics, 70, 357 – 371.

Odeniyi, M. A., Alfa, J., & Jaiyeoba, K. T. (2008). Effect of lubricants on flow properties and tablet strength of silicified microcrystalline cellulose. Fabad J Pharm Sci., 33, 71 – 75.

Ohwoavworhua, F. O., Adelakun, T. A. & Okhamafe, A. O. (2007). Correlating formulation performance with some physical properties of α-cellulose from corn cob and melon husk – A comparative study. Continental Journal Pharmaceutical Sciences, 1, 36 – 45.

Okunlola, A., & Odeku, O. A. (2011). Evaluation of starches obtained from four *Dioscorea* species as binding agent in chloroquine phosphate tablet formulations. Saudi Pharmaceutical Journal, 19, 95 – 105.

Özkan, Y., Özalp, Y., Savaşer, A., & Özkan, S. A. (2000). Comparative dissolution testing of Paracetamol commercial tablet dosage forms. Acta Poloniae Pharmaceutica – Drug Research, 57(1), 33 – 41.

Parmar, J., & Rane, M. (2009). Tablet formulation design and manufacture: Oral immediate release application. Pharma Time, 41(4), 21 – 29.

Paronen, P., & IIkka, J. (1996). Porosity–Pressure Functions. In G. Alderborn, & C. Nström, *Pharmaceutical powder compaction technology* (pp. 55 – 75). New York: Marcel Dekker Inc.

Parrott, E. L. (1989). Comparative evaluation of a new direct compression excipient, Soludex ™ 15. Drug Development and Industrial Pharmacy, 15(4), 561 – 583.

Patel, S., Kaushal, A. M. & Bansal, A. K.. (2007). Effect of particle size and compression force on compaction behaviour and derived mathematical parameters of compressibility. Pharmaceutical Research, 24(1), 111 – 124.

Patel, S. S. & Patel, N. M. (2009). Development of directly compressible co-processed excipient for dispersible tablets using 3^2 full factorial design. International Journal of Pharmacy and Pharmaceutical Sciences, 1(1), 125 – 148.

Pei-Ling, A. T., Mohamed, A. M. D., & Karim, A. A. (2006). Sago starch and composition of associated components in palms of different growth stages. Carbohydrate Polymers,63, 283 – 286.

Perera, C., Hoover, R., & Martin, A. M. (1997). The effect of hydroxypropylation on the structure and physicochemical properties of native, defatted and heat – moisture treated potato starches. Food Research International. 30(3-4): 235 – 247.

Picker, K. M., & Brink, D. (2006). Evaluation of powder and tableting properties of chitosan. AAPS PharSciTech, 7(3), E1 – E10.

Pimpa, B., Muhammad, S. K. S., Hassan, M. A., Ghazali, Z., Hashim, K., & Kanjanasopa, D. (2007a). Effect of electrone beam irradiation on physicochemical properties of sago starch. Songklanakarin J. Sci. Technol., 29(3), 759 – 768.

Pimpa, B., Muhammad, K., Ghazali, Z., Hashim, K., Hassan, M. A., & Mat Hashim, D. (2007b). Optimization of conditions for production of sago starch-based foam. Carbohydrate Polymers, 68, 751 – 760.

Prescott, J. K., & Hossfeld, R. J. (1994). Maintaining product uniformity and uninterrupted flow to direct compression tablet presses. Pharmaceutical Technology,18(6), 99 – 114.

Puspitowati, S., & Driscoll, R. H. (2007). Effect of degree of gelatinisation on the rheology and rehydration kinetics of instant rice produce by freeze drying. International Journal of Food Properties, 10(3), 445 – 453.

Radley, J. A. (1976). The Textile Industry. In Industrial Uses of Starch and its Derivatives (pp. 149 – 199). Great Britain: Applied Science Publisher.

Rai, S. M. (2006). Morphology and Functional Properties of Corn, Potato and Tapioca Starches. Food Hydrocolloids , 20, 557–566.

Randal, C. S. (1995). Particle Size Distribution. In H.G. Brittain, *Physical characterisation of pharmaceutical solids* (pp. 157 – 186). New York: Marcel Dekker Inc.

Ratnayake, W. S., & Jacson, D. S. (2006). Gelatinization and solubilty of corn starch during heating in excess water: New insight. Jounal of Agricultural and Food Chemiatry, 54, 3712 – 3716.

Reimerdes, D. (1993). The near future of tablet excipients. Manufacturing Chemist, 64, 14 – 15.

Riley, C. K., Wheatly, A. O., & Asemota, H. N. (2006). Isolation and Characterization of Starches From Eight Dioscorea Alata Cultivars Grown in Jamaica. African Journal of Biotechnology, 5(17), 1528-1536.

Riley, C. K., Adebayo, S. A., Wheatly, A. O., & Asemota, H. N. (2008). Surface properties of Yam (*Dioscorea sp*). Starch powders and potential for use as binders and disintegrants in drug formulations. Powder Technology, 185, 280 – 285.

Rowe, R. C., Shekey, P. J., & Owen, S. C. (2006). Handbook of pharmaceutical excipients. London: Pharmaceutical Press.

Rudnic, E. M., & Schwartz, J. B. (2005). Oral solid dosage forms. In *The Science and Practice of Pharmacy* (pp. 889 – 928). Philadelphia: Lippincott Williams & Wilkins.

Saigal, N., Baboota S., Ahuja, A., & Ali, J. (2009). Microcrysstalline cellulose as versatile excipient in drug reasearch. Journal of Young Pharmacists, 1(1), 6 – 12.

Santomaso, A., Lazzaro, P., & Canu, P. (2003). Powder floability and density ratios: the impact of granules packing. Chemical enginering Sciences, 58, 2857 – 2874.

Schüssele, A., & Bauer-Brandl, A. (2003). Note on the measurement of flowability according to the European Pharmacopoeia. International of Journal Pharmaceutics, 257, 3001 – 304.

Shah, R. B., Tawakkul, M. A., & Khan, M. A. (2008). Comparative evaluation of flow for pharmaceutical powders and granules. AAPS PharmSciTech, 9(1), 250 – 258.

Shangraw, R. F. (1989). Compressed tablet by direct compression. In H.A. Lieberman, L. Lachman, & J.B Schwartz, *Pharmaceutical Dosage Forms: Tablets* (pp. 195 – 247). New York and Basel: Marcel Decker Inc.

Shankar, K. R., Chowdary, K. P. R., Kumar, J. V., Srilakshmi, K. H., & Durga, K. N. (2012). Preparation, charakterization and evaluation of PGS – MCC co-processed excipient as directly compressible vehicle in tablet formulation. International Journal of Pharmaceutical Research and Development, 4(1), 37 – 43.

Shittu, A. O., Oyi, A. R., Isah, A. B., Kareem, S. O., & Ibramim, M. A. (2012). Formulation and evaluation of microcristalline tapioca starch as a filler-binder for direct compression. International Journal of Pharmaceutical Sciences and Research, 3(07), 2180 – 2190.

Shujun, W., Wenyuan, G., Hongyan, L., Haixia, C., Jiugao, Y., & Peigen, X. (2006). Study on the physicochemical, morphological, thermal and crystalline properties of starch separated from different *Dioscorea opposita* cultivars. Food Chemistry, 99, 38 – 44.

Sinchaipanid, N., Ketjinda, W., Pongwai, S., & Mitrevej, A. (1995). A preliminary study of sago starch as a tablet binder. Mahidol Journal Pharmaceutical Sciences, 22(3), 101 – 106.

Singh, A. V., & Nath, A. K. (2012). Evaluation of chemmically modified hydrophobic sago starch as a carrier for controlled drug delivery. Saudi Pharmaceutical Journal (in press).

Singh, A. V., Nath, A. K., Guha, M., & Kumar, K. (2011). Microwave assisted synthesis and evaluation of cross-linked carboxymethilated sago starch as superdisintegrant. Pharmacology & Pharmacy, 2, 42 – 46.

Singhal, R. S., Kennedy, J. F., Gopalakrishnan, S. M., Kaczmarek, A., Knill, C. J., & Akmar, P. F. (2008). Industrial production, processing, and utilization of sago palm-derived products. Carbohydrate Polymers, 72, 1 – 20.

Sinko, P. J. (2006). Martin's physical pharmacy and pharmaceutical sciences. United States of America: Lippincott Williams & Wilkins.

Solomans, T. W. G. & Fryhle, C. B. (2000) *Organic Chemistry*. 7th ed. New York: John Wiley & Sons Inc.

Sonnergaard, J. M. (1999). A critical evaluation of the Heckel equation. International Journal of Pharmaceutics, 193(1), 63 – 71.

Sonnergaard, J. M. (2000). Impact of particle density and initial volume on mathematical compression models. Eoropean Journal of Pharmaceutical Sciences, 11(4), 307 – 315.

Sopade, P. A., & Kiaka, A. (2001). Rheology and microstructure of sago starch from Papua New Guinea (2001). Journal of Food Enginering, 50, 47 – 57.

Staniforth, J. (2002). Powder Flow. In M.E. Aulton, *Pharmaceutics: The science of dosage form design* (pp. 200 – 210). London: Churchill Livingston.

Sun, C. C. (2006). A metrial-sparing method for simultaneous determination of true density and powder compaction properties-Aspartame as an example. International Journal of Pharmaceutics, 326(1-2), 93 – 99.

Sun, R. C., & Tomkinson, J. (2003). Fractional isolation and spectroskopic characterisation of sago starch. International Journal of Polymer Anal. Charact., 8, 29 – 46.

Sun, R. C., Tomkinson, J., Ma, P. L., & Liang, S. F. (2000). Comparative study of hemicelluloses from rice straw by alkali and hydrogen peroxyde treatments. Carbohydrate Polymers, 42, 111 – 122.

Swarbrick, J. & Boylan, J.C. eds. (2002) *Encyclopedia of pharmaceutical technology.* 2nd ed. New York: Marcel Dekker Inc.

Tattiyakul, J., Naksriarporn, T., & Pradipasena, P. (2010). X-ray Diffraction Pattern and Functional Properties of Dioscorea hispida Dennst Starch Hydrothermally Modified at Different Temperatures. Food Bioprocess Technology, doi : 10.1007/s11947-010-0424-3.

Teng, L. Y., Chin, N. L., & Yusof, Y. A. (2011). Rheological and textural studies of fresh and freeze-thawed of native sago starch – sugar gel. I. Optimisasion using response surface methodology. Food Hydrocolloids, 25, 1530 – 1537.

Terinte, N., Ibbett, R., & Schuster, K. C. (2011). Overview on native cellulose I and microcrystalline cellulose structure studied by X-Ray diffraction (WAXD): Comparison between measurement techniques. Lenzinger Berichte, 89, 118 – 131.

Tester, R. F., Karkalas, J., & Qi, X. (2004). Starch—Composition, Fine Structure andArchitecture. Journal of Cereal Science, 39, 151-165.

Tester, R. F., & Morrison, W. R. (1990). Swelling and Gelatinization of Cereal Starches. Effects of Amylopectin, Amylose, and Lipids. Cereal Chem., 67(6): 551-557

Thakur, R. R., & Kashi, M. (2011). An unlimited scope for novel formulations as orally disintegrating systems: Present and future prospects. Journal of Applied Pharmaceutical Science, 01(01), 13 – 19.

Tharanathan, R. N. (2005). Starch – value addition by modification. Critical Review in Food Sciences and Nutrition, 45, 371 – 384.

The British Pharmacopeia Commision. The British Pharmacopeia 2007. London 2006.

The United States of Pharmacopeial Convention. The United States of Pharmacopeia 27/The National Formulary 22: USP 27/ NF 22. Baltimore: Port City Press, 2004.

The United States of Pharmacopeial Convention. The United States of Pharmacopeia 30/The National Formulary 25: USP 30/ NF 25. Baltimore: Port City Press, 2007.

Tiwari, A. K., Shah, H., Rajpoot, A., & Singhal, M. (2011). Formulation and in-vitro evaluation of immediate release tablets of drotaverine HCl. Journal of Chemical and Pharmaceutical Research, 3(4), 333 – 341.

Tran, T., Piyachomkwan, K., & Sriroth, K. (2007). Gelatinization and thermal properties of modified cassava starches. Starch, 59, 46 – 55.

Tuovinen, L., Peltonen, S., & Jarvinen, K., (2003). Drug release from starch acetate films. Journal of Controlled Release, 91, 345 – 354.

Ummi-Shafiqah, M. S., Fazilah, A., Karim, A. A., Kaur, B., & Yusuf, Y. (2012). The effects of UV treatment on the properties of sago and mung bean films. International Food Research Journal, 19(1), 265 – 270.

Verwijs, M. (2007). Powder flow: The 4M bussniess and systems approach. Particle & Particle Systems Characterization, 24, 113 – 116.

Visvarungroj, N., & Remon, J. B. (1990). Crosslinked starch as sustained release agent. Drug Development and Industrial Pharmacy, 16 (7), 1091 – 1108.

Wang, W. J., Powell, A. D., & Oates, C. G. (1995). Pattern of enzyme hydrolysis in raw sago starch: Effect of processing history. Carbohydrate Polymers, 26, 91 – 97.

Weisser, E. M., Whaley, J. K., Enabosi, A. E., Shah, H., & Rege P. (2001). Polysaccharide material for direct compression. United States Patent, US6572887B2.

Wilkins, M. R., Wang, P., Xu, L., Nue, Y., Tumbleson, M. E., & Rausch, K. D. (2003). Variability in starch acetylation efficiency fromcommercial waxy corn hybrids. Cereal Chem, 80(1), 68 – 71.

Yaacob, B., Mohd Amin, M. C. I., Hashim, K., & Abu Bakar, B. (2011). Optimization of reaction conditions for carboxymethylated sago starch. Iranian Polymer Journal, 20(3), 195 – 204.

Yiu, P. H., Loh, S. L., Rajan, A., Wong, S. C., & Bong, C. F. J. (2008). Physiochemical properties of sago starch modified by acid treatment in alcohol. American Journal of Applied Sciences, 5(4), 307 – 311.

Yüksel, N., Türkmen, B., Kurdoğlu, A. H., Başaran, B., Erkin, J., & Baykara, T. (2007). Lubricant efficiency of magnesium stearate in direct compressible powder mixtures comprising Cellactose 80 and Pyridoxine Hydrochloride. Fabad J Pharm Sci., 32, 173 – 183.

Zavareze, E. R., & Dias, E. R. G (2011).Impact of heat-moisture treatment and annealing in starches: A review. Carbohydrate Polymers, 83, 317 – 328.

Zhang, Y., Law, Y., & Chakrabarti, S. (2003). Physical properties and compact analysis of commonly used direct compression binders. AAPS PharmSciTech, 4(4), 1 – 11.

Zou, J. J., Liu, C. J., & Eliasson, B.(2004). Modification of starch by glow discharge plasma. Carbohydrate Polymers, 55 (1), 23 – 26.

APPENDIX

Appendix A: Amylose, lipid and protein contents.

Test	Results			Mean±SD
	1	2	3	
Amylose (%)	26	26	27	26.3±30.58
Lipid (%)	0.12	0.13	0.12	0.12±0.01
Protein (%)	0.19	0.20	0.21	0.20±0.01

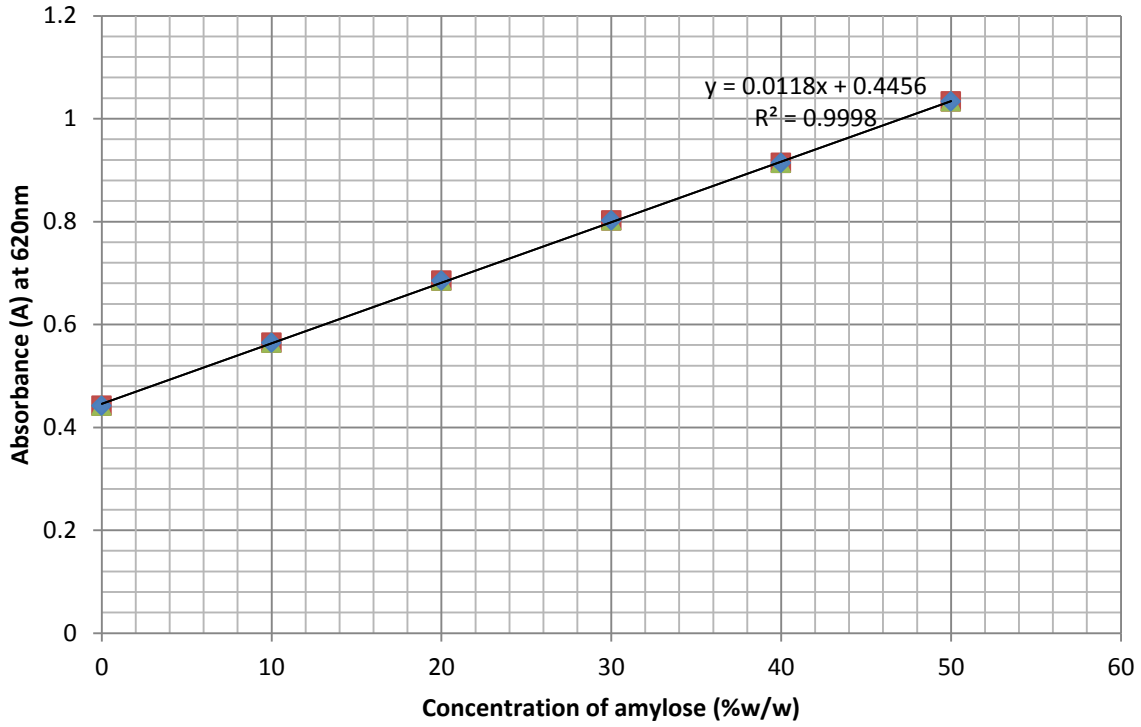

Figure 4.1: Standard curve of absorbance versus concentration of amylose measured at 620 nm.

Appendix B: Tabulated results for Differential scanning calorimetry.

Powder sample		To (°C)	Tp (°C)	Tc (°C)	Tc - To (°C)	ΔH (J/g)	DG (%)
Sago starch	1	66.09	71.50	78.61	12.52	-4.41	0.00
	2	66.78	71.78	78.11	11.33	-3.83	0.00
	3	67.09	71.98	78.63	11.54	-3.77	0.00
Mean ± SD		66.65± 0.51	71.75± 0.24	78.45± 0.29	11.80± 0.64	-4.00± 0.35	0.00± 0.00
PS1	1	72.44	74.56	79.35	6.91	-3.95	10.43
	2	73.35	75.44	79.67	5.32	-3.41	10.97
	3	72.17	74.02	77.65	5.48	-3.27	13.27
Mean ± SD		72.65± 0.62	74.67± 0.72	78.89± 1.09	5.90± 0.88	-3.54± 0.36	11.56± 1.51
PS2	1	73.32	75.53	79.98	6.66	-3.45	21.77
	2	72.33	74.80	78.46	6.13	-3.14	18.02
	3	72.44	74.54	77.93	5.49	-2.94	22.01
Mean ± SD		72.70± 0.54	74.96± 0.51	78.79 1.06	6.09± 0.59	-3.18± 0.26	20.60± 2.24
PS3	1	73.87	76.32	81.10	7.23	-2.79	36.73
	2	74.03	76.40	79.68	5.65	-2.35	38.64
	3	73.61	75.58	78.71	5.10	-2.27	39.78
Mean ± SD		73.84± 0.21	76.10± 0.45	79.83± 1.20	5.99± 1.11	-2.47± 0.28	38.38± 1.54
PS4	1	74.72	77.36	81.53	6.81	-2.37	46.23
	2	73.40	75.38	78.42	5.02	-2.21	42.29
	3	74.14	76.33	79.25	5.11	-2.17	42.44
Mean ± SD		74.07± 0.66	76.36± 0.99	79.73± 1.61	5.65± 1.01	-2.25± 0.11	43.65± 2.23

Appendix C: Swelling power (SP) and water solubility index (WSI).

Table 1: Swelling power (SP) and Water solubility Index (WSI) of sago starch.

Temperature	Weight of wet paste (mg)	Weight of dry paste (mg)	SP (%)	WSI (g/g)
25°C	570	190	3.00	5.00
	574	188	3.05	6.00
	569	192	2.96	4.00
Mean±SD			3.00±0.05	5.00±1.00
35°C	564	190	2.97	5.00
	561	189	3.00	5.50
	560	189	2.96	5.50
Mean±SD			2.98±0.02	5.33±0.29
45°C	564	187	3.02	6.50
	566	190	2.98	5.00
	563	188	2.99	6.00
Mean±SD			3.00±0.02	5,83±0.76
55°C	564	188	3.00	6.00
	564	188	3.00	6.00
	566	187	3.03	6.50
Mean±SD			3.01±0.02	6.17±0.29
65°C	561	187	3.00	6.50
	558	188	2.97	6.00
	557	185	3.01	7.50
Mean±SD			2.99±0.02	6.67±0.76
75°C	2860	130	22.00	35.00
	2855	132	21.63	34.00
	2868	155	18.50	22.5
Mean±SD			20.71±1.92	30.50±6.94
85°C	2160	80	27.00	60.00
	2166	84	25.79	58.00
	2170	82	26.46	59.00
Mean±SD			26.42±0.61	59.00±1.00

Note: initial weight of sago starch at 200 mg.

Table 2: Swelling power (SP) and Water solubility Index (WSI) of PS1.

Temperature	Weight of wet paste (mg)	Weight of dry paste (mg)	SP (%)	WSI (g/g)
25°C	580	188	3.09	6.00
	578	187	3.09	6.50
	576	189	3.05	5.50
Mean±SD			3.08±0.02	6.00±0.50
35°C	584	188	3.11	6.00
	579	186	3.11	7.00
	585	188	3.11	6.00
Mean±SD			3.11±0.00	6.33±0.58
45°C	582	186	3.13	7.00
	588	187	3.14	6.50
	579	186	3.11	7.00
Mean±SD			3.13±0.02	6.83±0.29
55°C	596	186	3.20	7.00
	603	187	3.22	6.50
	600	185	3.24	7.50
Mean±SD			3.22±0.22	7.00±0.50
65°C	897	187	4.80	6.50
	891	185	4.82	7.50
	894	185	4.83	7.50
Mean±SD			4.82±0.02	7.17±0.58
75°C	2888	152	19.00	24.00
	2876	154	18.68	23.00
	2880	152	18.95	24.00
Mean±SD			18.88±0.17	23.67±0.58
85°C	2880	120	24.00	40.00
	2887	119	24.26	40.50
	2875	121	23.76	39.50
Mean±SD			24.01±0.25	40.00±0.50

Note: initial weight of PS1 at 200 mg.

Table 3: Swelling power (SP) and Water solubility Index (WSI) of PS2.

Temperature	Weight of wet paste (mg)	Weight of dry paste (mg)	SP (%)	WSI (g/g)
25°C	651	186	3.50	7.00
	648	185	3.50	7.50
	646	185	3.49	7.50
Mean±SD			3.50±0.01	7.33±0.29
35°C	657	184	3.57	8.00
	650	185	3.51	7.50
	654	186	3.52	7.00
Mean±SD			3.53±0.03	7.50±0.50
45°C	658	184	3.58	8.00
	649	186	3.49	7.00
	651	184	3.54	8.00
Mean±SD			3.54±0.45	7.67±0.58
55°C	647	185	3.50	7.50
	658	185	3.56	7.50
	670	184	3.64	8.00
Mean±SD			3.57±0.07	7.67±0.29
65°C	768	183	4.20	8.50
	760	184	4.13	8.00
	770	182	4.23	9.00
Mean±SD			4.19±0.05	8.50±0.50
75°C	2220	148	15.00	26.00
	2211	152	14.55	24.00
	2277	152	14.98	24.00
Mean±SD			14.84±0.25	24.67±1.15
85°C	2648	132	20.06	34.00
	2640	134	19.70	33.00
	2630	131	20.08	34.50
Mean±SD			19.95±0.21	33.83±0.76

Note: initial weight of PS2 at 200 mg.

Table 4: Swelling power (SP) and Water solubility Index (WSI) of PS3.

Temperature	Weight of wet paste (mg)	Weight of dry paste (mg)	SP (%)	WSI (g/g)
25°C	630	180	3.50	10.00
	628	182	3.45	9.00
	635	179	3.55	10.50
Mean±SD			3.50±0.05	9.83±0.76
35°C	666	180	3.70	10.00
	655	181	3.62	9.50
	661	180	3.67	10.00
Mean±SD			3.66±004.	9.83±0.29
45°C	664	178	3.73	11.00
	660	181	3.65	9.50
	667	180	3.71	10.00
Mean±SD			3.70±0.04	10.17±0.76
55°C	665	179	3.72	10.50
	659	179	3.68	10.50
	662	180	3.68	10.00
Mean±SD			3.69±0.02	10.33±0.29
65°C	715	178	4.02	11.00
	725	179	4.05	10.50
	728	179	4.07	10.50
Mean±SD			4.05±0.03	10.67±0.29
75°C	1920	150	12.80	25.00
	1915	151	12.68	24.50
	1923	148	12.99	26
Mean±SD			12.82±0.16	25.17±0.76
85°C	2310	140	16.50	30.00
	2303	143	16.10	28.50
	2316	141	16.43	29.50
Mean±SD			16.34±0.21	29.33±0.76

Note: initial weight of PS3 at 200 mg.

Table 5: Swelling power (SP) and Water solubility Index (WSI) of PS4.

Temperature	Weight of wet paste (mg)	Weight of dry paste (mg)	SP (%)	WSI (g/g)
25°C	676	178	3.80	11.00
	671	178	3.77	11.00
	675	181	3.73	9.50
Mean±SD			3.77±0.04	10.50±0.87
35°C	674	179	3.77	10.50
	670	180	3.72	10.00
	672	178	3.78	11.00
Mean±SD			3.76±0.03	10.50±0.50
45°C	676	179	3.78	10.50
	672	178	3.78	11.00
	670	178	3.76	11.00
Mean±SD			3.77±0.01	10.83±0.29
55°C	712	178	4.00	11.00
	708	178	3.98	11.00
	711	179	3.97	10.50
Mean±SD			3.98±0.02	10.83±0.29
65°C	704	176	4.00	12.00
	700	176	3.98	12.00
	706	175	4.03	12.50
Mean±SD			4.00±0.03	12.17±0.29
75°C	1986	154	12.90	23.00
	1990	153	13.01	23.50
	1982	151	13.13	24.50
Mean±SD			13.01±0.12	23.67±0.76
85°C	2216	143	15.50	28.50
	2223	145	15.33	27.50
	2211	144	15.35	28.00
Mean±SD			15.39±0.09	28.00±0.50

Note: initial weight of PS4 at 200 mg.

Table 7: Swelling power (SP) and Water solubility Index (WSI) of Spress® B820.

Temperature	Weight of wet paste (mg)	Weight of dry paste (mg)	SP (%)	WSI (g/g)
25°C	960	158	6.08	23.83
	958	164	5.84	18.00
	962	166	5.80	17.00
Mean±SD			5.91±0.15	19.61±3.69
35°C	962	160	6.01	20.00
	963	164	5.87	18.00
	960	162	5.93	19.00
Mean±SD			5.94±0.07	19.00±1.00
45°C	961	165	5.82	17.50
	964	160	6.03	20.00
	959	160	5.99	20.00
Mean±SD			5.95±0.11	19.17±1.44
55°C	1027	158	6.50	23.83
	1020	156	6.53	22.00
	1023	161	6.35	19.50
Mean±SD			6.46±0.10	21.78±2.17
65°C	1560	156	10.00	22.00
	1566	154	10.17	23.00
	1558	156	9.99	22.00
Mean±SD			10.05±0.10	22.33±0.58
75°C	1584	132	12.00	34.00
	1576	128	12.31	36.00
	1579	132	11.96	34.00
Mean±SD			12.09±0.19	34.67±1.15
85°C	1750	125	14.00	37.50
	1756	127	13.83	36.50
	1754	128	13.70	36.00
Mean±SD			13.84±0.15	36.67±0.76

Note: initial weight of Spress®® B820 at 200 mg

Appendix D: Particle size and Size distribution for each powder tested using light microscopic method.

Table 1: Particle size distribution of Avicel PH 101.

Size range in µm	Mean of size range (d) in µm	Number of particles in each of size range (n)	n.d	% Frequency (% n)
20 - 30	25	9	225	3
30 - 40	35	12	420	4
40 - 50	45	33	1485	11
50 - 60	55	159	8745	53
60 - 70	65	45	2925	15
70 - 80	75	36	2700	12
80 - 90	85	6	510	2
		Σn = 300	Σnd =17010	Σ%n = 100%

Table 2: Particle size distribution of Spress® B820.

Size range in µm	Mean of size range (d) in µm	Number of particles in each of size range (n)	n.d	% Frequency (% n)
30 - 40	35	6	310	2
40 - 50	45	12	540	4
50 - 60	55	18	990	6
60 - 70	65	18	1170	6
70 - 80	75	27	2025	9
80 - 90	85	33	2805	11
90 - 100	95	90	8550	30
100 - 110	105	54	5670	18
110 - 120	115	42	4830	14
		Σn = 300	Σnd = 26890	Σ% n = 100%

Table 3: Particle size distribution of sago starch.

Size range in μm	Mean of size range (d) in μm	Number of particles in each of size range (n)	n.d	% Frequency (% n)
0 - 10	5	6	30	2
10 - 20	15	36	540	12
20 - 30	25	66	1650	22
30 - 40	35	141	4935	47
40 - 50	45	33	1485	11
50 - 60	55	18	990	6
		Σn = 300	Σnd = 9630	Σ%n = 100%

Table 4: Particle size distribution of PS1.

Size range in μm	Mean of size range (d) in μm	Number of particles in each of size range (n)	n.d	% Frequency (% n)
20 - 30	25	6	150	2
30 - 40	35	18	630	6
40 - 50	45	18	810	6
50 - 60	55	24	1320	8
60 - 70	65	30	1950	10
70 - 80	75	57	4275	19
80 - 90	85	75	6375	25
90 - 100	95	39	3705	13
100 - 110	105	24	2520	8
110 - 120	115	9	1035	3
		Σn = 300	Σnd =22770	Σ%n = 100%

Table 5: Particle size distribution of PS2.

Size range in μm	Mean of size range (d) in μm	Number of particles in each of size range (n)	n.d	% Frequency (% n)
30 - 40	35	9	315	3
40 - 50	45	12	540	4
50 - 60	55	18	990	6
60 - 70	65	21	1365	7
70 - 80	75	27	2025	9
80 - 90	85	36	3060	12
90 - 100	95	108	10260	36
100 - 110	105	48	5040	16
110 - 120	115	21	2415	7
		Σn = 300	Σnd =25695	Σ%n = 100%

Table 6: Particle size distribution of PS3.

Size range in μm	Mean of size range (d) in μm	Number of particles in each of size range (n)	n.d	% Frequency (% n)
30 - 40	35	3	105	1
40 - 50	45	9	405	3
50 - 60	55	15	825	5
60 - 70	65	18	1170	6
70 - 80	75	24	1800	8
80 - 90	85	54	4590	18
90 - 100	95	126	11970	42
100 - 110	105	39	4095	13
110 - 120	115	12	1380	4
		Σn = 300	Σnd =26340	Σ%n = 100%

Table 7: Particle size distribution of PS4.

Size range in µm	Mean of size range (d) in µm	Number of particles in each of size range (n)	n.d	% Frequency (% n)
30 - 40	35	6	210	2
40 - 50	45	12	540	4
50 - 60	55	15	825	5
60 - 70	65	21	1365	7
70 - 80	75	27	2025	9
80 - 90	85	36	3060	12
90 - 100	95	102	9690	34
100 - 110	105	63	6615	21
110 - 120	115	18	2070	6
		Σn = 300	Σnd =26400	Σ%n = 100%

Appendix E: Loss on drying, densities and porosity.

Table 1: Loss on drying.

Powder sample	Loss on Drying (%)			Mean±SD
	1	2	3	
Avicel pH 101	5.21	5.12	5.23	5.19±0.06
Spress®® B820	9.90	9,89	9,93	9.91±0.02
Sago starch	12.90	12.86	12.67	12.81±0.12
PGS 1	11.80	11.92	11.85	11.86±0.06
PGS 2	11.65	11.80	11.72	11.72±0.08
PGS 3	11.24	11.48	11.43	11.38±0.13
PGS 4	10.8	10.4	9.98	10.39±0.41

Table 2: True density (ρ_T), of the powders.

Powder sample	True density (ρ_T)			
	1	2	3	Mean±SD
Avicel pH 101	1.58	1.58	1.58	1.58 ± 0.00
Spress®® B820	1.50	1.50	1.50	1.50± 0.00
Sago starch	1.55	1.55	1.55	1.55± 0.00
PS 1	1.52	1.50	1.50	1.50± 0.00
PS 2	1.52	1.52	1.52	1.52± 0.00
PS 3	1.52	1.52	1.52	1.52± 0.00
PS 4	1.51	1.51	1.51	1.51± 0.00

Table 3: Bulk volume and tap volume of Avicel PH 101.

No.	W (g)	Vo (ml)	V10 (ml)	V50 (ml)	V100 (ml)	V200 (ml)	V500 (ml)	V2000 (ml)
1.	69.6	200	185	164	162	160	157	157
2.	69.6	200	185	166	162	159	157	157
3.	69.5	200	185	165	162	159	157	157

Note: W is weigh of the powder sample, Vo is bulk volume/initial volume, and V10, V50, V100, V200, V500, V 2000 is tap volume after 10, 50, 100, 200, 500, 2000 tapings respectively.

Table 4: Bulk density (ρ_0), and tap density (ρ_t) of Avicel PH 101.

No.	ρ_0 (g/ml)	ρ_t-10 (g/ml)	ρ_t-50 (g/ml)	ρ_t-100 (g/ml)	ρ_t-200 (g/ml)	ρ_t-500 (g/ml)	ρ_t-2000 (g/ml)
1.	0.35	0.38	0.42	0.43	0.44	0.44	0.44
2.	0.35	0.38	0.42	0.43	0.44	0.44	0.44
3.	0.35	0.38	0.42	0.43	0.44	0.44	0.44
Mean ±SD	0.35 ±0.00						0.44 ±0.00

Note: ρ_0 is bulk density and ρ_t-10, ρ_t-50, ρ_t-100, ρ_t-200, ρ_t-500, ρ_t-2000 is tap density after 10, 50, 100, 200, 500, 2000 tapings respectively

Table 5: Bulk volume and tap volume of Spress® B820.

No.	W (g)	Vo (ml)	V10 (ml)	V50 (ml)	V100 (ml)	V200 (ml)	V500 (ml)	V2000 (ml)
1.	127	200	187	184	181	179	178	178
2.	127	200	187	183	181	180	178	178
3.	127	200	186	183	180	179	178	178

Note: W is weigh of the powder sample, Vo is bulk volume/initial volume, and V10, V50, V100, V200, V500, V 2000 is tap volume after 10, 50, 100, 200, 500, 2000 tapings respectively.

Table 6: Bulk density (ρ_0), and tap density (ρ_t) of Spress® B820.

No.	ρ_0 (g/ml)	ρ_t-10 (g/ml)	ρ_t-50 (g/ml)	ρ_t-100 (g/ml)	ρ_t-200 (g/ml)	ρ_t-500 (g/ml)	ρ_t-2000 (g/ml)
1.	0.64	0.68	0.69	0.70	0.71	0.71	0.71
2.	0.64	0.68	0.69	0.70	0.71	0.71	0.71
3.	064	0.68	0.69	0.71	0.71	0.71	0.71
Mean ±SD	0.64 ±0.00						0.71 ±0.00

Note: ρ_0 is bulk density and ρ_t-10, ρ_t-50, ρ_t-100, ρ_t-200, ρ_t-500, ρ_t-2000 is tap density after 10, 50, 100, 200, 500, 2000 tapings respectively

Table 7: Bulk volume and tap volume of sago starch.

No.	W (g)	Vo (ml)	V10 (ml)	V50 (ml)	V100 (ml)	V200 (ml)	V500 (ml)	V2000 (ml)
1.	125	200	190	177	173	172	172	172
2.	125	200	190	176	173	172	172	172
3.	125	200	191	178	174	172	172	172

Note: W is weigh of the powder sample, Vo is bulk volume/initial volume, and V10, V50, V100, V200, V500, V 2000 is tap volume after 10, 50, 100, 200, 500, 2000 tapings respectively.

Table 8: Bulk density (ρ_0) and tap density (ρ_t) of sago starch.

No.	ρ_0 (g/ml)	ρ_t-10 (g/ml)	ρ_t-50 (g/ml)	ρ_t-100 (g/ml)	ρ_t-200 (g/ml)	ρ_t-500 (g/ml)	ρ_t-2000 (g/ml)
1.	0.63	0.66	0.71	0.72	0.73	0.73	0.73
2.	0.63	0.66	0.71	0.72	0.73	0.73	0.73
3.	0.63	0.65	0.70	0.72	0.73	0.73	0.73
Mean ±SD	0.63 ±0.00						0.73 ±0.00

Note: ρ_0 is bulk density and ρ_t-10, ρ_t-50, ρ_t-100, ρ_t-200, ρ_t-500, ρ_t-2000 is tap density after 10, 50, 100, 200, 500, 2000 tapings respectively

Table 9: Bulk volume and tap volume of PS1.

No.	W (g)	Vo (ml)	V10 (ml)	V50 (ml)	V100 (ml)	V200 (ml)	V500 (ml)	V2000 (ml)
1.	106	200	189	179	175	168	168	168
2.	106	200	190	178	176	169	168	168
3.	107	200	188	180	175	169	168	168

Note: W is weigh of the powder sample, Vo is bulk volume/initial volume, and V10, V50, V100, V200, V500, V 2000 is tap volume after 10, 50, 100, 200, 500, 2000 tapings respectively.

Table 10: Bulk density (ρ_0) and tap density (ρ_t) of PS1.

No.	ρ_0 (g/ml)	ρ_t-10 (g/ml)	ρ_t-50 (g/ml)	ρ_t-100 (g/ml)	ρ_t-200 (g/ml)	ρ_t-500 (g/ml)	ρ_t-2000 (g/ml)
1.	0.53	0.56	0.59	0.61	0.63	0.63	0.63
2.	0.53	0.56	0.60	0.60	0.63	0.63	0.63
3.	0.54	0.57	0.59	0.61	0.63	0.64	0.64
Mean ±SD	0.53 ±0.01						0.63 ±0.01

Note: ρ_0 is bulk density and ρ_t-10, ρ_t-50, ρ_t-100, ρ_t-200, ρ_t-500, ρ_t-2000 is tap density after 10, 50, 100, 200, 500, 2000 tapings respectively

Table 11: Bulk volume and tap volume of PS2.

No.	W (g)	Vo (ml)	V10 (ml)	V50 (ml)	V100 (ml)	V200 (ml)	V500 (ml)	V2000 (ml)
1.	105	200	187	181	175	169	169	169
2.	106	200	189	182	175	170	169	169
3.	106	200	189	181	176	170	169	169

Note: W is weigh of the powder sample, Vo is bulk volume/initial volume, and V10, V50, V100, V200, V500, V 2000 is tap volume after 10, 50, 100, 200, 500, 2000 tapings respectively.

Table 12: Bulk density (ρ_0) and tap density (ρ_t) of PS2.

No.	ρ_0 (g/ml)	ρ_t-10 (g/ml)	ρ_t-50 (g/ml)	ρ_t-100 (g/ml)	ρ_t-200 (g/ml)	ρ_t-500 (g/ml)	ρ_t-2000 (g/ml)
1.	0.53	0.56	0.58	0.60	0.62	0.62	0.62
2.	0.53	0.56	0.58	0.61	0.62	0.63	0.63
3.	0.53	0.56	0.59	0.60	0.62	0.63	0.63
Mean ±SD	0.53 ±0.00						0.63 ±0.01

Note: ρ_0 is bulk density and ρ_t-10, ρ_t-50, ρ_t-100, ρ_t-200, ρ_t-500, ρ_t-2000 is tap density after 10, 50, 100, 200, 500, 2000 tapings respectively

Table 13: Bulk volume and tap volume of PS3.

No.	W (g)	Vo (ml)	V10 (ml)	V50 (ml)	V100 (ml)	V200 (ml)	V500 (ml)	V2000 (ml)
1.	105	200	190	178	170	169	169	169
2.	106	200	189	179	171	169	169	169
3.	105	200	189	178	170	169	169	169

Note: W is weigh of the powder sample, Vo is bulk volume/initial volume, and V10, V50, V100, V200, V500, V 2000 is tap volume after 10, 50, 100, 200, 500, 2000 tapings respectively.

Table 14: Bulk density (ρ_0) and tap density (ρ_t) of PS3.

No.	ρ_0 (g/ml)	ρ_t-10 (g/ml)	ρ_t-50 (g/ml)	ρ_t-100 (g/ml)	ρ_t-200 (g/ml)	ρ_t-500 (g/ml)	ρ_t-2000 (g/ml)
1.	0.53	0.55	0.60	0.62	0.62	0.62	0.62
2.	0.53	0.55	0.60	0.62	0.63	0.63	0.63
3.	0.53	0.56	0.60	0.62	0.62	0.62	0.62
Mean ±SD	0.53 ±0.00						0.62 ±0.01

Note: ρ_0 is bulk density and ρ_t-10, ρ_t-50, ρ_t-100, ρ_t-200, ρ_t-500, ρ_t-2000 is tap density after 10, 50, 100, 200, 500, 2000 tapings respectively

Table 15: Bulk volume and tap volume of PS4.

No.	W (g)	Vo (ml)	V10 (ml)	V50 (ml)	V100 (ml)	V200 (ml)	V500 (ml)	V2000 (ml)
1.	104	200	188	178	171	170	170	170
2.	104	200	188	177	171	170	170	170
3.	105	200	189	177	170	170	170	170

Note: W is weigh of the powder sample, Vo is bulk volume/initial volume, and V10, V50, V100, V200, V500, V 2000 is tap volume after 10, 50, 100, 200, 500, 2000 tapings respectively.

Table 16: Bulk density (ρ_0) and tap density (ρ_t) of PS4.

No.	ρ_0 (g/ml)	ρ_t-10 (g/ml)	ρ_t-50 (g/ml)	ρ_t-100 (g/ml)	ρ_t-200 (g/ml)	ρ_t-500 (g/ml)	ρ_t-2000 (g/ml)
1.	0.52	0.55	0.58	0.61	0.61	0.61	0.61
2.	0.52	0.55	0.59	0.61	0.61	0.61	0.61
3.	0.53	0.55	0.58	0.62	0.62	0.62	0.62
Mean ±SD	0.52 ±0.01						0.61 ±0.01

Note: ρ_0 is bulk density and ρ_t-10, ρ_t-50, ρ_t-100, ρ_t-200, ρ_t-500, ρ_t-2000 is tap density after 10, 50, 100, 200, 500, 2000 tappings respectively.

Table 17: Calculation of % Porosity (ε).

Powder sample	1			2			3			Mean ε±SD
	ρ_0	ρ_T	ε	ρ_0	ρ_T	ε	ρ_0	ρ_T	ε	
Avicel PH 101	0.35	1.58	77.84	0.35	1.58	77.84	0.35	1.58	77.84	77.84±0.00
Spress®® B820	0.64	1.50	57.33	0.64	1.50	57.33	0.64	1.50	57.33	57.33±0.00
Sago starch	0.63	1.55	59.35	0.63	1.55	59.35	0.63	1.55	59.35	59.35±0.00
PS1	0.53	1.52	65.13	0.53	1.52	65.13	0.54	1.52	64.47	64.91±0.38
PS2	0.53	1.52	65.13	0.53	1.52	65.13	0.53	1.52	65.13	65.13±0.00
PS3	0.53	1.52	65.13	0.53	1.52	65.13	0.53	1.52	65.13	65.13±0.00
PS4	0.52	1.51	65.56	0.52	1.51	65.56	0.53	1.51	64.90	65.34±0.38

Appendix F: Flow properties.

Table 1: Calculation of Carr's Index (CI).

Sample powder	1			2			3			Mean CI(%)±SD
	ρ	ρ_t	CI (%)	ρ_0	ρ_t	CI (%)	ρ_0	ρ_t	CI (%)	
Avicel PH 101	0.35	0.44	20.45	0.35	0.44	20.45	0.35	0.44	20.45	20.45±0.00
Spress®® B820	0.64	0.71	9.86	0.64	0.71	9.86	0.64	0.71	9.86	9.86±0.00
Sago Starch	0.63	0.73	13.70	0.63	0.73	13.70	0.63	0.73	13.70	13.70±0.00
PS1	0.53	0.63	15.87	0.53	0.63	15.87	0.54	0.64	15.63	15.79±0.14
PS2	0.53	0.62	14.52	0.53	0.63	15.87	0.53	0.63	15.87	15.42±0.78
PS3	0.53	0.62	14.52	0.53	0.63	15.87	0.53	0.62	14.52	14.97±0.78
PS4	0.52	0.61	14.75	0.52	0.61	14.75	0.53	0.62	14.52	14.67±0.13

Table 2: Calculation of Hausner ratio (HR).

Sample powder	1			2			3			Mean HR±SD
	ρ	ρ_t	HR	ρ_0	ρ_t	HR	ρ_0	ρ_t	HR	
Avicel PH 101	0.35	0.44	1.26	0.35	0.44	1.26	0.35	0.44	1.26	1.26±0.00
Spress®® B820	0.64	0.71	1.11	0.64	0.71	1.11	0.64	0.71	1.11	1.11±0.00
Sago Starch	0.63	0.73	1.16	0.63	0.73	1.16	0.63	0.73	1.16	1.16±0.00
PS1	0.53	0.63	1.19	0.53	0.63	1.19	0.54	0.64	1.19	1.19±0.00
PS2	0.53	0.62	1.17	0.53	0.63	1.19	0.53	0.63	1.19	1.18±0.01
PS3	0.53	0.62	1.17	0.53	0.63	1.19	0.53	0.62	1.17	1.18±0.01
PS4	0.52	0.61	1.17	0.52	0.61	1.17	0.53	0.62	1.17	1.17±0.00

Table 3: Calculation of angle of repose, α (º).

Powder sample	1				2				3				Mean α(º)±SD
	X	Y	tg α	α(º)	X	Y	tg α	α(º)	X	Y	tg α	α(º)	
Avicel PH 101	-	-	-	-	-	-	-	-	-	-	-	-	-
Spress®® B820	4.4	2.5	0.57	29.7	4.4	2.6	0.59	30.5	4.4	2.6	0.59	30.5	30.23± 0.46
Sago Starch	-	-	-	-	-	-	-	-	-	-	-	-	-
PS1	4.6	2.9	0.63	32.2	4.4	2.8	0.64	32.6	4.5	2.8	0.62	31.8	32.20± 0.40
PS2	4.4	2.8	0.64	32.6	4.5	2.8	0.62	31.8	4.4	2.7	0.61	31.4	31.93± 0.61
PS3	4.5	2.7	0.6	31.0	4.6	2.7	0.59	30.5	4.6	2.8	0.61	31.4	30.97± 0.45
PS4	4.6	2.7	0.59	30.5	4.3	2.5	0.58	30.1	4.4	2.6	0.59	30.5	30.37± 0.23

Note: Y is height and X is diameter of the pile of the powder sample

Table 4: Calculation of flow rate.

Powder sample	1		2		3		Mean of flow rate (g/s)±SD
	Time (s)	Flow rate (g/s)	Time (s)	Flow rate (g/s)	Time (s)	Flow rate (g/s)	
Avicel PH 101	79	1.27	82	1.22	75	1.33	1.27±0.06
Spress®® B820	16	6.25	15	6.67	16	6.25	6.39±0.24
Sago starch	-	-	-	-	-	-	-
PS1	20	5.00	21	4.76	21	4.76	4.84±0.14
PS2	20	5.00	19	5.26	21	4.76	5.01±0.25
PS3	18	5.56	18	5.56	19	5.26	5.46±0.17
PS4	17	5.88	16	6.25	18	5.56	5.90±0.35

Appendix G: Powder Characterisation in compact form - Compression and Mechanical properties.

Table 1: Parameters for analysis of compression and mechanical properties of Avicel PH 101.

P (MPa)	No.	Hardness (N)	ρ_A (g/ml)	D (g/ml)	1 - D	ln 1/1 - D	C	P/C	T (N/mm^2)
20	1	92	0.88	0.56	0.44	0.82	0.60	33.33	1.11
	2	90	0.87	0.55	0.45	0.80	0.56	35.71	1.08
	3	89	0.88	0.56	0.44	0.82	0.60	33.33	1.06
Mean ±SD		90.33±1.53	0.88±0.01	0.56±0.01	0.44±0.01	0.81±0.01	0.59±0.02	34.12±1.37	1.08±0.03
40	1	200	1.12	0.71	0.29	1.24	0.69	57.97	3.04
	2	190	1.11	0.70	0.3	1.20	0.68	58.82	2.86
	3	198	1.11	0.70	0.3	1.20	0.68	58.82	3.00
Mean ±SD		196.00±5.29	1.11±0.01	0.70±0.01	0.30±0.01	1.21±0.02	0.68±0.01	58.54±0.49	2.97±0.09
60	1	295	1.26	0.79	0.21	1.56	0.72	83.33	5.09
	2	290	1.26	0.79	0.21	1.56	0.72	83.33	4.98
	3	288	1.26	0.79	0.21	1.56	0.72	83.33	4.93
Mean ±SD		291.00±3.61	1.26±0.00	0.79±0.00	0.21±0.00	1.56±0.00	0.72±0.00	83.33±0.00	5.00±0.08
80	1	350	1.32	0.83	0.17	1.77	0.73	109.59	6.30
	2	350	1.32	0.83	0.17	1.77	0.73	109.59	6.33
	3	349	1.31	0.83	0.17	1.77	0.73	109.59	6.22
Mean ±SD		349.67±0.58	1.32±0.01	0.83±0.01	0.17±0.00	1.77±0.00	0.73±0.00	109.59±0.00	6.28±0.06
100	1	401	1.36	0.86	0.14	1.97	0.74	135.14	7.49
	2	405	1.36	0.86	0.14	1.97	0.74	135.14	7.48
	3	402	1.36	0.86	0.14	1.97	0.74	135.14	7.47
Mean ±SD		402.67±2.08	1.36±0.00	0.86±0.00	0.14±0.00	1.97±0.00	0.74±0.00	135.14±0.00	7.48±0.01
120	1	452	1.39	0.88	0.12	2.12	0.75	160.00	8.63
	2	454	1.38	0.87	0.13	2.04	0.75	160.00	8.59
	3	450	1.40	0.89	0.11	2.21	0.75	160.00	8.58
Mean ±SD		452.00±2.00	1.39±0.01	0.88±0.01	0.12±0.01	2.12±0.09	0.75±0.00	160.00±0.00	8.60±0.03

‘Table 1, continued’

140	1	460	1.44	0.91	0.09	2.41	0.76	184.21	9.00
	2	457	1.44	0.91	0.09	2.41	0.76	184.21	8.90
	3	460	1.43	0.91	0.09	2.41	0.76	184.21	8.94
Mean ±SD		459.00±1.73	1.44±0.01	0.91±0.00	0.09±0.00	2.41±0.00	0.76±0.00	184.21±0.00	8.95±0.05
160	1	465	1.45	0.92	0.08	2.53	0.76	210.53	9.23
	2	465	1.45	0.92	0.08	2.53	0.76	210.53	9.19
	3	467	1.45	0.92	0.08	2.53	0.76	210.53	9.28
Mean ±SD		465.67±1.15	1.45±0.00	0.92±0.00	0.08±0.00	2.53±0.00	0.76±0.00	210.53±0.00	9.23±0.05
180	1	477	1.46	0.92	0.08	2.53	0.76	236.82	9.53
	2	478	1.48	0.94	0.06	2.81	0.76	236.82	9.67
	3	480	1.47	0.93	0.07	2.66	0.76	236.82	9.67
Mean ±SD		478.33±1.53	1.47±0.01	0.93±0.01	0.07±0.01	2.67±0.14	0.76±0.00	236.82±0.00	9.62±0.08
200	1	480	1.49	0.94	0.06	2.81	0.77	263.16	9.76
	2	479	1.48	0.94	0.06	2.81	0.76	263.16	9.70
	3	481	1.48	0.94	0.06	2.81	0.76	263.16	9.71
Mean ±SD		480.00±1.00	1.48±0.01	0.94±0.00	0.06±0.00	2.81±0.00	0.76±0.00	263.16±0.00	9.72±0.03

Note: P = compression pressure, ρ_A = apparent density, D = relative density, C= degree of volume reduction, T = tensile strength

Table 2: Parameters for analysis of compression and mechanical properties of Spress® B820.

P (MPa)	No.	Hardness (N)	ρ_A (g/ml)	D (g/ml)	1 - D	ln 1/1 - D	C	P/C	T (N/mm^2)
20	1	20	0.99	0.66	0.34	1.08	0.35	57.14	0.27
	2	22	1.00	0.67	0.33	1.11	0.36	55.55	0.29
	3	19	1.01	0.67	0.33	1.11	0.37	54.05	0.26
Mean ±SD		20.33±1.53	1.00±0.01	0.67±0.01	0.33±0.01	1.10±0.02	0.36±0.01	55.58±1.55	0.27±0.02
40	1	40	1.06	0.71	0.29	1.24	0.40	100.00	0.59
	2	42	1.07	0.71	0.29	1.24	0.40	100.00	0.62
	3	39	1.08	0.72	0.28	1.27	0.41	97.56	0.57
Mean ±SD		40.33±1.53	1.07±0.01	0.71±0.01	0.29±0.01	1.25±0.02	0.40±0.01	99.19±1.41	0.59±0.03
60	1	70	1.24	0.83	0.17	1.77	0.48	125.00	1.18
	2	72	1.24	0.83	0.17	1.77	0.48	125.00	1.21
	3	70	1.23	0.82	0.18	1.71	0.48	125.00	1.17
Mean ±SD		70.67±1.15	1.24±0.01	0.83±0.01	0.17±0.01	1.75±0.03	0.48±0.00	125.00±0.00	1.19±0.02
80	1	109	1.29	0.86	0.14	1.97	0.50	160.00	1.92
	2	106	1.27	0.85	0.15	1.90	0.50	160.00	1.84
	3	107	1.27	0.85	0.15	1.90	0.50	160.00	1.85
Mean ±SD		107.33±1.53	1.28±0.01	0.85±0.01	0.15±0.01	1.92±0.04	0.50±0,00	160.00±0.00	1.87±0.04
100	1	126	1.32	0.88	0.12	2.12	0.52	192.31	2.26
	2	127	1.32	0.88	0.12	2.12	0.52	192.31	2.30
	3	130	1.33	0.89	0.11	2.21	0.52	192.31	2.38
Mean ±SD		127.67±2.08	1.32±0.01	0.88±0.01	0.12±0.01	2.15±0.05	0.52±0.00	192.31±0.00	2.31±0.06
120	1	147	1.34	0.89	0.11	2.21	0.52	230.77	2.72
	2	148	1.36	0.91	0.09	2.41	0.53	226.42	2.78
	3	150	1.35	0.90	0.1	2.30	0.53	226.42	2.79
Mean ±SD		148.33±1.53	1.35±0.01	0.90±0.01	0.10±0.01	2.31±0.10	0.53±0.01	227.87±2.51	2.76±0.04

‘Table 2, continued’

140	1	180	1.37	0.91	0.09	2.41	0.53	264.15	3.41
	2	180	1.38	0.92	0.08	2.53	0.54	259.26	3.41
	3	185	1.37	0.91	0.09	2.41	0.53	264.15	3.51
Mean ±SD		181.67±2.89	1.37±0.01	0.91±0.01	0.09±0.01	2.45±0.07	0.53±0.01	262.52±2.82	3.44±0.06
160	1	186	1.39	0.93	0.07	2.66	0.54	296.30	3.54
	2	190	1.38	0.92	0.08	2.53	0.54	296.30	3.63
	3	189	1.40	0.93	0.07	2.66	0.54	296.30	3.63
Mean ±SD		188.33±2.08	1.39±0.01	0.93±0.01	0.07±0.01	2.62±0.08	0.54±0.00	296.30±0.00	3.60±0.05
180	1	220	1.40	0.93	0.07	2.66	0.54	333.33	4.20
	2	223	1.41	0.94	0.06	2.81	0.55	327.27	4.28
	3	225	1.42	0.95	0.05	3.00	0.55	327.27	4.35
Mean ±SD		222.67±2.52	1.41±0.01	0.94±0.01	0.06±0.01	2.82±0.17	0.55±0.01	329.29±3.50	4.28±0.08
200	1	226	1.42	0.95	0.05	3.00	0.55	363.64	4.38
	2	224	1.42	0.95	0.05	3.00	0.55	363.64	4.32
	3	222	1.42	0.95	0.05	3.00	0.55	363.64	4.28
Mean ±SD		224.00±2.00	1.42±0.00	0.95±0.00	0.05±0.00	3.00±0.00	0.55±0.00	363.64±0.00	4.33±0.05

Note: P = compression pressure, ρ_A = apparent density, D = relative density, C= degree of volume reduction, T = tensile strength

Table 3: Parameters for analysis of compression and mechanical properties of sago starch.

P (MPa)	No.	Hardness (N)	ρ_A (g/ml)	D (g/ml)	1 - D	ln 1/1 - D	C	P/C	T (N/mm^2)
20	1								
	2								
	3								
Mean ±SD									
40	1	21	0.99	0.64	0.36	1.02	0.36	111.11	0.29
	2	22	1.00	0.65	0.35	1.05	0.37	108.11	0.30
	3	18	0.99	0.64	0.36	1.02	0.36	111.11	0.25
Mean ±SD		20.33±2.08	0.99±0.01	0.64±0.01	0.36±0.01	1.03±0.02	0.36±0.01	110.11±1.73	0.28±0.03
60	1	32	1.02	0.66	0.34	1.08	0.38	157.89	0.44
	2	37	1.02	0.66	0.34	1.08	0.38	157.89	0.48
	3	30	1.00	0.65	0.35	1.05	0.37	162.16	0.41
Mean ±SD		33.00±3.61	1.01±0.01	0.66±0.01	0.34±0.01	1.07±0.02	0.38±0.01	159.31±2.47	0.44±0.04
80	1	37	1.05	0.68	0.32	1.12	0.40	200.00	0.53
	2	33	1.04	0.67	0.33	1.11	0.39	205.13	0.47
	3	31	1.03	0.66	0.34	1.08	0.39	205.13	0.44
Mean ±SD		33.67±3.06	1.04±0.01	0.67±0.01	0.33±0.01	1.10±0.02	0.39±0.01	203.42±2.96	0.48±0.05
100	1	39	1.06	0.68	0.32	1.14	0.41	243.90	0.57
	2	41	1.06	0.68	0.32	1.14	0.41	243.90	0.60
	3	41	1.06	0.68	0.32	1.14	0.41	243.90	0.60
Mean ±SD		40.33±1.15	1.06±0.01	0.68±0.00	0.32±0.00	1.14±0.00	0.41±0.00	243.90±0.00	0.59±0.02
120	1	47	1.07	0.69	0.31	1.17	0.41	292.68	0.70
	2	50	1.07	0.69	0.31	1.17	0.41	292.68	0.74
	3	48	1.07	0.69	0.31	1.17	0.41	292.68	0.71
Mean ±SD		48.33±1.53	1.07±0.00	0.69±0.00	0.31±0.00	1.17±0.00	0.41±0.00	292.68±0.00	0.72±0.02

'Table 3, continued'

140	1	52	1.10	0.71	0.29	1.24	0.43	325.58	0.79
	2	46	1.08	0.70	0.3	1.20	0.42	333.33	0.69
	3	49	1.09	0.70	0.3	1.20	0.42	333.33	0.74
Mean ±SD		49.00±3.00	1.09±0.01	0.70±0.01	0.30±0.01	1.21±0.02	0.42±0.01	330.75±4.47	0.74±0.05

Note: P = compression pressure, ρ_A = apparent density, D = relative density, C= degree of volume reduction, T = tensile strength

Table 4: Parameters for analysis of compression and mechanical properties of PS1.

P (MPa)	No.	Hardness (N)	ρ_A (g/ml)	D (g/ml)	1 - D	ln 1/1 - D	C	P/C	T (N/mm^2)
20	1								
	2								
	3								
Mean ±SD									
40	1	27	0.94	0.62	0.38	0.96	0.44	90.91	0.35
	2	26	0.93	0.62	0.38	0.96	0.43	93.02	0.33
	3	29	0.93	0.62	0.38	0.96	0.42	95.24	0.37
Mean ±SD		27.33±1.53	0.93±0.01	0.62±0.00	0.38±0.00	0.96±0.00	0.43±0.01	93.06±2.17	0.35±0.02
60	1	36	0.95	0.63	0.37	0.99	0.44	136.37	0.47
	2	38	0.96	0.64	0.36	1.02	0.45	133.33	0.50
	3	32	0.95	0.63	0.37	0.99	0.43	139.53	0.42
Mean ±SD		35.33±3.06	0.95±0.01	0.63±0.01	0.37±0.01	1.00±0.02	0.44±0.01	136.41±3.10	0.46±0.04
80	1	48	0.97	0.65	0.35	1.05	0.45	177.78	0.64
	2	50	0.98	0.65	0.35	1.05	0.46	173.91	0.67
	3	44	0.97	0.65	0.35	1.05	0.44	181.82	0.59
Mean ±SD		47.33±3.06	0.97±0.01	0.65±0.00	0.35±0.00	1.05±0.00	0.45±0.01	177.84±3.96	0.63±0.04
100	1	54	0.99	0.66	0.34	1.08	0.46	217.39	0.74
	2	55	0.99	0.66	0.34	1.08	0.46	217.39	0.75
	3	52	1.00	0.66	0.34	1.08	0.46	217.39	0.71
Mean ±SD		53.67±1.53	0.99±0.01	0.66±0.00	0.34±0.00	1.08±0.00	0.46±0.00	217.39±0.00	0.73±0.02

‘Table 4, continued’

120	1	64	1.01	0.67	0.33	1.11	0.48	250.00	0.89
	2	66	1.01	0.67	0.33	1.11	0.48	250.00	0.91
	3	63	1.01	0.67	0.33	1.11	0.47	255.32	0.87
Mean ±SD		64.33±1.53	1.01±0.00	0.67±0.00	0.33±0.00	1.11±0.00	0.48±0.01	251.77±3.07	0.89±0.02
140	1	71	1.02	0.68	0.32	1.14	0.48	291.67	1.00
	2	69	1.02	0.68	0.32	1.14	0.48	291.67	0.97
	3	73	1.03	0.68	0.32	1.14	0.48	291.67	1.04
Mean ±SD		71.00±2.00	1.02±0.00	0.68±0.00	0.32±0.00	1.14±0.00	0.48±0.00	291.67±0.00	1.00±0.04
160	1	76	1.03	0.69	0.31	1.17	0.49	326.53	1.08
	2	78	1.03	0.69	0.31	1.17	0.49	326.53	1.11
	3	74	1.04	0.69	0.31	1.17	0.48	333.33	1.06
Mean ±SD		76.00±2.00	1.03±0.01	0.69±0.00	0.31±0.00	1.17±0.00	0.49±0.01	328.80±3.93	1.08±0.03
180	1	81	1.05	0.70	0.3	1.20	0.50	360.00	1.17
	2	83	1.05	0.70	0.3	1.20	0.50	360.00	1.20
	3	79	1.05	0.70	0.3	1.20	0.48	375.00	1.14
Mean ±SD		81.00±2.00	1.05±0.00	0.70±0.00	0.30±0.00	1.20±0.00	0.49±0.01	365.00±8.66	1.17±0.03
200	1	83	1.06	0.71	0.29	1.24	0.50	400.00	1.21
	2	85	1.06	0.71	0.29	1.24	0.50	400.00	1.23
	3	83	1.06	0.71	0.29	1.24	0.49	408.16	1.20
Mean ±SD		83.67±1.15	1.06±0.00	0.71±0.00	0.29±0.00	1.24±0.00	0.50±0.01	402.72±4.71	1.21±0.02

Note: P = compression pressure, ρ_A = apparent density, D = relative density, C= degree of volume reduction, T = tensile strength

Table 5: Parameters for analysis of compression and mechanical properties of PS2.

P (MPa)	No.	Hardness (N)	ρ_A (g/ml)	D (g/ml)	1 - D	ln 1/1 - D	C	P/C	T (N/mm^2)
20	1								
	2								
	3								
Mean ±SD									
Mean ±SD	1	28	0.95	0.63	0.37	0.99	0.44	90.91	0.37
	2	25	0.94	0.62	0.38	0.97	0.44	90.91	0.31
	3	31	0.96	0.63	0.37	0.99	0.45	88.89	0.41
Mean ±SD		28.00±3.00	0.95±0.01	0.63±0.01	0.37±0.01	0.98±0.01	0.44±0.01	90.24±1.17	0.36±0.05
60	1	48	0.99	0.65	0.35	1.05	0.46	130.43	0.66
	2	53	1.00	0.66	0.34	1.08	0.47	127.66	0.73
	3	42	0.99	0.65	0.35	1.05	0.46	130.43	0.57
Mean ±SD		47.67±5.51	0.99±0.01	0.65±0.01	0.35±0.01	1.06±0.02	0.46±0.01	129.51±1.60	0.65±0.08
80	1	70	1.02	0.67	0.33	1.11	0.48	166.67	0.99
	2	68	1.03	0.68	0.32	1.14	0.49	163.27	0.96
	3	72	1.03	0.68	0.32	1.14	0.49	163.27	1.03
Mean ±SD		70.00±2.00	1.03±0.01	0.68±0.01	0.32±0.01	1.13±0.02	0.49±0.01	164.40±1.96	0.99±0.04
100	1	80	1.06	0.70	0.3	1.20	0.50	200.00	1.17
	2	83	1.07	0.70	0.3	1.20	0.50	200.00	1.22
	3	75	1.06	0.70	0.3	1.20	0.50	200.00	1.09
Mean ±SD		79.33±4.04	1.06±0.01	0.70±0.00	0.30±0.00	1.20±0.00	0.50±0.00	200.00±0.00	1.16±0.07
120	1	90	1.09	0.72	0.28	1.27	0.51	235.29	1.35
	2	91	1.09	0.72	0.28	1.27	0.51	235.29	1.37
	3	88	1.09	0.72	0.28	1.27	0.51	235.29	1.32
Mean ±SD		89.67±1.53	1.09±0.00	0.72±0.00	0.28±0.00	1.27±0.00	0.51±0.00	235.29±0.00	1.35±0.03
140	1	98	1.11	0.73	0.27	1.31	0.52	269.23	1.50
	2	95	1.10	0.72	0.28	1.27	0.52	269.23	1.44
	3	100	1.12	0.74	0.26	1.35	0.53	264.15	1.54
Mean ±SD		97.67±2.52	1.11±0.01	0.73±0.01	0.27±0.01	1.31±0.04	0.52±0.01	267.54±2.93	1.49±0.05

‘Table 5, continued’

160	1	102	1.13	0.74	0.26	1.34	0.53	301.89	1.60
	2	100	1.13	0.74	0.26	1.34	0.53	301.89	1.56
	3	105	1.13	0.74	0.26	1.34	0.53	301.89	1.65
Mean ±SD		102.33±2.52	1.13±0.00	0.74±0.00	0.26±0.00	1.34±0.00	0.53±0.00	301.89±0.00	1.60±0.05
180	1	109	1.14	0.75	0.25	1.39	0.54	333.33	1.72
	2	106	1.14	0.75	0.25	1.39	0.54	333.33	1.66
	2	104	1.14	0.75	0.25	1.39	0.54	333.33	1.64
Mean ±SD		106.33±2.52	1.14±0.00	0.75±0.00	0.25±0.00	1.39±0.00	0.54±0.00	333.33±0.00	1.67±0.04
200	1	112	1.17	0.77	0.23	1.47	0.55	363.64	1.80
	2	116	1.20	0.79	0.21	1.56	0.56	357.14	1.92
	2	110	1.16	0.76	0.24	1.42	0.54	370.37	1.77
Mean ±SD		112.67±3.06	1.18±0.02	0.77±0.02	0.23±0.02	1.48±0.07	0.55±0.01	363.72±6..61	1.83±0.08

Note: P = compression pressure, ρ_A = apparent density, D = relative density, C= degree of volume reduction, T = tensile strength

Table 6: Parameters for analysis of compression and mechanical properties of PS3.

P (MPa)	No.	Hardness (N)	ρ_A (g/ml)	D (g/ml)	1 - D	ln 1/1 - D	C	P/C	T (N/mm^2)
20	1								
	2								
	3								
Mean ±SD									
40	1	35	0.95	0.63	0.37	0.99	0.44	90.91	0.46
	2	36	0.95	0.63	0.37	0.99	0.44	90.91	0.47
	3	35	0.95	0.63	0.37	0.99	0.44	90.91	0.46
Mean ±SD		35.33±0.58	0.95±0.00	0.63±0.00	0.37±0.00	0.99±0.00	0.44±0.00	90.91±0.00	0.46±0.01
60	1	72	0.97	0.64	0.36	1.02	0.45	133.33	0.96
	2	70	0.98	0.64	0.36	1.02	0.46	130.43	0.94
	3	69	0.97	0.64	0.36	1.02	0.45	133.33	0.92
Mean ±SD		70.33±1.53	0.97±0.01	0.64±0.00	0.36±0.00	1.02±0.00	0.45±0.01	132.36±1.67	0.94±0.02
80	1	77	1.02	0.67	0.33	1.12	0.48	166.67	1.07
	2	75	1.02	0.67	0.33	1.12	0.48	166.67	1.04
	3	80	1.02	0.67	0.33	1.12	0.48	166.67	1.13
Mean ±SD		77.33±2.52	1.02±0.00	0.67±0.00	0.33±0.00	1.12±0.00	0.48±0.00	166.67±0.00	1.08±0.05
100	1	85	1.04	0.68	0.32	1.14	0.49	204.08	1.21
	2	87	1.04	0.68	0.32	1.14	0.49	204.08	1.24
	3	79	1.03	0.68	0.32	1.14	0.49	204.08	1.12
Mean ±SD		83.67±4.16	1.04±0.01	0.68±0.00	0.32±0.00	1.14±0.00	0.49±0.00	204.08±0.00	1.19±0.06
120	1	94	1.05	0.69	0.31	1.17	0.50	240.00	1.36
	2	90	1.06	0.70	0.3	1.20	0.50	240.00	1.31
	3	97	1.06	0.70	0.3	1.20	0.50	240.00	1.42
Mean ±SD		93.67±3.51	1.06±0.01	0.70±0.01	0.30±0.01	1.19±0.02	0.50±0.00	240.00±0.00	1.36±0.06

‘Table 6, continued’

140	1	100	1.10	0.72	0.28	1.27	0.52	269.23	1.50
	2	103	1.09	0.72	0.28	1.27	0.51	274.51	1.55
	3	98	1.09	0.72	0.28	1.27	0.51	274.51	1.47
Mean ±SD		100.33±2.52	1.09± 0.01	0.72± 0.00	0.28± 0.00	1.27±0.00	0.51±0.01	272.75±3.05	1.51±0.04
160	1	117	1.15	0.76	0.24	1.43	0.54	296.30	1.82
	2	113	1.11	0.73	0.27	1.31	0.52	311.54	1.74
	3	108	1.11	0.73	0.27	1.31	0.52	311.54	1.66
Mean ±SD		112.67±4.51	1.12± 0.02	0.74± 0.02	0.26± 0.02	1.35±0.07	0.53±0.01	306.46±8.80	1.74±0.08
180	1	126	1.17	0.77	0.23	1.47	0.55	327.27	2.02
	2	120	1.15	0.76	0.24	1.43	0.54	333.33	1.90
	2	124	1.16	0.76	0.24	1.43	0.54	333.33	1.98
Mean ±SD		123.33±3.01	1.16± 0.01	0.76± 0.01	0.24± 0.01	1.44±0.02	0.54±0.01	331.31±3.50	1.97±0.06
200	1	137	1.21	0.80	0.2	1.61	0.56	357.14	2.29
	2	134	1.21	0.80	0.2	1.61	0.56	357.14	2.23
	2	131	1.20	0.79	0.21	1.56	0.56	357.14	2.17
Mean ±SD		134.00±3.00	1.21± 0.01	0.80± 0.01	0.20± 0.01	1.59±0.03	0.56±0.00	357.14±0.00	2.23±0.06

Note: P = compression pressure, ρ_A = apparent density, D = relative density, C= degree of volume reduction, T = tensile strength

Table 7: Parameters for analysis of compression and mechanical properties of PS4.

P (MPa)	No.	Hardness (N)	ρ_A (g/ml)	D (g/ml)	1 - D	ln 1/1 - D	C	P/C	T (N/mm^2)
20	1	40	1.01	0.66	0.34	1.08	0.48	41.67	0.55
	2	38	1.00	0.66	0.34	1.08	0.48	41.67	0.52
	3	37	1.00	0.66	0.34	1.08	0.47	42.55	0.51
Mean ±SD		38.33±1.53	1.00±0.01	0.66±0.00	0.34±0.00	1.08±0.00	0.48±0.01	41.96±0.51	0.53±0.02
40	1	58	1.04	0.68	0.32	1.14	0.50	80.00	0.83
	2	62	1.05	0.69	0.31	1.17	0.50	80.00	0.89
	3	59	1.03	0.68	0.32	1.14	0.49	81.63	0.84
Mean ±SD		59.67±2.08	1.04±0.01	0.68±0.01	0.32±0.01	1.15±0.02	0.50±0.01	80.54±0.94	0.85±0.03
60	1	73	1.07	0.70	0.3	1.20	0.51	117.65	1.07
	2	71	1.06	0.70	0.3	1.20	0.51	117.65	1.03
	3	74	1.06	0.70	0.3	1.20	0.50	120.00	1.08
Mean ±SD		72.67±1.53	1.06±0.01	0.70±0.00	0.30±0.00	1.20±0.00	0.51±0.01	118.43±1.36	1.06±0.03
80	1	101	1.11	0.73	0.27	1.31	0.53	150.94	1.55
	2	104	1.12	0.74	0.26	1.35	0.54	148.15	1.61
	3	102	1.11	0.73	0.27	1.31	0.52	153.85	1.56
Mean ±SD		102.33±1.53	1.11±0.01	0.73±0.01	0.27±0.01	1.32±0.02	0.53±0.01	150.98±2.85	1.57±0.03
100	1	120	1.16	0.76	0.24	1.43	0.55	181.82	1.92
	2	124	1.18	0.78	0.22	1.51	0.56	178.57	2.01
	3	118	1.15	0.76	0.24	1.43	0.54	185.19	1.88
Mean ±SD		120.67±3.06	1.16±0.02	0.76±0.01	0.23±0.01	1.46±0.05	0.55±0.01	181.86±3.31	1.94±0.07
120	1	145	1.24	0.82	0.18	1.71	0.58	206.90	2.45
	2	144	1.23	0.81	0.19	1.66	0.58	206.90	2.43
	3	140	1.22	0.80	0.2	1.61	0.57	210.53	2.34
Mean ±SD		143.00±2.65	1.23±0.01	0.81±0.01	0.19±0.01	1.66±0.05	0.58±0.01	208.11±2.10	2.41±0.06

‘Table 7, continued’

140	1	163	1.32	0.87	0.13	2.04	0.61	229.51	2.93
	2	160	1.26	0.83	0.17	1.77	0.59	237.29	2.78
	3	158	1.26	0.83	0.17	1.77	0.58	241.38	2.72
Mean ±SD		160.33±2.52	1.28±0.03	0.84±0.02	0.16±0.02	1.86±0.16	0.59±0.02	236.06±6.03	2.81±0.11
160	1	178	1.32	0.87	0.13	2.04	0.61	262.30	3.23
	2	179	1.32	0.87	0.13	2.04	0.61	262.30	3.24
	3	180	1.33	0.88	0.12	2.12	0.60	266.67	3.29
Mean ±SD		179.00±1.00	1.32±0.01	0.87±0.01	0.13±0.01	2.07±0.05	0.61±0.01	263.76±2.52	3.25±0.03
180	1	188	1.36	0.89	0.11	2.21	0.62	290.32	3.50
	2	188	1.35	0.89	0.11	2.21	0.61	295.08	3.48
	3	190	1.37	0.90	0.1	2.30	0.61	295.08	3.57
Mean ±SD		188.67±1.15	1.36±0.01	0.89±0.01	0.11±0.01	2.24±0.05	0.61±0.01	293.49±2.75	3.52±0.05
200	1	204	1.41	0.93	0.07	2.66	0.63	317.46	3.92
	2	203	1.39	0.91	0.09	2.41	0.63	317.46	3.87
	3	206	1.39	0.91	0.09	2.41	0.62	322.58	3.96
Mean ±SD		204.33±1.53	1.40±0.01	0.92±0.01	0.08±0.01	2.49±0.14	0.63±0.01	319.17±2.97	3.92±0.05

Note: P = compression pressure, ρ_A = apparent density, D = relative density, C= degree of volume reduction, T = tensile strength

Appendix H: Powder Characterisation in compact form - Lubricant sensitivity.

Table 1: Mixture of Avicel PH 101and Magnesium stearate.

P (MPa)	Compact	Hardness (N)				
		Concentration of magnesium stearate (%)				
		0	0.25	0.5	0.75	1
20	1	92	64	59	51	50
	2	90	62	62	48	52
	3	89	65	60	52	48
Mean± SD		90.33±1.53	63.67±1.52	60.33±1.52	50.33±2.08	50.00±2.00
40	1	200	160	154	147	149
	2	190	160	155	149	150
	3	198	163	152	150	147
Mean± SD		196.00±5.29	161.00±1.73	153.67±1.52	148.67±1.53	148.67±1.53
60	1	295	254	253	240	239
	2	290	256	248	242	242
	3	288	254	251	243	242
Mean± SD		291.00±3.61	254.67±1.15	250.67±2.52	241.67±1.53	241.67±1.53
80	1	350	337	324	310	310
	2	350	335	321	316	315
	3	349	331	322	312	312
Mean± SD		349.67±0.58	334.33±3.06	322.33±1.52	312.67±3.06	312.33±2.52
100	1	401	377	369	362	360
	2	405	380	366	365	365
	3	402	376	370	361	362
Mean± SD		402.67±2.08	377.67±2.08	368.33±2.08	362.67±2.08	362.33±2.52
120	1	452	430	420	410	408
	2	454	430	418	408	410
	3	450	429	422	412	412
Mean± SD		452.00±2.00	429.67±0.58	420.00±2.00	410.00±2.00	410.00±2.00

Note: P = compression pressure

Table 2: Mixture of Spress® B820 and Magnesium stearate.

P (MPa)	Compact	Hardness (N)				
		Concentration of magnesium stearate (%)				
		0	0.25	0.5	0.75	1
20	1	20				
	2	22				
	3	19				
Mean± SD		20.33±1.53				
40	1	40	5	7	8	3
	2	42	5	6	9	4
	3	39	5	7	8	3
Mean± SD		40.33±1.53	5.00±0.00	6.67±0.58	8.33±0.58	3.33±0.58
60	1	70	22	15	10	6
	2	72	21	13	9	6
	3	70	20	11	10	7
Mean± SD		70.67±1.15	21.00±1.00	13.00±2.00	9.67±0.58	6.33±0.58
80	1	109	24	16	11	7
	2	106	24	15	11	7
	3	107	23	14	11	6
Mean± SD		107.33±1.53	23.67±0.58	15.00±1.00	11.00±0.00	6.67±0.58
100	1	126	27	18	12	9
	2	127	25	19	13	7
	3	130	30	17	12	7
Mean± SD		127.67±2.08	27.33±2.52	18.00±1.00	12.33±0.58	7.67±1.15
120	1	147	34	20	13	8
	2	148	34	21	13	7
	3	150	34	19	14	8
Mean± SD		148.33±1.53	34.00±0.00	20.00±1.00	13.33±0.58	7.67±0.58

Note: P = compression pressure

Table 3: Mixture of sago starch and Magnesium stearate.

P (MPa)	Compact	Hardness (N)				
		Concentration of magnesium stearate (%)				
		0	0.25	0.5	0.75	1
20	1					
	2					
	3					
Mean± SD						
40	1	21	17	16	5	5
	2	22	17	13	5	6
	3	18	15	15	5	5
Mean± SD		20.33±2.08	16.33±1.15	14.67±1.53	5.00±0.00	5.33±0.58
60	1	32	25	26	20	18
	2	37	22	23	24	16
	3	30	28	23	22	15
Mean± SD		33.00±3.61	25.00±3.00	24.00±1.73	22.00±2.00	16.33±1.53
80	1	37	28	26	23	21
	2	33	26	25	28	19
	3	31	27	27	27	20
Mean± SD		33.67±3.06	27.00±1.00	26.00±1.00	26.00±2.65	20.00±1.00
100	1	39	31	30	26	20
	2	41	30	29	25	21
	3	41	33	28	30	22
Mean± SD		40.33±1.15	31.33±1.53	29.00±1.00	27.00±2.65	21.00±1.00
120	1	47	36	31	29	23
	2	50	37	34	30	25
	3	48	38	33	29	28
Mean± SD		48.33±1.53	37.00±1.00	32.67±1.53	29.33±0.58	25.33±2.52

Note: P = compression pressure

Table 4: Mixture of PS1and Magnesium stearate.

P (MPa)	Compact	Hardness (N)				
		Concentration of magnesium stearate (%)				
		0	0.25	0.5	0.75	1
20	1					
	2					
	3					
Mean± SD						
40	1	27	8	8	4	2
	2	26	9	6	4	3
	3	29	8	9	4	3
Mean± SD		27.33±1.53	8.33±0.58	7.67±1.53	4.00±0.00	3.00±0.00
60	1	36	13	12	11	6
	2	38	12	12	9	6
	3	32	12	10	9	5
Mean± SD		35.33±3.06	12.33±0.58	11.33±1.15	9.67±1.15	5.67±0.58
80	1	48	15	13	16	8
	2	50	13	14	12	9
	3	44	14	12	10	8
Mean± SD		47.33±3.06	14.00±1.00	13.00±1.00	12.67±3.06	8.33±0.58
100	1	54	21	15	15	11
	2	55	16	16	14	9
	3	52	17	17	14	8
Mean± SD		53.67±1.53	18.00±2.65	16.00±1.00	14.33±0.58	9.33±1.53
120	1	64	24	19	17	12
	2	66	26	21	16	13
	3	63	23	19	17	11
Mean± SD		64.33±1.53	24.33±1.53	19.67±1.15	16.67±0.58	12.00±1.00

Note: P = compression pressure

Table 5: Mixture of PS2 and Magnesium stearate.

P (MPa)	Compact	Hardness (N)				
		Concentration of magnesium stearate (%)				
		0	0.25	0.5	0.75	1
20	1					
	2					
	3					
Mean± SD						
40	1	28	15	8	5	3
	2	25	13	7	4	3
	3	31	14	7	5	3
Mean± SD		28.00±3.00	14.00±1.00	7.33±0.58	4.67±0.58	3.00±0.00
60	1	48	21	14	11	7
	2	53	22	13	11	6
	3	42	22	16	11	7
Mean± SD		47.67±5.51	21.67±0.58	14.33±1.53	11.00±0.00	6.67±0.58
80	1	70	24	14	14	8
	2	68	26	15	14	8
	3	72	28	16	14	7
Mean± SD		70.00±2.00	26.00±2.00	15.00±1.00	14.00±0.00	7.67±0.58
100	1	80	30	24	15	9
	2	83	33	25	16	9
	3	75	31	26	14	10
Mean± SD		79.33±4.04	31.33±1.53	25.00±1.00	15.00±1.00	9.33±0.58
120	1	90	31	28	20	12
	2	91	33	26	19	11
	3	88	31	24	19	11
Mean± SD		89.67±1.53	31.67±1.15	26.00±2.00	19.33±0.58	11.33±0.58

Note: P = compression pressure

Table 6: Mixture of PS3 and Magnesium stearate.

P (MPa)	Compact	Hardness (N)				
		Concentration of magnesium stearate (%)				
		0	0.25	0.5	0.75	1
20	1					
	2					
	3					
Mean± SD						
40	1	35	11	9	7	4
	2	36	12	10	5	3
	3	35	10	10	5	3
Mean± SD		35.33±0.58	11.00±1.00	9.67±0.58	5.67±1.15	3.65±0.92
60	1	72	23	20	14	5
	2	70	20	17	12	6
	3	69	22	15	10	7
Mean± SD		70.33±1.53	21.67±1.53	17.33±2.52	12.00±2.00	6.00±1.00
80	1	77	25	21	14	7
	2	75	26	22	14	8
	3	80	27	19	15	6
Mean± SD		77.33±2.52	26.00±1.00	20.67±1.53	14.33±0.58	7.00±1.00
100	1	85	28	22	17	8
	2	87	28	24	19	10
	3	79	27	22	16	10
Mean± SD		83.67±4.16	27.68±0.58	22.67±1.15	17.33±1.53	9.33±1.15
120	1	94	32	26	18	11
	2	90	30	24	16	10
	3	97	33	24	20	10
Mean± SD		93.67±3.51	31.67±1.53	24.67±1.15	18.00±2.00	10.33±0.58

Note: P = compression pressure

Table 7: Mixture of PS4 and Magnesium stearate.

P (MPa)	Compact	Hardness (N)				
		Concentration of magnesium stearate (%)				
		0	0.25	0.5	0.75	1
20	1	40	7	6	4	2
	2	38	6	6	5	4
	3	37	8	6	5	3
Mean± SD		38.33±1.53	7.00±1.00	6.00±0.00	4.67±0.58	3.00±1.00
40	1	58	11	11	8	6
	2	62	14	11	8	6
	3	59	11	12	9	6
Mean± SD		59.67±2.08	12.00±1.73	11.33±0.58	8.33±0.58	6.00±1.00
60	1	73	20	17	11	7
	2	71	18	15	10	8
	3	74	21	14	12	8
Mean± SD		72.67±1.53	19.67±1.53	15.33±1.53	11.00±1.00	7.67±0.58
80	1	101	28	22	12	8
	2	104	31	22	14	10
	3	102	30	24	15	10
Mean± SD		102.33±1.53	29.67±1.53	22.67±1.15	13.67±1.53	9.33±1.15
100	1	120	36	29	18	12
	2	124	34	27	16	12
	3	118	33	30	15	10
Mean± SD		120.67±3.06	34.33±1.53	28.67±1.53	16.33±1.53	11.33±1.15
120	1	145	44	34	21	12
	2	144	42	30	25	12
	3	140	45	32	24	11
Mean± SD		143.00±2.65	43.67±1.53	32.00±2.00	23.33±2.08	11.67±0.58

Note: P = compression pressure

Table 8: Hardness of compacts without lubricant (H_0) and with lubricant magnesium stearate (H) at highest compression pressure applied (120 MPa).

Powder	Compact	Hardness (N)				
		Concentration of magnesium stearate (%)				
		0.00	0.25	0.50	0.75	1.00
Avicel PH 101	1	452	430	420	410	408
	2	454	430	418	408	410
	3	450	429	422	412	412
Mean± SD		452.00±2.00	429.67±0.58	420.00±2.00	410.00±2.00	410.00±2.00
Spress® B820	1	147	34	20	13	8
	2	148	34	21	13	7
	3	150	34	19	14	8
Mean± SD		148.33±1.53	34.00±0.00	20.00±1.00	13.33±0.58	7.67±0.58
Sago starch	1	47	36	31	29	23
	2	50	37	34	30	25
	3	48	38	33	29	28
Mean± SD		48.33±1.53	37.00±1.00	32.67±1.53	29.33±0.58	25.33±2.52
PS1	1	64	20	19	17	5
	2	66	23	20	16	6
	3	63	18	16	17	7
Mean± SD		64.33±1.53	24.33±1.53	19.67±1.15	16.67±0.58	12.00±1.00
PS2	1	90	31	28	16	12
	2	91	33	26	17	11
	3	88	31	24	14	11
Mean± SD		89.67±1.53	31.67±1.15	26.00±2.00	19.33±0.58	11.33±0.58
PS3	1	94	70	47	36	17
	2	90	69	47	36	19
	3	97	65	46	39	20
Mean± SD		93.67±3.51	31.67±1.53	24.67±1.15	18.00±2.00	10.33±0.58
PS4	1	145	94	67	49	36
	2	144	91	65	51	37
	3	140	98	66	50	35
Mean± SD		143.00±2.65	43.67±1.53	32.00±2.00	23.33±2.08	11.67±0.58

Table 9: Lubricant sensitivity ratio (LSR).

Powder	LSR (%)			
	Concentration of magnesium stearate (%)			
	0.25	0.5	0.75	1
Avicel PH 101	4.87	7.08	9.29	9.73
	5.29	7.93	10.13	9.69
	4.67	6.22	8.44	8.44
Mean±SD	4.94 ±0.32	7.08±0.86	9.29±0.88	9.29±0.73
Spress® B820	76.87	86.39	91.16	94.56
	77.03	85.81	91.22	95.27
	77.33	87.33	90.67	94.67
Mean±SD	77.08 ±0.23	86.51±0.77	91.02±0.30	94.83±0.38
Sago starch	23.4	34.04	38.3	51.06
	26	32	40	50
	20.83	31.25	39.58	41.67
Mean±SD	23.41 ±2.56	32.43±1.44	39.29±0.89	47.58±5.14
PS1	62.50	67.19	73.44	79.69
	60.61	71.21	75.76	81.82
	63.49	68.25	73.02	82.54
Mean±SD	62.20±1.46	68.88±2.08	74.07±1.48	81.35±1.48
PS2	65.56	68.89	77.78	86.67
	63.74	71.43	79.12	87.91
	64.77	72.73	78.41	87.5
Mean±SD	64.96 ±0.91	71.02±1.95	78.44±0.67	87.36±0.63
PS3	65.96	72.34	80.85	88.30
	66.67	73.33	82.22	88.89
	65.98	75.26	79.38	89.69
Mean±SD	66.20±0.44	73.64±1.49	80.82±1.42	88.96±0.70
PS4	69.66	76.55	85.52	91.72
	70.83	79.17	82.64	91.67
	67.86	77.14	82.86	92.14
Mean±SD	69.45±1.50	77.62±1.37	83.67±1.60	91.84±2.58

Appendix I: Powder Characterisation in compact form - Loading capacity.

Table 1: Mixture of Avicel PH 101 and Paracetamol.

P (MPa)	Compact	Tensile strength, T (N/mm^2)					
		Concentration of paracetamol (%)					
		0	10	20	30	40	50
20	1	1.11	1.07	1.00	0.70	0.48	0.32
	2	1.08	1.06	1.00	0.68	0.48	0.40
	3	1.06	1.06	1.02	0.71	0.45	0.38
Mean±SD		1.08±0.03	1.06±0.01	1.01±0.01	0.70±0.02	0.47±0.02	0.37±0.04
40	1	3.04	2.86	2.36	1.84	1.19	0.93
	2	2.86	2.97	2.36	1.74	1.18	0.89
	3	3.00	2.98	2.51	1.84	1.18	0.92
Mean±SD		2.97±0.09	2.94±0.07	2.41±0.09	1.81±0.06	1.18±0.01	0.91±0.02
60	1	5.09	4.92	3.23	2.68	2.07	1.66
	2	4.98	4.83	3.21	2.73	2.07	1.62
	3	4.93	4.95	3.37	2.72	1.99	1.72
Mean±SD		5.00±0.08	4.90±0.06	3.27±0.09	2.71±0.03	2.04±0.05	1.67±0.05
80	1	6.30	6.26	4.08	3.71	2.69	1.99
	2	6.33	6.12	4.20	3.92	2.56	2.10
	3	6.22	6.22	4.17	3.70	2.62	2.06
Mean±SD		6.28±0.06	6.20±0.07	4.15±0.06	3.78±0.12	2.62±0.07	2.05±0.06
100	1	7.49	6.98	4.88	4.61	2.98	2.43
	2	7.48	7.07	4.82	4.53	3.28	2.60
	3	7.47	7.34	4.80	4.46	3.05	2.51
Mean±SD		7.48±0.01	7.13±0.19	4.83±0.04	4.53±0.08	3.10±0.16	2.51±0.09
120	1	8.63	7.24	5.70	4.69	3.75	2.63
	2	8.59	7.25	5.61	4.79	3.73	2.61
	3	8.58	7.56	5.59	4.61	3.81	2.66
Mean±SD		8.60±0.03	7.35±0.18	5.63±0.06	4.70±0.09	3.76±0.04	2.63±0.03

Note: P = compression pressure

Table 2: Mixture of Spress® B820 and Paracetamol.

P (MPa)	Compact	Tensile strength, T (N/mm^2)					
		Concentration of paracetamol (%)					
		0	10	20	30	40	50
20	1	0.27	0.16	0.11	0.10	0.07	0.03
	2	0.29	0.16	0.13	0.10	0.06	0.03
	3	0.26	0.15	0.13	0.09	0.06	0.03
Mean±SD		0.27±0.02	0.16±0.01	0.12±0.01	0.10±0.01	0.06±0.01	0.03±0.00
40	1	0.59	0.41	0.28	0.20	0.15	0.07
	2	0.62	0.39	0.31	0.21	0.13	0.09
	3	0.57	0.43	0.25	0.21	0.12	0.09
Mean±SD		0.59±0.03	0.41±0.02	0.28±0.03	0.21±0.01	0.13±0.02	0.08±0.01
60	1	1.18	0.73	0.61	0.33	0.25	0.12
	2	1.21	0.75	0.55	0.36	0.20	0.19
	3	1.17	0.75	0.54	0.33	0.28	0.15
Mean±SD		1.19±0.02	0.74±0.01	0.57±0.04	0.34±0.02	0.24±0.04	0.15±0.04
80	1	1.92	1.34	1.08	0.61	0.38	0.29
	2	1.84	1.26	1.00	0.56	0.44	0.25
	3	1.85	1.32	1.13	0.66	0.42	0.32
Mean±SD		1.87±0.04	1.31±0.04	1.07±0.07	0.61±0.05	0.41±0.03	0.29±0.04
100	1	2.26	1.57	1.33	0.99	0.69	0.62
	2	2.30	1.61	1.37	0.94	0.64	0.56
	3	2.38	1.59	1.34	0.88	0.66	0.56
Mean±SD		2.31±0.06	1.59±0.02	1.35±0.02	0.94±0.06	0.66±0.03	0.58±0.03
120	1	2.72	2.15	1.82	1.65	1.15	0.82
	2	2.78	2.15	1.72	1.55	1.06	0.91
	3	2.79	2.07	1.77	1.62	1-08	0.89
Mean±SD		2.76±0.04	2.12±0.05	1.77±0.05	1.61±0.05	1.10±0.05	0.87±0.05

Note: P = compression pressure

Table 3: Mixture of PS4 and Paracetamol.

P (MPa)	Compact	Tensile strength, T (N/mm^2)					
		Concentration of paracetamol (%)					
		0	10	20	30	40	50
20	1	0.55	0.29	0.16	0.10	0.07	0.04
	2	0.52	0.28	0.19	0.11	0.09	0.04
	3	0.51	0.28	0.19	0.11	0.07	0.04
Mean±SD		0.53±0.02	0.28±0.01	0.18±0.02	0.11±0.01	0.08±0.01	0.04±0.00
40	1	0.83	0.57	0.33	0.21	0.16	0.12
	2	0.89	0.56	0.32	0.24	0.16	0.12
	3	0.84	0.57	0.34	0.21	0.17	0.09
Mean±SD		0.85±0.03	0.57±0.01	0.33±0.01	0.22±0.02	0.16±0.01	0.11±0.02
60	1	1.07	0.73	0.59	0.35	0.29	0.16
	2	1.03	0.74	0.52	0.40	0.24	0.18
	3	1.08	0.69	0.55	0.35	0.23	0.16
Mean±SD		1.06±0.03	0.72±0.03	0.55±0.04	0.37±0.03	0.25±0.03	0.17±0.01
80	1	1.55	1.27	1.01	0.63	0.39	0.24
	2	1.61	1.18	1.02	0.59	0.41	0.28
	3	1.56	1.20	1.07	0.56	0.40	0.25
Mean±SD		1.57±0.03	1.22±0.05	1.03±0.03	0.59±0.04	0.40±0.01	0.26±0.02
100	1	1.92	1.53	1.39	0.91	0.69	0.59
	2	2.01	1.57	1.43	0.89	0.67	0.60
	3	1.88	1.58	1.38	0.87	0.62	0.55
Mean±SD		1.94±0.07	1.56±0.03	1.40±0.03	0.89±0.02	0.66±0.04	0.58±0.03
120	1	2.45	1.97	1.72	1.55	1.13	0.81
	2	2.43	1.93	1.67	1.52	1.03	0.84
	3	2.34	1.95	1.75	1.58	1.09	0.87
Mean±SD		2.41±0.06	1.95±0.02	1.71±0.04	1.55±0.03	1.08±0.05	0.84±0.03

Note: P = compression pressure

Appendix J: Evaluation of tablet properties – Tap testing powder mixtures.

Table 1: Tap testing of the formulations (powder mixtures).

	Formulation				
	1	2	3	4	5
Bulk density (g/cm^3) ± SD	0.36	0.60	0.54	0.54	0.50
	0.36	0.60	0.55	0.54	0.50
	0.35	0.61	0.55	0.54	0.51
Average Bulk density (g/cm^3) ± SD	0.36±0.01	0.60±0.01	0.55±0.01	0.54±0.00	0.50±0.01
Tapped density (g/cm^3) ± SD	0.46	0.68	0.63	0.63	0.60
	0.46	0.68	0.63	0.63	0.60
	0.46	0.68	0.65	0.62	0.61
Average Tapped density (g/cm^3) ± SD	0.46±0.01	0.68±0.00	0.64±0.01	0.63±0.01	0.60±0.01
Carr's compressibility index (CI, %) ± SD	21.74	11.76	14.28	14.28	16.67
	21.74	11.76	12.70	14.28	16.67
	23.91	10.29	15.38	12.90	16.39
Average Carr's compressibility index (CI, %) ± SD	22.46±1.25	11.27±0.85	14.12±1.35	13.82±0.80	16.58±0.16
Hausner ratio (HR) ± SD	1.28	1.13	1.17	1.17	1.20
	1.28	1.13	1.15	1.17	1.20
	1.31	1.11	1.18	1.15	1.20
Average Hausner ratio (HR) ± SD	1.29±0.02	0.12±0.01	1.17±0.02	1.16±0.01	1.20±0.00

Appendix K: Evaluation of tablet properties - Thickness, diameter and hardness test.

Table 1: Thickness, diameter and hardness test for Formulation 1.

No. tablet	Thickness (mm)	Diameter (mm)	Hardness (N)
1	3.91	9.90	93
2	3.94	9.89	94
3	3.94	9.89	92
4	3.90	9.90	95
5	3.98	9.90	91
6	3.96	9.89	92
7	4.09	9.93	90
8	3.98	9.90	90
9	3.95	9.90	90
10	3.98	9.90	105
Mean±SD	3.96±0.05	9.90±0.01	92.91±4.37

Table 2: Thickness, diameter and hardness test for Formulation 2.

No. tablet	Thickness (mm)	Diameter (mm)	Hardness (N)
1	3.53	9.87	110
2	3.56	9.87	101
3	3.56	9.88	99
4	3.52	9.87	110
5	3.59	9.89	90
6	3.54	9.88	105
7	3.58	9.88	101
8	3.54	9.87	110
9	3.59	9.88	99
10	3.52	9.87	110
Mean±SD	3.55±0.03	9.88±0.01	103.50±6.72

Table 3: Thickness, diameter and hardness test for Formulation 3.

No. tablet	Thickness (mm)	Diameter (mm)	Hardness (N)
1	3.69	9.91	100
2	3.68	9.90	102
3	3.67	9.90	94
4	3.66	9.89	103
5	3.63	9.89	108
6	3.67	9.90	91
7	3.59	9.88	110
8	3.65	9.89	115
9	3.67	9.91	110
10	3.67	9.90	102
Mean±SD	3.66±0.03	9.90±0.01	103.50±7.46

Table 4: Thickness, diameter and hardness test for Formulation 4 (reference).

No. tablet	Thickness (mm)	Diameter (mm)	Hardness (N)
1	3.60	9.88	102
2	3.57	9.88	100
3	3.62	9.87	97
4	3.58	9.88	93
5	3.56	9.88	100
6	3.61	9.87	105
7	3.59	9.88	91
8	3.59	9.88	104
9	3.62	9.88	92
10	3.58	9.88	103
Mean±SD	3.59±0.02	9.88±0.00	98.70±5.17

Table 5: Thickness, diameter and hardness test for Formulation 4 (stability test: 3 months storage).

No. tablet	Thickness (mm)	Diameter (mm)	Hardness (N)
1	3.62	9.88	99
2	3.60	9.90	98
3	3.60	9.87	100
4	3.59	9.93	102
5	3.60	9.89	97
6	3.58	9.89	102
7	3.61	9.91	104
8	3.62	9.94	99
9	3.60	9.88	101
10	3.60	9.90	98
Mean±SD	3.60±0.01	9.90±0.02	100.00±2.21

Table 6: Thickness, diameter and hardness test for Formulation 4 (stability study: 6 months storage).

No. tablet	Thickness (mm)	Diameter (mm)	Hardness (N)
1	3.62	9.90	99
2	3.64	9.89	103
3	3.59	9.90	96
4	3.58	9.94	101
5	3.60	9.90	98
6	3.59	9.90	107
7	3.62	9.86	97
8	3.58	9.89	105
9	3.63	9.87	100
10	3.60	9.92	98
Mean±SD	3.61±0.02	9.90±0.02	100.40±3.60

Table 7: Thickness, diameter and hardness test for Formulation 5 (reference).

No. tablet	Thickness (mm)	Diameter (mm)	Hardness (N)
1	3.63	9.90	114
2	3.62	9.90	115
3	3.63	9.90	112
4	3.62	9.90	101
5	3.62	9.90	110
6	3.61	9.90	111
7	3.62	9.91	106
8	3.62	9.90	103
9	3.60	9.90	105
10	3.60	9.90	114
Mean±SD	3.62±0.01	9.90±0.00	109.10±5.00

Table 8: Thickness, diameter and hardness test for Formulation 5 (stability study: 3 months storage).

No. tablet	Thickness (mm)	Diameter (mm)	Hardness (N)
1	3.60	9.88	110
2	3.60	9.91	111
3	3.66	9.90	107
4	3.64	9.91	108
5	3.61	9.93	103
6	3.61	9.89	105
7	3.65	9.92	110
8	3.60	9.94	108
9	3.59	9.90	107
10	3.63	9.90	105
Mean±SD	3.62±0.02	9.91±0.02	107.40±2.55

Table 9: Thickness, diameter and hardness test for Formulation 5 (stability study: 6 months storage).

No. tablet	Thickness (mm)	Diameter (mm)	Hardness (N)
1	3.60	9.88	103
2	3.66	9.94	105
3	3.60	9.93	110
4	3.60	9.89	107
5	3.66	9.93	107
6	3.60	9.93	104
7	3.63	9.95	110
8	3.65	9.96	105
9	3.61	9.90	106
10	3.59	9.92	108
Mean±SD	3.62±0.03	9.92±0.03	106.50±2.37

Table 10: Uniformity of weight (reference).

No. tablet	Weight (mg)				
	Formulation 1	Formulation 2	Formulation 3	Formulation 4	Formulation 5
1	347.9	348.1	348.1	349.5	350.1
2	348.3	350.0	349.5	350.0	349.3
3	347.0	349.5	349.0	350.6	351.2
4	346.9	348.3	349.8	348.0	347.6
5	346.9	348.9	352.2	350.8	349.0
6	349.2	348.1	349.3	349.9	348.7
7	348.5	349.1	352.6	351.1	348.9
8	346.6	348.3	350.9	349.6	350.6
9	348.7	349.5	348.7	350.1	348.2
10	346.4	349.2	351.2	350.3	350.8
11	346.8	347.5	352.3	348.5	349.5
12	347.3	349.7	350.5	349.6	349.6
13	349.3	347.7	349.6	349.3	348.2
14	349.0	349.0	350.6	351.1	349.9
15	348.4	349.7	348.8	351.3	348.4
16	347.9	348.9	350.6	350.1	349.6
17	346.1	349.1	349.2	351.1	347.8
18	349.0	347.5	349.0	348.9	349.5
19	348.1	349.3	349.0	350.2	350.9
20	348.1	348.3	350.1	351.2	350.2
Mean±SD	347.82±1.00	348.79±0.76	350.05±1.29	350.06±0.93	349.40±1.05

Table 11: Uniformity of weight (stability study: 3months storage).

No. tablet	Weight (mg)	
	Formulation 4	Formulation 5
1	349.2	348.2
2	348.8	349.0
3	348.5	348.5
4	347.9	350.0
5	349.2	347.6
6	348.6	349.1
7	350.0	350.1
8	349.3	349.4
9	347.8	348.7
10	348.4	349.9
11	348.6	348.5
12	347.9	347.8
13	349.0	349.0
14	348.9	348.5
15	350.0	348.6
16	349.6	349.8
17	348.7	348.6
18	348.6	350.0
19	349.0	349.7
20	347.8	348.4
Mean±SD	348.79±0.66	348.97±0.76

Table 12: Uniformity of weight (stability study: 6 months storage).

No. tablet	Weight (mg)	
	Formulation 4	Formulation 5
1	350.0	347.8
2	348.6	349.3
3	349.4	348.5
4	348.0	348.4
5	348.1	349.0
6	349.9	350.2
7	349.6	348.3
8	347.6	348.6
9	347.8	348.8
10	348.6	349.0
11	349.1	348.7
12	349.6	348.2
13	349.8	349.4
14	347.3	347.9
15	348.6	348.6
16	348.1	348.3
17	349.6	348.8
18	348.3	349.2
19	348.4	349.0
20	347.2	348.9
Mean±SD	348.68±0.89	348.75±0.55

Table 13: Friability test (reference).

Formulation	Total weight of 20 tablets before testing (mg)	Total weight of 20 tablets after testing (mg)	Friability (%)
1	6972.3	6946.0	0.38
2	6992.7	6959.4	0.48
3	7007.9	6972.4	0.51
4	7006.9	6969.1	0.54
5	7001.0	6970.8	0.43

Table 14: Friability test (stability study: 3 months storage)

Formulation	Total weight of 20 tablets before testing (mg)	Total weight of 20 tablets after testing (mg)	Friability (%)
4	6997.6	6619.7	0.54
5	7010.2	6687.5	0.46

Table 15: Friability test (stability study: 6 months storage).

Formulation	Total weight of 20 tablets before testing (mg)	Total weight of 20 tablets after testing (mg)	Friability (%)
4	7000.2	6594.2	0.58
5	7015.1	6692.4	0.46

Appendix L: Evaluation of tablet properties – Disintegration test.

Table 1: Disintegration test (reference).

Formulation	Time (minutes)						Mean±SD (minutes)
	No. of tablet						
	1	2	3	4	5	6	
1	0.17	0.23	0.28	0.18	0.25	0.28	0.23±0.05
2	1.22	1.30	1.38	1.35	1.58	1.63	1.41±0.16
3	1.23	1.23	1.50	1.25	1.33	1.45	1.33±0.12
4	0.50	0.58	0.60	0.57	0.58	0.60	0.57±0.37
5	0.42	0.43	0.45	0.43	0.47	0.45	0.44±0.18

Table 2: Disintegration test (stability study: 3months storage).

Formulation	Time (minutes)						Mean±SD (minutes)
	No. of tablet						
	1	2	3	4	5	6	
4	0.58	0.62	0.57	0.55	0.49	0.54	0.56±0.04
5	0.46	0.50	0.47	0.50	0.44	0.43	0.47±0.03

Table 3: Disintegration test (stability study: 6months storage).

Formulation	Time (minutes)						Mean±SD (minutes)
	No. of tablet						
	1	2	3	4	5	6	
4	0.53	0.61	0.50	0.62	0.55	0.64	0.58±0.06
5	0.50	0.40	0.47	0.44	0.42	0.48	0.45±0.04

Appendix M: Evaluation of tablet properties -Dissolution test.

Table 1: Formulation 1.

Time (min)	No. Tablet												Mean±SD Paracetamol released	
	1		2		3		4		5		6			
	Paracetamol released		Paracetamol released		Paracetamol released		Paracetamol released		Paracetamol released		Paracetamol released			
	µg/ml	%	µg/ml	%	µg/ml	%	µg/ml	%	µg/ml	%	µg/ml	%	µg/ml	%
5	2.56	19.20	4.23	31.73	3.38	25.36	2.94	22.06	4.21	31.58	2.99	22.43	3.39± 0.70	25.39± 5.23
10	3.90	29.26	6.37	47.79	4.76	35.71	4.40	33.01	5.10	38.26	4.43	33.23	4.83± 0.86	36.21± 6.42
15	4.59	34.43	7.62	57.16	5.61	42.09	5.00	37.51	5.87	44.04	4.65	34.88	5.56± 1.13	41.69± 8.50
20	5.28	39.61	8.89	66.69	6.77	50.79	5.75	43.14	6.51	48.83	5.61	42.09	6.47± 1.31	48.53± 9.85
25	6.49	48.69	10.73	80.50	7.70	57.76	7.00	52.51	7.39	55.44	6.92	51.91	7.71± 1.54	57.80± 11.55
30	7.67	57.54	10.07	75.54	8.21	61.59	8.39	62.94	7.99	59.94	7.65	57.39	8.33± 0.90	62.49± 6.76

Table 2: Formulation 2.

Time (min)	No. Tablet												Mean±SD Paracetamol released	
	1		2		3		4		5		6			
	Paracetamol released		Paracetamol released		Paracetamol released		Paracetamol released		Paracetamol released		Paracetamol released			
	µg/ml	%	µg/ml	%	µg/ml	%	µg/ml	%	µg/ml	%	µg/ml	%	µg/ml	%
5	5.98	44.86	6.26	46.96	4.15	31.13	7.03	52.74	4.76	35.71	5.70	42.76	5.65± 1.04	42.36± 7.82
10	9.59	71.94	9.29	69.69	6.24	46.81	10.20	76.52	7.88	59.11	8.70	65.27	8.65± 1.42	64.89± 10.66
15	10.36	77.71	10.62	79.67	8.30	62.27	10.87	81.55	10.02	75.17	10.85	81.40	10.17± 0.97	76.30± 7.28
20	10.92	81.92	10.96	82.22	10.96	82.22	11.21	84.10	11.06	82.97	11.18	83.87	11.05± 0.12	82.88± 0.92
25	13.38	100.38	13.30	99.77	13.38	100.38	13.36	100.23	13.42	100.68	13.32	99.92	13.36± 0.04	100.23 ± 0.33
30	13.41	100.60	13.44	100.83	13.44	100.83	13.41	100.60	13.41	100.60	13.39	100.45	13.42 ±0.09	100.65 ± 0.15

Table 3: Formulation 3.

Time (min)	No. Tablet												Mean±SD Paracetamol released	
	1		2		3		4		5		6			
	Paracetamol released		Paracetamol released		Paracetamol released		Paracetamol released		Paracetamol released		Paracetamol released			
	µg/ml	%	µg/ml	%	µg/ml	%	µg/ml	%	µg/ml	%	µg/ml	%	µg/ml	%
5	7.23	54.24	8.70	65.27	6.85	51.39	6.33	47.49	7.40	55.51	8.33	62.49	7.47 ±0.89	56.07± 6.71
10	7.76	58.21	9.59	71.94	8.08	60.62	9.48	71.11	8.63	64.74	8.98	67.37	8.75 ±0.74	65.67± 5.55
15	8.38	62.87	10.47	78.54	8.94	67.07	9.82	73.67	9.40	70.52	9.45	70.89	9.41 ±0.72	70.59± 5.38
20	10.92	81.92	10.89	81.70	10.89	81.70	11.50	86.27	11.69	87.70	11.74	88.07	11.27 ±0.42	84.56± 3.11
25	13.39	100.45	13.32	99.92	13.33	100.00	13.44	100.83	13.39	100.45	13.33	100.00	13.37 ±0.05	100.28 ± 0.36
30	13.44	100.83	13.36	100.23	13.42	100.68	13.50	101.28	13.41	100.60	13.39	100.45	13.42 ±0.05	100.68 ± 0.36

Table 4: Formulation 4 (reference).

Time (min)	No. Tablet												Mean±SD Paracetamol released	
	1		2		3		4		5		6			
	Paracetamol released		Paracetamol released		Paracetamol released		Paracetamol released		Paracetamol released		Paracetamol released			
	µg/ml	%	µg/ml	%	µg/ml	%	µg/ml	%	µg/ml	%	µg/ml	%	µg/ml	%
5	10.82	81.17	10.79	80.95	10.74	80.57	10.68	80.12	11.15	83.65	11.81	88.60	10.10± 0.43	82.51± 3.23
10	10.99	82.45	12.21	91.60	10.96	82.22	11.04	82.82	11.30	84.77	11.81	88.60	11.39± 0.51	85.41± 3.86
15	13.30	99.77	13.30	99.77	13.33	100.00	13.38	100.38	13.35	100.15	13.32	99.92	13.33± 0.03	100.00 ± 0.24
20	13.39	100.45	13.39	100.45	13.36	100.23	13.39	100.45	13.38	100.38	13.39	100.45	13.38± 0.01	100.40 ± 0.09
25	13.41	100.60	13.41	100.60	13.41	100.60	13.41	100.60	13.41	100.60	13.42	100.68	13.41± 0.00	100.61 ± 0.03
30	13.42	100.68	13.41	100.60	13.42	100.68	13.42	100.68	13.44	100.83	13.42	100.68	13.42± 0.01	100.69 ± 0.07

Table 5: Formulation 4 (stability study: 3months storage).

Time (min)	No. Tablet												Mean±SD Paracetamol released	
	1		2		3		4		5		6			
	Paracetamol released		Paracetamol released		Paracetamol released		Paracetamol released		Paracetamol released		Paracetamol released			
	µg/ml	%	µg/ml	%	µg/ml	%	µg/ml	%	µg/ml	%	µg/ml	%	µg/ml	%
5	11.12	83.42	10.73	80.50	10.75	80.65	10.78	80.87	11.74	88.07	10.60	79.52	10.95± 0.42	82.17± 3.17
10	11.24	84.32	10.92	81.92	12.16	91.22	10.96	82.22	11.76	88.22	10.98	82.37	11.34± 0.51	85.05± 3.84
15	13.32	99.92	13.31	99.85	13.30	99.77	13.24	99.32	13.34	100.08	13.34	100.08	13.31± 0.04	99.84± 0.28
20	13.38	100.38	13.37	100.30	13.32	99.92	13.35	100.15	13.38	100.38	13.37	100.30	13.36± 0.02	100.24 ± 0.18
25	13.40	100.53	13.41	100.60	13.38	100.38	13.38	100.38	13.40	100.53	13.38	100.38	13.39± 0.01	100.47 ± 0.10
30	13.41	100.60	13.41	100.60	13.39	100.45	13.40	100.53	13.42	100.68	13.40	100.53	13.41± 0.01	100.57 ± 0.08

Table 6: Formulation 4 (stability study: 6months storage).

Time (min)	No. Tablet												Mean±SD Paracetamol released	
	1		2		3		4		5		6			
	Paracetamol released		Paracetamol released		Paracetamol released		Paracetamol released		Paracetamol released		Paracetamol released			
	µg/ml	%	µg/ml	%	µg/ml	%	µg/ml	%	µg/ml	%	µg/ml	%	µg/ml	%
5	10.46	78.47	10.37	77.79	10.56	79.22	10.35	77.64	10.65	79.89	10.70	80.27	10.52± 0.15	78.88 ±1.09
10	11.24	84.32	11.86	88.97	11.67	87.55	11.48	86.12	11.21	84.10	11.19	83.95	11.44± 0.28	85.83 ±2.09
15	13.28	99.62	13.18	98.87	13.33	100.00	13.27	99.55	13.30	99.77	13.25	99.40	13.27± 0.05	99.54 ±0.38
20	13.33	100.00	13.32	99.92	13.36	100.23	13.35	100.15	13.34	100.08	13.33	100.00	13.34± 0.01	100.06 ±0.11
25	13.34	100.08	13.35	100.15	13.36	100.23	13.34	100.08	13.35	100.15	13.34	100.08	13.35± 0.01	100.13 ±0.06
30	13.33	100.00	13.34	100.08	13.35	100.15	13.37	100.30	13.35	100.15	13.34	100.08	13.35± 0.01	100.13 ±0.10

Table 7: Formulation 5 (reference).

Time (min)	No. Tablet												Mean±SD Paracetamol released	
	1		2		3		4		5		6			
	Paracetamol released		Paracetamol released		Paracetamol released		Paracetamol released		Paracetamol released		Paracetamol released			
	µg/ml	%	µg/ml	%	µg/ml	%	µg/ml	%	µg/ml	%	µg/ml	%	µg/ml	%
5	11.10	83.27	10.98	82.37	10.92	81.92	10.89	81.70	10.89	81.70	10.84	81.32	10.94± 0.09	82.05± 0.69
10	11.16	83.72	11.30	84.77	11.13	83.50	11.10	83.27	11.06	82.97	12.12	90.92	11.31± 0.40	84.86± 3.03
15	13.33	100.00	13.32	99.92	13.33	100.00	13.35	100.15	13.36	100.23	13.25	99.40	13.32± 0.04	99.95± 0.29
20	13.36	100.23	13.33	100.00	13.36	100.23	13.38	100.38	13.41	100.60	13.35	100.15	13.37± 0.03	100.27 ± 0.04
25	13.38	100.38	13.41	100.60	13.44	100.83	13.41	100.60	13.46	100.98	13.36	100.23	13.41± 0.04	100.60 ± 0.28
30	13.42	100.68	13.44	100.83	13.46	100.98	13.47	101.05	13.46	100.98	13.44	100.83	13.45± 0.02	100.89 ± 0.14

Table 8: Formulation 5 (stability study: 3months storage).

Time (min)	No. Tablet												Mean±SD Paracetamol released	
	1		2		3		4		5		6			
	Paracetamol released		Paracetamol released		Paracetamol released		Paracetamol released		Paracetamol released		Paracetamol released			
	µg/ml	%	µg/ml	%	µg/ml	%	µg/ml	%	µg/ml	%	µg/ml	%	µg/ml	%
5	10.90	81.77	10.88	81.62	11.09	83.20	10.80	81.02	10.86	81.47	10.90	81.77	10.91± 0.10	81.81± 0.74
10	11.31	84.84	11.10	83.27	11.14	83.57	12.10	90.77	11.00	82.52	11.11	83.35	11.29± 0.41	84.72± 3.06
15	13.33	100.00	13.21	99.10	13.34	100.08	13.23	99.25	13.32	99.92	13.33	100.00	13.29± 0.06	99.73± 0.43
20	13.34	100.08	13.36	100.23	13.36	100.23	13.35	100.15	13.39	100.45	13.39	100.45	13.37± 0.02	100.27 ± 0.15
25	13.38	100.38	13.40	100.53	13.37	100.30	13.38	100.38	13.43	100.75	13.42	100.62	13.40± 0.02	100.49 ± 0.17
30	13.43	100.75	13.43	100.75	13.43	100.75	13.42	100.62	13.44	100.83	13.44	100.83	13.43± 0.01	100.76 ± 0.08

Table 9: Formulation 5 (stability study: 6months storage).

Time (min)	No. Tablet												Mean±SD Paracetamol released	
	1		2		3		4		5		6			
	Paracetamol released		Paracetamol released		Paracetamol released		Paracetamol released		Paracetamol released		Paracetamol released			
	µg/ml	%	µg/ml	%	µg/ml	%	µg/ml	%	µg/ml	%	µg/ml	%	µg/ml	%
5	10.36	77.72	10.47	78.54	10.83	81.25	10.74	80.57	10.68	80.12	10.23	76.74	10.55± 0.24	79.16 ±1.76
10	11.21	84.10	11.23	84.25	11.26	84.47	11.40	85.52	11.16	83.72	10.98	82.37	11.21± 0.14	84.07 ±1.03
15	13.27	99.55	13.29	99.70	13.29	99.70	13.33	100.00	13.30	99.77	13.26	99.47	13.29± 0.02	99.70 ±0.18
20	13.33	100.00	13.34	100.08	13.33	100.00	13.35	100.15	13.36	100.23	13.36	100.23	13.35± 0.01	100.11 ±0.10
25	13.34	100.08	13.33	100.00	13.33	100.00	13.35	100.15	13.35	100.15	13.36	100.23	13.34± 0.01	100.10 ±0.09
30	13.36	100.23	13.33	100.00	13.35	100.15	13.33	100.00	13.35	100.15	13.35	100.15	13.35± 0.01	100.11 ±0.09

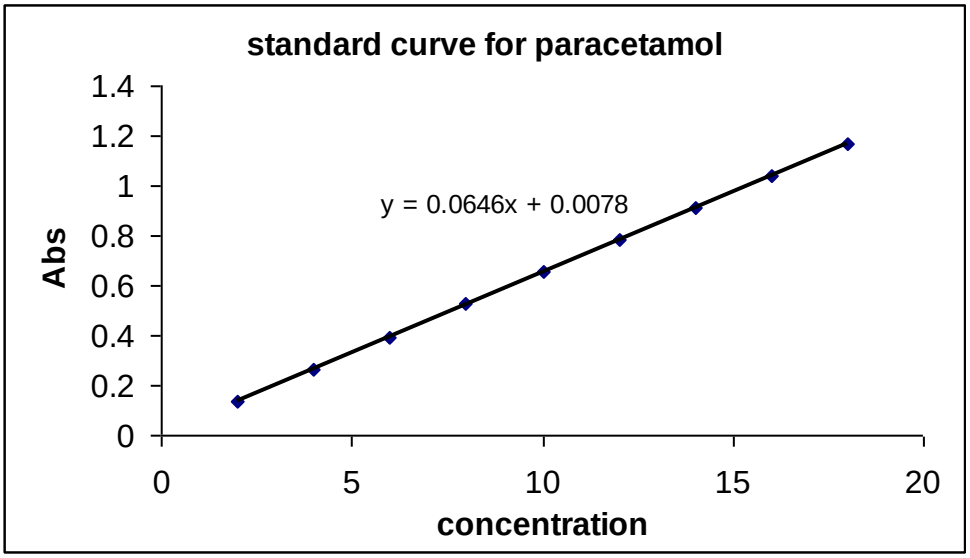

Figure 3: The standard curve for the absorbance of paracteamol at different concentrations.

Appendix N: Statistical Analysis

Table 1: Statistical analysis for powder properties.

No	Analysis	Types of test	Result significance: < 0.05, Significantly different	Correlation
1	The significant of amylose content	One Sample t – test	0.0004	
2	Impact of heating time on amylose content	One way anova & Correlate bivariate (Paired sample t-test)	0.00001	0.374
3	The significant degree of crystallinity by: i. Area method ii. Peak high method	One Sample t-test	 0.00 0.000004	
4	Impact of heating time to the degree of crystallinity i. Area method ii. Peak high method	One way anova & Correlate bivariate (Paired sample t-test)	 0.00 0.00	 - 0.748 - 0.528
5	Comparison the values of the degree of crystalinity by high method and area method	One sample t-test	0.00	
6	Impact degree of crystallinity to moisture content i. Area method ii. Peak high method	One way anova & Correlate bivariate (Paired sample t-test)	 0.00 0.00	 0.790 0.580
7	The significant of viscosity	One Sample t – test	0.002	
8	Impact of heating time and amylose content to the viscosity of sago, PS1, PS2, PS2, PS3, PS4	Two way anova univariate	0.028	0.980
9	Impact of amylose content to the viscosity of sago, PS1, PS2, PS2, PS3, PS4	One way anova & Correlate bivariate (Paired sample t-test)	0.0000002	-0.932
10	Impact of the heating time to the viscosity of sago, PS1, PS2, PS3, PS4	One way anova & Correlate bivariate (Paired sample t-test)	0.00	0.971
11	Impact of the viscosity on DG For sago,PS1,PS2,PS3,PS4	One way anova & Correlate bivariate (Paired sample t-test)	0.077	0.972

'Table 1, continued'

No	Analysis	Types of test	Result: < 0.05, Significantly different	Correlation
12	Impact of amylose content to the viscosity and DG for sago, PS1,PS2,PS3,PS4	Two way anova multivariate		
	i. viscosity		0.012	0.910
	ii. DG		0.001	0.961
13	Impact of DG, amylose content on viscosity for sago,PS1,PS2,PS3,PS4	Two way anova Univariate	0.028	0.980
14	Impact of heating time, DG, amylose content on viscosity for PS1,PS2,PS3, PS4	Two way anova univariate	0.028	0.980
15	The significant of viscosities for sago starch, PS1, PS2,PS3 and PS4	One sample t-test	0.002	
19	Impact of heating time and amylose content to the	Two way anova multivariate		
	i. To		0.014	0.942
	ii. TP		0.089	0.787
	iii. Tc		0.290	0.471
	iv. Tc – To		0.022	0.921
20	Impact of temperature on swelling power	One way anova & Correlate bivariate (Paired sample t-test)	0.00	0.771
21	Impact of heating time to swelling power	One way anova & Correlate bivariate (Paired sample t-test)	0.00	-0.125
22	Impact of temperature and heating time on swelling power	Two way anova univariate	0.00	0.910
23	Impact of temperature, heating time and amylose content on swelling power	Two way anova univariate	0.00	0.999
24	The significant of swelling index with in group sago starch, PS1,PS2,PS3 and PS4 up to temperature 55˚C	One sample t-test	0.03	

‘Table 1, continued’

No	Analysis	Types of test	Result: < 0.05, Significantly different	Correlation
25	Impact of temperature up to 55˚C on swelling index For sago starch, PS1,PS2,PS3 and PS4	One way anova & Correlate bivariate (Paired sample t-test)	0.000	0.890
26	Impact of temperature up to 55˚C and heating time on swelling power For sago starch, PS1,PS2,PS3 and PS4	Two way anova univariate	0.000	0.998
27	Impact of temperature up to 55˚C and amylose content on swelling power For sago starch, PS1,PS2,PS3 and PS4	Two way anova univariate	0.000	0.986
28	Impact of temperature up to 55˚C, heating time and amylose content on swelling power For sago starch, PS1,PS2,PS3 and PS4	Two way anova univariate	0.000	1.000
29	Impact of temperature up to 55˚C and DG on swelling power For sago starch, PS1,PS2,PS3 and PS4	Two way anova univariate	0.000	0.998
30	Impact of temperature up to 55˚C, heating time and DG on swelling power For sago starch, PS1,PS2,PS3 and PS4	Two way anova univariate	0.000	0.998
31	Impact of temperature up to 55˚C, amylose content and DG on swelling power For sago starch, PS1,PS2,PS3 and PS4	Two way anova univariate	0.000	1.000
32	Impact of temperature up to 55˚C, heating time, amylose content and DG on swelling power For sago starch, PS1,PS2,PS3 and PS4	Two way anova univariate	0.000	1.000
33	Impact of temperature on Water Solubility Index	One way anova & Correlate bivariate (Paired sample t-test)	0.00	0.713

'Table 1, continued'

No	Analysis	Types of test	Result: < 0.05, Significantly different	Correlation
34	Impact of heating time to Water Solubility Index	One way anova & Correlate bivariate (Paired sample t-test)	0.00	-0.172
35	Impact of temperature and heating time on Water Solubility Index	Two way anova univariate	0.00	0.860
36	Impact of temperature, heating time and amylose content on Water Solubility Index	Two way anova univariate	0.00	0.997
37	Correlation between swelling power and water solubility index	One way anova & Correlate bivariate (Paired sample t-test)	0.00	0.926
38	Impact of temperature, heating time and amylose content on Water Solubility Index and SP	Two way anova multivariate	Significant	
	i. Water solubility index		0.00	0.999
	ii. Swelling power		0.00	1.000
39	The significant of solubility index with in group sago starch, PS1,PS2,PS3 and PS4 up to temperature 65˚C	One sample t-test	0.000	
40	Impact of temperature up to 65˚C On solubility index For sago starch, PS1,PS2,PS3 and PS4	One way anova & Correlate bivariate (Paired sample t-test)	0.00	0.860
41	Impact of temperature up to 65˚C and heating time on solubility index For sago starch, PS1,PS2,PS3 and PS4	Two way Anova Univariate	0.000	0.987
42	Impact of temperature up to 65˚C and amylose content on solubility index For sago starch, PS1,PS2,PS3 and PS4	Two way Anova Univariate	0.000	0.957

‘Table 1, continued’

No	Analysis	Types of test	Result: < 0.05, Significantly different	Correlation
43	Impact of temperature up to 65˚C, heating time and amylose content on solubility index For sago starch, PS1,PS2,PS3 and PS4	Two way Anova Univariate	0.000	0.999
44	Impact of temperature up to 65˚C and DG on solubility index For sago starch, PS1,PS2,PS3 and PS4	Two way anova univariate	0.002	0.988
45	Impact of temperature up to 65˚C, heating time and DG on solubility index For sago starch, PS1,PS2,PS3 and PS4	Two way anova univariate	0.002	0.988
46	Impact of temperature up to 65˚C, amylose content and DG on solubility index For sago starch, PS1,PS2,PS3 and PS4	Two way anova univariate	0.000	1.000
47	Impact of temperature up to 65˚C, heating time, amylose content and DG on swelling power For sago starch, PS1,PS2,PS3 and PS4	Two way anova univariate	0.000	1.000
48	The significant of the following	One sample t – test		
	i. Mean particle size		0.00	
	ii. loss on Drying		0.0002	
	iii. True Density		0.001	
	iv. Bulk Density		0.0001	
	v. Tap Density		0.00003	
	vi. % Porosity		0.0005	

'Table 1, continued'

No	Analysis	Types of test	Result: < 0.05, Significantly different	Correlation
49	The significance of each of the following For only Sago starch, PS1,PS2,PS3,PS4	One sample t – test		
	i. Mean particle size		0.00	
	ii. loss on Drying		0.00	
	iii. True Density		0.00	
	iv. Bulk Density		0.00	
	v. Tap Density		0.00	
	vi. % Porosity		0.00	
50	Impact of particle sizes on the	One way anova &		
	i. Loss on drying (Moisture content),	Correlate bivariate (Paired sample t-test)	0.00	0.535
	ii. bulk density,		0.0000002	0.162
	iii. tap Density		0.0000003	0.200
	iv. porosity		0.00	-0.19
	v. true density		0.00	-0.735
51	Impact of the Loss on drying (Moisture content) to	One way anova & Correlate bivariate (Paired sample t-test)		
	i. bulk density,		0.00	0.781
	ii. tap density,		0.00	0.836
	iii. porosity		0.00	-0.774
52	Impact of particle sizes and loss on drying (Moisture content) to	Two way anova univariate		
	i. bulk density,		0.00	0.999
	ii. tap density,		0.00	0.998
	iii. porosit		0.00	0.999

‘Table 1, continued’

No	Analysis	Types of test	Result significancy: < 0.05, Significantly different	Correlation
53	Impact of particle sizes and loss on drying (Moisture content) for only sago starch, PS1, PS2, PS3 and PS4 to	Two way anova multivariate		
	i. bulk density,		0.00	0.995
	ii. tap density,		0.00	0.990
	iii. porosity		0.00	0.993
54	Impact of True density on porosity	One way anova & Correlate bivariate (Paired sample t-test)	0.00	0.669
56	Impact of heating time for sago starch, PS1, PS2, PS3, PS4 to moisture content	One way anova & Correlate bivariate (Paired sample t-test)	0.00	0.260
58	Impact of heating time for sago starch, PS1, PS2, PS3, PS4 to bulk density	One way anova & Correlate bivariate (Paired sample t-test)	0.000	-0.755
59	Impact of heating time for sago starch, PS1, PS2, PS3, PS4 to tap density	One way anova & Correlate bivariate (Paired sample t-test)	0.000	-0.800
60	Impact of heating time for sago starch, PS1, PS2, PS3, PS4 to true density	One way anova & Correlate bivariate (Paired sample t-test)	0.000	-0.594

'Table 1, continued'

No	Analysis	Types of test	Result: < 0.05, Significantly different	Correlation
61	Impact of heating time for sago starch, PS1, PS2, PS3, PS4 to porosity	One way anova & Correlate bivariate (Paired sample t-test)	0.000	0.743
62	The significance of	One Sample t-test		
	i. CI		0.064	
	ii. HR		0.059	
	iii. Angle of repose		0.00	
	iv. Flow rate (g/s)		0.00	
63	Impact of particle size on	One way anova &		
	i. CI	Correlate bivariate	0.00	-0.284
	ii. HR	(Paired sample t-test)	0.00	-0.298
	iii. Angle of repose		0.00	-0.997
	iv. flow rate		0.00	0.958
64	Impact of moisture content (loss on drying) on	One way anova & Correlate bivariate		
	i. CI,	(Paired sample t-	0.0003	-0.574
	ii. HR,	test)	0.00	-0.611
	iii. Angle of repose,		0.00	-0.195
	iv. flow rate		0.00	0.806
65	Impact of porosity on	One way anova &		
	i. CI,	Correlate bivariate	0.00	0.945
	ii. HR,	(Paired sample t-test)	0.00	0.951
	iii. Angle of repose,		0.00	0.240
	iv. flow rate		0.00	-0.939

‘Table 1, continued’

No	Analysis	Types of test	Result: < 0.05, Significantly different	Correlation
66	Impact of particle size and Loss on drying (moisture content) on	Two way anova multivariate		
	i. CI,		0.00	0.986
	ii. HR,		0.00	0.985
	iii. Angle of repose,		0.001	0.996
	iv. flow rate		0.00	0.988
67	Impact of particle size, loss on drying (moisture content) and porosity on	Two way anova multivariate		
	i. CI,		0.00	0.986
	ii. HR,		0.00	0.985
	iii. Angle of repose,		0.00	0.997
	iv. flow rate		0.00	0.992
68	Impact of particle size and porosity on	Two way anova multivariate		
	i. CI,		0.00	0.986
	ii. HR,		0.00	0.985
	iii. Angle of repose,		0.00	0.997
	iv. flow rate		0.00	0.992
69	Impact of Loss on drying (moisture content) and porosity on	Two way anova multivariate		
	i. CI,		0.00	0.986
	ii. HR,		0.00	0.985
	iii. Angle of repose,		0.00	0.997
	iv. flow rate		0.00	0.992

‘Table 1, continued’

No	Analysis	Types of test	Result: < 0.05, Significantly different	Correlation
70	Correlation between CI and HR	Correlate - Bivariate	0.00	0.998
71	Correlation between angle of repose and flow rate	Correlate - Bivariate	0.00	-0.979
72	Relationship of CI , HR and angle of repose	Correlate - Bivariate		
	1. CI & HR		0.00	0.998
	2. CI & angle of repose		0.095	0.373
	3. HR & angle of repose		0.08	0.391
73	Relationship of CI , HR and flow rate	Correlate - Bivariate		
	1. CI & HR		0.00	0.998
	2. CI & flow rate		0.00	-0.885
	3. HR & flow rate		0.00	-0.913
74	Relationship of CI, HR, angle of repose and flow rate	Correlate - Bivariate		
	1. CI & HR		0.00	0.998
	2. CI & angle of repose		0.095	0.373
	3. CI & flow rate		0.00	-0.885
	4. HR & angle of repose		0.08	0.391
	5. HR & flow rate		0.00	-0.913
	6. Flow rate & angle of repose		0.00	-0.979

'Table 1, continued'

No	Analysis	Types of test	Result: < 0.05, Significantly different	Correlation
75	The significance of sago starch, PS1, PS2, PS3, PS4 for	One sample t-test		
	i. Particle size		0.00	
	ii. Moisture content		0.0001	
	iii. Amylose content		0.001	
	iv. Viscosity		0.0002	
	v. DG		0.0001	
	vi. CI		0.0001	
	vii. HR		0.0002	
	viii. Angle of repose		0.000003	
	ix. Flow rate		0.00	
	x. Porosity		0.000003	
76	Impact of DG on	One way anova &		
	i. CI,	Correlate bivariate	0.504	0.183
	ii. HR,	(Paired sample t-test)	0.0003	0.071
	iii. Angle of repose,		0.002	-0.771
	iv. flow rate		0.0001	0.896
77	Significances of Avicel PH 101, Spress B820 and PS4 for	One sample t-test		
	i. CI		0.00001	
	ii. HR		0.00	
	iii. Angle of repose		0.0000001	
	iv. Flow rate		0.001	

‘Table 1, continued’

78	Significances between Spress® B820 and PS4 for		One sample t-test	
	i.	CI		0.001
	ii.	HR		0.00
	iii.	Angle of repose		0.00
	iv.	Flow rate		0.0000002

Table 2: Statistical analysis for powder compact properties.

No	Analysis	Types of test	Result: < 0.05, Significantly different	Correlation
1	The significant of Py	One sample t-test	0.018	
2	Impact particle size on Py	One way anova & Correlate bivariate (Paired sample t-test)	0.036	-0.430
3	Impact of DG on Py for sago starch, PS1, PS2, PS3, PS4	One way anova & Correlate bivariate (Paired sample t-test)	0.00	-0.954
4	Impact of DG and particle size on Py for sago starch, PS1, PS2, PS3, PS4	Two way anova univariate	0.00	0.996
5	Comparison Py value of Avicel PH 101, PS4 and Spress® B820	One sample t-test	0.00	
6	Comparison Py value of PS4 and Spress® B820	One sample t-test	0.00001	
7	The significant Py values for sago starch, PS1, PS2, PS3 and PS4 diferent?	One sample t-test	0.002	
8	The significant of a	One sample t-test	0.000001	
9	The significant of Pk	One sample t-test	0.02	
10	Impact of DG of sago starch, PS1, PS2, PS3, PS4 on	One way anova & Correlate bivariate		
	i. a,	(Paired sample t-test)	0.00007	0.950
	ii. Pk		0.00	0.734

'Table 2, continued'

No	Analysis	Types of test	Result: < 0.05, Significantly different	Correlation
11	Comparison of a, b, Pk values of Avicel PH 101, PS4 and Spress® B820	One sample t-test		
	i. a		0.00	
	ii. b		0.0003	
	iii. Pk		0.00004	
12	Comparison of a, b, Pk values of PS4 and Spress® B820	One sample t-test		
	i. a		0.00	
	ii. b		0.00	
	iii. Pk		0.00	
13	Impact of irregularity particle shape on Py	One way anova & Correlate bivariate (Paired sample t-test)	0.000002	-0.950
14	Comparison Py values between Spress® B820 and PS4	One sample t-test	0.00001	
15	Comparison Py values between PS1 and Sago starch	One sample t-test	0.001	
16	Comparoson DG values between PS1 and Sago starch	One sample t-test	0.076	
17	Impact of DG to Da For PS1,PS2,PS3, PS4 and sago	One way anova & Correlate bivariate (Paired sample t-test)	0.0001	-0.934
18	Impact of Particle size to Da For PS1,PS2,PS3, PS4 and sago	One way anova & Correlate bivariate (Paired sample t-test)	0.00	-0.778
19	Impact of DG and particle size to Da For PS1,PS2,PS3, PS4 and sago	Two way anova univariate	0.001	0.938

'Table 2, continued'

No	Analysis	Types of test	Result: < 0.05, Significantly different	Correlation
20	Comparison between Spress® B820 and PS4 for	One sample t-test		
	i. Particle size		0.00	
	ii. Moisture content		0.002	
	iii. DG		0.002	
	iv. Area degree of crystalinity		0.00	
	v. Height peak degree of crystalinity		0.00	
	vi. K		0.00	
	vii. A		0.00	
	viii. Py		0.00	
	ix. a		0.00	
	x. b		0.00	
	xi. Pk		0.00	
21	Impact of Particle size and shape irregularity (Avicel, Spress® B820, PS4, PS3, PS2, PS1, and sago) to Py	Two way anova univariate	0.00	0.994
22	Impact of particle size to Do	One way anova & Correlate bivariate (Paired sample t-test)	0.00	0.070
23	Impact of particle size to Do For PS1,PS2,PS3, PS4 and sago	One way anova & Correlate bivariate (Paired sample t-test)	0.00	-0.981
24	The significant of hardness	One sample t-test	0.00	
25	The significant of tensile strength (T)	One sample t-test	0.00	

'Table 2, continued'

No	Analysis	Types of test	Result: < 0.05, Significantly different	Correlation
26	Impact of P on hardness	One way anova & Correlate bivariate (Paired sample t-test)	0.00	
27	Impact of P on T	One way anova & Correlate bivariate (Paired sample t-test)	0.00	
28	Impact of P on relative density (D)	One Way Anova	Significant	
29	Impact of P and particle size of sago starch, PS1, PS2, PS3, PS4 and Spress® B820 on hardness	Two way anova univariate	0.00	0.999
30	Impact of P and particle size of sago starch, PS1, PS2, PS3, PS4 and Spress® B820 on T	Two way anova univariate	0.00	0.999
31	Impact of moisture content of sago starch, PS1, PS2, PS3, PS4 and Spress® B820 on hardness	One way anova & Correlate bivariate (Paired sample t-test)	0.00	-0.591
32	Impact of P and moisture content of sago starch, PS1, PS2, PS3, PS4 and Spress® B820 on T	One way anova & Correlate bivariate (Paired sample t-test)	0.00	-0.617
33	Impact of P, particle size and moisture content of sago starch, PS1, PS2, PS3, PS4 and Spress® B820 on hardness	Two way anova univariate	0.00	0.998

'Table 2, continued'

No	Analysis	Types of test	Result: < 0.05, Significantly different	Correlation
34	Impact of P, particle size and moisture content of sago starch, PS1, PS2, PS3, PS4 and Spress® B820 on T	Two way anova univariate	0.00	0.998
35	Impact of P and DG of sago starch, PS1, PS2, PS3, PS4 and Spress® B820 on hardness	Two way anova univariate	0.00	0.997
36	Impact of P and DG of sago starch, PS1, PS2, PS3, PS4 and Spress® B820 on T	Two way anova univariate	0.00	0.998
37	Comparison of hardness between PS4 and Spress® B820	One sample t-test	0.00	
39	Comparison of T between PS4 and Spress® B820	One sample t-test	0.00	
40	The significant of hardness in the lubricant sensitivity test for • Avicel PH 101 • Spress® B820 • PS1 • PS2 • PS3 • PS4	One sample t-test	 0.00 0.00 0.00 0.00 0.00 0.00	
41	Impact of P and magnesium stearate concentration on the hardness of Avicel PH 101, Spress® B820, Sago, PS1, PS2, PS3,PS4	Two way Anova Univariate	0.025	0.03
42	The significant of LSR values of Sago starch,PS1,PS2,PS3,PS4	One Sample t-test	0.00	
43	Impact of magnesium stearate concentration on LSR	One way anova & Correlate bivariate (Paired sample t-test)	0.00	0.249

'Table 2, continued'

No	Analysis	Types of test	Result: < 0.05, Significantly different	Correlation
44	Impact of magnesium stearate concentration and particle size on LSR	Two way anova univariate	0.00	0.997
45	Impact of magnesium stearate concentration and flow rate on LSR	Two way anova univariate	0.00	0.990
46	Impact of magnesium stearate concentration, particle size and flow rate on LSR	Two way anova univariate	0.00	0.995
47	Impact of magnesium stearate concentration on LSR sago starch, PS1, PS2, PS3, PS4	One way anova & Correlate bivariate (Paired sample t-test)	0.00	0.443
48	Impact of magnesium stearate concentration and particle size on LSR Sago starch, PS1, PS2, PS3, PS4	Two way anova univariate	0.00	0.991
49	Impact of magnesium stearate concentration and flow rate on LSR Sago starch, PS1, PS2, PS3, PS4	Two way anova univariate	0.00	0.982
50	Impact of magnesium stearate concentration, particle size and flow rate on LSR Sago starch, PS1, PS2, PS3, PS4	Two way anova univariate	0.00	0.984
51	Impact of magnesium stearate concentration and DG on LSR Sago starch, PS1, PS2, PS3, PS4	Two way anova univariate	0.000003	0.974
52	Comparison LSR of Avicel PH 101, PS4 ,Spress® B820	One sample t-test	0.01	
53	Comparison LSR of PS4 and Spress® B820	One sample t-test	0.00	
54	The significant of T in loading capacity test (in group and among group) of Avicel PH 101, PS4 and Spress® B820	On Sample t-test	0.00	
55	Impact of compression pressure P and concentration of paracetamol on the tensile strength of Avicel PH 101, Spress® B820, PS4	Two way anova Univariate	0.00	0.388

'Table 2, continued'

No	Analysis	Types of test	Result: < 0.05, Significantly different	Correlation
56	Impact of compression pressure P and concentration of paracetamol on the tensile strength of Spress® B820 and PS4	Two way anova Univariate	0.00	0.989
57	The significant of loading capacity (in group and among group) of Avicel PH 101, PS4 and Spress® B820	One sample t-test	0.00	

Table 3: Statistical analysis for tablet properties.

No	Analysis	Types of test	Result: < 0.05, Significantly different	Correlation
1	The significant of all formulations for:	One sample t-test		
	i. Thickness		0.00	
	ii. Diameter		0.00	
	iii. Hardness		0.00	
	iv. Friability		0.00	
	v. Disintegration Time		0.00	
	vi. Dissolution Rate		0.00	
2	The significant of formulation 1, 2, 3 for:	One sample t-test		
	i. Thickness		0.00	
	ii. Diameter		0.00	
	iii. Hardness		0.00	
	iv. Friability		0.00	
	v. Disintegration Time		0.00	
	vi. Dissolution Rate			

'Table 3, continued'

No	Analysis	Types of test	Result: < 0.05, Significantly different	Correlation
3	The significant of formulation 4 and 5 for:	One sample t-test		
	i. Thickness		0.00	
	ii. Diameter		0.00	
	iii. Hardness		0.00	
	iv. Friability		0.00	
	v. Disintegration Time		0.00	
	vi. Dissolution Rate		0.00	
4	The significant of formulation 4 and 5 for:	One sample t-test		
	i. Thickness		0.00	
	ii. Diameter		0.00	
	iii. Hardness		0.00	
	iv. Friability		0.00	
	v. Disintegration Time		0.00	
	vi. Dissolution Rate		0.00	
5	Impact Avicel PH 101 on formulation 4 and 5 for:	One way anova & Correlate bivariate (Paired sample t-test)		
	i. Hardness		0.00	-
	ii. Friability		0.00	-
	iii. Disintegration Time		0.00	-
	iv. Dissolution Rate		0.00	-
6	Impact Sodium starch glycolate on formulation 4 and 5 for:	One way anova & Correlate bivariate (Paired sample t-test)		
	i. Hardness		0.00	-
	ii. Friability		0.00	-
	iii. Disintegration Time		0.00	-
	iv. Dissolution Rate		0.00	-

'Table 3, continued'

No	Analysis	Types of test	Result: < 0.05, Significantly different	Correlation
7	Impact of Avicel PH 101 and Sodium starch glycolate on formulation 4 and 5 for:	Two way anova Multivariate		-
	vii. Hardness		0.00	-
	viii. Friability		0.00	-
	ix. Disintegration Time		0.00	
	x. Dissolution Rate		0.00	-
8	Impact of Spress® B820 and Sodium starch glycolate on formulation 4 for:	Two way anova Multivariate		
	i. Hardness		0.00	-
	ii. Friability		0.00	-
	iii. Disintegration Time		0.00	-
	iv. Dissolution Rate		0.00	-
9	Impact of PS4 and Sodium starch glycolate on formulation 5 for:	Two way anova Multivariate		
	i. Hardness		0.00	-
	ii. Friability		0.00	-
	iii. Disintegration Time		0.00	-
	iv. Dissolution Rate		0.00	-
10	Impact of Avicel PH 101, Spress® B820 and Sodium starch glycolate on formulation 5 for:	Two way anova Multivariate		
	i. Hardness		0.00	-
	ii. Friability		0.00	-
	iii. Disintegration Time		0.00	-
	iv. Dissolution Rate		0.00	-
11	Impact of Avicel PH 101, PS4 and Sodium starch glycolate on formulation 5 for:	Two way anova Multivariate		
	i. Hardness		0.00	-
	ii. Friability		0.00	-
	iii. Disintegration Time		0.00	-
	iv. Dissolution Rate		0.00	-

'Table 3, continued'

No	Analysis	Types of test	Result: < 0.05, Significantly different	Correlation
12	Correlation between hardness and disintegration time	One way anova & Correlate bivariate (Paired sample t-test)	0.00	0.311
13	Correlation between hardness and dissolution rate	One way anova & Correlate bivariate (Paired sample t-test)	0.000000001	-0.036
14	Correlation between hardness and friability	One way anova & Correlate bivariate (Paired sample t-test)	0.00	0.037
15	Correlation between disintegration time and dissolution rate	One way anova & Correlate bivariate (Paired sample t-test)	0.00	0.150
16	Correlation between disintegration time and friability	One way anova & Correlate bivariate (Paired sample t-test)	0.00002	0.549
17	Correlation between dissolution rate and friability	One way anova & Correlate bivariate (Paired sample t-test)	0.00	0.573
18	Impact hardness and disintegration time on dissolution rate	Two way anova Univariate	0.06	0.983
19	Impact hardness and friability on dissolution rate	Two way anova Univariate	0.121	0.948
20	Impact hardness, disintegration time and friability on dissolution rate	Two way anova Univariate	0.351	0.996
21	Impact of swelling power on the disintegration time	One way anova & Correlate bivariate (Paired sample t-test)	0.00000002	0.700

‘Table 3, continued’

No	Analysis	Types of test	Result: < 0.05, Significantly different	Correlation
22	Impact of viscosity on dissolution rate	One way anova & Correlate bivariate (Paired sample t-test)	0.00	0.259
23	The significant of disintegration time of formulation 4 (references, 3mth, 6,mth)	One sample t-test	0.00	
24	The significant of thickness of formulation 4 (references, 3mth, 6,mth)	One sample t-test	0.00	
25	The significant of diameter of formulation 4 (references, 3mth, 6,mth)	One sample t-test	0.00	
26	The significant of hardness of formulation 4 (references, 3mth, 6,mth)	One sample t-test	0.00	
27	The significant of uniformity of weigh of formulation 4 (references, 3mth, 6,mth)	One sample t-test	0.00	
28	The significant of friability of formulation 4 (references, 3mth, 6,mth)	One sample t-test	0.00	
29	The significant of dissolution rate of formulation 4 (references, 3mth, 6,mth)	One sample t-test	0.00	
30	The significant of disintegration time of formulation 5 (references, 3mth, 6,mth)	One sample t-test	0.00	
31	The significant of thickness of formulation 5 (references, 3mth, 6,mth)	One sample t-test	0.00	
32	The significant of diameter of formulation 5 (references, 3mth, 6,mth)	One sample t-test	0.00	
33	The significant of hardness of formulation 5 (references, 3mth, 6,mth)	One sample t-test	0.00	
34	The significant of uniformity of weigh of formulation 5 (references, 3mth, 6,mth)	One sample t-test	0.00	

‘Table 3, continued’

No	Analysis	Types of test	Result: < 0.05, Significantly different	Correlation
35	The significant of friability of formulation 5 (references, 3mth, 6,mth)	One sample t-test	0.00	
36	The significant of dissolution rate of formulation 5 (references, 3mth, 6,mth)	One sample t-test	0.00	

Appendix 0: Awards, intellectual property rights and publications.

1. List of awards

(a) BioInno Awards 2009

(b) BioInno Awards 2010

2. Intellectual property right

Current title: A method for producing directly compressible sago starch

Old title: Pres-Go: A new directly compressible sago starch

3. Revision a manuscript for publication in Powder Technology Journal

Title: COMPRESSION AND MECHANICAL PROPERTIES OF DIRECTLY COMPRESSIBLE PREGELATINIZED SAGO STARCHES

4. A manuscript submitted for publication in International Journal of Pharmaceutics

Title: COMPRESSION AND MECHANICAL PROPERTIES OF DIRECTLY COMPRESSIBLE PREGELATINIZED SAGO STARCHES